HEPATIC TRANSPORTER FUNCTION IN LIVER DISEASE: IMPACT ON HEPATOBILIARY DISPOSITION AND PHARMACOKINETICS

Jason Robert Slizgi

A dissertation submitted to the faculty of the University of North Carolina at Chapel Hill in partial fulfillment of the requirements for the degree of Doctor of Philosophy at the Eshelman School of Pharmacy (Pharmacotherapy and Experimental Therapeutics)

Chapel Hill
2016

Approved by:

Kim L.R. Brouwer

Dhiren Thakker

A. Sidney Barritt IV

William J. Brock

Robert Dupuis

©2016
Jason Robert Slizgi
ALL RIGHTS RESERVED

ABSTRACT

Jason Robert Slizgi: Hepatic Transporter Function in Liver Disease: Impact on Hepatobiliary Disposition and Pharmacokinetics
(Under the direction of Kim L.R. Brouwer)

The objective of this doctoral dissertation research was to understand how hepatic transporter function in liver disease affects hepatobiliary disposition and pharmacokinetics of endogenous and exogenous compounds. In particular, this dissertation focused on two forms of liver disease: non-alcoholic steatohepatitis (NASH) and autosomal dominant polycystic kidney disease (ADPKD). A multi-experimental, translational approach including transporter over-expressing membrane vesicles, sandwich-cultured human hepatocytes, isolated perfused rat livers, metabolomic profiling, imaging, and an *in vivo* study in humans was employed. Based on reported changes in *in vitro* expression of organic anion transporting polypeptide (OATP), multidrug resistance-associated protein (MRP) 2 and MRP3 in liver tissue from patients with NASH, we tested the hypothesis that the disposition of ^{99m}Technetium-mebrofenin (MEB), an OATP, MRP2, and MRP3 probe, was altered in this patient population. Systemic and hepatic concentrations of MEB were increased in patients with NASH compared to age- and sex-matched healthy volunteers, consistent with impaired uptake and biliary excretion, and enhanced basolateral efflux of MEB.

Tolvaptan and two metabolites, DM-4103 and DM-4107, were shown to be inhibitors of the major human hepatic bile acid transporters Na^+-taurocholate cotransporting polypeptide (NTCP), bile salt export pump (BSEP), and MRP2, MRP3, and MRP4, which may contribute to

tolvaptan-associated liver injury in patients with ADPKD. Although impaired bile acid transport by tolvaptan and/or its metabolites may negatively impact bile acid homeostasis, the fact that liver injury has been observed only in patients with ADPKD suggests that other mechanism(s) and/or patient susceptibility factors may contribute to drug-induced liver injury (DILI) in this patient population. Metabolomic profiling of bile acids in polycystic kidney (PCK) rats, a rodent model of human ADPKD, revealed significantly increased concentrations of total bile acids and bile acids associated with hepatotoxicity in the serum and liver when compared to wild-type rats. Total serum bile acids positively correlated with measures of liver impairment (i.e. liver weight, total liver bile acids, total liver bile acids associated with hepatotoxicity, and cystic volume) suggesting that serum bile acids may be useful biomarkers for liver impairment in ADPKD. Further mechanistic studies revealed, for the first time, decreased biliary excretion of 5(6)-carboxy-2',7'-dichlorofluorescein (CDF), a fluorescent Oatp, Mrp2, and Mrp3 probe, in PCK rats using the isolated perfused rat liver model. In total, these data suggest that drug- and disease-specific factors may play a role in the potential for bile acid-mediated hepatotoxicity associated with tolvaptan use in patients with ADPKD.

This research has resulted in novel contributions that provide important insight into the impact of liver disease on hepatic transporter function. This information will significantly enhance our ability to understand and predict altered hepatic transporter function, which will improve the safety and effectiveness of drugs.

ACKNOWLEDGEMENTS

I want to thank my major advisor, Kim Brouwer, for allowing me to work in her research laboratory. I want to also thank my committee chair, Dhiren Thakker, for his scientific and personal support during my time at UNC. Dhiren's calm in times of adversity is a unique ability of his. It is no wonder why he is so revered by his colleagues and students; I am now among one of them. I want to thank Sid Barritt for his clinical expertise and always being flexible despite his busy schedule; Bob Dupuis, for his support throughout the program; and Bill Brock, for is insightful comments, thought-provoking questions related to my dissertation work, and his mentorship.

I would be remiss if I didn't thank my past and present colleagues whom have undoubtedly contributed to the work presented herein and to my progression through the program: Cen Guo, Vadryn Pierre, Kyunghee Yang, Izna Ali, James Beaudoin, Melina Malinen, Yang Lu, Brian Ferslew, Nathan Pfeifer, Brandon Swift, Rhiannon Hardwick, Kevin Watt, Eleftheria Tsakalozou, and Danny Gonzalez, among others. Big shout out to Josh Kaullen who spent many many many hours with me during our clinical study. Don't forget to use that second attack in war, my friend.

I also want to acknowledge all the friendships I have made here in North Carolina for keeping me sane and reminding me that a (happy) life exists outside of graduate school: Jen Grant (my awesome roommate of three years), Ben Murray and Katie Starr (my awesome roommates of two years and fellow music/beer connoisseurs), and everyone on the best damn

kickball team (Julie Vo, Doug Huey, Stephen Morrison, Carly Dickerson, Daniel Bessa, Tim Ferris, Andrew Butler, Erin Wilson, Felix Sebera, Holly Schroder, Shaye Hagler, Kat Fol, Rebekah Morrison)! I will miss y'all from our trips to the beach, to the mountains, but most importantly, to our raucous nights at Star Karaoke! It's tearin' up my heart!

Lastly, I dedicate this work to my family. Any formulation of words to describe the amount of love and support you have given me would be an injustice – thank you Mom and Dad!

TABLE OF CONTENTS

LIST OF TABLES

LIST OF FIGURES

LIST OF ABBREVIATIONS

ADPKD	Autosomal dominant polycystic kidney disease
ARPKD	Autosomal recessive polycystic kidney disease
ALP	Alkaline phosphatase
ALT	Alanine transaminase
AMP	Adenosine monophosphate
AST	Aspartate transaminase
ATP	Adenosine triphosphate
AUC	Area under the curve
BEI	Biliary excretion index
BMI	Body mass index
BSEP	Bile salt export pump
CDCA	Chenodeoxycholic acid
CDF	5(6)-carboxy-2',7'-dichlorofluorescein
CHO	Chinese hamster ovary
CI	Confidence interval
$Cl_{biliary}$	Biliary clearance

C_{max}	Maximal concentration
DILI	Drug-induced liver injury
DHEAS	Dehydroepiandrosteronesulfate
GCDCA	Glycochenodeoxycholic acid
GDCA	Glycodeoxycholic acid
HBSS	Hank's balanced salt solution
HOMA-IR	Homeostatic model assessment for insulin resistance
$E_2$17G	Estradiol-17β-glucuronide
FDA	Food and Drug Administration
IC_{50}	Concentration of inhibitor where the transport activity is reduced by half
IHC	Immunohistochemistry
K_i	Inhibition constant
K_m	Concentration that yields half maximal substrate transport
LC-MS/MS	Liquid chromatography-tandem mass spectrometry
NAFLD	Non-alcoholic fatty liver disease
NAS	Non-alcoholic fatty liver disease activity score
NASH	Nonalcoholic steatohepatitis

NTCP	Na^+-taurocholate cotransporting polypeptide
MANOVA	Multiple analysis of variance
MEB	^{99m}Technetium–mebrofenin
MRI	Magnetic resonance imaging
MRP	Multidrug resistance-associated protein
NCA	Noncompartmental analysis
OATP	Organic anion transporting polypeptide
PCA	Principal component analysis
PCK	Polycystic kidney
PK	Pharmacokinetics
PKD	Polycystic kidney disease
TCA	Taurocholic acid
TDCA	Taurodeoxycholic acid
TCDCA	Taurochenodeoxycholic acid
SCHH	Sandwich-cultured human hepatocytes
V_{max}	Maximal rate of substrate transport
X_{max}	Maximal liver activity

CHAPTER 1. Introduction[1]

Effect of Liver Disease on Hepatic Transporter Expression and Function

INTRODUCTION

The liver is an important organ in the biotransformation, disposition, and elimination of endogenous (e.g. macromolecules, bile acids) and exogenous molecules (e.g. drugs). Drug metabolizing enzymes play a central role in hepatic drug elimination; however, efforts over the past decade have revealed that transport proteins are also important determinants of hepatic clearance. Hepatic transporters are transmembrane proteins anchored in polarized hepatocytes, the primary parenchymal cell type of the liver, that facilitate the transport of molecules to and from sinusoidal blood and hepatocytes (basolateral transporters) or from hepatocytes into the biliary canaliculus (canalicular transporters). These transporters are classified into two superfamilies: the solute carrier (SLC) protein family and the adenosine triphosphate (ATP)-binding cassette (ABC) protein family.

The expression and function of transporters are subject to complex regulatory mechanisms and are contributing factors to interindividual variability. Characterizing sources that contribute to individual variability in drug transporter expression/function, and thus hepatic clearance, will improve the efficient development of new and safer pharmacological interventions and improve our mechanistic understanding of disease genesis/progression. The identification of drug-drug interactions (DDIs) and more recently, genetic polymorphisms, which

[1] A portion of this chapter is in preparation as a review article; Dr. Nilay Thakker authored the review of hepatocellular carcinoma and primary biliary cholangitis in this chapter.

influence the expression and/or function of drug transporters, have been under extensive investigation over the years. However, DDIs and genetic polymorphisms represent only a portion of the total contribution to interindividual variability.

Liver disease may influence the expression and function of hepatic transporters. Chronic liver disease is a significant source of morbidity and mortality in both industrialized and developing nations. It is estimated that one million deaths worldwide were attributed to liver cirrhosis alone in 2010, while many more were due to liver cancer and hepatitis (Mokdad et al., 2014). The etiologies of liver disease are diverse and can include chronic alcohol abuse, viral/bacterial infection, fatty liver disease, and drug-induced injury – all of which may have genetic components that can influence the development, manifestation, and severity of disease. The purpose of this article is to review the literature characterizing and quantifying the effects of liver disease on the expression and function of hepatic transporters in humans. First, a brief overview of hepatic transporters will be provided. Then, the effects of cholestasis, hepatitis C (HCV) infection, hepatocellular carcinoma (HCC), human immunodeficiency virus (HIV) infection, non-alcoholic steatohepatitis (NASH), and primary biliary cholangitis (PBC) on hepatic transporter expression and function will be provided. In addition to highlighting current knowledge regarding the effect of liver disease on hepatic transporters, this review will identify knowledge gaps in our understanding of the contribution of liver disease to the complexity of variable drug disposition and elimination.

Basolateral Uptake Transporters

Sodium-Taurocholate Cotransporting Polypeptide (NTCP)

The *SLC10A1* gene encodes NTCP, a key transport protein involved in the enterohepatic recirculation of bile acids (Hagenbuch et al., 1994). NTCP is homogenously expressed throughout the liver acinus and specifically coordinates the sodium-dependent uptake of bile acids from the sinusoidal blood to hepatocytes by electrogenically co-transporting two sodium ions and one bile acid molecule (Hagenbuch et al., 1996; Weinman et al., 1997). NTCP transports a variety of bile acids but appears to have higher affinity for glycine- and taurine-conjugated bile acids compared to their unconjugated counterparts, and a higher affinity for dihydroxy bile acids (e.g. chendodeoxycholate and deoxycholate conjugates) than trihydroxy bile acids (e.g. cholate conjugates). Although little emphasis is placed on NTCP-mediated interactions during drug development, NTCP has been shown to transport drugs. For example, drug-conjugated bile acids have been proposed as a potential strategy for drug delivery (Vallejo et al., 2007). Approximately 35% of total rosuvastatin uptake into hepatocytes was accounted for by NTCP (Ho et al., 2006); however, it is not clear if this contribution is relevant in the presence of systemic bile acids, which may selectively outcompete rosuvastatin *in vivo*. Interestingly, NTCP was shown to be a functional receptor for the hepatitis B virus and thus, may serve as a novel therapeutic target to inhibit the viral entry mechanism (Watashi et al., 2014; Yan et al., 2012).

Organic Anion Transporters (OATs)

OATs, classified in the *SLC22A* superfamily, are a ubiquitously expressed group of organic anion transporters that have broad distribution in such tissues as kidney, liver, brain,

pancreas, salivary glands, and skeletal muscle (Bleasby et al., 2006). These transporters generally mediate the transport of negatively charged endogenous and exogenous molecules in a bidirectional manner in exchange for dicarboxylate ions (Burckhardt et al., 2001; Simonson et al., 1994; Van Aubel et al., 2000), although uncharged and even cationic molecules have been reported as substrates (Cropp et al., 2008; Sweet et al., 1999). OATs also transport endogenous substances including cGMP, bile acids, and hormone derivatives (Kobayashi et al., 2002; Sekin et al., 1997; Sun et al., 2001). Prostaglandins and glutamate are examples of endogenous substrates of OAT2, whereas examples of xenobiotics include methotrexate, valproic acid, and allopurinol (Enomoto et al., 2002; Sekin et al., 1997; Shin et al., 2007; Sun et al., 2001). OAT7 is another liver-specific OAT that appears to have similar and overlapping substrate specificity with other OATs (Sekin et al., 1997; Shin et al., 2007). Despite the expression and function of OATs in the liver, there is little evidence demonstrating the clinical relevance of these transporters in the context of DDIs and/or genetic polymorphisms, although pravastatin recently was identified as a novel OAT7 substrate (Emami Riedmaier et al., 2016; Giacomini et al., 2010).

Organic Anion-Transporting Polypeptides (OATPs)

OATPs are a class of proteins that belong to the *SCLO* superfamily with 12-transmembrane spanning domains that are localized on the basolateral membrane of many epithelial cells. OATPs are highly expressed in the liver (predominantly OATP1B1, OATP1B3, and OATP2B1) (Badée et al., 2015; Hagenbuchand et al., 2008; Mikkaichi et al., 2004; Satlin et al., 1997). OATPs transport a wide variety of amphipathic and anionic substances in a bidirectional manner through countertransport with either bicarbonate or reduced glutathione (Li et al., 1998; Li et al., 2000; Kalliokoski et al., 2009). OATP substrates include endogenous

compounds such as bile acids, bilirubin, thyroid hormones, and steroid conjugates. Several drug classes have been characterized, or even specifically designed, as substrates for OATPs including 3-hydroxy-3methylglutarylcoenzyme A (HMG-CoA) reductase inhibitors (i.e. statins), angiotensin II receptor antagonists, angiotensin converting enzyme inhibitors, and cardiac glycosides (FDA Guidance, 2012; Kalliokoski et al., 2009). The liver-specific OATP1B1, OATP1B3, and to a lesser extent, OATP2B1, are considered clinically relevant drug transporters by the Food and Drug Administration (FDA) and are routinely evaluated during drug development (FDA Guidance, 2012).

Organic Cation Transporters (OCTs)

The first OCT (i.e. OCT1) was isolated and cloned from rat kidney by Gründemann et al. in 1994 and was later shown to display a 12-transmembrane structure that mediates the bidirectional transport of various small molecules (~60-350 Da) in an electrogenic manner (Koepsell et al., 2003). Similar to other transporters of the SLC family, OCTs display broad tissue distribution in such organs as the kidney, liver, and intestine. Three OCT isoforms have been identified in humans. OCT1 exhibits greatest expression in the liver. OCTs generally mediate the transport of small hydrophilic compounds with at least one positive charged amine moiety, although uncharged or anionic substrates have been reported (Koepsell et al., 2003). Classic substrates include tetraethylammonium (TEA) and the parkinsonian neurotoxin 1-methyl-4-phenylpyridinium (MPP^+); clinically relevant drug substrates include famotidine, ranitidine, and more recently, metformin (Bourdet et al., 2005; Cai et al., 2016; Han et al., 2015).

Canalicular Efflux Transporters

Breast Cancer Resistance Protein (BCRP)

BCRP (*ABCG2*) was first cloned by Doyle et al. (2003) and although its name suggests otherwise, BCRP is expressed in a variety of tissues and cell types (e.g. intestine, brain, liver, cardiac muscle). BCRP is a half transporter hypothesized to function as a homodimer or potentially a tetramer (Litman et al., 2001; Xu et al., 2004). In the liver, BCRP is localized to the canalicular membrane with broad substrate specificity, which includes organic ions, sulfate conjugates, and both negatively and positively charged molecules. BCRP substrates have been characterized primarily in the context of oncology due to the resistance of certain cancer types against chemotherapeutic agents. Some examples include mitoxantrone, SN-38, topotecan, and doxorubicin (Kawabata et al., 2001; Maliepaard et al., 1999; Nakagawa et al., 1992). However, BCRP can transport sulfate and glucuronide bile acid conjugates and may play a compensatory role when the function of other transporters (e.g. MRP2) are impaired (Pauli-Magnus et al., 2006; Zamek-Gliszczynski et al., 2006).

Bile Salt Export Pump (BSEP)

ABCB11 encodes BSEP, a member of the ABC transporter family, which is the primary hepatocellular transporter responsible for secretion of bile acids into the bile canaliculus. BSEP is predominantly expressed throughout the human liver acinus. Bile acid transport requires the hydrolysis of ATP, which drives the conformational change in the transmembrane domain of BSEP, hence translocating bile acids from hepatocytes to the canalicular space. In addition to bile acids, BSEP has been reported to transport pravastatin (Hirano et al., 2005). Monoanionic and conjugated bile acids represent the majority of BSEP substrates; unconjugated bile acids do not appear to be substrates as evidenced by in vitro and in vivo human data (Carlton et al., 2003;

Gerloff et al., 1999). Differences in substrate specificity between species have been reported; for example, human BSEP is able to transport taurolithocholate-3-sulfate although this is not true for the rodent orthologue (Byrne et al., 2002). The affinity (i.e., K_m) for bile acids is generally in the low micromolar range across species, but differences in rank-order and specificity have been noted. For example, human BSEP has a higher affinity for taurocholate than mouse BSEP (human K_m: 4.25 μM compared to mouse K_m: 15-30 μM) (Byrne et al., 2002).

Multidrug and Toxin Extrusion Protein 1 (MATE1)

MATE1 (*SLC47A1*) is an H^+/organic cation transporter first identified in 2005 that mediates the electrogenic transport of organic cations independent of a sodium gradient (Otsuka et al., 2005). It is primarily expressed on the canalicular membrane of hepatocytes and the luminal membrane of the proximal tubules and is thought to play a physiological role in the excretion of toxic endogenous substances, although several drugs have been identified as substrates (e.g. metformin, cimetidine, and acyclovir) (Nies et al., 2011).

Multidrug Resistance-Associated Protein 2 (MRP2)

MRP2 is a member of the *ABCC* family and one of nine recognized MRPs. First identified in the canalicular membrane of hepatocytes, MRP2 has been characterized in the kidney, small intestine, gallbladder, and placenta (Kepplerand et al., 1996; Meyer zu Schwabedissen et al., 2005; Sandusky et al., 2002; Schaub et al., 1999). MRP2 is a major driving force for bile-acid independent bile flow through the secretion of reduced glutathione, although it transports divalent and glucuronide- and sulfate-conjugated bile acids into the bile canaliculus. MRP2 is responsible for the biliary transport of many anionic drug/metabolites including methotrexate, acetaminophen-glucuronide, and etoposide (Büchler et al., 1996; Fahrmayr et al., 2012). The physiological role of MRP2 is demonstrated by the characteristic elimination of

bilirubin (specifically, the conjugated species) as evidenced by in vitro data and in patients with Dubin-Johnson Syndrome, who harbor polymorphisms in the *ABCC2* gene (Jemnitz et al., 2010; Keppler et al., 2014). This is further supported by the naturally occurring Mrp2-deficient rats (i.e. Eisai hyperbilirubinemic and CY/TR$^-$ mutant rat strains), which have been a valuable *in vivo* model for understanding the role of MRP2 in drug disposition (Büchler et al., 1996; Kepplerand et al., 1996; Oswald et al., 2006).

Multidrug Resistance Protein 1 (MDR1)

MDR1, commonly known as P-glycoprotein (P-gp), was one of the first ABC proteins identified due to its important role in drug resistance in chemotherapy. Like other ABC transporters, P-gp is comprised of two membrane-bound domains each consisting of six transmembrane helices (Looand et al., 1995). Expression has been quantified in many tissues such as the liver, brain, testis, gut, and colon (Cordon-Cardo et al., 2000). Although the physiological role of P-gp has been debated, it likely plays a general role in the protection from xenobiotics and disposition of endogenous substances, as evidenced by its ability to transport a variety of amphipathic drugs, natural products, and peptides. P-gp transports immunosuppressants, hormones, calcium channel blockers, and cardiac glycosides, but P-gp expression and function have been studied the most in the context of cancer chemotherapy. Apart from being expressed in major organs governing drug disposition (e.g. the liver, gut), P-gp is overexpressed in many cancer cell types, which limits the distribution/exposure of chemotherapeutics to the site of action (Amin et al., 2013; Mechetner et al., 1998; Vredenburg et al., 2001).

Basolateral Efflux Transporters

Multidrug Resistance-Associated Protein 1 (MRP1)

The clinical relevance of MRP1, encoded by the *ABCC1* gene, was first recognized in the transport of hydrophobic and hydrophilic anticancer agents such as vincristine and etoposide (Keppler et al., 2011; Slot et al., 2011; Zhou et al., 2008). Under normal conditions, the expression of MRP1 in the liver is low (Deeley et al., 2006; Stride et al., 1997). In vitro studies have established that MRP1 can transport a variety of physiological organic anions including drugs and their conjugated metabolites. For example, MRP1 can transport endogenous substances such as 17 beta-estradiol glucuronide, glutathione, leukotriene C4, folic acid, and vitamin B12, which may indicate its physiological role in cellular defense and oxidative stress (Deeley et al., 2006; Stride et al., 1997).

Multidrug Resistance-Associated Protein 3 (MRP3)

MRP3, encoded by the *ABCC3* gene, actively transports organic ions using energy generated by the hydrolysis of ATP. MRP3 is localized on the basolateral membrane of hepatocytes but is expressed in other tissues such as the gut, kidney, and adrenal cortex (Scheffer et al., 2002). In the context of the liver, MRP3 is thought to play an adaptive role in response to hepatocellular stress as evidenced by the upregulation of MRP3 in cholestatic conditions (Chai et al., 2012; Donner et al., 2001). MRP3 transports bulky organic anions from the hepatocyte to the systemic circulation and preferentially mediates the transport of glucuronide and, to a lesser extent, sulfate conjugates (e.g. bilirubin glucuronide, bile acid conjugates) (Borst et al., 2002; Hirohashi et al., 2000). Although MRP3 has been studied in the context of bile acid transport, several drugs and/or metabolites have been identified as MRP3 substrates such as acetaminophen

glucuronide, methotrexate, and sorafenib (Canet et al., 2015; Tomonari et al., 2016; Xiong et al., 2002; Zeng et al., 2001).

Multidrug Resistance-Associated Protein 4 (MRP4)

In contrast to MRP3, MRP4 (*ABCC4*) transports a dynamic range of endogenous molecules such as folate, bile acids, uric acid, eicosanoids, steroid hormones, and cyclic nucleotides (Borst et al., 2002; Zelcer et al., 2003). Although first characterized as a transporter that confers resistance to cytotoxic agents, MRP4 has since shown broad substrate specificity to drugs from many classes including antibiotics, antivirals, and cardiovascular agents. MRP4 is generally expressed in tissues with a barrier function such as the liver, brain, and intestine. In the liver, MRP4 is localized on the basolateral membrane and translocates molecules from the hepatocyte back to the systemic circulation. Similar to MRP3, it is thought that the physiological role of MRP4 is to protect the liver from toxic accumulation of bile acids as evidenced by marked increases in MRP4 expression in cholestasis (Gradhand et al., 2008). This hypothesis is further supported in Mrp4-knockout mice that exhibited severe obstructive cholestasis in the absence of Mrp4 (Mennone et al., 2006).

Liver Disease

The effects of liver disease on hepatic transporter expression and function in humans are described in the following section.

Cholestasis

Cholestasis is the impairment of bile formation (hepatocellular) and/or flow (obstructive) that can arise from a number of intrinsic and extrinsic factors. In response to accumulating bile constituents, adaptive mechanisms induce hepatoprotective systems (e.g. bile acid transporter

expression) aimed at reducing intracellular accumulation of bile acids, which can be hepatotoxic due to their detergent-like properties.

The functional role of transporters in cholestasis is highlighted in patients harboring mutations in the *ABC11* (BSEP) gene known as progressive familial intrahepatic cholestasis 2 (PFIC2). First described by Clayton et al. (1969), the PFIC-2 phenotype is illustrated by pruritus, jaundice, and clinical signs of cholestasis (discolored stools, dark urine), which often leads to fulminant liver failure and death early in life (Clayton et al., 1969; Jacquemin et al., 2012). Message and protein analysis of hepatic bile acid uptake transporters (e.g. NTCP, OATP1B1 and OATP1B3) were found to be downregulated compared to control samples, whereas OATP2B1was unaffected (Keitel et al., 2005). Interestingly, MRP4, but not MRP3 was strongly upregulated in PFIC-2 livers, consistent with an adaptive response to increased hepatocellular bile acid concentrations. Although it is not clear why the authors did not observe increased MRP3 as would be expected in cholestasis, it must be noted that the sample size was small (n=4 PFIC-2 and n=3 control samples). MRP2 was localized to the canalicular membrane and appeared to be downregulated in PFIC-2; however, this result did not reach statistical significance (Keitel et al., 2005).

Because the etiologies of cholestasis can be diverse, altered transporter function may be causal or an adaptive response to cholestasis, or both. For example, intrahepatic cholestasis of pregnancy (ICP) is an acute form of cholestasis that typically presents in the third trimester of pregnancy and is associated with premature delivery, respiratory distress, and intrauterine death (Rook et al., 2012). In vivo studies revealed that the transcriptional dynamics of BSEP were inversely correlated with serum 17β-estradiol (E2) levels, implicating E2 levels in the repression of BSEP, which may increase susceptibility to ICP (Chen et al., 2015; Song et al., 2014). In the

same study, repression of BSEP expression also was demonstrated in human primary hepatocytes (Song et al., 2014). The procholestatic effects of estrogens and progesterone may also alter Mrp2; E2 administration causes endocytic internalization, as well as decreased expression and function of Mrp2 in rodents (Mottino et al., 2002; Trauner et al., 1997). Downregulation of hepatic sinusoidal transporters (i.e. Oatp1a1, Oatp1a4, and Oatp1b2) are likely an adaptive response to increased bile acid concentrations and cholestasis (Geier et al., 2003; Simon et al., 1996). Although ethical considerations may preclude the quantification of hepatic transporter expression in ICP, the expression of OATP1B3 in placenta was decreased in pregnant women diagnosed with ICP, consistent with altered transporter expression revealed in animal studies (Wang et al., 2012). Zollner et al. (2001) reported that NTCP mRNA correlated with serum bile acids in patients with inflammatory cholestasis. Similar observations were reported for OATP1B1 and BSEP, but MRP2 mRNA was unchanged (Zollner et al., 2001).

Given the limited availability of human samples, the application of animal models has provided information about the mechanisms underlying transporter expression/function in cholestasis. For example, ligation of the common bile duct in rodents leading to cholestasis decreased Mrp2 protein levels without a corresponding change in mRNA expression, suggestive of an impaired posttranslational modification effect (Paulusma et al., 2000). Immunofluorescent staining revealed intracellular localization of Mrp2, which may indicate that the Mrp2 trafficking pathway(s) to the canalicular membrane are compromised resulting in the endocytic retention of Mrp2 and possible lysosomal degradation. Indeed, retrieval of MRP2 from the canalicular membrane into the cytoplasm of hepatocytes has been reported in patients with cholestasis (Kojima et al., 2008). Although the exact mechanism underlying this observation has yet to be fully elucidated, altered binding and subsequent improper anchoring in the canalicular membrane

via radixin and/or other actin filament interactions appears to play a role (Elferink et al., 2015; He et al., 2012; Kojima et al., 2008).

Few studies have investigated the effect of cholestasis on the pharmacokinetics and hepatobiliary disposition of drugs. Bile duct ligation in rats significantly increased the systemic concentrations of morphine-3-glucuronide, the active metabolite of the analgesic morphine, due, in part to increased expression of hepatic Mrp3 (Hasegawa et al., 2009). Message and protein expression of MRP3 were significantly increased by ~3-fold in patients with obstructive cholestasis (Chai et al., 2012); hence, it is conceivable that increased systemic exposure of morphine glucuronide(s) could impact pharmacodynamic activity and/or toxicity in this patient population. In experimental intrahepatic cholestasis induced by 17α-ethynylestradiol in rats, the antidiabetic effect of metformin was reduced due to impaired hepatic uptake of Oct1 (Jin et al., 2009). Although clinical data are needed, these observations suggest that metformin efficacy (e.g. in gestational diabetes) may be impaired in diabetic patients with estrogen-associated ICP. In the same rodent model, systemic concentrations of doxorubicin were increased by ~60%, which was partially attributed to a ~67% reduction in Mrp2-mediated biliary excretion (Choi et al., 2013). Lastly, the apparent half-life and systemic exposure of digoxin was decreased in a rodent model of cholestasis, presumably through impaired P-gp-mediated enterohepatic recirculation (Harrison et al., 1976).

Hepatitis C Infection

Hepatitis C virus (HCV) is a prevalent form of viral hepatitis. The risk of developing cirrhosis, liver cancers, or both is increased in HCV-infected patients (Gower et al., 2014). HCV induces hepatoprotective response pathways in response to fibrosis and hepatocellular injury that can affect normal gene expression patterns (Kurzawski et al., 2012). The World Health

Organization estimates that more than 150 million individuals are chronically infected with HCV (Chu et al., 2008). Thus, understanding altered expression and/or function genes involved in absorption, distribution, metabolism, and excretion (ADME) is crucial to pharmacotherapeutic intervention in this population.

Due to inflammation associated with viral infection, prevailing evidence implicates the coordinate downregulation of ADME genes by nuclear transcription factors [e.g. PXR, CAR, aryl hydrocarbon receptor (AHR), RXR), although interaction(s) with the HCV virus and the transcriptional factor RXR have be reported (Clément et al., 2009; Congiu et al., 2009; Tsutsumi et al., 2002). Therefore, the pathophysiological role of HCV in altered ADME expression cannot be dismissed. Relative mRNA expression of OATP1B1 and OATP2B1 was reduced in the livers of patients with chronic HCV infection, although the mechanistic link between inflammatory cytokines and OATP downregulation is not clear (Hanada et al., 2012; Nakai et al., 2008). Downregulation of NTCP, OAT2, and OCT1 correlated with fibrosis state but another study observed no difference compared to control samples (Hanada et al., 2012; Nakai et al., 2008). In the presence of HCV-induced cirrhosis, expression of NTCP, OATP1B3, and OCT1 are decreased compared to control samples using proteomic analysis (Wang et al., 2016).

Hepatic basolateral efflux transporters MRP3 and MRP4 are elevated compared to the livers of non-infected controls using mRNA analysis. These data are consistent with Ogasawara et al. (2010) who identified MRP4 mRNA as a potential marker for liver disease (Kurzawski et al., 2012; Ogasawara et al., 2010; Ros et al., 2003). Under normal physiological conditions, MRP3 and MRP4 protein are expressed at low levels but are significantly increased in cholestatic and inflammatory conditions, possibly due to the activation of AHR and/or Nrf2 observed in end-stage liver disease (Donner et al., 2001; Klaassen et al., 2010; Mennone et al.,

2006; Ros et al., 2003; Zollner et al., 2007). In contrast, the canalicular transporters BCRP and BSEP appeared to be downregulated whereas MRP1 and P-gp were upregulated. Some observations report that MRP2 is unaffected, although Hanada et al. (2012) found a negative correlation between fibrosis stage and MRP2 mRNA expression (Hanada et al., 2012; Kurzawski et al., 2012; Ogasawara et al., 2010; Ros et al., 2003). The impact of altered mRNA expression on protein expression has yet to be quantified, although immunohistochemistry shows increased MRP1 and P-gp staining in HCV liver biopsies (Ros et al., 2003). In HCV-induced cirrhosis, protein expression of BSEP, MRP2, and P-gp are downregulated whereas BCRP and MATE1 are unchanged (Wang et al., 2016). To date, the clinical relevance of these findings in HCV-infected patients is unclear. The systemic clearance of nelfinavir, a P-gp substrate, was reduced in HIV/HCV-co-infected patients compared to HIV-infected patients without HCV (Regazzi et al., 2005). However, P-gp is expressed in other tissues (e.g. gut, blood brain barrier) and thus, must be considered as a contributing factor to altered pharmacokinetics in HCV-associated P-gp function. Hepatic uptake and excretion of ^{99m}Tc-mebrofenin was decreased in HCV-infected patients, suggestive of altered OATP-, MRP2-, and MRP3mediated function (Kula et al., 2010).

Hepatocellular carcinoma

Hepatocellular carcinoma (HCC) is a malignancy of the liver cells that often occurs in patients with hepatic diseases such as cirrhosis or chronic hepatitis associated with HCV. There is a substantial body of evidence indicating that the expression of hepatic uptake and efflux transporters is altered in HCC. NTCP and OATP1B1 are the key transporters responsible for the uptake of drugs linked to bile acids as carrier molecules (Briz et al., 2002; Kramer et al., 1992; Zollner et al., 2005). Studies have shown that the expression of NTCP and OATP1B1 is significantly reduced in patients with HCC (Zollner et al., 2005). This is consistent with previous

in vitro studies that demonstrated reduced bile acid uptake in hepatoma cell lines (Kullak-Ublick et al., 1996; Marchegiano et al., 1992; von Dippe et al., 1990). These studies highlight the risk of liver toxicity during bile salt coupled chemotherapy because of reduced expression of NTCP and OATP1B1 (Zollner et al., 2005). OATP1B1 and OATP1B3 have been studied extensively in different types of cancers including HCC (Thakkar et al., 2015; Vavricka et al., 2004). Although initially considered to be liver specific, subsequent studies have shown that OATP1B1 and OATP1B3 frequently are expressed in multiple types of cancer tissues (Abe et al., 2001; Hamada et al., 2008; Kounnis et al., 2011; Muto et al., 2007; Thakkar et al., 2013; Thakkar et al., 2015). After the initial study reporting the reduced expression of OATP1B1 protein in HCC cell lines, many other in vitro studies reported similar findings (Cui et al., 2003; Libra et al., 2006; Monks et al., 2007; Vander Borght et al., 2005; Zollner et al., 2005). However, one study reported no significant change in expression of OATP1B1 compared to normal liver (Muto et al., 2007). These apparent differences may arise due to different detection methods (Muto et al., 2007; Zollner et al., 2005). Similarly, OATP1B3 mRNA and protein are reduced in HCC (Libra et al., 2006; Muto et al., 2007; Tsuboyama et al., 2010). Although studies in other cancer types have implied a potential association between OATP1B3 expression and clinical outcomes, the functional role of OATP1B3 in HCC remains to be investigated (Lockhart et al., 2008; Muto et al., 2007).

Interestingly, mRNA and protein expression of some other OATPs (e.g. OATP2A1, OATP3A1, OATP4A1 and OATP5A1) are reported to be upregulated in primary and metastatic liver cancer suggesting the potential role of these OATPs in supplying nutrients and hormones to tumor cells (Buxhofer-Ausch et al., 2013; Wlcek et al., 2011). OCT1 is downregulated in HCC compared to nonmalignant tissues, apparently through epigenetic mechanisms (Schaeffeler et al.,

2011). The downregulation of OCT1 expression is clinically associated with tumor progression and poor outcomes in patients with HCC (Heise et al., 2012; Schaeffeler et al., 2011).

Several studies indicate that the expression of canalicular and basolateral efflux transporters are altered in HCC. Although Borel et al. (2012) reported BCRP mRNA was unchanged, other studies reported a significant elevation of BCRP mRNA and protein expression in HCC compared to normal liver tissues (Sukowati et al., 2012; Sun et al., 2010). Interestingly, BCRP expression increased following chemotherapy in hepatoblastoma patients, which highlights its potential role in drug resistance in HCC (Sukowati et al., 2012; Vander Borght et al., 2008). On the other hand, BSEP expression was reported to be reduced secondary to inflammation-induced decreases in farnesoid X receptor (FXR) (Chen et al., 2013). Although the role of BSEP in resistance to chemotherapy is unclear, many studies have shown that elevated serum bile acid concentrations in the liver contribute to HCC pathogenesis (Bernstein et al., 2009; Chen et al., 2013; Gadaleta et al., 2010; Jansen et al., 2007; Knisely et al., 2006; Strautnieks et al., 2008). In fact, children with BSEP deficiency demonstrated a higher risk of cholestasis and HCC (Knisely et al., 2006; Strautnieks et al., 2008). Collectively, these findings highlight the potential role of BSEP and altered bile acid homeostasis in HCC progression (Chen et al., 2013).

P-gp expression in HCC displays divergent results at the mRNA and protein levels in some in vitro and in vivo studies, which may be related to different detection methods as well as tumor heterogeneity (Borel et al., 2012; Ng et al., 2000; Ros et al., 2003; Takanishi et al., 2009; Teeter et al., 1993; Zollner et al., 2005). The protein expression of P-gp showed a trend towards a reduction in HCC compared to normal hepatocytes (Ng et al., 2000; Takanishi et al., 2009; Zollner et al., 2005). In regard to its function, P-gp expression was inversely correlated with

chemotherapeutic response in patients with inoperable HCC (Chou et al., 1997; Ng et al., 2000). MRP2 expression in HCC was unchanged compared to normal hepatocyte tissues (Namisaki et al., 2014; Pfeifer et al., 2014; Zollner et al., 2005). MRP1, which is not expressed in normal hepatocytes, is overexpressed at both the mRNA and protein levels in HCC (Bonin et ak,m 2002; Sukowati et al., 2012; Zhao et al., 2010). One study showed that the MRP1 promoter (-1666GG) polymorphism was a predictor of poor survival in patients with HCC from Southeast China (Zhao et al., 2010). MRP3 and MRP4 mRNA levels were reported to be upregulated in HCC (Borel et al., 2012; Nies et al., 2001; Ros et al., 2003). Although several studies have noted the altered expression of drug transporters in HCC, further investigations are necessary to examine their clinical significance in HCC.

Human Immunodeficiency Virus (HIV) Infection

Similar to viral hepatitis, HIV is associated with chronic inflammation as evidenced by the presence of elevated proinflammatory cytokines such as interleukin (IL)-6 and tumor necrosis factor (TNF)-α (Appay et al., 2008). For example, mRNA and protein expression of major sinusoidal uptake transporters (i.e. OATP1B1, OATP1B3, OATP2B1, OCT1, OCT2, and NTCP) were downregulated in human hepatocytes when incubated with TNF- α, which resulted in reduced functional activity (Vee et al., 2009). Message and protein levels of MRP2 were increased by IL-6 or IL-1β exposure in sandwich-cultured human hepatocytes whereas BSEP protein expression appeared to decrease (Diao et al., 2010). In another study, MRP2 and BCRP were reported to be downregulated following exposure of IL-6 or IL-1β in primary human hepatocytes; therefore, additional mechanistic studies are required to definitively conclude that canalicular transporters are upregulated or downregulated. (Vee et al., 2009).). Based on these data, it is conceivable that liver transporter expression and/or function may be impacted in HIV-

infected patients because such signaling molecules can modulate transporters in vitro. It also must be noted that the administration of antiretroviral therapy is associated with a reduction in cytokine levels that may contribute to interindividual variability in hepatic transporter expression in HIV-infected patients (Brazille et al., 2003).

Despite the aforementioned data, the effect of HIV infection on the expression of transporters has not been evaluated systematically. In addition, coinfection (e.g. bacterial infection) could contribute to altered transporter regulation. For example, gene expression of hepatic Mrp2, Bcrp, and Oatps was downregulated in HIV-1 transgenic rats co-infected with endotoxin (Ghoneim et al., 2016). P-gp and MRP2 protein levels in the rectal-sigmoid colon were lower in antiretroviral-naïve patients compared to non-infected subjects; whether similar expression patterns occur in the liver remains to be evaluated (De Rosa et al., 2013; Kis et al., 2016). Data quantifying hepatic transporter protein expression followed by subsequent functional studies are needed. Altered ADME processes in clearance organs (i.e. intestine, liver, and kidney) in combination with the potential for induction by co-medications (e.g. protease inhibitors) highlights the complexity of predicting transporter-mediated drug disposition in HIV-infected patients (Dixit et al., 2007; Foisy et al., 2008).

Non-Alcoholic Fatty Liver Disease and Non-Alcoholic Steatohepatitis

Non-alcoholic fatty liver disease (NAFLD) consists of liver pathology ranging from simple steatosis to non-alcoholic steatohepatitis (NASH), an advanced inflammatory state of liver disease. NAFLD has become the most common form of liver disease in Western and industrialized nations driven by the prevailing obesity epidemic; it is estimated that ~20-30% of the general population is affected, although some reports are as high as 50% (Ali et al., 2009; Bedogni et al., 2005; Lomonaco et al., 2013; Younossi et al., 2016). For reasons not fully known,

some patients with NAFLD develop NASH, which may lead to hepatocarcinoma, cirrhosis, and/or fulminant liver failure. Due to the increasing prevalence of NAFLD and NASH, considerable research has been dedicated to quantifying how NASH affects ADME enzymes/transporters. These findings may have important implications in the treatment and disposition of drugs in this patient population.

Global gene expression analysis first implicated a coordinated down regulation of hepatic uptake transporters (e.g., OATPs) in patients with NASH (Lake et al., 2011). Further reports by Cherrington and colleagues revealed a significant increase in OATP1B1, but a decrease in OATP1B3, and no change in OATP2B1 in human liver biopsies using immunoblot techniques. Interestingly, no differences were observed in these transporters based on mRNA analysis (Clarke et al., 2014b). These findings are in contrast to data obtained from a commonly used diet-induced rodent model of NASH; mRNA and protein analyses were in agreement that rodent orthologues of human OATPs were decreased (Clarke et al., 2014a; Clarke et al., 2014b). These results support increased systemic concentrations of simvastatin acid, an OATP/Oatp substrate, in the rodent model of NASH compared to wild-type rats (Clarke et al., 2014a). NTCP, the primary hepatic bile acid transporter, is decreased in patients with NASH compared to patients with simple steatosis based on real-time reverse transcription polymerase chain reaction and immunoblot techniques; these data are consistent with a recent publication reporting that serum bile acids are increased in patients with NASH (Aguilar-Olivos et al., 2015; Ferslew et al., 2015b). Rat Ntcp and Oat2 also were shown to decrease in an experimental rodent model of NASH, presumably mediated through pro-inflammatory cytokines known to decrease hepatic transporter expression (Fisher et al., 2009; Tanaka et al., 2012). Pharmacokinetic studies that quantify the functional impact of altered uptake transporter expression are limited in humans.

However, our group recently reported increased systemic concentrations of ^{99m}Tc-mebrofenin, a hepatobiliary diagnostic agent and OATP/MRP2/MRP3 substrate, in patients with biopsy-confirmed NASH (Slizgi et al., (in preparation)).

In what appears to be an adaptation to prevent further damage by toxicants, hepatic efflux transporters are increased in NASH. For example, MRP3-6 are induced in liver biopsies from NASH patients, similar to findings in a rodent model of NASH (Hardwick et al., 2011; Lickteig et al., 2007; Tanaka et al., 2012). Similarly, Mrp1 mRNA is increased ~5-fold compared to control animals (Tanaka et al., 2012). Functional drug disposition studies corroborate these findings as evidenced by increased plasma acetaminophen glucuronide concentrations in diet-induced NASH animals attributable to increased Mrp3 expression (Lickteig et al., 2007). Administration of morphine and acetaminophen to patients with NASH resulted in increased systemic concentrations of the glucuronide conjugates, consistent with increased function of MRP3 in this patient population (Canet et al., 2015; Ferslew et al., 2015a). Although MRP2 is increased, a growing body of evidence supports a functional decrease in MRP2 due to disruption of cellular trafficking and/or improper localization away from the canalicular membrane (Fisher et al., 2009). This is supported by reports of reduced biliary excretion of acetaminophen glucuronide and pemetrexed, consistent with impaired Mrp2 function (Dzierlenga et al., 2016; Lickteig et al., 2007). These findings corroborate enhanced hepatic retention and a prolonged half-life of the liver contrast agent gadolinium ethoxybenzyl diethylenetriamine pentaacetic acid (Gd-EOB-DTPA) in NASH-induced rats (Tsuda et al., 2011). In contrast to Hardwick et al. (2011), who reported an increase in total MRP2 in human liver biopsies, a recent study reported decreased MRP2 in NASH patients, which correlated inversely with progression of NAFLD (Okushin et al., 2015). Decreased Mrp2 mRNA and protein expression were reported in a diet-

induced rodent model of hypercholesterolemia (Okushin et al., 2016). Apparent discrepancies may be due to differences in analytical method(s) or to the heterogeneous population of NASH patients and interindividual variability in MRP2 expression. Regardless, functional studies in humans are needed to evaluate the impact of altered MRP2 expression and/or localization. Although pharmacokinetic studies are limited, our group recently reported increased hepatic exposure of ^{99m}Tc-mebrofenin in patients with biopsy-confirmed NASH, which lends credence to the hypothesis that altered trafficking and localization of MRP2 result in a functional decrease in MRP2-mediated efflux (Slizgi et al., (in preparation)). BCRP mRNA and protein expression is increased in NASH liver biopsies, but this finding was not observed in rodent models of NASH (Canet et al., 2014; Hardwick et al., 2011). Finally, rodent P-gp and BSEP/Bsep expression appear to be increased in NASH but protein expression has not been quantified (Aguilar-Olivos et al., 2015; Canet et al., 2014; Okushin et al., 2015).

Primary Biliary Cholangitis

Primary biliary cholangitis (PBC) is a disease that causes bile duct inflammation and chronic damage over time. This leads to a buildup of bile acids and toxins that can cause cholestasis, fibrosis, and cirrhosis. Several studies have reported that the mRNA and protein expression of NTCP, OATP1B1, and OATP1B3 are downregulated in PBC as compared to normal liver (Kojima et al., 2003; Takeyama et al., 2012; Takeyama et al., 2015; Zollner et al., 2003). These findings suggest the potential adaptation by hepatocytes to limit the accumulation of toxic bile acids (Zollner et al., 2003).

Studies performed in in vitro systems and human liver confirmed that efflux transporter expression is maintained or had a trend towards increased expression in PBC as compared to normal liver (Kojima et al., 2003; Takeyama et al., 2012; Zollner et al., 2003). Zollner et al.

(2003) reported that BSEP and MRP2 expression were unchanged whereas expression of P-gp and MRP3 was upregulated in PBC. Interestingly, it was reported that these alterations may be related to the adaptation of transporters and the expression patterns may change from the early to late stage PBC (Takeyama et al., 2009; Takeyama et al., 2012). In addition to the changes in expression, the localization of MRP2 was altered in PBC stage III (Kojima et al., 2003). MRP1 and organic solute transporter (OST) α/β are upregulated in patients with PBC, presumably in inflamed tissue (Boyer et al., 2006; Kula et al., 2010; Takeyama et al., 2009; Teeter et al., 1993). MRP1 expression has been reported in macrophages, which may further supports the hypothesis that MRP1 is upregulated during inflammation (Jorajuria et al., 2004). Further studies are required to better understand the functional role of MRP1 and OST α/β in PBC.

Summary and Perspective

Among the challenges in diagnosing and treating liver disease is understanding its impact on hepatic transporter function and the disposition of clinically-relevant drugs, which may be further influenced by genetic and other environmental factors. The field of drug transport continues to evolve as more transporter-specific substrates and inhibitors are identified. However, clinically relevant probes are lacking due, in part, to the multiplicity of drug transporters (i.e. overlapping substrate specificity between transporters), the dynamic interplay between uptake, efflux, and metabolism processes, and the inability to quantify tissue-specific drug concentrations. Advances in magnetic resonance imaging (MRI) and positron emission tomography (PET), coupled with development of MRI and PET probes that are substrates for specific transporters, will continue to facilitate the quantification of hepatic transporter function, particularly canalicular efflux transporters, which should improve our ability to assess transporter function in diseases afflicting the liver. Finally, the amalgamation of such functional data can be

applied to pharmacokinetic modeling and systems pharmacology approaches to better understand and predict drug disposition in patients with liver disease. This will improve our fundamental understanding of drug efficacy and safety in these patient populations.

Table 1.1 Altered Expression of Hepatic Transporters in Liver Disease

Transporter	Liver Disease	Alterations (mRNA)	Alterations (protein)	Technique	Reference
NTCP/Ntcp	Cholestasis	↓ (~2-fold, human); ↓ (~3-fold, rodent)	↓ (~3-fold, human); ↓ (~3-fold, rodent)	RT-qPCR; NB; WB	Chai et al., 2012; Chen et al., 2008; Geier et al., 2003; Zollner et al., 2001
	HCV	↑ (human) or ↔ (human); ↔ (rodent)	-	RT-qPCR	Hanada et al., 2012; Kikuchi et al., 2010; Nakai et al., 2008
	HCC	↓ (~2-fold, human)	↓ (human)	RT-qPCR; NB	Kullak-Ublick et al., 1996; Zollner et al., 2005
	HIV	-	-	-	-
	NASH	↑ (~1.5-fold, human) or ↓ (~2-5-fold, human); ↓ (~2-fold, rodent)	↓ (~5-fold, human)	ISH; RT-qPCR WB	Aguilar-Olivos et al., 2015; Fisher et al., 2009; Okushin et al., 2015; Tanaka et al., 2012
	PBC/cirrhosis	↓ (~1.5-3-fold, human)	↓ (~2-fold, human)	RT-qPCR; WB; IF	Kojima et al., 2003; Takeyama et al., 2012; Zollner et al., 2003

Transporter	Liver Disease	Alterations (mRNA)	Alterations (protein)	Technique	Reference
OATP1B1/ Oatp1b2	Cholestasis	↓ (~2-fold, human); ↓ (~2-fold, rodent)	↔ (rodent)	NB; RT-qPCR; WB	Chen et al., 2008; Geier et al., 2003; Zollner et al., 2001
	HCV	↓ (~1.5-fold human); ↔ (rodent)	-	RT-qPCR	Hanada et al., 2012; Kikuchi et al., 2010; Nakai et al., 2008
	HCC	↓ (~2-3-fold, human) or ↔ (human)	↓ (human)	RT-qPCR; IF; IHC; WB	Cui et al., 2003; Kullak-Ublick et al., 1996; Libra et al., 2006; Monks et al., 2007; Vavricka et al., 2004
	HIV	-	-	-	-
	NASH	↔ (human); ↑ (~10-fold, rodent) or ↔ (rodent) or ↓ (~2-fold, rodent)	↑ (~5-fold, human); ↑ (~10-fold, rodent) or ↔ (rodent)	ISH; RT-qPCR; WB	Bedogni et al., 2005; Canet et al., 2014; Clarke et al., 2014; Fisher et al., 2009
	PBC/cirrhosis	↔ (human) or ↓ (~2-3-fold, human)	↔ (human) or ↓ (~2-fold, human)	RT-qPCR; IF; WB	Kojima et al., 2003; More et al., Takeyama et al., 2012; 2013; Zollner et al., 2003

Transporter	Liver Disease	Alterations (mRNA)	Alterations (protein)	Technique	Reference
OATP1B3	Cholestasis	↓ (~2-fold, human); ↓ (~2-fold, rodent)	↔ (rodent)	NB; RT-qPCR; WB	Chen et al., 2008; Geier et al., 2003
	HCV	-	-	-	-
	HCC	↓ (~5-50-fold, human)	↓ (human)	NB; RT-qPCR; WB; IHC; IF	Libra et al., 2006; Tsuboyama et al., 2010; Vavricka et al., 2004
	HIV	-	-	-	-
	NASH	↔ (human)	↓ (~10-fold, human)	ISH; WB	Clarke et al., 2014
	PBC/cirrhosis	↔ (human) or ↓ (~2-fold, human)	↔ (human) or ↓ (~2-3-fold, human)	RT-qPCR; IF; WB	Kojima et al., 2003; More et al., 2013; Takeyama et al., 2012; Zollner et al., 2003
OATP2B1/ Oatp2b1	Cholestasis	-	-	-	-
	HCV	↓ (, human); ↑ (~2-fold rodent)	-	RT-qPCR	Hanada et al., 2012; Kikuchi et al., 2010
	HCC	-	-	-	-
	HIV	↔ (rodent)	-	RT-qPCR	Ghoneim et al., 2016
	NASH	↔ (human); ↔ (rodent)	↔ (human); ↓ (~2-fold, rodent)	ISH; WB	Canet et al., 2014; Clarke et al., 2014
	PBC/cirrhosis	↑ (human)	↑ (human)	RT-qPCR ; WB	More et al., 2013

Transporter	Liver Disease	Alterations (mRNA)	Alterations (protein)	Technique	Reference
OAT2/Oat2	Cholestasis	-	-	-	-
	HCV	↓ (human); ↔ (rodent)	-	RT-qPCR	Hanada et al., 2012; Kikuchi et al., 2010
	HCC	-	-	-	-
	HIV	-	-	-	-
	NASH	↓ (~2-fold, rodent)		RT-qPCR	Fisher et al., 2009
	PBC/cirrhosis	-	-	-	-

Transporter	Liver Disease	Alterations (mRNA)	Alterations (protein)	Technique	Reference
OCT1/Oct1	Cholestasis	↓ (~3-fold rodent)	↓ (~2-fold rodent)	RT-qPCR; WB	Trauner et al., 1997
	HCV	↔ (human) or ↓ (human); ↓ (~2-fold rodent)	-	RT-qPCR	Hanada et al., 2012; Nakai et al., 2008 Kikuchi et al., 2010;
	HCC	↓ (~2-3-fold, human)	↓ (human)	RT-qPCR; WB; IF	Heise et al., 2012; Schaeffeler et al., 2011
	HIV	-	-	-	-
	NASH	-	-	-	-
	PBC/cirrhosis	-	-	-	-
MRP1/Mrp1	Cholestasis	-	-	-	-
	HCV	↑ (10-fold human)	↑ (human)	RT-qPCR; IHC	Ros et al., 2003
	HCC	↑ (human)	↑ (human)	RT-qPCR ; WB	Bonin et al., 2002; Ros et al., 2003; Zhao et al., 2010
	HIV	↔ (rodent)	-	RT-qPCR	Ghoneim et al., 2016
	NASH	↑ (~2-fold, human); ↑ (~2-fold, rodent)	↑ (~2-fold, human)	ISH; RT-qPCR; WB	Canet et al., 2014; Hardwick et al., 2011; Tanaka et al., 2012
	PBC/cirrhosis	↑ (human)	↑ (human)	RT-qPCR ; IHC	More et al., 2013; Ros et al., 2003

Transporter	Liver Disease	Alterations (mRNA)	Alterations (protein)	Technique	Reference
MRP3/Mrp3	Cholestasis	↑ (~3-fold, human)	↑ (~3-fold, human)	RT-qPCR ; IHC	Chai et al., 2012
	HCV	↑ (~10-fold, human); ↔ (rodent)	↑ (~2-20-fold, human)	RT-qPCR ; WB	Kikuchi et al., 2010; Ogasawara et al., 2010; Ros et al., 2003;
	HCC	↑ (~2-fold, human); ↔ (human)	-	RT-qPCR	Bonin et al., 2002; Borel et al., 2012; Nies et al., 2001; Ros et al., 2003
	HIV	↑ (~3-fold, rodent)	-	RT-qPCR	Ghoneim et al., 2016
	NASH	↑ (~2-fold, human); ↓ (~2-fold, rodent) or ↑ (~5-fold, rodent)	↑ (~2-fold, human); ↓ (~2-fold, rodent) or ↑ (~3-fold, rodent)	ISH; WB	Canet et al. 2014; Clarke et al., 2014; Hardwick et al., 2011
	PBC/cirrhosis	↑ (~10-fold, human) or ↓ (human, diabetic cirrhosis); ↔ (human, alcohol cirrhosis)	↑ (human) and ↑ (human, diabetic and alcohol cirrhosis)	RT-qPCR ; IHC	Kojima et al., 2003; More et al., 2013; Ros et al., 2003; Zollner et al., 2003

Transporter	Liver Disease	Alterations (mRNA)	Alterations (protein)	Technique	Reference
MRP4/Mrp4	Cholestasis	↑ (~1.5-fold, human)		RT-qPCR	Chai et al., 2012; Chen et al., 2008
	HCV	↑ (~2-fold, human); ↑ (~2-fold, rodent)	↑ (~3-fold, human)	RT-qPCR; WB	Kikuchi et al., 2010; Kurzawski et al., 2012; Ogasawara et al., 2010
	HCC	↑ (~ 2-fold, human)	-	RT-qPCR	Borel et al., 2012
	HIV	↔ (rodent)	-	RT-qPCR	Ghoneim et al., 2016
	NASH	↑ (~3-fold, human); ↑ (~3-40-fold, rodent)	↑ (~3-fold, human); ↑ (~3-fold, rodent)	ISH; RT-qPCR; WB	Canet et al., 2014; Clarke et al., 2012; Hardwick et al., 2011; Tanaka et al., 2012
	PBC/cirrhosis	↔ (human) or ↑ (human)	↑ (human)	RT-qPCR; IHC; WB	More et al., 2013; Takeyama et al., 2012
BCRP/Bcrp	Cholestasis	-	-	-	-
	HCV	↓ (~2-fold, human); ↓ (~2-fold, rodent)	-	RT-qPCR	Kikuchi et al., 2010; Kurzawski et al., 2012
	HCC	↑ (human); ↔ (human)	↑ (human)	RT-qPCR ; IHC	Borel et al., 2012; Sukowati et al., 2012; Sun et al., 2010
	HIV	↔ (rodent)	-	RT-qPCR	Ghoneim et al., 2016
	NASH	↑ (~2-fold, human); ↑ (~5-fold, rodent)	↑ (~2-fold, human); ↔ (rodent)	RT-qPCR; WB	Canet et al., 2014; Hardwick et al., 2011
	PBC/cirrhosis	↑ (~ 2-fold, human)	↑ (human)	RT-qPCR ; WB; IHC	Hardwick et al., 2014; More et al., 2013

Transporter	Liver Disease	Alterations (mRNA)	Alterations (protein)	Technique	Reference
BSEP/Bsep	Cholestasis	↔ (human) or ↓ (~2-fold, human); ↓ (~2-fold, rodent)	↔ (human); ↓ (~2-fold, rodent)	RT-qPCR; WB; IHC	Chai et al., 2012; Chen et al., 2008; Song et al., 2007; Zollner et al., 2001
	HCV	↑ (~2-fold human) or ↓ (human); ↔ (rodent)	↔ (human)	RT-qPCR ; IHC	Hanada et al., 2012; Kikuchi et al., 2010 Ogasawara et al., 2010; Ros et al., 2003
	HCC	↓ (human)	↓ (human)	RT-qPCR; WB	Chen et al., 2013; Knisely et al., 2006
	HIV	-	-	-	-
	NASH	↑ (~5-fold, human) or ↓ (~2-fold, human); ↔ (rodent)	-	RT-qPCR	Aguilar-Olivos et al., 2015; Okushin et al., 2015; Tanaka et al., 2012
	PBC/cirrhosis	↔ (human) or ↓ (human)	↔ (human) or ↓ (human)	IHC; RT-qPCR; WB	Kojima et al., 2003; Takeyama et al., 2012

Transporter	Liver Disease	Alterations (mRNA)	Alterations (protein)	Technique	Reference
MRP2/Mrp2	Cholestasis	↔ (human) or ↓ (~2-fold, human)	↓ (human)	RT-qPCR; IHC	Chen et al., 2008; Chai et al., 2012; Zollner et al., 2001
	HCV	↔ (human) or ↓ (~2-fold human); ↔ (rodent)	↔ (human)	RT-qPCR; IHC	Hanada et al., 2012; Kikuchi et al., 2010 Kurzawski et al., 2012; Ogasawara et al., 2010; Ros et al., 2003
	HCC	↔ (human)	↔ (human)	RT-qPCR; IHC	Hanada et al., 2012; Namisaki et al., 2014
	HIV	↑ (~2-fold, rodent)	↑ (~1.5-fold, rodent)	qPCR; WB	Ghoneim et al., 2016
	NASH	↔ (human) or ↓ (~2-fold, human); ↔ (rodent) or ↑ (~2-fold, rodent)	↑ (~3-fold, human); ↑ (~2-fold, rodent) or ↔ (rodent)	ISH; RT-qPCR; WB	Canet et al., 2014; Clarke et al., 2014; Fisher et al., 2009; Hardwick et al., 2011; Okushin et al., 2015; Tanaka et al., 2012
	PBC/cirrhosis	↔ (human)	↔ (human)	RT-qPCR; WB; IHC	Kojima et al., 2003; More et al., 2013; Takeyama et al., 2012; Zollner et al., 2003

Transporter	Liver Disease	Alterations (mRNA)	Alterations (protein)	Technique	Reference
P-gp	Cholestasis	-	↔ (human)	IHC	Zollner et al., 2001
	HCV	↑ (~2-5-fold, human); ↔ (rodent)	↑ (~20-fold, human)	RT-qPCR; IHC	Kikuchi et al., 2010; Kurzawski et al., 2012; Ogasawara et al., 2010; Ros et al., 2003
	HCC	↑ (~ 2-5-fold, human)	↑ (human)	RT-qPCR; WB	Borel et al., 2012; Ng et al., 200; Ros et al., 2003; Takanishi et al., 2009; Teeter et al., 1993; Zollner et al., 2005
	HIV	-	↑ (~1.5-fold, rodent)	WB	Ghoneim et al., 2016
	NASH	↑ (~2-fold, rodent)	↑ (~2-fold, rodent)	ISH;WB	Canet et al., 2014
	PBC/cirrhosis	↑ (human)	↑ (5-fold, human)	RT-qPCR; WB; IHC	Ros et al., 2003; Zollner et al., 2003

Abbreviations: no data available (-); hepatocellular carcinoma (HCC); hepatitis C virus (HCV); human immunodeficiency virus (HIV); immunofluorescence microscopy (IF); immunohistochemistry (IHC); in situ hybridization (ISH); nonalcoholic steatohepatitis (NASH); northern blot (NB); primary biliary cholangitis (PBC); quantitative reverse transcription polymerase chain reaction (RT-qPCR); western blot (WB)

Table 1.2 Altered Transporter-Mediated Drug Disposition in Liver Disease

Liver Disease	Drug	Drug Class	Altered Drug Disposition	Implicated Transport Protein	Reference
Cholestasis	Diethylstilbestrol	Estrogen-replacement therapy	↓ systemic clearance and ↑ liver injury	ND (rodent)	Klaassen et al., 1973
	Rifampin	Antibiotic	↑ half-life	ND (human)	Spring 1968
	Digoxin	Cardiac glycoside	↓ half-life	ND (impaired enterohepatic recirculation)	Harrison et al., 1976
	Doxorubicin	Chemotherapeutic	↑ systemic concentrations	Mrp2 (rodent)	Choi et al., 2013
	Metformin	Antidiabetic	↓ systemic clearance and hepatic uptake; ↓ suppression of glucose production	Oct1 (rodent)	Jin et al., 2009
	Metformin	Antidiabetic	↓ systemic clearance and hepatic uptake; ↓ suppression of glucose production	Oct1 (rodent)	Jin et al., 2009
HCV	Nelfinavir	Antiretroviral	↑ systemic concentrations	P-gp (human)	Regazzi et al., 2015
	^{99m}Tc-mebrofenin	Hepatobiliary radiodiagnostic	↓ hepatic uptake, ↑ T_{max}, ↓ hepatic excretion	OATP, MRP2 (human)	Hanada et al., 2012
HCC	Gd-EOB-DTPA	Hepatobiliary contrast agent	↑ or ↓ signal intensity	OATP1B1 (human) OATP1B3 (human) MRP2 (human)	Enomoto et al., 2002; Shin et al., 2007
HIV	-	-	-	-	-

Liver Disease	Drug	Drug Class	Altered Drug Disposition	Implicated Transport Protein	Reference
NASH	APAP/APAP-glucuronide	Analgesic	↑ systemic concentrations; ↓ biliary excretion	MRP3 (human); Mrp2/Mrp3 (rodent)	Ferslew et al., 2015a
	Morphine/morphine-glucuronide	Analgesic	↑ systemic concentrations	MRP3 (human)	Canet et al., 2015
	^{99m}Tc-mebrofenin	Hepatobiliary diagnostic	↑ systemic concentrations; ↑ hepatic exposure	OATP, MRP2, MRP3 (human)	Slizgi et al., (in preparation)
	Gd-EOB-DTPA	Hepatobiliary diagnostic	↑ hepatic exposure	Mrp2 (rodent)	Tsuda et al., 2011
	Methotrexate	Chemotherapeutic	↑ liver and ↑ GI toxicity	ND (rodent)	Hardwick et al., 2014
	Pemetrexed	Chemotherapeutic	↑ systemic concentrations; ↓ biliary excretion	Mrp2 (rodent)	Dzierlenga et al., 2016
	Simvastatin	Cholesterol-lowering	↑ systemic concentrations	Oatp (rodent)	Clarke et al., 2014a
PBC/cirrhosis	Gd-EOB-DTPA	Hepatobiliary contrast agent	↓ hepatic signal intensity	OATP (human)	Takeyama et al., 2015

Abbreviations: data not available (-); hepatocellular carcinoma (HCC); hepatitis C virus (HCV); human immunodeficiency virus (HIV); immunohistochemistry (IHC); nonalcoholic steatohepatitis (NASH); primary biliary cholangitis (PBC)

Bile Acids and their Pathophysiological Role in Drug-Induced Liver Injury

Bile acids are a family of cholesterol-derived acidic steroids that function as emulsifying agents in the digestion and absorption of triglycerides and other complex lipids. Despite their well-known role in digestion/absorption, bile acids also act as signaling molecules and have been implicated in the etiology and pathogenesis of disease (Chiang et al., 2013). Hence, there is significant interest in understanding the role of bile acids in the pathophysiology of disease. This section will briefly review bile acids and their role in drug-induced liver injury (DILI), a liver pathology that is a focus of this dissertation.

Synthesis and Transport

Bile acids are amphipathic molecules consisting of four linked hydrocarbon rings with two or three hydroxyl groups and a terminal carboxyl group. Bile acid species are defined by their differences in side chain structure, stereochemistry of the six-member ring, and the position and stereochemistry of various hydroxyl groups; an excellent review of bile acid structure is provided by Monte et al. (2009). In humans, primary bile acids (i.e. cholic acid and chenodeoxycholic acid) are synthesized by the hydroxylation of cholesterol by P450 cholesterol 7alpha-hydroxylase (CYP7A1), a rate-limiting enzyme in bile acid synthesis, followed by hydroxylation by P450 sterol 12α-hydroxylase (CYP8B1) (Martin et al., 1993; Swell et al., 1981; Zhang et al., 2001). This synthetic pathway is known as the "classic" pathway and accounts for ~90% of total bile acid production (Ferdinandusse et al., 2006). The "alternative" pathway accounts for remaining bile acid synthesis and is initiated by P450 oxysterol 7α-hydroxylase (CYP27A1) in extrahepatic tissues (e.g. vascular endothelium) followed by hydroxylation by CYP7A1 in the liver (Norlin et al., 2007; Wu et al., 1999). Finally, bile acids are conjugated with taurine or glycine catalyzed by bile acid CoA:amino acid N-acyltransferase (Falany et al., 1994;

Scherstén et al., 1967); bile acids also can be conjugated with glucuronide or sulfate moieties, although to a less extent than amine conjugates. In total, over 16 enzymes have been identified in the conversion of cholesterol to various bile acid species (Russell et al., 2009).

Amidated bile acids are actively excreted from hepatocytes into the canalicular membrane by the bile salt export pump (BSEP) in an adenosine triphosphate (ATP)-dependent manner. Other canalicular transport proteins, such as the multidrug resistance-associated protein (MRP) 2 and the breast cancer resistance protein (BCRP), have been shown to transport glucuronide and sulfate-bile acid conjugates (Blazquez et al., 2007; Akita et al., 2001). Alternatively, bile acids can be transported into the systemic circulation by basolateral efflux transporters including organic solute transporter (OST)α and OSTβ, MRP3, and MRP4 (Trauner and Boyer et al., 2003). Following excretion into the bile canaliculus, bile acids are stored in the gallbladder prior to secretion into the duodenum through the sphincter of Oddi. Although less recognized, cholangiocytes, epithelial cells lining the bile duct, are also capable of transporting bile acids. For example, the organic anion-transporting polypeptide (OATP) 1A2 is located on the apical membrane of cholangiocytes (Lee et al., 2005). Various OATP1A2 substrates including bile acids (e.g. taurocholic acid), steroid conjugates, and xenobiotics have been identified (Franke et al., 2009). The sodium-dependent bile acid transporter (ASBT) is another apical transporter capable of translocating bile acids from the canalicular space into cholangiocytes (Alpini et al., 1997; Alpini et al., 2001). Basolateral transporter expression (i.e. OSTα/OSTβ, MRP2, and MRP3) has been reported in cholangiocytes and these transporters are thought to play a role in the cholehepatic shunt pathway under pathophysiological conditions (Pauli-Magnus et al., 2006). For example, ASBT is induced in response to chronic cholestasis,

which is hypothesized to enhance biliary lipid secretion and choleresis (Alpini et al., 2001; Alpini et al., 2005).

Following gallbladder contraction by cholecystokinin and subsequent release into the intestinal tract, bile acids are efficiently reabsorbed in the terminal ileum by ASBT and OSTα/OSTβ (Balakrishnan et al., 2006; Ballatori et al., 2005; Dawson et al., 2005; Shneider et al., 1995; Wong et al., 1994). It is estimated that 95% of bile acids are reabsorbed by the intestine and returned to the portal vein for active hepatic uptake by Na^+-taurocholate cotransporting polypeptide (NTCP) and OATPs (e.g. OATP1B1 and OATP1B3), thus completing the enterohepatic recirculation of bile acids. It must be noted that bile acids undergo extensive modification in the intestinal tract mediated by bacterial and host enzymatic processes. Bacterial enzymes deconjugate/dehydroxylate bile acids back to their primary bile acid form, which can facilitate passive diffusion across the plasma membrane of enterocytes, although intestinal transporters readily transport bile acids as well. For example, bacterial 7α-dehydroxylase converts cholic acid to dehydroxycholic acid by the removal of hydrogen at the C7 position (Bokkenheuser et al., 1969). Hydrolysis and dehydroxylation reactions are mediated by a board spectrum of anaerobic bacterial and are not detailed here. An extensive review of intestinal bile acid metabolism is provided by Ridlon et al. (2006). Bile acids also can be metabolized by human cytochrome P450 enzymes; for example, CYP3A converts lithocholic acid to hyocholic acid and ursodeoxycholic acid (Bodin et al., 2005; Chang et al., 1993; Chen et al., 2014).

Bile Acids and Toxicity

Although bile acids have important physiological functions, they can be cytotoxic and induce and/or contribute to organ dysfunction. Obstructive cholestasis, for example, is a condition in which the flow of bile to the gallbladder is impaired, resulting in hepatocellular buildup of bile acids and subsequent hepatotoxicity. Supraphysiological concentrations of hydrophobic secondary bile acids, such as lithocholic acid, have been associated with the risk of colon cancer (Ajouz et al., 2014; Cook et al., 1940). The detergent effects of bile acids appear to be correlated with hydrophobicity. Attili et al. (1986) reported the rank order of toxicity from greatest to least: lithocholic acid > deoxycholic acid > chenodeoxycholic acid > cholic acid > ursodeoxycholic acid.

Bile acid-induced oxidative stress is a primary mechanism underlying bile acid toxicity (Sokol et al., 1991; Togashi et al., 1990). Due to their detergent like effects, it is suggested that bile acids directly impair mitochondrial respiration. Indeed, bile acids have been shown to enhance mitochondrial membrane permeability to protons, disrupt the structural integrity of mitochondrial components, and decrease enzymatic activity involved in the electron transport chain (Krähenbühl et al., 1994; Rolo et al., 2000). The generation of intracellular reactive oxygen species appears to be an early event in mitochondria-associated toxicity in rodents and humans (Soko et al., 1995; Soko et al., 2005). Subsequent depletion of antioxidants (e.g. glutathione) and constituents of the electron transport chain (e.g. ubiquinone-9 and ubiquinone-10) induce the mitochondrial permeability transition (MPT) leading to the initiation of apoptotic and necrotic pathways (Krähenbühl et al., 1995; Lemasters et al. 1998; Yerushalmi et al., 2001). More recent studies demonstrate that hydrophobic bile acids also can induce endoplasmic reticulum stress. For example, glycochenodeoxycholic acid induced the release of Ca^{2+} in rat hepatocytes and

subsequent activation of calpain and caspase-12, two signaling molecules involved in the initiation of apoptosis (Iizaka et al., 2007; Tsuchiya et al., 2006).

Bile Acid-Mediated Hepatotoxicity and Drug Administration

The administration of drugs can impair synthesis and excretory processes involved in bile acid homeostasis and increase hepatocellular concentrations of bile acids, which can lead to hepatotoxicity. Other mechanisms that induce and/or contribute to DILI are discussed in Chen et al. (2015). Insight into the specific mechanism(s) underlying altered bile acid homeostasis during drug therapy first implicated inhibition of canalicular bile acid transporters, and subsequent increase in hepatocellular bile acids, by drugs. For example, impaired biliary bile acid secretion in rodents was reported with drugs associated with DILI such as troglitazone, cyclosporine A, and bosentan (Bohme et al., 1993; Fattinger et al., 2001; Funk et al., 2001). Particular interest has focused on BSEP inhibition, the rate-limiting step in bile acid-dependent biliary clearance of bile acids. A systematic evaluation by Morgan et al. (2010) revealed an association with inhibition of BSEP by drugs and DILI; data from this study demonstrated that drugs with an inhibitory potency (IC_{50}) greater than 25 μM correlated with liver injury in humans. Subsequent studies indicated that inhibition of compensatory bile acid transporters (e.g. MRP2-4) increase the correlation between bile acid transporter inhibition and DILI (Köck et al., 2014; Morgan et al., 2013). Hence, high-throughput in vitro screening tools are used routinely in drug development to assess the potential for liver liabilities in humans. Other mechanisms involved in altered bile acid homeostasis that were not explored in this dissertation (e.g. impaired bile canaliculus dynamics, inhibition of bile acid metabolism, modulation of nuclear hormone receptors, altered phospholipid flux) have been demonstrated and are reviewed elsewhere (Burbank et al., 2016; He et al., 2015; Rodrigues et al. 2014).

Bile Acids as Biomarkers of DILI

Biochemical measures such as serum transaminases, alkaline phosphatase, gamma-glutamyl transferase, and total bilirubin remain the gold standard for the diagnosis of many liver diseases and the adjudication of DILI (Ozer et al., 2008; Watkins et al., 2009; Wolf et al. 1999). However, these measurements have limitations (e.g. lack specificity and/or sensitivity) and are sometimes difficult for clinicians to interpret (Knight et al., 2005; Thapa et al. 2007). Serum bile acids have been proposed as biomarkers of hepatobiliary disease including primary biliary cirrhosis, nonalcoholic and alcoholic steatohepatitis, intrahepatic cholestasis of pregnancy, and hepatitis C infection (Ferslew et al., 2015; Heikkinen et al. 1983; Murphy et al., 1972; Shlomai et al., 2013; Trinchet et al., 1994). Furthermore, signature patterns in the bile acid pool have been investigated to differentiate liver disease (Bathena et al., 2015; Ferslew et al., 2015; Kamano et al., 1999). For example, the ratio of cholic acid to chenodeoxycholic acid was significantly different in patients with compensated liver cirrhosis compared to patients with decompensated liver cirrhosis (Adachi et al., 1988). To date, serum bile acids are used for the clinical diagnosis of intrahepatic cholestasis of pregnancy (Huang et al., 2007; Pusl et al., 2007). Otherwise, bile acids are not used routinely in clinical practice to diagnose other hepatobiliary diseases, perhaps due to lack of specificity, interindividual variability, or difficulty in implementing bile acid profiling in routine clinical practice, among others reasons (Heaton et al., 1979; Steiner et al., 2011).

Recent research suggests that using serum bile acids to identify or diagnose DILI is promising. Yamazaki et al. (2013) first identified altered bile acid homeostasis as an early hepatotoxic signal after the administration of several hepatotoxins (e.g. acetaminophen, bendazac, cyclosporine A, carbamazepine) in rats. Serum glycocholate,

glycochenodeoxycholate, taurocholate, and taurochenodeoxycholate concentrations were consistently elevated in response to hepatotoxic drugs (Yamazaki et al., 2013). Another study by Luo et al. (2014) reported that animals with histopathological signs of hepatocellular necrosis displayed increases in serum cholic acid, glycholic acid, and taurocholic acid, whereas animals with signs of bile duct hyperplasia displayed increases in only the amidated conjugates of glycholic acid, and taurocholic acid; these data suggest that signature bile acid profiles may be able to differentiate different forms of DILI. Indeed, serum conjugated bile acid concentrations were higher in patients diagnosed with DILI (any form) compared to healthy controls (Luo et al., 2015); elevated bile acid concentrations also have been reported in cyclosporine A-associated liver injury (Beger et al., 2015). The Safer And Faster Evidence-based Translation (SAFE-T) Consortium is currently assessing the utility of serum bile acids, among others, as biomarkers of DILI, which may aid in the diagnosis and prognosis of DILI before irreversible and/or fatal injury occurs (Weiler et al., 2015).

Autosomal Dominant Polycystic Kidney Disease: Basic Biology and Protein Transporter Function

Polycystic kidney disease (PKD) is a common cause of renal failure due to the development of fluid-filled cysts and subsequent displacement/destruction of renal nephrons. PKD is genetically transmitted in a dominant form (autosomal dominant polycystic kidney disease; ADPKD) or in a recessive form (autosomal recessive polycystic kidney disease; ARPKD). ADPKD is slowly progressive whereas ARPKD is typically more severe. For example, newborns with ARPKD are often born with massively enlarged cysts, congenital hepatic fibrosis, and aberrant intrahepatic bile ducts (Zerres et al., 1998). Nearly one-half of affected newborns die shortly after birth, although children who are not symptomatic until later in life have a better prognosis (Deget et al., 1995; Zerres et al., 1996). This dissertation focused on ADPKD; a review of ARPKD is provided by Kaplan et al. (1988) and more recently, Hartung et al. (2014).

Genetics and Cell Biology

ADPKD arises from mutations in the PKD1 (~85% of cases) or PKD2 (~15% of cases) gene. Although the hepatorenal manifestations are similar between both mutations, symptomatic renal decline presents later in life and is associated with longer survival and less complications in patients with PKD2 mutations compared to patients with PKD1 mutations (Hateboer et al., 1999). PKD1 encodes polycystin-1, a large integral membrane protein expressed in the primary cilia of many tissues such as the kidney, heart, muscle, and liver (Geng et al., 1997; Ong et al., 1999; Zhou et al., 2009). Although the function of polycystin-1 is not fully understood, it has been proposed that polycystin-1 acts as cell surface signaling receptor that regulates intracellular

Ca^{2+} homoeostasis through the interaction with polycystin-2 (Dalagiorgou et al., 2010). Further studies indicate polycystin-1 behaves like a G protein-coupled receptor involved in regulating cell cycle arrest, presumably by the indirect inhibition of cyclin-dependent kinases, activators of cellular proliferation (Bhunia et al., 2002; Delmas et al., 2002; Hanaoka et al., 2000). PKD2 encodes polycystin-2, a Ca^{2+}-permeable cation channel that either localizes to the cilium, where it can interact with polycystin-1, or in intracellular compartments where it can modulate the release of intracellular Ca^{2+} (González-Perrett et al., 2001; Nauli et al., 2003).

Cystogenesis

The natural history of cystogenesis in ADPKD patients is variable and not well understood. Bae et al. (2013) reported that the number of identifiable kidney cysts can range from as low as 10 cysts to more than 200 cysts using magnetic resonance imaging. Although all cells within the kidney contain the same germline (i.e. inherited) mutation, only a small portion of these cells become cystic. To explain this apparent anomaly, Reeders (1992) proposed a two-hit hypothesis suggesting that a second "hit" to the wild-type PKD1 (or PKD2) allele is a prerequisite for focal cyst initiation and development, similar to the multi-hit hypotheses underlying the initiation of cancer cells. Indeed, germline and somatic mutations have been identified in patients with ADPKD (Qian et al., 1996; Watnick et al., 2000). Although mechanistic studies in mouse models of ADPKD support the hypothesis that somatic conversion is conceivable, recent studies indicate that gene dosage effects may help explain large interindividual variability in disease severity (Rossetti et al., 2009; Wu et al., 1998; Vujic et al., 2010). Gene dosage, or haploinsufficiency, refers to the concept that mutation(s) affect the expressivity of particular genes (i.e. the number of gene products cells can produce), which may

lead to interindividual variability in a clinical phenotype, such as seen in ADPKD. This concept is fully explored in Eccles and Staynder (2014).

Fluid Transport in ADPKD

Altered planar cell polarity and cyclic adenosine monophosphate (cAMP)-mediated cell proliferation is central to the macroscopic development of cysts (Grantham et al., 1987; Grantham, 1996). Furthermore, the accumulation of fluid within cysts suggests that cystic endothelium display unique ion-driven absorptive properties that results in subsequent osmotic movement of water into the cyst lumen. Investigation into the transport properties of cysts sparked interest when cysts were observed to rapidly refill after aspiration, although an early study by Jacobsson et al. (1977) was first to demonstrate the accumulation of water in cysts after the administration of $^{3}H\text{-}H_20$ (Bennett et al., 1987).

Current data suggest that ion transport into the cyst cavity is driven by two transporters: the cystic fibrosis transmembrane regulator (CFTR) and Na^+K^+-ATPase. CFTR is a Cl^- channel that facilitates the movement of Cl^- ions into cysts whereas Na^+K^+-ATPase is an antiporter that exchanges Na^+ for K^+, both of which are present at the apical surface of cystic epithelium (Nakanishi et al., 2001; Wilson et al., 1991). Interestingly, the severity of ADPKD was diminished in patients with coexisting cystic fibrosis, a genetic disease in which patients lack functional CFTR (Xu et al., 2006). Elevated concentrations of cAMP appear to drive secretory processes associated with cystogenesis, which may be secondary to altered Ca^{2+} homeostasis and/or upregulation of vasopressin receptor(s) due to disruption of polycystin-1 binding to heterotrimeric G proteins (Gattone et al., 2003; Parnell et al., 1998; Wang et al., 2010). Indeed, cAMP is consistently elevated in both animal models of PKD and in patients with ADPKD

(Devuyst et al., 2013; Nagao et al., 2006; Starremans et al., 2008; Yamaguchi et al., 1997). Therapeutic strategies targeting fluid accumulation (e.g. vasopressin receptor antagonists, somatostatin receptor agonists) have been evaluated or are currently under investigation, although the long term efficacy and safety of successfully blocking fluid accumulation in cysts is unknown at this time.

Hepatic cysts

The liver is the most commonly affected extrarenal organ in ADPKD. Hogan et al. (2015) reported that ~70% of men and ~80% of women (age 15-49 years old) have detectable liver cysts using magnetic resonance imaging. The observation that hepatic cyst burden (i.e. number of cysts and cystic volume) is increased in women compared to men is consistent among studies (Bae et al., 2006; Chauvea et al. 2000; Levine et al., 1985; Hogan et al. 2015). The underlying mechanism appears to be related to the stimulatory effects of hormones (e.g. estrogens) and subsequent epithelial hyperproliferation (Everson et al., 2005; Sherstha et al., 1997); hence, clinicians recommend avoiding hormonal therapy or hormone-containing oral contraceptive therapy when symptomatic liver cystic disease presents (Chapman et al., 2015; Sherstha et al., 1997).

Hepatic cysts derive from the biliary epithelium and thus display phenotypic and functional characteristics similar to cholangiocytes (Perrone et al., 1995). Similar to cell types of the kidney, cholangiocytes express polycystin-1 and polycystin-2; altered Ca^{2+} homeostasis due to genetic mutation(s) increases adenylyl cyclase6 activity and cAMP levels (Masyk et al., 2006). cAMP-mediated fluid transport appears to be driven by CFTR and subsequent generation of an osmotic gradient, which facilitates water entry into the lumen. Interestingly, aquaporins,

transmembrane proteins that mediate the passive movement of water across epithelial cells, are abnormally expressed in ADPKD (Banales et al., 2008; Li et al., 2016). Overexpression of aquaporin-1 correlated with the cyst size, which may indicate that aquaporin(s) contribute to fluid accumulation and cystogenesis (Li et al., 2016).

The polycystic kidney disease rat, a model of human ADPKD

The polycystic kidney (PCK) rat was discovered by Katsuyama et al. (2000). Further characterization by Lager et al., (2001), among others, have demonstrated that the PCK rat displays a natural history of hepatorenal features most similar to human ADPKD. PCK rat kidneys are normal at birth but progressively develop focal renal cysts that diminish renal function over time (Lager et al., 2001; Mason et al., 2010). Abnormal serum biochemistries (e.g. serum creatinine, proteinuria, blood urea nitrogen) are consistent with that seen in patients with ADPKD (Mason et al., 2010; Woon et al., 2015). PCK rats also develop hepatic cysts, which up until their discovery, had not been demonstrated in other rat models. For example, the Han:SPRD rat and chin rat models do not display progressive hepatic cyst development and even exhibit skeletal abnormalities, inconsistent with human ADPKD. (Gretz et al., 1996; Nauta et al., 1999; Ohno et al., 1989; Schäfer et al., 1994). Remodeling of the biliary epithelium and dilatation of the intrahepatic bile ducts contribute to the formation of isolated cysts that are disconnected from the biliary tree in PCK rats over time (Masyuk et al., 2004). Cholangiocyte cilia were also structurally abnormal and shorter compared to normal cholangiocytes, similar to reports in ADPKD (Alvaro et al., 2008; Masyuk et al., 2003; Masyuk et al., 2004). Hence, the similar hepatorenal phenotype observed in PCK rats has provided tremendous value towards understanding the pathogenesis of ADPKD and therapeutic interventions (Blazer-Yost et al., 2010; Wang et al., 2004; Wang et al., 2010). It must be noted that genetic analysis revealed

polycystic kidney disease in PCK rats is due to mutation(s) in the polycystic kidney and hepatic disease 1 (Pkhd1) gene, the rat orthologue of human PKHD1, and thus is genetically orthologous to human ARPKD (Ward et al., 2002). Therefore, genetic differences underlying the etiology of disease in PCK rats and human ADPKD may limit the extrapolation of information generated in this rodent model to humans.

Drug transporters in ADPKD

The effect of ADPKD on the expression and function of clinically relevant drug transporters, as those outlined in Chapter 1 of this dissertation, have not been investigated. Because ion transporter function, cellular proliferation, extracellular matrix remodeling, and neovascularization all play an important role in cyst growth, it is conceivable that drug transporters may be affected due to overlapping signaling processes that are altered in this disease state. For example, cAMP, the signaling molecule elevated in ADPKD, has been shown to influence the translocation of Mrp2 and Mrp3 in *in vitro* studies (Chandra et al., 2005; Park et al., 2014; Roelofsen et al., 1998).

Project Rationale and Specific Aims

The objective of this dissertation research was to understand how hepatic transporter function in liver disease affects the hepatobiliary disposition and pharmacokinetics of endogenous and exogenous compounds. In order to describe and predict the effect of liver disease on hepatobiliary disposition and pharmacokinetics, the expression and function of hepatic transporters in disease states must be better understood. This dissertation focused on two pathophysiological states of liver impairment: non-alcoholic steatohepatitis (NASH) and autosomal dominant polycystic kidney disease (ADPKD).

Non-alcoholic steatohepatitis (NASH)

NASH is an advanced inflammatory form of non-alcoholic fatty liver disease defined by histological confirmation of hepatic steatosis, hepatocyte ballooning, and lobular inflammation (Chalasani et al., 2012). NASH is a significant health concern, which can progress to advanced fibrosis/cirrhosis, hepatocellular carcinoma, and liver failure. Dysregulation of transporter expression has been reported in rodent models of NASH and in patients with NASH, as reviewed in the introductory section of this dissertation (Canet et al., 2015; Clarke et al., 2014; Ferslew et al., 2015; Hardwick et al., 2011). Specifically, hepatic uptake transporters (e.g. organic anion-transporting polypeptides (OATPs)) are down-regulated while excretory transporters are up-regulated (e.g. multidrug resistance protein (MRP) 3) in NASH. There are conflicting reports of altered MRP2 expression patterns in NASH that warrant further investigation. For example, Hardwick et al. (2011) reported that MRP2 protein expression was upregulated in patients with NASH but Okushin et al. (2015) observed downregulation of MRP2 mRNA expression in liver tissue. It must be noted that mRNA expression does not always correlate with protein expression,

so it is unclear how the findings from Okushin et al. (2015) translate to MRP2 protein expression, and more importantly to MRP2 function (Maier et al., 2009; Vogel et al., 2012). Furthermore, MRP2 appears mislocalized off the canalicular membrane, presumably internalized to intracellular vesicles in the subapical domain (Hardwick et al. 2011). Vesicular retrieval of Mrp2/MRP2 has been demonstrated in lipopolysaccharide-induced oxidative stress and in several forms of human liver injury such as autoimmune hepatitis, primary sclerosing cholangitis, and obstructive jaundice (Kojima et al., 2003; Kojima et al., 2008; Saeki et al., 2011). More recently, Dzierlenga et al. (2016) demonstrated that radixin and Rab11-mediated active insertion of Mrp2 is impaired in a rodent model of NASH, providing a mechanistic basis for these observations. Therefore, the objective of Aim #1 was to evaluate the pharmacokinetics of ^{99m}Tc-mebrofenin (MEB), an OATP, MRP2 and MRP3 substrate, in patients with biopsy-confirmed NASH compared to healthy volunteers. The evaluation of systemic pharmacokinetics, coupled with liver scintigraphy to assess hepatic exposure, provides a powerful approach to assess, for the first time, the functional effects of OATP, MRP2, and/or MRP3 modulation due to NASH.

MEB was selected as a phenotypic probe substrate to assess the effect of altered OATP, MRP2, and MRP3 function in patients with NASH compared to healthy volunteers. To date, quantitative scintigraphy and pharmacokinetic analysis of MEB have only been conducted in healthy volunteers (Ghibellini at al., 2008; Pfeifer et al., 2013a). In vitro studies indicate that MEB is a substrate for OATP1B1, OATP1B3, MRP2, and MRP3 (de Graaf et al., 2011; Ghibellini at al., 2008); OATP1B1-mediated intrinsic clearance (i.e. V_{max}/K_m) of MEB is ~1.5-fold higher compared to OATP1B3 and pharmacokinetic modeling indicated that MRP2-mediated excretion of MEB is ~3-4-fold greater compared to MRP3-mediated efflux (Ghibellini

at al., 2008; Pfeifer et al., 2013a). In humans, MEB is efficiently extracted by the liver (~98% of dose) and excreted into bile with minimal urinary excretion (~1-2% up to 24 hrs) and negligible metabolism (Krishnamurthy et al., 1990; Choletec package insert). Altered function of OATP- and MRP2-mediated transport would be expected to impact the systemic and hepatic exposure of MEB. Indeed, inhibition of OATP by ritonavir increased the systemic concentrations of MEB in healthy volunteers although hepatic exposure was unaffected by ritonavir because intracellular hepatic concentrations were below concentrations necessary to inhibit MRP2-mediated biliary excretion (Pfeifer et al., 2013a). Furthermore, increased hepatic exposure of MEB and other iminodiacetic acid analogs due to genetic impairment in Mrp2-deficient rats and patients with Dubin-Johnson syndrome is well established and supports the use of MEB as a phenotypic probe for MRP2 (Bhargava et al., 2009; Doo et al., 1991; Hendrikse et al., 2004; Pinós et al., 1990; Pinós et al., 1991). It must be noted that MRP3 also has been shown to transport MEB. MRP3-mediated clearance of MEB appears to be significantly lower compared to MRP2-mediated clearance, but increased MRP3 expression and/or function may impact systemic concentrations or liver exposure of MEB (Ghibellini et al., 2008; Pfeifer et al., 2013a). To date, altered function of MRP3-mediated transport has been demonstrated in patients with NASH. Ferslew et al. (2015) reported increased serum concentrations of morphine glucuronide, an MRP3 substrate, in patients with NASH; similarly, Canet et al. (2015) also demonstrated that acetaminophen glucuronide serum concentrations, another MRP3 substrate, were increased in pediatric patients with NASH.

Although systemic concentrations are routinely measured to estimate drug exposure, it has become increasingly evident that drug exposure in a particular compartment or tissue may be altered without significantly affecting systemic concentrations (Rose et al., 2014; Swift et al.,

2009). Gamma scintigraphy is a powerful imaging technique that enables the direct visualization of a radiolabeled molecule in real time. Apart from their routine use as diagnostic agents, gamma emitting radionuclides have been used for drug development purposes (e.g. capsule disintegration, drug disposition) (Damle et al., 2002; Fischman et al., 2002; Newman et al., 1995). Therefore, administration of MEB, coupled with gamma scintigraphy, provides a noninvasive method to quantify tissue exposure (i.e. liver exposure) in vivo. This approach allows for simultaneous evaluation of blood and liver pharmacokinetics; this will improve the elucidation of the functional consequences of NASH-associated changes in transporter function compared to the use of blood sampling alone.

Autosomal dominant polycystic kidney disease (ADPKD)

ADPKD is a monogenic inheritable disease characterized by progressive renal cyst development, often leading to end-stage renal disease. Supportive care and surgical interventions represent the mainstay of ADPKD treatment because no Food and Drug Administration (FDA)-approved therapy currently exists. Tolvaptan, an orally available vasopressin V_2-receptor antagonist, recently has shown promise for delaying renal cyst progression in ADPKD (Torres et al., 2012). In the pivotal clinical trial, however, tolvaptan was associated with liver injury evident by increased liver enzymes and bilirubin in some patients (Torres et al., 2012; Watkins et al., 2015). The etiology of liver injury in this patient population, to date, is unknown. Furthermore, it is also unclear whether DILI observed in ADPKD patients is due to the parent compound, a metabolite of tolvaptan (e.g. DM-4103 or DM-4107), or some other specie(s). Bile acid-mediated hepatotoxicity is one mechanism of drug-induced liver injury (DILI). Although bile acids are important in digestion/absorption and normal hepatic function, they can be hepatotoxic when present at high concentrations due to drug- and/or patient-specific mechanism(s). Therefore, **Aim**

#2 of this dissertation was designed to test the hypothesis that altered bile acid homeostasis is an underlying mechanism in tolvaptan-associated liver injury in patients with ADPKD.

DILI is one of the most frequent adverse events that can lead to market withdrawal, additional labeling requirements, or failure during clinical development (Senior et al., 2014). Although many mechanisms have been implicated in the pathogenesis and development of DILI (e.g. reactive metabolites, mitochondrial toxicity, adaptive and innate immunity), bile acids can accumulate and induce cholestasis and/or liver injury in humans (Rodrigues et al., 2016; Yang et al., 2013). The bile salt export pump (BSEP) plays a major role in the biliary clearance of bile acids. Thus, inhibition of BSEP by drugs and/or metabolites, which may lead to subsequent accumulation of bile acids, has been associated with DILI (Morgan et al., 2010). In addition to the inhibition of BSEP, inhibition of other bile acid transporters (e.g. MRP2-4) correlated with evidence of DILI in humans (Morgan et al., 2013). Therefore, inhibition of bile acid transporters by tolvaptan and two major metabolites (i.e. DM-4103 and DM-4107) was evaluated in **Subaim #2a**, which may help elucidate the biological etiology of tolvaptan-associated liver injury.

To examine the effect of tolvaptan and metabolites on the transport of bile acids, in vitro systems were employed. Membrane vesicles or transfected cell lines that overexpress a transporter of interest are widely used to characterize the kinetics (e.g. Michaelis-Menten constant, maximal transport velocity) of substrate transport in vitro. To study the kinetics of efflux transporters (e.g. BSEP), inside-out membrane vesicles are prepared to orient the adenosine triphosphate (ATP) binding site of the transporter to the buffer, which facilitates the uptake of substrate(s) into vesicles (Vogel et al., 2013). This assay allows the direct measurement of transporter-mediated translocation of a substrate across the cell membrane in a high-throughput fashion and is a commonly used approach to detect drug-drug or drug-bile acid

interactions (Giacomini et al., 2010; Vogel et al., 2013). Therefore, this model system was used in **Subaim #2a** to evaluate the effect of tolvaptan, DM-4103, and DM-4107 on human bile acid transporter function. Although transporter-overexpressing systems are convenient in vitro tools, human hepatocytes are the most physiologically-relevant cell-based model to study hepatic drug transport. Sandwich-cultured human hepatocytes (SCHH) are useful to study drug disposition and hepatotoxicity due to the preservation of cellular architecture and relevant metabolism and transporter genes (Marion et al., 2007; Swift et al., 2010). Therefore, SCHH were used as a secondary model system to evaluate the disposition of tolvaptan and the effect of tolvaptan on bile acid disposition in **Subaim #2a**.

Interestingly, no hepatic events were observed in tolvaptan-treated patients with hyponatremia, heart failure, or cirrhosis, which may indicate that ADPKD patients may be particularly susceptible to liver injury (Watkins et al., 2015). It is possible that impaired transporter function and bile acid homeostasis, independent of tolvaptan treatment, may predispose this patient population to hepatotoxicity. Indeed, literature reports indicate that bile acids are increased in DILI and may contribute to the pathogenesis of liver injury (James et al., 2015; Luo et al., 2014; Yamazaki et al., 2013). Altered bile acid homeostasis and hepatic transporter function in ADPKD have not been systematically evaluated to date, although Salam et al. (1989) reported prolonged hepatic retention of MEB, a MRP2 substrate, in a patient with ADPKD. To investigate bile acid homeostasis and hepatic transporter function in ADPKD, polycystic kidney (PCK) rats were selected as a surrogate model for studies outlined in **Subaim #2b and #2c**.

Several rodent models of polycystic kidney disease have been described; however, many of these rodent models do not display the progressive hallmarks and natural history of

hepatorenal abnormalities observed in human ADPKD (McDonald et al., 2006; Schieren et al., 1996). For example, the polycystic kidney disease (pcy) and polycystin 2 (pkd2) mouse model exhibits progressive enlargement of renal cysts, subsequent renal decline and early death, but display mild or no hepatic cyst involvement (Fry et al., 1985; Guay-Woodford et al., 2003; Woo et al., 1997). Other models are embryonic lethal (e.g. polycystin 1 mouse) or display skeletal and vascular defects (e.g. Oak Ridge polycystic kidney mutation) that are inconsistent with the human ADPKD phenotype (Boulter et al., 2001; Moyer et al., 1994). A spontaneous mutation in a colony of Sprague-Dawley rats displaying bilateral renal and hepatic cysts, now known as the PCK rat, was described by Katsuyama et al. (2000). Subsequent studies indicated that the natural progression and hepatorenal features in PCK rats, such as progressive renal cyst growth, biliary dysgenesis, and hepatic cyst development, most resemble human ADPKD (Hogan et al., 2015; Lager et al., 2001; Mason, et al. 2010; Masyuk et al., 2004). Therefore, the PCK rat model was selected to evaluate bile acid homeostasis and hepatic transporter function outlined in **Subaim #2b and #2c**.

To study hepatic transporter function in PCK rats in **Subaim #2c**, the isolated perfused liver model was selected. The isolated perfused rat liver is an ex vivo or in situ model widely used to investigate the physiology and function of the liver. Although hepatocyte cultures and liver slices are useful whole-cell models, the primary advantages of the isolated perfused rat liver are the retention of normal hepatic architecture, microcirculation, and bile production in a system that approaches normal physiology (Bessems et al., 2006). Additionally, the influence of extrahepatic mechanism(s) (e.g. hormonal influences, nonhepatic routes of elimination) is eliminated. The liver can be perfused in a nonrecirculating (single-pass) or recirculating manner (Brouwer and Thurman et al., 1996). Single-pass systems perfuse probe-containing buffer into

the liver that enables direct sampling of the outflow perfusate and bile to facilitate the calculation of hepatic extraction and biliary excretion, respectively. Furthermore, experimental protocols in which the steady-state hepatic extraction ratio is achieved and then switched to blank buffer (i.e. perfusate without the probe substrate) for additional sampling is an established experimental design to estimate basolateral efflux (Akita et al., 2001; Pfeifer et al., 2013b; Tian et al., 2008). Coupled with pharmacokinetic modeling, the isolated perfused rat liver model is a powerful tool to study hepatobiliary disposition and the multiplicity of transport in isolation (Chandra et al., 2005; Pfeifer et al., 2013b; Zamek-Gliszczynski et al., 2003). In addition, this model has been applied successfully to study the effect of chemical modulation and naturally occurring mutant strains (e.g., Mrp2-deficient rats) on transporter function (Chandra et al., 2005; Pfeifer et al., 2013b). Given the accompanying pathological changes that are expected in PCK rats (i.e. hepatic cysts), the isolated perfused liver model was chosen as a suitable model to test the effect of polycystic kidney disease on hepatic transporter function outlined in **Subaim #2c**. The fluorescent probe, 5(6)-carboxy-2',7'-dichlorofluorescein (CDF), was chosen as the phenotypic probe because: (1) it is a substrate for the hepatic uptake transporter Oatp1 and rapidly secreted into bile via Mrp2; (2) it is a fluorescent molecule and thus readily detectable using fluorescence spectroscopy; (3) the hepatobiliary disposition of CDF is well described (Chandra et al., 2005; Zamek-Gliszczynski et al., 2003). Additional review regarding the transport kinetics of CDF is provided in **Chapter 5**.

Summary

In summary, the first aim of this research project was to evaluate the pharmacokinetics of MEB in patients with biopsy-confirmed NASH compared to age- and sex-matched healthy volunteers (**Aim #1**). The second aim of this research project was to determine whether altered

bile acid homeostasis is a biologically plausible mechanism underlying tolvaptan-associated liver injury in patients with ADPKD (**Aim #2**).

Aim #1. Determine the functional consequences of hepatic transport modulation by non-alcoholic steatohepatitis (NASH) on the pharmacokinetics of ^{99m}Technetium-mebrofenin (MEB).

Hypothesis: NASH modulates the expression/function of OATP, MRP2 and/or MRP3 transport proteins responsible for drug disposition. Thus, NASH will affect the systemic and hepatic disposition of MEB.

1.a. Quantify MEB pharmacokinetics in patients with NASH versus healthy human volunteers.

Aim #2. Determine the inhibitory potency of tolvaptan and its metabolites on major efflux hepatic transporters; characterize the functional consequences of autosomal dominant polycystic disease (ADPKD) on bile acid homeostasis and hepatic transport function using polycystic kidney (PCK) rats.

Hypothesis: Altered bile acid homeostasis is a contributing mechanism underlying tolvaptan-associated liver injury in patients with ADPKD.

1.a. Determine the inhibitory potency of tolvaptan and its metabolites on hepatic bile acid transporters.

1.b. Characterize the consequences of ADPKD on bile acid homeostasis using PCK rats.

1.c. Characterize the functional consequences of ADPKD on hepatic transport function using the isolated-perfused rat liver model in PCK rats.

REFERENCES

Abe T, Unno M, Onogawa T, Tokui T, Kondo TN, Nakagomi R, Adachi H, Fujiwara K, Okabe M, Suzuki T, Nunoki K, Sato E, Kakyo M, Nishio T, Sugita J, Asano N, Tanemoto M, Seki M, Date F, Ono K, Kondo Y, Shiiba K, Suzuki M, Ohtani H, Shimosegawa T, Iinuma K, Nagura H, Ito S, Matsuno S. LST-2, a human liver-specific organic anion transporter, determines methotrexate sensitivity in gastrointestinal cancers. Gastroenterology. 2001 Jun;120(7):1689–99.

Adachi Y, Nanno T, Itoh T, Kurumi Y, Yamazaki K, Sawada Y, Yamamoto T. Determination of individual serum bile acids in chronic liver diseases: fasting levels and results of oral chenodeoxycholic acid tolerance test. Gastroenterol Jpn. 1988 Aug;23(4):401-7.

Aguilar-Olivos NE, Carrillo-Córdova D, Oria-Hernández J, Sánchez-Valle V, Ponciano-Rodríguez G, Ramírez-Jaramillo M, Chablé-Montero F, Chávez-Tapia NC, Uribe M, Méndez-Sánchez N. The nuclear receptor FXR, but not LXR, up-regulates bile acid transporter expression in non-alcoholic fatty liver disease. Ann Hepatol. 2015 Jul-Aug;14(4):487-93.

Ajouz H, Mukherji D, Shamseddine A. Secondary bile acids: an underrecognized cause of colon cancer. World J Surg Oncol. 2014 May 24;12:164.

Akita H, Suzuki H, Ito K, Kinoshita S, Sato N, Takikawa H, Sugiyama Y. Characterization of bile acid transport mediated by multidrug resistance associated protein 2 and bile salt export pump. Biochim Biophys Acta 2001; 1511: 7-16.

Akita H, Suzuki H, Sugiyama Y. Sinusoidal efflux of taurocholate is enhanced in Mrp2-deficient rat liver. Pharm Res. 200118:1119-25.

Ali R, Cusi K. New diagnostic and treatment approaches in non-alcoholic fatty liver disease (NAFLD). Ann Med. 2009 41(4):265-78.

Alpini G, Glaser S, Baiocchi L, Francis H, Xia X, Lesage G. Secretin activation of the apical Na+-dependent bile acid transporter is associated with cholehepatic shunting in rats. Hepatology. 2005 May;41(5):1037-45.

Alpini G, Glaser SS, Rodgers R. et al. Functional expression of the apical Na+-dependent bile acid transporter in large but not small rat cholangiocytes. Gastroenterology. 1997;113:1734–1740.

Alpini SG, Phinizy JL, Kanno N. et al. Regulation of cholangiocyte apical bile acid transporter (ABAT) activity by biliary bile acids: Different potential compensatory changes for intrahepatic and extrahepatic cholestasis. Gastroenterology. 2001;120:A6.

Alvaro, Onori P, Alpini G, Franchitto A, Jefferson DM, Torrice A, Cardinale V, Stefanelli F, Mancino MG, Strazzabosco M, Angelico M, Attili A, Gaudio E. Morphological and functional features of hepatic cyst epithelium in autosomal dominant polycystic kidney disease. Am J Pathol. 2008 Feb;172(2):321-32.

Amin ML. P-glycoprotein Inhibition for Optimal Drug Delivery. Drug Target Insights. 2013 Aug 19;7:27-34.

Appay V, Sauce D Immune activation and inflammation in HIV-1 infection: causes and consequences. J Pathol. 2008 214:231–241.

Attili AF, Angelico M, Cantafora A, Alvaro D, Capocaccia L. Bile acid-induced liver toxicity: relation to the hydrophobic-hydrophilic balance of bile acids. Med Hypotheses. 1986 Jan;19(1):57-69.

Badée J, Achour B, Rostami-Hodjegan A, Galetin A. Meta-analysis of expression of hepatic organic anion-transporting polypeptide (OATP) transporters in cellular systems relative to human liver tissue. Drug Metab Dispos. 2015 Apr;43(4):424-32.

Bae KT, Bumwoo P, Hongliang S, et al. Segmentation of Individual Renal Cysts from MR Images in Patients with Autosomal Dominant Polycystic Kidney Disease. Clin J Am Soc Nephrol. 2013 Jul 3; 8(7): 1089–1097.

Bae KT, Zhu F, Chapman AB, Torres VE, Grantham JJ, Guay-Woodford LM, Baumgarten DA, King BF Jr, Wetzel LH, Kenney PJ, Brummer ME, Bennett WM, Klahr S, Meyers CM, Zhang X, Thompson PA, Miller JP. Magnetic resonance imaging evaluation of hepatic cysts in early autosomal-dominant polycystic kidney disease: the Consortium for Radiologic Imaging Studies of Polycystic Kidney Disease cohort. Clin J Am Soc Nephrol. 2006 Jan;1(1):64-9.

Balakrishnan A, Polli J. Apical Sodium Dependent Bile Acid Transporter (ASBT, SLC10A2): A Potential Prodrug Target. Mol Pharm. 2006 May–Jun; 3(3): 223–230.

Ballatori N, Christian WV, Lee JY, Dawson PA, Soroka CJ, Boyer JL, Madejczyk MS, Li N. OSTalpha-OSTbeta: a major basolateral bile acid and steroid transporter in human intestinal, renal, and biliary epithelia. Hepatology. 2005 Dec;42(6):1270-9.

Banales JM, Masyuk TV, Bogert PS, Huang BQ, Gradilone SA, Lee SO, Stroope AJ, Masyuk AI, Medina JF, LaRusso NF. Hepatic cystogenesis is associated with abnormal expression and location of ion transporters and water channels in an animal model of autosomal recessive polycystic kidney disease. Am J Pathol. 2008 Dec;173(6):1637-46.

Bathena SP, Thakare R, Gautam N, Mukherjee S, Olivera M, Meza J, Alnouti Y. Urinary bile acids as biomarkers for liver diseases II. Signature profiles in patients. Toxicol Sci. 2015 Feb;143(2):308-18.

Bedogni G, Miglioli L, Masutti F, Tiribelli C, Marchesini G, Bellentani S. Prevalence of and risk factors for nonalcoholic fatty liver disease: the dionysos nutrition and liver study. Hepatology. 2005 42:44–52.

Bernstein H, Bernstein C, Payne CM, Dvorak K. Bile acids as endogenous etiologic agents in gastrointestinal cancer. World J Gastroenterol. 2009 Jul 21;15(27):3329–40.

Bleasby K, Castle JC, Roberts CJ, Cheng C, Bailey WJ, Sina JF, Kulkarni AV, Hafey MJ, Evers

R, Johnson JM, Ulrich RG, Slatter JG. Expression profiles of 50 xenobiotic transporter genes in humans and pre-clinical species: a resource for investigations into drug disposition. Xenobiotica. 2006 Oct-Nov;36(10-11):963-88.

Bonin S, Pascolo L, Crocé LS, Stanta G, Tiribelli C. Gene Expression of ABC Proteins in Hepatocellular Carcinoma, Perineoplastic Tissue, and Liver Diseases. Mol Med. 2002 8(6):318–25.

Borel F, Han R, Visser A, Petry H, van Deventer SJ, Jansen PL, Konstantinova P; Réseau Centre de Ressources Biologiques Foie (French Liver Biobanks Network), France. Adenosine triphosphate-binding cassette transporter genes up-regulation in untreated hepatocellular carcinoma is mediated by cellular microRNAs. Hepatology. 2012 Mar;55(3):821–32.

Borst P, Elferink RO. Mammalian ABC transporters in health and disease. Annu Rev Biochem. 2002;71:537-92.

Beger RD, Bhattacharyya S, Yang X, Gill PS, Schnackenberg LK, Sun J, James LP. Translational biomarkers of acetaminophen-induced acute liver injury. Arch Toxicol. 2015 Sep;89(9):1497-522.

Bennett WM, Elzinga L, Golper TA, Barry JM. Reduction of cyst volume for symptomatic management of autosomal dominant polycystic kidney disease. J Urol. 1987 Apr;137(4):620-2.

Bessems M, 't Hart NA, Tolba R, Doorschodt BM, Leuvenink HG, Ploeg RJ, Minor T, van Gulik TM. The isolated perfused rat liver: standardization of a time-honoured model. Lab Anim. 2006 Jul;40(3):236-46.

Bhargava KK, Joseph B, Ananthanarayanan M, Balasubramaniyan N, Tronco GG, Palestro CJ, Gupta S. Adenosine triphosphate-binding cassette subfamily C member 2 is the major transporter of the hepatobiliary imaging agent (99m)Tc-mebrofenin. J Nucl Med. 2009 Jul;50(7):1140-6.

Bhunia AK, Piontek K, Boletta A, Liu L, Qian F, Xu PN, Germino FJ, Germino GG: PKD1 induces p21waf1 and regulation of the cell cycle via direct activation of the JAK-STAT signaling pathway in a process requiring PKD2. Cell 109: 157–168, 2002

Blazer-Yost BL, Haydon J, Eggleston-Gulyas T, Chen JH, Wang X, Gattone V, Torres VE. Pioglitazone Attenuates Cystic Burden in the PCK Rodent Model of Polycystic Kidney Disease. PPAR Res. 2010; 2010:274376.

Blazquez AG, Briz O, Serrano MA, Marin JJG. Role of human breast cancer resistance protein (BCRP/ABCG2) in the canalicular transport of bile acid derivatives. Acta Physiol 2007; 190: 103.

Bodin K, Lindbom U, Diczfalusy U. Novel pathways of bile acid metabolism involving CYP3A4. Biochim Biophys Acta. 2005 Feb 21;1687(1-3):84-93.

Bohme M, Buchler M, Muller M, Keppler D. Differential inhibition by cyclosporins of primary-active ATP-dependent transporters in the hepatocyte canalicular membrane. FEBS Lett 1993;333:193-196.

Bokkenheuser V, Hoshita T, Mosbach EH. Bacterial 7-dehydroxylation of cholic acid and allocholic acid. J Lipid Res. 1969 Jul;10(4):421-6.

Boulter C, Mulroy S, Webb S, Fleming S, Brindle K, and Sandford R. Cardiovascular, skeletal, and renal defects in mice with a targeted disruption of the Pkd1 gene. Proc Natl Acad Sci USA 2001 98: 12174–12179.

Bourdet DL, Pritchard JB, Thakker DR. Differential substrate and inhibitory activities of ranitidine and famotidine toward human organic cation transporter 1 (hOCT1; SLC22A1), hOCT2 (SLC22A2), and hOCT3 (SLC22A3). J Pharmacol Exp Ther. 2005 Dec;315(3):1288-97.

Boyer JL, Trauner M, Mennone A, Soroka CJ, Cai SY, Moustafa T, Zollner G, Lee JY, Ballatori N. Upregulation of a basolateral FXR-dependent bile acid efflux transporter OSTalpha-OSTbeta in cholestasis in humans and rodents. Am J Physiol Gastrointest Liver Physiol. 2006 Jun;290(6):G1124–30.

Brazille P, Dereuddre-Bosquet N, Leport C, Clayette P, Boyer O, Vilde JL, Dormont D, Benveniste O. Decreases in plasma TNF-alpha level and IFN-gamma mRNA level in peripheral blood mononuclear cells (PBMC) and an increase in IL-2 mRNA level in PBMC are associated with effective highly active antiretroviral therapy in HIV-infected patients. Clin Exp Immunol. 2003 131(2):304-311.

Briz O, Serrano MA, Rebollo N, Hagenbuch B, Meier PJ, Koepsell H, Marin JJ. Carriers involved in targeting the cytostatic bile acid-cisplatin derivatives cis-diammine-chloro-cholylglycinate-platinum(II) and cis-diammine-bisursodeoxycholate-platinum(II) toward liver cells. Mol Pharmacol. 2002 Apr;61(4):853–60.

Büchler M, König J, Brom M, Kartenbeck J, Spring H, Horie T, Keppler D. cDNA cloning of the hepatocyte canalicular isoform of the multidrug resistance protein, cMrp, reveals a novel conjugate export pump deficient in hyperbilirubinemic mutant rats. J Biol Chem. 1996 Jun 21;271(25):15091-8.

Burckhardt G, Burckhardt BC. In vitro and in vivo evidence of the importance of organic anion transporters (OATs) in drug therapy. Handb Exp Pharmacol. 2011 201:29–104.

Buxhofer-Ausch V, Secky L, Wlcek K, Svoboda M, Kounnis V, Briasoulis E, Tzakos AG, Jaeger W, Thalhammer T. Tumor-specific expression of organic anion-transporting polypeptides: transporters as novel targets for cancer therapy. J Drug Deliv. 2013;2013:863539.

Byrne JA, Strautnieks SS, Mieli-Vergani G, Higgins CF, Linton KJ, Thompson RJ. The human bile salt export pump: characterization of substrate specificity and identification of inhibitors. Gastroenterology. 2002 Nov;123(5):1649-58.

Cai H, Zhang Y, Han TK, Everett RS, Thakker DR. Cation-selective transporters are critical to the AMPK-mediated antiproliferative effects of metformin in human breast cancer cells. Int J Cancer. 2016 May 1;138(9):2281-92.

Canet MJ, Hardwick RN, Lake AD, Dzierlenga AL, Clarke JD, Cherrington NJ. Modeling human nonalcoholic steatohepatitis-associated changes in drug transporter expression using experimental rodent models. Drug Metab Dispos. 2014 Apr;42(4):586-95.

Canet MJ, Merrell MD, Hardwick RN, Bataille AM, Campion SN, Ferreira DW, Xanthakos SA, Manautou JE, A-Kader HH, Erickson RP, Cherrington NJ. Altered Regulation of Hepatic Efflux Transporters Disrupts Acetaminophen Disposition in Pediatric Nonalcoholic Steatohepatitis. Drug Metab Dispos. 2015 June; 43(6): 829–835.

Canet MJ, Merrell MD, Hardwick RN, Bataille AM, Campion SN, Ferreira DW, Xanthakos SA, Manautou JE, A-Kader HH, Erickson RP, Cherrington NJ. Altered regulation of hepatic efflux transporters disrupts acetaminophen disposition in pediatric nonalcoholic steatohepatitis. Drug Metab Dispos. 2015 Jun;43(6):829-35.

Carlton VE, Harris BZ, Puffenberger EG, Batta AK, Knisely AS, Robinson DL, Strauss KA, Shneider BL, Lim WA, Salen G, Morton DH, Bull LN. Complex inheritance of familial hypercholanemia with associated mutations in TJP2 and BAAT. Nat Genet. 2003 May;34(1):91-6.

Chai J, He Y, Cai SY, Jiang Z, Wang H, Li Q, Chen L, Peng Z, He X, Wu X, Xiao T, Wang R, Boyer JL, Chen W. Elevated hepatic multidrug resistance-associated protein 3/ATP-binding cassette subfamily C 3 expression in human obstructive cholestasis is mediated through tumor necrosis factor alpha and c-Jun NH2-terminal kinase/stress-activated protein kinase-signaling pathway. Hepatology. 2012 May;55(5):1485-94.

Chai J, He Y, Cai SY, Jiang Z, Wang H, Li Q, Chen L, Peng Z, He X, Wu X, Xiao T, Wang R, Boyer JL, Chen W. Elevated hepatic multidrug resistance-associated protein 3/ATP-binding cassette subfamily C 3 expression in human obstructive cholestasis is mediated through tumor necrosis factor alpha and c-Jun NH2-terminal kinase/stress-activated protein kinase-signaling pathway. Hepatology. 2012 May;55(5):1485-94.

Chen HL, Liu YJ, Chen HL, Wu SH, Ni YH, Ho MC, Lai HS, Hsu WM, Hsu HY, Tseng HC, Jeng YM, Chang MH. Expression of hepatocyte transporters and nuclear receptors in children with early and late-stage biliary atresia. Pediatr Res. 2008 Jun;63(6):667-73.

Chen Y, Song X, Valanejad L, Vasilenko A, More V, Qiu X, Chen W, Lai Y, Slitt A, Stoner M, Yan B, Deng R. Bile salt export pump is dysregulated with altered farnesoid X receptor isoform expression in patients with hepatocellular carcinoma. Hepatology. 2013 Apr;57(4):1530–41.

Chen Y, Vasilenko A, Song X, Valanejad L, Verma R, You S, Yan B, Shiffka S, Hargreaves L, Nadolny C, Deng R. Estrogen and Estrogen Receptor-α-Mediated Transrepression of Bile Salt Export Pump. Mol Endocrinol. 2015 Apr;29(4):613-26.

Choi YH, Lee YK, Lee MG. Effects of 17α-ethynylestradiol-induced cholestasis on the pharmacokinetics of doxorubicin in rats: reduced biliary excretion and hepatic metabolism of doxorubicin. Xenobiotica. 2013 Oct;43(10):901-7.

Chou YY, Cheng AL, Hsu HC. Expression of P-glycoprotein and p53 in advanced hepatocellular carcinoma treated by single agent chemotherapy: clinical correlation. J Gastroenterol Hepatol. 1997 Aug;12(8):569–75.

Chu CJ, Lee SD. Hepatitis B virus/hepatitis C virus coinfection: epidemiology, clinical features, viral interactions and treatment. J Gastroenterol Hepatol. 2008 Apr;23(4):512-20.

Clarke JD, Hardwick RN, Lake AD, Canet MJ, Cherrington NJ.Experimental nonalcoholic steatohepatitis increases exposure to simvastatin hydroxy acid by decreasing hepatic organic anion transporting polypeptide expression. J Pharmacol Exp Ther. 2014 Mar;348(3):452-8.

Clarke JD, Hardwick RN, Lake AD, Lickteig AJ, Goedken MJ, Klaassen CD, Cherrington NJ4. Synergistic interaction between genetics and disease on pravastatin disposition. J Hepatol. 2014 Jul;61(1):139-47.

Clayton RJ, Iber FL, Ruebner BH, McKusick VA. Byler disease. Fatal familial intrahepatic cholestasis in an Amish kindred. Am J Dis Child. 1969 Jan;117(1):112-24.

Clément S, Pascarella S, Negro F. Hepatitis C virus infection: molecular pathways to steatosis, insulin resistance and oxidative stress. Viruses. 2009 Sep;1(2):126-43.

Congiu M, Mashford ML, Slavin JL, Desmond PV. Coordinate regulation of metabolic enzymes and transporters by nuclear transcription factors in human liver disease. J Gastroenterol Hepatol. 2009 Jun;24(6):1038-44.

Cordon-Cardo C, O'Brien JP, Boccia J, Casals D, Bertino JR, Melamed MR. Expression of the multidrug resistance gene product (P-glycoprotein) in human normal and tumor tissues. J Histochem Cytochem. 1990 Sep;38(9):1277-87.

Cropp CD, Komori T, Shima JE, Urban TJ, Yee SW, More SS, Giacomini KM. Organic anion transporter 2 (SLC22A7) is a facilitative transporter of cGMP. Mol Pharmacol. 2008 Apr;73(4):1151-8.

Cui Y, König J, Nies AT, Pfannschmidt M, Hergt M, Franke WW, Alt W, Moll R, Keppler D. Detection of the human organic anion transporters SLC21A6 (OATP2) and SLC21A8 (OATP8) in liver and hepatocellular carcinoma. Lab Invest. 2003 Apr;83(4):527–38.

De Rosa MF, Robillard KR, Kim CJ, Hoque MT, Kandel G, Kovacs C, Kaul R, and Bendayan R. Expression of membrane drug efflux transporters in the sigmoid colon of HIV-infected and uninfected men. J Clin Pharmacol. 2013 53:934–945.

Deeley RG, Cole SPC. Substrate recognition and transport by multidrug resistance protein 1

(ABCC1). FEBS Lett. 2006 580:1103–11.

Diao L, Li N, Brayman TG, Hotz KJ, Lai Y. Regulation of MRP2/ABCC2 and BSEP/ABCB11 expression in sandwich cultured human and rat hepatocytes exposed to inflammatory cytokines TNF-{alpha}, IL-6, and IL-1{beta}. J Biol Chem. 2010 285(41):31185-31192.

Dixit V, Hariparsad N, Li F, Desai P, Thummel K, Unadkat J. Cytochrome P450 enzymes and transporters induced by anti-human immunodeficiency virus protease inhibitors in human hepatocytes: implications for predicting clinical drug interactions. Drug Metab Dispos. 2007 35(10):1853-1859.

Donner MG, Keppler D. Up-regulation of basolateral multidrug resistance protein 3 (Mrp3) in cholestatic rat liver. Hepatology. 2001 Aug;34(2):351-9.

Brouwer KLR and Thurman RG. Isolated perfused liver. Pharm Biotechnol 1996 8:161–192.

Burbank MG, Burban A, Sharanek A, Weaver RJ, Guguen-Guillouzo C, Guillouzo A. Early alterations of bile canaliculi dynamics and the ROCK/MLCK pathway are characteristics of drug-induced intrahepatic cholestasis. Drug Metab Dispos. 2016 Aug 18.

Canet MJ, Merrell MD, Hardwick RN, Bataille AM, Campion SN, Ferreira DW, Xanthakos SA, Manautou JE, Hesham A-Kader H, Erickson RP, Cherrington NJ. Altered regulation of hepatic efflux transporters disrupts acetaminophen disposition in pediatric nonalcoholic steatohepatitis. Drug Metab Dispos. 2015 Jun;43(6):829-35.

Chalasani N, Younossi Z, Lavine JE, Diehl AM, Brunt EM, Cusi K, Charlton M, SanyalAJ; American Association for the Study of Liver Diseases; American College of Gastroenterology; American Gastroenterological Association. The diagnosis and management of non-alcoholic fatty liver disease: Practice guideline by the American Association for the Study of Liver Diseases, American College of Gastroenterology, and the American Gastroenterological Association. Am J Gastroenterol. 2012 Jun;107(6):811-26.

Chandra P, Johnson BM, Zhang P, Pollack GM, and Brouwer KLR. Modulation of hepatic canalicular or basolateral transport proteins alters hepatobiliary disposition of a model organic anion in the isolated perfused rat liver. Drug Metab Dispos. 2005 33:1238–1243

Chandra P, Zhang P, Brouwer KL. Short-term regulation of multidrug resistance-associated protein 3 in rat and human hepatocytes. Am J Physiol Gastrointest Liver Physiol. 2005 Jun;288(6):G1252-8.

Chang TK, Teixeira J, Gil G, Waxman DJ. The lithocholic acid 6 beta-hydroxylase cytochrome P-450, CYP 3A10, is an active catalyst of steroid-hormone 6 beta-hydroxylation. Biochem J. 1993 Apr 15;291 (Pt 2):429-33.

Chapman AB, Devuyst O, Eckardt KU, Gansevoort RT, Harris T, Horie S, Kasiske BL, Odland D, Pei Y, Perrone RD, Pirson Y, Schrier RW, Torra R, Torres VE, Watnick T, Wheeler DC; Conference Participants. Autosomal-dominant polycystic kidney disease (ADPKD): executive

summary from a Kidney Disease: Improving Global Outcomes (KDIGO) Controversies Conference. Kidney Int. 2015 Jul;88(1):17-27.

Chauveau D, Fakhouri F, Grünfeld JP.Liver Involvement in Autosomal-Dominant Polycystic Kidney Disease Therapeutic Dilemma. J Am Soc Nephrol. 2000 Sep;11(9):1767-75.

Chen J, Zhao KN, Chen C. The role of CYP3A4 in the biotransformation of bile acids and therapeutic implication for cholestasis. Ann Transl Med. 2014 Jan;2(1):7.

Chen M, Suzuki A, Borlak J, Andrade RJ, Lucena MI. Drug-induced liver injury: Interactions between drug properties and host factors. J Hepatol. 2015 Aug;63(2):503-14.

Chiang JY. Bile acid metabolism and signaling. Compr Physiol. 2013 Jul;3(3):1191-212.

Choletec® [package insert]. Bracco Diagnostics. Princeton, NJ; 2014.

Clark JD, Hardwick RN, Lake AD, Canet M, Cherrington NJ. Experimental Nonalcoholic Steatohepatitis Increases Exposure to Simvastatin Hydroxy Acid by Decreasing Hepatic Organic Anion Transporting Polypeptide Expression. J Pharmacol Exp Ther. 2014 Mar; 348(3): 452–458.

Cook JW, Kennaway EL, Kennaway NM. Production of tumors in mice by deoxycholic acid. Nature. 1940;145:627.

Dalagiorgou G, Basdra EK, Papavassiliou AG. Polycystin-1: function as a mechanosensor. Int J Biochem Cell Biol. 2010 Oct;42(10):1610-3.

Damle B, Ullah, Doll W, Wiley G, Knupp C. Pharmacokinetics and gamma scintigraphy evaluation of two enteric coated formulations of didanosine in healthy volunteers. Br J Clin Pharmacol. 2002 Sep;54(3):255-61.

Dawson PA, Hubbert M, Haywood J, Craddock AL, Zerangue N, Christian WV, Ballatori N. The heteromeric organic solute transporter alpha-beta, Ostalpha-Ostbeta, is an ileal basolateral bile acid transporter. J Biol Chem. 2005 Feb 25;280(8):6960-8.

de Graaf W, Häusler S, Heger M, van Ginhoven TM, van Cappellen G, Bennink RJ, Kullak-Ublick GA, Hesselmann R, van Gulik TM, Stieger B. Transporters involved in the hepatic uptake of (99m)Tc-mebrofenin and indocyanine green. J Hepatol. 2011 Apr;54(4):738-45.

Deget F, Rudnik-Schoneborn S, Zerres K: Course of autosomal recessive polycystic kidney disease (ARPKD) in siblings: A clinical comparison of 20 sibships. Clin Genet 47: 248–253, 1995.

Delmas P, Nomura H, Li X, Lakkis M, Luo Y, Segal Y, Fernandez-Fernandez JM, Harris PC, Frischauf AM, Brown DA, Zhou J: Constitutive activation of G-proteins by polycystin-1 is antagonized by polycystin-2. J Biol Chem 277: 11276–11283, 2002

Devuyst O, Torres VE. Osmoregulation, vasopressin, and cAMP signaling in autosomal dominant polycystic kidney disease. Curr Opin Nephrol Hypertens. 2013 Jul;22(4):459-70.

Donner MG, Keppler D.Up-regulation of basolateral multidrug resistance protein 3 (Mrp3) in cholestatic rat liver. Hepatology. 2001 Aug;34(2):351-9.

Doyle L, Ross DD. Multidrug resistance mediated by the breast cancer reistance protein BCRP (ABCG2). Oncogene. 2003 22, 7340-7358.

Doo E, Krishnamurthy GT, Eklem MJ, Gilbert S, Brown PH. Quantification of hepatobiliary function as an integral part of imaging with technetium-99m-mebrofenin in health and disease. J Nucl Med. 1991 Jan;32(1):48-57.

Dzierlenga AL, Clarke JD, Cherrington NJ. Nonalcoholic Steatohepatitis Modulates Membrane Protein Retrieval and Insertion Processes. Drug Metab Dispos. 2016 Nov;44(11):1799-1807.
Dzierlenga AL, Clarke JD, Klein DM, Anumol T, Snyder SA, Li HY, Cherrington N. Biliary Elimination of Pemetrexed is Dependent on Mrp2 in Rats: Potential Mechanism of Variable Response in Nonalcoholic Steatohepatitis. J Pharmacol Exp Ther. 2016 Aug;358(2):246-53.

Eccles MR and Staynder CA. Polycystic kidney disease – where gene dosage counts. F1000Prime Rep. 2014; 6: 24.

Elferink RP, Paulusma CC2. MRP2 in cholestasis: Putting down the anchor. J Hepatol. 2015 Dec;63(6):1309-10.

Emami Riedmaier A, Burk O, Eijck BA, Schaeffeler E, Klein K, Fehr S, Biskup S, Müller S, Winter S, Zanger UM, Schwab M, Nies AT. Variability in hepatic expression of organic anion transporter 7/SLC22A9, a novel pravastatin uptake transporter: impact of genetic and regulatory factors. Pharmacogenomics J. 2016 Aug;16(4):341-51.

Enomoto A, Takeda M, Shimoda M, Narikawa S, Kobayashi Y, Kobayashi Y, Yamamoto T, Sekine T, Cha SH, Niwa T, Endou H. Interaction of human organic anion transporters 2 and 4 with organic anion transport inhibitors. J Pharmacol Exp Ther. 2002 Jun;301(3):797-802.

Fahrmayr C, König J, Auge D, Mieth M, Fromm MF. Identification of drugs and drug metabolites as substrates of multidrug resistance protein 2 (MRP2) using triple-transfected MDCK-OATP1B1-UGT1A1-MRP2 cells. Br J Pharmacol. 2012 Mar;165(6):1836-47.

FDA Guidance: Guidance for Industry. Drug Interaction Studies — Study Design, Data Analysis, Implications for Dosing, and Labeling Recommendations. 2012, http://www.fda.gov/downloads/Drugs/GuidanceComplianceRegulatoryInformation/Guidances/UCM193282.pdf.

Ferslew BC, Johnston CK, Tsakalozou E, Bridges AS, Paine MF, Jia W, Stewart PW, Barritt AS 4th, Brouwer KL. Altered morphine glucuronide and bile acid disposition in patients with nonalcoholic steatohepatitis. Clin Pharmacol Ther. 2015a Apr;97(4):419-27.

Ferslew BC, Xie G, Johnston CK, Su M, Stewart PW, Jia W, Brouwer KL, Sidney Barritt A 4th. Altered Bile Acid Metabolome in Patients with Nonalcoholic Steatohepatitis. Dig Dis Sci. 2015b Nov;60(11):3318-28.

Fisher CD, Lickteig AJ, Augustine LM, Oude Elferink RP, Besselsen DG, Erickson RP,

Cherrington NJ. Experimental non-alcoholic fatty liver disease results in decreased hepatic uptake transporter expression and function in rats. Eur J Pharmacol. 2009 Jun 24;613(1-3):119-27

Foisy M, Yakiwchuk E, Hughes C. Induction effects of ritonavir: implications for drug interactions. Ann Pharmacother. 2008 42(7):1048-1059.

Gadaleta RM, van Mil SWC, Oldenburg B, Siersema PD, Klomp LWJ, van Erpecum KJ. Bile acids and their nuclear receptor FXR: Relevance for hepatobiliary and gastrointestinal disease. Biochim Biophys Acta. 2010 Jul;1801(7):683–92.

Everson GT, Taylor MR. Management of polycystic liver disease. Curr Gastroenterol Rep. 2005;7:19–25.

Falany CN, Johnson MR, Barnes S, Diasio RB. Glycine and taurine conjugation of bile acids by a single enzyme. Molecular cloning and expression of human liver bile acid CoA:amino acid N-acyltransferase. J Biol Chem. 1994 Jul 29;269(30):19375-9.

Fattinger K, Funk C, Pantze M, Weber C, Reichen J, Stieger B, Meier PJ. The endothelin antagonist bosentan inhibits the canalicular bile salt export pump: a potential mechanism for hepatic adverse reactions. Clin Pharmacol Ther. 2001 Apr;69(4):223-31.

Ferdinandusse S, Houten SM. Peroxisomes and bile acid synthesis. Biochim et Biophys Acta. 2006;1763:1427–1440.

Ferslew BC, Johnston CK, Tsakalozou E, Bridges AS, Paine MF, Jia W, Stewart PW, Barritt AS 4th, Brouwer KL. Altered morphine glucuronide and bile acid disposition in patients with nonalcoholic steatohepatitis. Clin Pharmacol Ther. 2015 Apr;97(4):419-27.

Ferslew BC, Xie G, Johnston CK, Su M, Stewart PW, Jia W, Brouwer KL, Barritt AS. Altered Bile Acid Metabolome in Patients with Nonalcoholic Steatohepatitis. Dig Dis Sci. 2015 Nov;60(11):3318-28.

Fischman AJ, Alpert NM, Rubin RH. Pharmacokinetic imaging: a noninvasive method for determining drug distribution and action. Clin Pharmacokinet. 2002;41(8):581-602.

Franke RM, Scherkenbach LA, Sparreboom A. Pharmacogenetics of the organic anion transporting polypeptide 1A2. Pharmacogenomics. 2009 Mar;10(3):339-44.

Fry J, Koch W, Jennette J, McFarland E, Fried F, Mandell J. A genetically determined murine model of infantile polycystic kidney disease. J Urol. 1985;134:828–833.

Funk C, Ponelle C, Scheuermann G, Pantze M. Cholestatic potential of troglitazone as a possible factor contributing to troglitazone-induced hepatotoxicity: in vivo and in vitro interaction at the canalicular bile salt export pump (Bsep) in the rat. Mol Pharmacol 2001;59:627-635.

Gattone VH, Wang X, Harris PC, Torres VE. Inhibition of renal cystic disease development and progression by a vasopressin V2 receptor antagonist. Nat Med. 2003; 9:1323–1326.

Geier A, Dietrich CG, Gerloff T, Haendly J, Kullak-Ublick GA, Stieger B, Meier PJ, Matern S, Gartung C. Regulation of basolateral organic anion transporters in ethinylestradiol-induced cholestasis in the rat. Biochim Biophys Acta. 2003 1609(1): 87–94.

Geng L, Segal Y, Pavlova A, Barros EJ, Lohning C, Lu W, Nigam SK, Frischauf AM, Reeders ST, Zhou J: Distribution and developmentally regulated expression of murine polycystin. Am J Physiol 272: F451–F459, 1997.

Gerloff T, Stieger B, Hagenbuch B, Madon J, Landmann L, Roth J, Hofmann AF, Meier PJ. The sister of P-glycoprotein represents the canalicular bile salt export pump of mammalian liver. J Biol Chem .1998 273:10046–10050.

Ghibellini G, Leslie EM, Pollack GM, Brouwer KL. Use of tc-99m mebrofenin as a clinical probe to assess altered hepatobiliary transport: integration of in vitro, pharmacokinetic modeling, and simulation studies. Pharm Res. 2008 Aug;25(8):1851-60.

Ghoneim RH, Piquette-Miller M. Endotoxin-Mediated Downregulation of Hepatic Drug Transporters in HIV-1 Transgenic Rats. Drug Metab Dispos. 2016 May;44(5):709-19.

Giacomini KM, Huang SM, Tweedie DJ, Benet LZ, Brouwer KL, Chu X, Dahlin A, Evers R, Fischer V, Hillgren KM, Hoffmaster KA, Ishikawa T, Keppler D, Kim RB, Lee CA, Niemi M, Polli JW, Sugiyama Y, Swaan PW, Ware JA, Wright SH, Yee SW, Zamek-Gliszczynski MJ, Zhang L. Membrane transporters in drug development. Nat Rev Drug Discov. 2010 Mar;9(3):215-36.

Giacomini KM, Huang SM, Tweedie DJ, Benet LZ, Brouwer KL, Chu X, Dahlin A, Evers R, Fischer V, Hillgren KM, Hoffmaster KA, Ishikawa T, Keppler D, Kim RB, Lee CA, Niemi M, Polli JW, Sugiyama Y, Swaan PW, Ware JA, Wright SH, Yee SW, Zamek-Gliszczynski MJ, Zhang L. Membrane transporters in drug development. Nat Rev Drug Discov. 2010 Mar;9(3):215-36.

González-Perrett S, Kim K, Ibarra C, Damiano AE, Zotta E, Batelli M, Harris PC, Reisin IL, Arnaout MA, Cantiello HF. Polycystin-2, the protein mutated in autosomal dominant polycystic kidney disease (ADPKD), is a Ca2+-permeable nonselective cation channel. Proc Natl Acad Sci U S A. 2001 Jan 30;98(3):1182-7.

Gower E, Estes C, Blach S, Razavi-Shearer K, Razavi H. Global epidemiology and genotype distribution of the hepatitis C virus infection. J Hepatol. 2014 Nov;61(1 Suppl):S45-57.

Gradhand U, Lang T, Schaeffeler E, Glaeser H, Tegude H, Klein K, Fritz P, Jedlitschky G, Kroemer HK, Bachmakov I, Anwald B, Kerb R, Zanger UM, Eichelbaum M, Schwab M, Fromm MF.Variability in human hepatic MRP4 expression: influence of cholestasis and genotype. Pharmacogenomics J. 2008 Feb;8(1):42-52.

Grantham JJ, Geiser JL, Evan AP. Cyst formation and growth in autosomal dominant polycystic kidney disease. Kidney Int. 1987 May;31(5):1145-52.

Grantham JJ. The etiology, pathogenesis, and treatment of autosomal dominant polycystic kidney disease: recent advances. Am J Kidney Dis. 1996 Dec;28(6):788-803.

Gretz N, Kränzlin B, Pey R, Schieren G, Bach J, Obermüller N, Ceccherini I, Klöting I, Rohmeiss P, Bachmann S, Hafner M. Rat models of autosomal dominant polycystic kidney disease. Nephrol Dial Transplant. 1996;11 Suppl 6:46-51.

Grundemann D, Gorboulev V, Gambaryan S, Veyhl M, and Koepsell H. Drug excretion mediated by a new prototype of polyspecific transporter. Nature. 1994 Dec 8;372(6506):549-52.

Guay-Woodford LM. Murine models of polycystic kidney disease: molecular and therapeutic insights. Am J Physiol. 2003;285:F1034–F1049.

Hagenbuch B, Meier PJ. Molecular cloning, chromosomal localization, and functional characterization of a human liver Na+/bile acid cotransporter. J Clin Invest. 1994 Mar;93(3):1326-31.

Hagenbuch B, Meier PJ. Sinusoidal (basolateral) bile salt uptake systems of hepatocytes. Semin Liver Dis. 1996 May;16(2):129-36.

Hagenbuchand B, Gui C. Xenobiotic transporters of the human organic anion transporting polypeptides (OATP) family. Xenobiotica. 2008 38: 778-801.

Hamada A, Sissung T, Price DK, Danesi R, Chau CH, Sharifi N, Venzon D, Maeda K, Nagao K, Sparreboom A, Mitsuya H, Dahut WL, Figg WD. Effect of SLCO1B3 haplotype on testosterone transport and clinical outcome in caucasian patients with androgen-independent prostatic cancer. Clin Cancer Res. 2008 Jun 1;14(11):3312–8.

Han TK, Proctor WR, Costales CL, Cai H, Everett RS, Thakker DR. Four cation-selective transporters contribute to apical uptake and accumulation of metformin in Caco-2 cell monolayers. J Pharmacol Exp Ther. 2015 Mar;352(3):519-28.

Hanada K, Nakai K, Tanaka H, Suzuki F, Kumada H, Ohno Y, Ozawa S, Ogata H. Effect of nuclear receptor downregulation on hepatic expression of cytochrome P450 and transporters in chronic hepatitis C in association with fibrosis development. Drug Metab Pharmacokinet. 2012;27(3):301-6.

Hanaoka K, Qian F, Boletta A, Bhunia AK, Piontek K, Tsiokas L, Sukhatme VP, Guggino WB, Germino GG. Co-assembly of polycystin-1 and -2 produces unique cation-permeable currents. Nature. 2000 Dec 21-28;408(6815):990-4.

Hardwick RN, Clarke JD, Lake AD, Canet MJ, Anumol T, Street SM, Merrell MD, Goedken MJ, Snyder SA, Cherrington NJ. Increased susceptibility to methotrexate-induced toxicity in nonalcoholic steatohepatitis. Toxicol Sci. 2014 Nov;142(1):45-55.
Hardwick RN, Fisher CD, Canet MJ, Scheffer GL, Cherrington NJ. Variations in ATP-binding cassette transporter regulation during the progression of human nonalcoholic fatty liver disease. Drug Metab Dispos. 2011 Dec;39(12):2395-402.

Harrison LI, Gibaldi M. Influence of cholestasis on drug elimination: pharmacokinetics. J Pharm Sci. 1976 Sep;65(9):1346-8.

Hartung EA, Guay-Woodford LM. Autosomal recessive polycystic kidney disease: a hepatorenal fibrocystic disorder with pleiotropic effects. Pediatrics. 2014 Sep;134(3):e833-45.

Hasegawa Y, Kishimoto S, Takahashi H, Inotsume N, Takeuchi Y, Fukushima S. Altered expression of MRP2, MRP3 and UGT2B1 in the liver affects the disposition of morphine and its glucuronide conjugate in a rat model of cholestasis. J Pharm Pharmacol. 2009 Sep;61(9):1205-10.

Hateboer N, v Dijk MA, Bogdanova N, Coto E, Saggar-Malik AK, San Millan JL, Torra R, Breuning M, Ravine D: Comparison of phenotypes of polycystic kidney disease types 1 and 2. Lancet 353: 103–107, 1999.

He K, Cai L, Shi Q, Liu H, Woolf TF. Inhibition of MDR3 Activity in Human Hepatocytes by Drugs Associated with Liver Injury. Chem Res Toxicol. 2015 Oct 19;28(10):1987-90.

He XJ, Wang WR, Zhang Y, Yang Q. The effect of radixin knockdown on the expression and efflux function of MRP2 in SGC-7901 cells. Eur J Pharm Sci. 2012 Aug 15;46(5):426-34.

Heise M, Lautem A, Knapstein J, Schattenberg JM, Hoppe-Lotichius M, Foltys D, Weiler N, Zimmermann A, Schad A, Gründemann D, Otto G, Galle PR, Schuchmann M, Zimmermann T. Downregulation of organic cation transporters OCT1 (SLC22A1) and OCT3 (SLC22A3) in human hepatocellular carcinoma and their prognostic significance. BMC Cancer. 2012 12:109.

Heaton K. Bile salt tests in clinical practice. Br Med J. 1979 Mar 10; 1(6164): 644–646.

Heikkinen J. Serum bile acids in the early diagnosis of intrahepatic cholestasis of pregnancy. Obstet Gynecol. 1983 May;61(5):581-87.

Hendrikse NH, Kuipers F, Meijer C, Havinga R, Bijleveld CM, van der Graaf WT, Vaalburg W, de Vries EG. In vivo imaging of hepatobiliary transport function mediated by multidrug resistance associated protein and P-glycoprotein. Cancer Chemother Pharmacol. 2004 Aug;54(2):131-8.

Hirano M, Maeda K, Hayashi H, Kusuhara H, Sugiyama Y. Bile salt export pump (BSEP/ ABCB11) can transport a nonbile acid substrate, pravastatin. J Pharmacol Exp Ther. 2005 314:876–88.

Hirohashi T, Suzuki H, Takikawa H, Sugiyama Y. ATP-dependent transport of bile salts by rat multidrug resistance-associated protein 3 (Mrp3). J Biol Chem. 2000 Jan 28;275(4):2905-10.

Ho RH, Tirona RG, Leake BF, Glaeser H, Lee W, Lemke CJ, Wang Y, Kim RB. Drug and bile acid transporters in rosuvastatin hepatic uptake: function, expression, and pharmacogenetics. Gastroenterology. 2006 130:1793–1806.

Jacquemin E. Progressive familial intrahepatic cholestasis. Clin Res Hepatol Gastroenterol. 2012

Sep;36 Suppl 1:S26-35.

Jansen PLM. Endogenous bile acids as carcinogens. J Hepatol. 2007;47(3):434–5.

Jemnitz K, Heredi-Szabo K, Janossy J, Ioja E, Vereczkey L, Krajcsi P. 2010. ABCC2/Abcc2: a multispecific transporter with dominant excretory functions. Drug Metab Rev 42:402-36.

Jin HE, Hong SS, Choi MK, Maeng HJ, Kim DD, Chung SJ, Shim CK. Reduced antidiabetic effect of metformin and down-regulation of hepatic Oct1 in rats with ethynylestradiol-induced cholestasis. Pharm Res. 2009 Mar;26(3):549-59.

Jorajuria S, Dereuddre-Bosquet N, Naissant-Storck K, Dormont D, Clayette P. Differential Expression Levels of MRP1, MRP4, and MRP5 in Response to Human Immunodeficiency Virus Infection in Human Macrophages. Antimicrob Agents Chemother. 2004 May;48(5):1889-91.

Kalliokoski A and Niemi M. Impact of OATP transporters on pharmacokinetics. Br J Pharmacol. 2009 Oct; 158(3): 693–705.

Kawabata S, Oka M, Shiozawa K, Tsukamoto K, Nakatomi K, Soda H, Fukuda M, Ikegami Y, Sugahara K, Yamada Y, Kamihira S, Doyle LA, Ross DD, Kohno S. Breast cancer resistance protein directly confers SN-38 resistance of lung cancer cells. Biochem Biophys Res Commun. 2001 Feb 9;280(5):1216-23.

Keitel V, Burdelski M, Warskulat U, Kühlkamp T, Keppler D, Häussinger D, Kubitz R. Expression and localization of hepatobiliary transport proteins in progressive familial intrahepatic cholestasis. Hepatology. 2005 May;41(5):1160-72.

Keppler D. Multidrug resistance proteins (MRPs, ABCCs): importance for pathophysiology and drug therapy. Handb. Exp. Pharmacol. 2011 201:299–323.

Keppler D. The roles of MRP2, MRP3, OATP1B1, and OATP1B3 in conjugated hyperbilirubinemia. Drug Metab Dispos. 2014 Apr;42(4):561-5.

Kepplerand D, Kartenbeck J. The canalicular conjugate export pump encoded by the cmrp/cmoat gene. Prog Liver Dis. 1996 14: 55-67.

Kepplerand, DKartenbeck J. The canalicular conjugate export pump encoded by the cmrp/cmoat gene. Prog Liver Dis. 1996 14: 55-67.

Kikuchi R, McCown M, Olson P, Tateno C, Morikawa Y, Katoh Y, Bourdet DL, Monshouwer M, Fretland AJ. Effect of hepatitis C virus infection on the mRNA expression of drug transporters and cytochrome p450 enzymes in chimeric mice with humanized liver. Drug Metab Dispos. 2010 Nov;38(11):1954-61.

Kis O, Sankaran-Walters S, Hoque MT, Walmsley SL, Dandekar S, Bendayan R. HIV-1 Alters Intestinal Expression of Drug Transporters and Metabolic Enzymes: Implications for

Antiretroviral Drug Disposition. Antimicrob Agents Chemother. 2016 Apr 22;60(5):2771-81.

Klaassen CD, Reisman SA. Nrf2 the rescue: effects of the antioxidative/electrophilic response on the liver. Toxicol Appl Pharmacol. 2010 Apr 1;244(1):57-65.

Klaassen CD. The effect of altered hepatic function on the toxicity, plasma disappearance and biliary excretion of diethylstilbestrol. Toxicol Appl Pharmacol. 1973 Jan;24(1):142-9.

Knisely AS, Strautnieks SS, Meier Y, Stieger B, Byrne JA, Portmann BC, Bull LN, Pawlikowska L, Bilezikçi B, Ozçay F, László A, Tiszlavicz L, Moore L, Raftos J, Arnell H, Fischler B, Németh A, Papadogiannakis N, Cielecka-Kuszyk J, Jankowska I, Pawłowska J, Melín-Aldana H, Emerick KM, Whitington PF, Mieli-Vergani G, Thompson RJ. Hepatology. 2006 Aug;44(2):478–86.

Kobayashi Y, Ohshiro N, Shibusawa A, Sasaki T, Tokuyama S, Sekine T, Endou H, and Yamamoto T. Isolation, characterization and differential gene expression of multispecific organic anion transporter 2 in mice. Mol Pharmacol. 2002 62:7–1.

Koepsell H, Schmitt BM, Gorboulev V. Organic cation transporters. Rev Physiol Biochem Pharmacol. 2003;150:36-90.

Kojima H, Nies AT, König J, Hagmann W, Spring H, Uemura M, Fukui H, Keppler D. Changes in the expression and localization of hepatocellular transporters and radixin in primary biliary cirrhosis. J Hepatol. 2003 Nov;39(5):693–702.

Hogan MC, Abebe K, Torres VE, Chapman AB, Bae KT, Tao C, Sun H, Perrone RD, Steinman TI, Braun W, Winklhofer FT, Miskulin DC, Rahbari-Oskoui F, Brosnahan G, Masoumi A, Karpov IO, Spillane S, Flessner M, Moore CG, Schrier RW. Liver involvement in early autosomal-dominant polycystic kidney disease. Clin Gastroenterol Hepatol. 2015 Jan;13(1):155-64.

Huang WM, Seubert DE, Donnelly JG, Liu M, Javitt NB. Intrahepatic cholestasis of pregnancy: detection with urinary bile acid assays. J Perinat Med. 2007;35(6):486-91.

Iizaka T, Tsuji M, Oyamada H, Morio Y, Oguchi K. Interaction between caspase-8 activation and endoplasmic reticulum stress in glycochenodeoxycholic acid-induced apoptotic HepG2 cells. Toxicology. 2007;241:146–156.

Jacobsson L, Lindqvist B, Michaelson G, Bjerle P. Fluid turnover in renal cysts. Acta Med Scand. 1977;202(4):327-9.

James L, Yan K, Pence L, Simpson P, Bhattacharyya S, Gill P, Letzig L, Kearns G, Beger R. Comparison of Bile Acids and Acetaminophen Protein Adducts in Children and Adolescents with Acetaminophen Toxicity. PLoS One. 2015 Jul 24;10(7):e0131010.

Kamano T, Mikami Y, Kurasawa T, Tsurumaru M, Matsumoto M, Kano M, Motegi K. Ratio of primary and secondary bile acids in feces: possible marker for colorectal cancer? Dis Colon Rectum. 1999 May;42(5):668-72.

Kaplan BS, Fay J, Shah V, Dillon MJ, Barratt TM: Autosomal recessive polycystic kidney disease. Pediatr Nephrol 3: 43–49, 1989.

Katsuyama M, Masuyama T, Komura I, Hibino T, Takahashi H. Characterization of a novel polycystic kidney rat model with accompanying polycystic liver. Exp Anim. 2000 Jan;49(1):51-5.

Katsuyama M, Masuyama T, Komura I, Hibino T, Takahashi H. Characterization of a novel polycystic kidney rat model with accompanying polycystic liver. Exp Anim. 2000 Jan;49(1):51-5.

Knight JA. Liver function tests: their role in the diagnosis of hepatobiliary diseases. J Infus Nurs. 2005 Mar-Apr;28(2):108-17.

Köck K, Ferslew BC, Netterberg I, Yang K, Urban TJ, Swaan PW, Stewart PW, Brouwer KL. Risk factors for development of cholestatic drug-induced liver injury: inhibition of hepatic basolateral bile acid transporters multidrug resistance-associated proteins 3 and 4. Drug Metab Dispos. 2014 Apr;42(4):665-74.

Kojima H, Nies AT, König J, Hagmann W, Spring H, Uemura M, Fukui H, Keppler D. Changes in the expression and localization of hepatocellular transporters and radixin in primary biliary cirrhosis. J Hepatol. 2003 39:693–702.

Kojima H, Sakurai S, Uemura M, Kitamura K, Kanno H, Nakai Y, Fukui H. Disturbed colocalization of multidrug resistance protein 2 and radixin in human cholestatic liver diseases. J Gastroenterol Hepatol. 2008 Jul;23(7 Pt 2):e120-8.

Kounnis V, Ioachim E, Svoboda M, Tzakos A, Sainis I, Thalhammer T, Steiner G, Briasoulis E. Expression of organic anion-transporting polypeptides 1B3, 1B1, and 1A2 in human pancreatic cancer reveals a new class of potential therapeutic targets. Onco Targets Ther. 2011;4:27–32.

Krähenbühl S, Talos C, Fischer S, Reichen J. Toxicity of bile acids on the electron transport chain of isolated rat liver mitochondria. Hepatology. 1994;19:471–479.

Krähenbühl S, Talos C, Lauterburg BH, Reichen J. Reduced antioxidative capacity in liver mitochondria from bile duct ligated rats. Hepatology. 1995;22:607–612.

Kramer W1, Wess G, Schubert G, Bickel M, Girbig F, Gutjahr U, Kowalewski S, Baringhaus KH, Enhsen A, Glombik H, et al. Liver-specific drug targeting by coupling to bile acids. J Biol Chem. 1992 Sep 15;267(26):18598–604.

Krishnamurthy GT, Turner FE. Pharmacokinetics and clinical application of technetium 99m-labeled hepatobiliary agents. Semin Nucl Med. 1990 Apr;20(2):130-49.

Kula M, Karacavus S, Baskol M, Deniz K, Abdulrezzak U, Tutus A. Hepatobiliary function assessed by 99mTc-mebrofenin cholescintigraphy in the evaluation of fibrosis in chronic hepatitis: histopathological correlation. Nucl Med Commun. 2010 Apr;31(4):280-5.

Kullak-Ublick GA, Beuers U, Paumgartner G. Molecular and functional characterization of bile

acid transport in human hepatoblastoma HepG2 cells. Hepatology. 1996 May;23(5):1053–60.

Kurzawski M, Dziedziejko V, Post M, Wójcicki M, Urasińska E, Miętkiewski J, Droździk M. Expression of genes involved in xenobiotic metabolism and transport in end-stage liver disease: up-regulation of ABCC4 and CYP1B1. Pharmacol Rep. 2012;64(4):927-39.

Lager DJ, Qian Q, Bengal RJ, Ishibashi M, Torres VE. The pck rat: a new model that resembles human autosomal dominant polycystic kidney and liver disease. Kidney Int. 2001 Jan;59(1):126-36.

Lake AD, Novak P, Fisher CD, Jackson JP, Hardwick RN, Billheimer DD, Klimecki WT, Cherrington NJ. Analysis of global and absorption, distribution, metabolism, and elimination gene expression in the progressive stages of human nonalcoholic fatty liver disease. Drug Metab Dispos. 2011 Oct;39(10):1954-60.

Lee W, Belkhiri A, Lockhart AC, Merchant N, Glaeser H, Harris EI, Washington MK, Brunt EM, Zaika A, Kim RB, El-Rifai W. Overexpression of OATP1B3 confers apoptotic resistance in colon cancer. Cancer Res. 2008 Dec 15;68(24):10315–23.

Lee W, Glaeser H, Smith LH, et al. Polymorphisms in human organic anion-transporting polypeptide 1A2 (OATP1A2): implications for altered drug disposition and central nervous system drug entry. J Biol Chem. 2005;280:9610–9617.

Lemasters JJ, Nieminen AL, Qian T, Trost LC, Elmore SP, Nishimura Y, Crowe RA, Cascio WE, Bradham CA, Brenner DA, et al. The mitochondrial permeability transition in cell death: a common mechanism in necrosis, apoptosis and autophagy. Biochim Biophys Acta. 1998;1366:177–196.

Levine E, Cook LT, Grantham JJ. Liver cysts in autosomal-dominant polycystic kidney disease: clinical and computed tomographic study. AJR Am J Roentgenol. 1985 Aug;145(2):229-33.

Li D, Shi X, Zhao L, Liang Z, Xie S, Wang G. Overexpression of Aquaporin 1 on cysts of patients with polycystic liver disease. Rev Esp Enferm Dig. 2016 Feb;108(2):71-8.

Li L, Lee TK, Meier PJ, Ballatori N. Identification of glutathione as a driving force and leukotriene C4 as a substrate for oatp1, the hepatic sinusoidal organic solute transporter. J Biol Chem. 1998 Jun 26;273(26):16184-91.

Li L, Lee TK, Meier PJ, Ballatori N. Oatp2 mediates bidirectional organic solute transport: a role for intracellular glutathione. Mol Pharmacol. 2000 58: 335-40.

Libra A, Fernetti C, Lorusso V, Visigalli M, Anelli PL, Staud F, Tiribelli C, Pascolo L. Molecular determinants in the transport of a bile acid-derived diagnostic agent in tumoral and nontumoral cell lines of human liver. J Pharmacol Exp Ther. 2006 Nov;319(2):809–17.

Lickteig AJ, Fisher CD, Augustine LM, Aleksunes LM, Besselsen DG, Slitt AL, Manautou JE, Cherrington NJ. Efflux transporter expression and acetaminophen metabolite excretion are altered in rodent models of nonalcoholic fatty liver disease. Drug Metab Dispos. 2007 Oct;35(10):1970-8.

Litman T, Druley TE, Stein WD, Bates SE. From MDR to MXR: new understanding of multidrug resistance systems, their properties and clinical significance. Cell Mol Life Sci. 2001 Jun;58(7):931-59.

Liu Y, Pu QH, Wu MJ, Yu C. Proteomic analysis for the impact of hypercholesterolemia on expressions of hepatic drug transporters and metabolizing enzymes. Xenobiotica. 2016 Oct;46(10):940-7.

Lockhart AC, Harris E, Lafleur BJ, Merchant NB, Washington MK, Resnick MB, Yeatman TJ, Lee W. Organic anion transporting polypeptide 1B3 (OATP1B3) is overexpressed in colorectal tumors and is a predictor of clinical outcome. Clin Exp Gastroenterol. 2008;1:1–7.

Lomonaco R, Sunny NE, Bril F, Cusi K. Nonalcoholic fatty liver disease: current issues and novel treatment approaches. Drugs. 2013;73(1):1-14.

Looand TW, Clarke DM. Membrane topology of a cysteine-less mutant of human P-glycoprotein. J Biol Chem. 1995 270: 843-8.

Maliepaard M, van Gastelen MA, de Jong LA, Pluim D, van Waardenburg RC, Ruevekamp-Helmers MC, Floot BG, Schellens JH. Overexpression of the BCRP/MXR/ABCP gene in a topotecan-selected ovarian tumor cell line. Cancer Res. 1999 Sep 15;59(18):4559-63.

Luo L, Kenny J, Warner R, Johnson K, Colangelo, JL. Profiling individual bile acids in human populations using a UPLC/MS/MS method [abstract]. Toxicol Suppl Toxicol Sci. 2015 Volume 144, Issue 1, Page 256.

Luo L, Schomaker S, Houle C, Aubrecht J, Colangelo JL. Evaluation of serum bile acid profiles as biomarkers of liver injury in rodents. Toxicol Sci. 2014 Jan;137(1):12-25.

Luo L, Schomaker S, Houle C, Aubrecht J, Colangelo JL. Evaluation of serum bile acid profiles as biomarkers of liver injury in rodents. Toxicol Sci. 2014 Jan;137(1):12-25.

Maier T, Güell M, Serrano L. Correlation of mRNA and protein in complex biological samples. FEBS Lett. 2009 Dec 17;583(24):3966-73.

Marchegiano P1, Carubbi F, Tiribelli C, Amarri S, Stebel M, Lunazzi GC, Levy D, Bellentani S. Transport of sulfobromophthalein and taurocholate in the HepG2 cell line in relation to the expression of membrane carrier proteins. Biochem Biophys Res Commun. 1992 Mar 31;183(3):1203–8.

Marion TL, Leslie EM, Brouwer KL Use of sandwich-cultured hepatocytes to evaluate impaired bile acid transport as a mechanism of drug-induced hepatotoxicity. Mol Pharm. 2007 Nov-Dec;4(6):911-8.

Martin KO, Budai K, Javitt NB. Cholesterol and 27-hydroxycholesterol 7 alpha-hydroxylation: evidence for two different enzymes. J Lipid Res. 1993 Apr;34(4):581-8.

Mason SB, Liang Y, Sinders RM, Miller CA, Eggleston-Gulyas T, Crisler-Roberts R, Harris PC, Gattone VH 2nd. Disease stage characterization of hepatorenal fibrocystic pathology in the PCK rat model of ARPKD. Anat Rec (Hoboken). 2010 Aug;293(8):1279-88.

Masyuk AI, Masyuk TV, Splinter PL, Huang BQ, Stroope AJ, LaRusso NF. Cholangiocyte cilia detect changes in luminal fluid flow and transmit them into intracellular Ca2+ and cAMP signaling. Gastroenterology. 2006 Sep;131(3):911-20.

Masyuk TV, Huang BQ, Masyuk AI, Ritman EL, Torres VE, Wang X, Harris PC, Larusso NF. Biliary dysgenesis in the PCK rat, an orthologous model of autosomal recessive polycystic kidney disease. Am J Pathol. 2004 Nov;165(5):1719-30.

Masyuk TV, Huang BQ, Ward CJ, Masyuk AI, Yuan D, Splinter PL, Punyashthiti R, Ritman EL, Torres VE, Harris PC, LaRusso NF. Defects in cholangiocyte fibrocystin expression and ciliary structure in the PCK rat. Gastroenterology. 2003 Nov;125(5):1303-10.

McDonald RA, Avner ED. Watson ML, editor. New York: Oxford University Press; Mouse Models of Polycystic Kidney Disease. 1996:pp 63–87.

Mechetner E, Kyshtoobayeva A, Zonis S, Kim H, Stroup R, Garcia R, Parker RJ, Fruehauf JP. Levels of multidrug resistance (MDR1) P-glycoprotein expression by human breast cancer correlate with in vitro resistance to taxol and doxorubicin. Clin Cancer Res. 1998 Feb;4(2):389-98.

Mennone A, Soroka CJ, Cai SY, Harry K, Adachi M, Hagey L, Schuetz JD, Boyer JL. Mrp4-/- mice have an impaired cytoprotective response in obstructive cholestasis. Hepatology. 2006 May;43(5):1013-21.

Mennone A, Soroka CJ, Cai SY, Harry K, Adachi M, Hagey L, Schuetz JD, Boyer JL. Mrp4-/- mice have an impaired cytoprotective response in obstructive cholestasis. Hepatology. 2006 May;43(5):1013-21.

Meyer zu Schwabedissen HE, Jedlitschky G, Gratz M, Haenisch S, Linnemann K, Fusch C, Cascorbi I, Kroemer HK. Variable expression of MRP2 (ABCC2) in human placenta: influence of gestational age and cellular differentiation. Drug Metab Dispos. 2005 Jul;33(7):896-904.

Mikkaichi T, Suzuki T, Onogawa T, Tanemoto M, Mizutamari H, Okada M, Chaki T, Masuda S, Tokui T, Eto N, Abe M, Satoh F, Unno M, Hishinuma T, Inui K, Ito S, Goto J, Abe T. Isolation and characterization of a digoxin transporter and its rat homologue expressed in the kidney. Proc Natl Acad Sci USA. 2004 Mar 9;101(10):3569-74.

Mokdad AA, Lopez AD, Shahraz S, Lozano R, Mokdad AH, Stanaway J, Murray CJL, Naghavi M. Liver cirrhosis mortality in 187 countries between 1980 and 2010: a systematic analysis. BMC Med. 2014 12:145.

Monks NR, Liu S, Xu Y, Yu H, Bendelow AS, Moscow JA. Potent cytotoxicity of the phosphatase inhibitor microcystin LR and microcystin analogues in OATP1B1- and OATP1B3-expressing HeLa cells. Mol Cancer Ther. 2007 Feb;6(2):587–98.

Monte MJ, Marin JJ, Antelo A, Vazquez-Tato J. Bile acids: chemistry, physiology, and pathophysiology. World J Gastroenterol. 2009 Feb 21;15(7):804-16.

More VR, Cheng Q, Donepudi AC, Buckley DB, Lu ZJ, Cherrington NJ, Slitt AL. Alcohol cirrhosis alters nuclear receptor and drug transporter expression in human liver. Drug Metab Dispos. 2013 May;41(5):1148-55.

Morgan RE, Trauner M, van Staden CJ, Lee PH, Ramachandran B, Eschenberg M, Afshari CA, Qualls CW Jr., Lightfoot-Dunn R, and Hamadeh HK. Interference with bile salt export pump function is a susceptibility factor for human liver injury in drug development. Toxicol Sci. 2010 118:485–500.

Morgan RE, Trauner M, van Staden CJ, Lee PH, Ramachandran B, Eschenberg M, Afshari CA, Qualls CW Jr, Lightfoot-Dunn R, Hamadeh HK. Interference with bile salt export pump function is a susceptibility factor for human liver injury in drug development. Toxicol Sci. 2010 Dec;118(2):485-500.

Morgan RE, van Staden CJ, Chen Y, Kalyanaraman N, Kalanzi J, Dunn RT 2nd, Afshari CA, Hamadeh HK. A multifactorial approach to hepatobiliary transporter assessment enables improved therapeutic compound development. Toxicol Sci. 2013 Nov;136(1):216-41.

Morgan RE, van Staden CJ, Chen Y, Kalyanaraman N, Kalanzi J, Dunn RT 2nd, Afshari CA, Hamadeh HK. A multifactorial approach to hepatobiliary transporter assessment enables improved therapeutic compound development. Toxicol Sci. 2013 Nov;136(1):216-41.

Mottino AD, Cao J, Veggi LM, Crocenzi F, Roma MG, Vore M. Altered localization and activity of canalicular Mrp2 in estradiol-17beta-D-glucuronide-induced cholestasis. Hepatology. 2002 35(6):1409–19.

Moyer J, Lee-Tischler M, Kwon HY, Schrick J, Avner E, Sweeney W, Godfrey V, Cacheiro N, Wilkinson J, and Woychik R. Candidate gene associated with a mutation causing recessive polycystic kidney disease in mice. Science. 1994 264: 1329–1333.

Murphy GM, Ross A, Billing BH. Serum bile acids in primary biliary cirrhosis. Gut. 1972 Mar;13(3):201-6.

Muto M, Onogawa T, Suzuki T, Ishida T, Rikiyama T, Katayose Y, Ohuchi N, Sasano H, Abe T, Unno M. Human liver-specific organic anion transporter-2 is a potent prognostic factor for human breast carcinoma. Cancer Sci. 2007 Oct;98(10):1570–6.

Nagao S, Nishii K, Katsuyama M, Kurahashi H, Marunouchi T, Takahashi H, Wallace DP. Increased water intake decreases progression of polycystic kidney disease in the PCK rat. J Am Soc Nephrol. 2006 Aug;17(8):2220-7.

Nakagawa M, Schneider E, Dixon KH, Horton J, Kelley K, Morrow C, Cowan KH.. Reduced intracellular drug accumulation in the absence of P-glycoprotein (mdr1) overexpression in mitoxantrone-resistant human MCF-7 breast cancer cells. Cancer Res. 1992 Nov 15;52(22):6175-81.

Nakai K, Tanaka H, Hanada K, Ogata H, Suzuki F, Kumada H, Miyajima A, Ishida S, Sunouchi M, Habano W, Kamikawa Y, Kubota K, Kita J, Ozawa S, Ohno Y. Decreased expression of cytochromes P450 1A2, 2E1, and 3A4 and drug transporters Na+-taurocholate-cotransporting polypeptide, organic cation transporter 1, and organic anion-transporting peptide-C correlates with the progression of liver fibrosis in chronic hepatitis C patients. Drug Metab Dispos. 2008 Sep;36(9):1786-93.

Nakanishi K, Sweeney WE Jr, Macrae Dell K, Cotton CU, Avner ED. Role of CFTR in autosomal recessive polycystic kidney disease. J Am Soc Nephrol. 2001 Apr;12(4):719-25.

Namisaki T, Schaeffeler E, Fukui H, Yoshiji H, Nakajima Y, Fritz P, Schwab M, Nies AT. Differential expression of drug uptake and efflux transporters in Japanese patients with hepatocellular carcinoma. Drug Metab Dispos. 2014 Dec;42(12):2033–40.

Nauli SM, Alenghat FJ, Luo Y, Williams E, Vassilev P, Li X, Elia AE, Lu W, Brown EM, Quinn SJ, Ingber DE, Zhou J. Polycystins 1 and 2 mediate mechanosensation in the primary cilium of kidney cells. Nat Genet. 2003 Feb;33(2):129-37.

Nauta J, Goedbloed MA, Luider TM, Hoogeveen AT, van den Ouweland AM, Halley DJ. The Han:SPRD rat is not a genetic model of human autosomal dominant polycystic kidney disease type 1. Lab Anim. 1997 Jul;31(3):241-7.

Newman S, Steed K, Hooper G, Källén A, Borgström L. Comparison of gamma scintigraphy and a pharmacokinetic technique for assessing pulmonary deposition of terbutaline sulphate delivered by pressurized metered dose inhaler. Pharm Res. 1995 Feb;12(2):231-6.

Ng IO, Liu CL, Fan ST, Ng M. Expression of P-glycoprotein in hepatocellular carcinoma. A determinant of chemotherapy response. Am J Clin Pathol. 2000 Mar;113(3):355–63.

Nichols MT, Gidey E, Matzakos T, Dahl R, Stiegmann G, Shah RJ, Grantham JJ, Fitz JG, Doctor RB: Secretion of cytokines and growth factors into autosomal dominant polycystic kidney disease liver cyst fluid. Hepatology 2004, 40:836–846.

Nies AT, Koepsell H, Damme K, Schwab M. Organic cation transporters (OCTs, MATEs), in vitro and in vivo evidence for the importance in drug therapy. Handb Exp Pharmacol. 2011 201:105–167.

Nies AT, König J, Pfannschmidt M, Klar E, Hofmann WJ, Keppler D. Expression of the multidrug resistance proteins MRP2 and MRP3 in human hepatocellular carcinoma. Int J cancer. 2001 Nov;94(4):492–9.

Norlin M, Wikvall K. Enzymes in the Conversion of Cholesterol into Bile Acids. Curr Mol Med. 2007;7:199–218.

Ogasawara K, Terada T, Katsura T, Hatano E, Ikai I, Yamaoka Y, Inui K. Hepatitis C virus-related cirrhosis is a major determinant of the expression levels of hepatic drug transporters. Drug Metab Pharmacokinet. 2010;25(2):190-9.

Ohno K, Kondo K. A mutant rat with congenital skeletal abnormalities and polycystic kidneys. Jikken Dobutsu. 1989 Apr;38(2):139-46.

Okushin K, Tsutsumi T, Enooku K, Fujinaga H, Kado A, Shibahara J, Fukayama M, Moriya K, Yotsuyanagi H, Koike K. The intrahepatic expression levels of bile acid transporters are inversely correlated with the histological progression of nonalcoholic fatty liver disease. J Gastroenterol. 2015 Nov 25.

Oswald S, Westrup S, Grube M, Kroemer HK, Weitschies W, Siegmund W. Disposition and sterol-lowering effect of ezetimibe in multidrug resistance-associated protein 2-deficient rats. J Pharmacol Exp Ther. 2006 Sep;318(3):1293-9.

Okushin K, Tsutsumi T, Enooku K, Fujinaga H, Kado A, Shibahara J, Fukayama M, Moriya K, Yotsuyanagi H, Koike K. The intrahepatic expression levels of bile acid transporters are inversely correlated with the histological progression of nonalcoholic fatty liver disease. J Gastroenterol. 2015 Nov 25 1-11.

Ong AC, Ward CJ, Butler RJ, Biddolph S, Bowker C, Torra R, Pei Y, Harris PC. Coordinate expression of the autosomal dominant polycystic kidney disease proteins, polycystin-2 and polycystin-1, in normal and cystic tissue. Am J Pathol. 1999 Jun;154(6):1721-9.

Otsuka M, Matsumoto T, Morimoto R, Arioka S, Omote H, Moriyama Y. A human transporter protein that mediates the final excretion step for toxic organic cations. Proc Natl Acad Sci USA. 2005 Dec 13; 102(50):17923-8.

Ozer J, Ratner M, Shaw M, Bailey W, Schomaker S. The current state of serum biomarkers of hepatotoxicity. Toxicology. 2008 Mar 20;245(3):194-205.

Park SW, Schonhoff CM1, Webster CR2, Anwer MS3. Rab11, but not Rab4, facilitates cyclic AMP- and tauroursodeoxycholate-induced MRP2 translocation to the plasma membrane. Am J Physiol Gastrointest Liver Physiol. 2014 Oct 15;307(8):G863-70.

Parnell SC, Magenheimer BS, Maser RL, et al. The polycystic kidney disease-1 protein, polycystin-1, binds and activates heterotrimeric G-proteins in vitro. Biochem Biophys Res Commun. 1998; 251:625–631.

Pauli-Magnus C, Meier PJ. Hepatobiliary transporters and drug-induced cholestasis. Hepatology. 2006 44:778-87.

Paulusma CC, Kothe MJ, Bakker CT, Bosma PJ, van Bokhoven I, van Marle J, Bolder U, Tytgat GN, Oude Elferink RP. Zonal down-regulation and redistribution of the multidrug resistance protein 2 during bile duct ligation in rat liver. Hepatology. 2000 31:684-693.

Perrone RD, Grubman SA, Rogers LC, Lee DW, Moy E, Murray SL, Torres VE, Jefferson DM: Continuous epithelial cell lines from ADPKD liver cysts exhibit characteristics of intrahepatic biliary epithelium. Am J Physiol 1995, 269:G335–G345

Pfeifer ND, Bridges AS, Ferslew BC, Hardwick RN, Brouwer KL. Hepatic basolateral efflux contributes significantly to rosuvastatin disposition II: characterization of hepatic elimination by basolateral, biliary, and metabolic clearance pathways in rat isolated perfused liver. J Pharmacol Exp Ther. 2013b Dec;347(3):737-45.

Pfeifer ND, Goss SL, Swift B, Ghibellini G, Ivanovic M, Heizer WD, Gangarosa LM, and Brouwer LR. Effect of Ritonavir on 99mTechnetium–Mebrofenin Disposition in Humans: A Semi-PBPK Modeling and In Vitro Approach to Predict Transporter-Mediated DDIs. CPT Pharmacometrics Syst Pharmacol. 2013a Jan; 2(1): e20.

Pfeifer ND, Hardwick RN, Brouwer KLR. Role of hepatic efflux transporters in regulating systemic and hepatocyte exposure to xenobiotics. Annu Rev Pharmacol Toxicol. 2014 54:509–35.

Pinós, T., Constansa, J.M., Palacin, A. & Figueras, C. A new diagnostic approach to the Dubin-Johnson syndrome. Am J Gastroenterol. 1990 Jan;85(1):91-3.

Pinós, T., Figueras, C. & Herranz, R. Scintigraphic diagnosis of Dubin-Johnson syndrome: DISIDA is also useful. Am J Gastroenterol. 1991 Nov;86(11):1687-8.

Pusl T and Ulrich B. Intrahepatic cholestasis of pregnancy. Orphanet J Rare Dis. 2007; 2: 26.

Qian F, Watnick TJ, Onuchic LF, Germino GG. The molecular basis of focal cyst formation in human autosomal dominant polycystic kidney disease type I. Cell. 1996;87:979–87.

Reeders ST. Multilocus polycystic disease. Nat Genet. 1992;1:235–7.

Regazzi M, Maserati R, Villani P, Cusato M, Zucchi P, Briganti E, Roda R, Sacchelli L, Gatti F, Foglie PD, Nardini G, Fabris P, Mori F, Castelli P, Testa L. Clinical Pharmacokinetics of Nelfinavir and Its Metabolite M8 in Human Immunodeficiency Virus (HIV)-Positive and HIV-Hepatitis C Virus-Coinfected Subjects. Antimicrob Agents Chemother. 2005 Feb; 49(2): 643–649.

Ridlon JM, Kang DJ, Hylemon PB. Bile salt biotransformations by human intestinal bacteria. J Lipid Res. 2006 Feb;47(2):241-59.

Rodrigues AD, Lai Y, Cvijic ME, Elkin LL, Zvyaga T, Soars MG. Drug-induced perturbations of the bile acid pool, cholestasis, and hepatotoxicity: mechanistic considerations beyond the direct inhibition of the bile salt export pump. Drug Metab Dispos. 2014 Apr;42(4):566-74.

Roelofsen H, Soroka CJ, Keppler D, Boyer JL. Cyclic AMP stimulates sorting of the canalicular organic anion transporter (Mrp2/cMoat) to the apical domain in hepatocyte couplets. J Cell Sci. 1998 Apr;111 (Pt 8):1137-45.

Rolo AP, Oliveira PJ, Moreno AJ, Palmeira CM. Bile acids affect liver mitochondrial bioenergetics: possible relevance for cholestasis therapy. Toxicol Sci. 2000;57:177–185.

Rook M, Vargas J, Caughey A, Bacchetti P, Rosenthal P, Bull L.. Fetal Outcomes in pregnancies complicated by intrahepatic cholestasis of pregnancy in a Northern California Cohort. PLoS One. 2012;7(3):e28343.

Ros JE, Libbrecht L, Geuken M, Jansen PL, Roskams TA. High expression of MDR1, MRP1, and MRP3 in the hepatic progenitor cell compartment and hepatocytes in severe human liver disease. J Pathol. 2003 Aug;200(5):553-60.

Ros JE, Libbrecht L, Geuken M, Jansen PLM, Roskams TAD. High expression of MDR1, MRP1, and MRP3 in the hepatic progenitor cell compartment and hepatocytes in severe human liver disease. J Pathol. 2003 Aug;200(5):553–60.

Rose RH, Neuhoff S, Abduljalil K, Chetty M, Rostami-Hodjegan A, Jamei M. Application of a Physiologically Based Pharmacokinetic Model to Predict OATP1B1-Related Variability in Pharmacodynamics of Rosuvastatin. CPT Pharmacometrics Syst Pharmacol. 2014 Jul 9;3:e124.

Rossetti S, Kubly VJ, Consugar MB, Hopp K, Roy S, Horsley SW, Chauveau D, Rees L, Barratt TM, van't Hoff WG, Niaudet P, Niaudet WP, Torres VE, Harris PC. Incompletely penetrant PKD1 alleles suggest a role for gene dosage in cyst initiation in polycystic kidney disease. Kidney Int. 2009;75:848–55.

Russell DW. Fifty years of advances in bile acid synthesis and metabolism. J Lipid Res. 2009 Apr; 50(Suppl): S120–S125.

Saeki J, Sekine S, Horie T. LPS-induced dissociation of multidrug resistance-associated protein 2 (Mrp2) and radixin is associated with Mrp2 selective internalization in rats. Biochem Pharmacol. 2011 81:178–18

Salam M, Keeffe EB. Liver cysts associated with polycystic kidney disease: role of Tc-99m hepatobiliary imaging. Clin Nucl Med. 1989 Nov;14(11):803-7.

Sandusky GE, Mintze KS, Pratt SE, Dantzig AH. Expression of multidrug resistance-associated protein 2 (MRP2) in normal human tissues and carcinomas using tissue microarrays. Histopathology. 2002 Jul;41(1):65-74.

Satlin LM, Amin V, Wolkoff AW. Organic anion transporting polypeptide mediates organic anion/HCO3- exchange. J Biol Chem. 1997 Oct 17;272(42):26340-5.

Schaeffeler E, Hellerbrand C, Nies AT, Winter S, Kruck S, Hofmann U, van der Kuip H, Zanger UM, Koepsell H, Schwab M. DNA methylation is associated with downregulation of the organic cation transporter OCT1 (SLC22A1) in human hepatocellular carcinoma. Genome Med. 2011 Dec 23;3(12):82.

Schaub TP, Kartenbeck J, König J, Spring H, Dörsam J, Staehler G, Störkel S, Thon WF, Keppler D.. Expression of the MRP2 gene-encoded conjugate export pump in human kidney proximal tubules and in renal cell carcinoma. J Am Soc Nephrol. 1999 Jun;10(6):1159-69.

Schäfer K, Gretz N, Bader M, Oberbäumer I, Eckardt KU, Kriz W, Bachmann S. Characterization of the Han:SPRD rat model for hereditary polycystic kidney disease. Kidney Int. 1994 Jul;46(1):134-52.

Scheffer GL, Kool M, de Haas M, de Vree JM, Pijnenborg AC, Bosman DK, Elferink RP, van der Valk P, Borst P, Scheper RJ. Tissue distribution and induction of human multidrug resistant protein 3. Lab Invest. 2002 Feb;82(2):193-201.

Scherstén T. The synthesis of taurocholic and glycocholic acids in human liver homogenates and subcellular fractions in obstructive jaundice. Scand J Gastroenterol. 1967;2(1):49-58.

Schieren G, Pey R, Bach J, Hafner M, Gretz N. Murine models of polycystic kidney disease. Nephrol Dial Transplant. 1996;11 Suppl 6:38-45.

Sekine T, Watanabe N, Hosoyamada M, Kanai Y, Endou H. Expression cloning and characterization of a novel multispecific organic anion transporter. J Biol Chem. 1997 272:18526–18529.

Senior JR. Evolution of the Food and Drug Administration approach to liver safety assessment for new drugs: current status and challenges. Drug Saf. 2014 Nov;37 Suppl 1:S9-17.

Sherstha R, McKinley C, Russ P, Scherzinger A, Bronner T, Showalter R, Everson GT. Postmenopausal estrogen therapy selectively stimulates hepatic enlargement in women with autosomal dominant polycystic kidney disease. Hepatology. 1997 Nov;26(5):1282-6.

Shin HJ, Anzai N, Enomoto A, He X, Kim DK, Endou H, Kanai Y. Novel liver-specific organic anion transporter OAT7 that operates the exchange of sulfate conjugates for short chain fatty acid butyrate. Hepatology. 2007 Apr;45(4):1046-55.

Shlomai A, Halfon P, Goldiner I, Zelber-Sagi S, Halpern Z, Oren R, Bruck R. Serum bile acid levels as a predictor for the severity of liver fibrosis in patients with chronic hepatitis C. J Viral Hepat. 2013 Feb;20(2):95-102.

Shneider BL, Dawson PA, Christie DM, Hardikar W, Wong MH, and Suchy FJ. Cloning and molecular characterization of the ontogeny of a rat ileal sodium-dependent bile acid transporter. J Clin Invest. 1995 Feb; 95(2): 745–754.

Simon FR, Fortune J, Iwahashi M, Gartung C, Wolkoff A, Sutherland E. Ethinyl estradiol cholestasis involves alterations in expression of liver sinusoidal transporters. Am J Physiol. 1996 271(6 Pt 1):G1043–52.

Simonson GD, Vincent AC, Roberg KJ, Huang Y, Iwanij V. Molecular cloning and characterization of a novel liver-specific transport protein. J Cell Sci. 1994 107:1065–1072.

Slizgi JR et al. Hepatic Disposition of 99mTechnetium–Mebrofenin is Altered in Patients with Non-Alcoholic Steatohepatitis (NASH) (in preparation).

Slot AJ, Molinski SV, Cole SPC. Mammalian multidrug resistance proteins (MRPs). Essays Biochem. 2011 50:179–207.

Sokol RJ, Dahl R, Devereaux MW, Yerushalmi B, Kobak GE, Gumpricht E. Human hepatic mitochondria generate reactive oxygen species and undergo the permeability transition in response to hydrophobic bile acids. J Pediatr Gastroenterol Nutr. 2005;41:235–243.

Sokol RJ, Devereaux M, Khandwala RA. Effect of dietary lipid and vitamin E on mitochondrial lipid peroxidation and hepatic injury in the bile duct-ligated rat. J Lipid Res. 1991;32:1349–1357.

Sokol RJ, Winklhofer-Roob BM, Devereaux MW, McKim JM Jr. Generation of hydroperoxides in isolated rat hepatocytes and hepatic mitochondria exposed to hydrophobic bile acids. Gastroenterology. 1995;109:1249–1256.

Song X, Vasilenko A, Chen Y, Valanejad L, Verma R, Yan B, Deng R. Transcriptional dynamics of bile salt export pump during pregnancy: mechanisms and implications in intrahepatic cholestasis of pregnancy. Hepatology. 2014 Dec;60(6):1993-2007.

Spring P, in "A Symposium on Rimactane," Ciba Ltd., Basel, Switzerland, 1968, pp. 32-34.

Starremans PG, Li X, Finnerty PE, Guo L, Takakura A, Neilson EG, Zhou J. A mouse model for polycystic kidney disease through a somatic in-frame deletion in the 5' end of Pkd1. Kidney Int. 2008 Jun;73(12):1394-405.

Steiner C, Othman A, Saely CH, Rein P, Drexel H, von Eckardstein A, Rentsch KM. Bile acid metabolites in serum: intraindividual variation and associations with coronary heart disease, metabolic syndrome and diabetes mellitus. PLoS One. 2011;6(11):e25006.

Strautnieks SS, Byrne JA, Pawlikowska L, Cebecauerová D, Rayner A, Dutton L, Meier Y, Antoniou A, Stieger B, Arnell H, Ozçay F, Al-Hussaini HF, Bassas AF, Verkade HJ, Fischler B, Németh A, Kotalová R, Shneider BL, Cielecka-Kuszyk J, McClean P, Whitington PF, Sokal E, Jirsa M, Wali SH, Jankowska I, Pawłowska J, Mieli-Vergani G, Knisely AS, Bull LN, Thompson RJ. Severe bile salt export pump deficiency: 82 different ABCB11 mutations in 109 families. Gastroenterology. 2008 Apr;134(4):1203–14.

Stride BD, Grant CE, Loe DW, Hipfner DR, Cole SPC, Deeley RG. Pharmacological characterization of the murine and human orthologs of multidrug resistance protein in transfected human embryonic kidney cells. Mol. Pharmacol. 1997 52:344–53.

Sukowati CH, Rosso N, Pascut D, Anfuso B, Torre G, Francalanci P, Crocè LS, Tiribelli C. Gene and functional up-regulation of the BCRP/ABCG2 transporter in hepatocellular carcinoma. BMC Gastroenterol. 2012 Dec 15;12(1):160.

Sun W, Wu RR, van Poelje PD, and Erion MD. Isolation of a family of organic anion transporters from human liver and kidney. Biochem Biophys Res Commun. 2001 283:417– 422.

Sun Z, Zhao Z, Li G, Dong S, Huang Z, Ye L, Liang H, Qu J, Ai X, Zhang W, Chen X. Relevance of two genes in the multidrug resistance of hepatocellular carcinoma: in vivo and

clinical studies. Tumori. 2010 Jan-Feb;96(1):90-6.

Sweet DH, Pritchard JB. The molecular biology of renal organic anion and organic cation transporters. Cell Biochem Biophys. 1999 31:89–118.

Swell L, Schwartz CC, Gustafsson J, Danielsson H, Vlahcevic ZR. A quantitative evaluation of the conversion of 25-hydroxycholesterol to bile acids in man. Biochim Biophys Acta. 1981 Jan 26;663(1):163-8.

Swift B, Pfeifer ND, Brouwer KL. Sandwich-cultured hepatocytes: an in vitro model to evaluate hepatobiliary transporter-based drug interactions and hepatotoxicity. Drug Metab Rev. 2010 Aug;42(3):446-71.

Swift B, Tian X, Brouwer, KL. Integration of Preclinical and Clinical Data with Pharmacokinetic Modeling and Simulation to Evaluate Fexofenadine as a Probe for Hepatobiliary Transport Function. Pharm Res. 2009 Aug;26(8):1942-51.

Takanishi K, Miyazaki M, Ohtsuka M, Nakajima N. Inverse Relationship between P-Glycoprotein Expression and Its Proliferative Activity in Hepatocellular Carcinoma. Oncology. Karger Publishers; 2009 Jun 30;54(3):231–7.

Takeyama Y, Sakisaka S. Hepatobiliary membrane transporters in primary biliary cirrhosis. Hepatol Res. Blackwell Publishing Asia; 2012 Feb;42(2):120–30.

Takeyama Y, Tsuchiya N, Kunimoto H, Fukunaga A, Sakurai K, Hirano G, Yokoyama K, Morihara D, Anan A, Irie M, Shakado S, Sohda T, Sakisaka S. Gadolinium-ethoxybenzyl-diethylenetriamine pentaacetic acid-enhanced magnetic resonance imaging as a useful detection method for advanced primary biliary cirrhosis. Hepatol Res. 2015 Oct;45(10):E108–14.

Takeyama Y, Uehara Y, Inomata S, Morihara D, Nishizawa S, Ueda S, Matsumoto T, Tanaka T, Anan A, Nishimura H, Irie M, Iwata K, Shakado S, Sohda T, Sakisaka S. Alternative transporter pathways in patients with untreated early-stage and late-stage primary biliary cirrhosis. Liver Int. 2009 Mar;29(3):406–14.

Tanaka N, Matsubara T, Krausz KW, Patterson AD, Gonzalez FJ. Disruption of phospholipid and bile acid homeostasis in mice with nonalcoholic steatohepatitis. Hepatology. 2012 Jul;56(1):118-29.

Teeter L, Hsu H, Curley S, Tong M, Kuo M. Expression of multidrug resistance (p-glycoprotein) mdr1 and mdr2 genes in human hepatocellular carcinomas and liver metastases of colonic tumors. Int J Oncol. 1993 Jan;2(1):73–80.

Thakkar N, Kim K, Jang ER, Han S, Kim K, Kim D, Merchant N, Lockhart AC, Lee W. A cancer-specific variant of the slco1b3 gene encodes a novel human organic anion transporting polypeptide 1B3 (OATP1B3) localized mainly in the cytoplasm of colon and pancreatic cancer cells. Mol Pharm. 2013;10(1):406–16.

Thakkar N, Lockhart AC, Lee W. Role of Organic Anion-Transporting Polypeptides (OATPs) in

Cancer Therapy. AAPS J. 2015 May;17(3):535–45.

Tomonari T, Takeishi S, Taniguchi T, Tanaka T, Tanaka H, Fujimoto S, Kimura T, Okamoto K, Miyamoto H, Muguruma N, Takayama T. MRP3 as a novel resistance factor for sorafenib in hepatocellular carcinoma. Oncotarget. 2016 Feb 9;7(6):7207-15.

Thapa BR and Anuj Walia A. Liver Function Tests and their Interpretation. Indian J Pediatr. 2007; 74 (7): 663-671.

Tian X, Swift B, Zamek-Gliszczynski MJ, Belinsky MG, Kruh GD, Brouwer KL. Impact of basolateral multidrug resistance-associated protein (Mrp) 3 and Mrp4 on the hepatobiliary disposition of fexofenadine in perfused mouse livers. Drug Metab Dispos. 2008 36:911-5

Togashi H, Shinzawa H, Wakabayashi H, Nakamura T, Yamada N, Takahashi T, Ishikawa M. Activities of free oxygen radical scavenger enzymes in human liver. J Hepatology. 1990;11:200–205.

Torres VE, Chapman AB, Devuyst O, et al. Tolvaptan in patients with autosomal dominant polycystic kidney disease. N Engl J Med. 2012;367:2407–18.

Trauner , Arrese M, Soroka CJ, Ananthanarayanan M, Koeppel TA, Schlosser SF, Suchy FJ, Keppler D, Boyer JL. The rat canalicular conjugate export pump (Mrp2) is down-regulated in intrahepatic and obstructive cholestasis. Gastroenterology. 1997 113(1):255–64.

Trauner M and Boyer JL. Bile salt transporters: molecular characterization, function, and regulation. Physiol Rev. 2003 83 :633–671.

Trinchet JC, Gerhardt MF, Balkau B, Munz C, Poupon RE. Serum bile acids and cholestasis in alcoholic hepatitis. Relationship with usual liver tests and histological features. J Hepatol. 1994 Aug;21(2):235-40.

Tsuboyama T, Onishi H, Kim T, Akita H, Hori M, Tatsumi M, Nakamoto A, Nagano H, Matsuura N, Wakasa K, Tomoda K. Hepatocellular carcinoma: hepatocyte-selective enhancement at gadoxetic acid-enhanced MR imaging--correlation with expression of sinusoidal and canalicular transporters and bile accumulation. Radiology. 2010 Jun;255(3):824–33.

Tsuchiya S, Tsuji M, Morio Y, Oguchi K. Involvement of endoplasmic reticulum in glycochenodeoxycholic acid-induced apoptosis in rat hepatocytes. Toxicol Lett. 2006;166:140–149.

Tsuda N, Matsui O. Signal profile on Gd-EOB-DTPA-enhanced MR imaging in non-alcoholic steatohepatitis and liver cirrhosis induced in rats: correlation with transporter expression. Eur Radiol. 2011 Dec;21(12):2542-50.

Tsutsumi T, Suzuki T, Shimoike T, Suzuki R, Moriya K, Shintani Y, Fujie H, Matsuura Y, Koike K, Miyamura T. Interaction of hepatitis C virus core protein with retinoid X receptor alpha modulates its transcriptional activity. Hepatology. 2002 Apr;35(4):937-46.

Vallejo M, Castro MA, Medarde M, Macias RI, Romero MR, El-Mir MY, Monte MJ, Briz O, Serrano MA, Marin JJ. Novel bile acid derivatives (BANBs) with cytostatic activity obtained by conjugation of their side chain with nitrogenated bases. Biochem Pharmacol. 2007 73:1394–1404

Van Aubel RA, Masereeuw R, Russel F. Molecular pharmacology of renal organic anion transporters. Am J Physiol Renal Physiol. 2000 279:F216–F232.

Vander Borght S, Libbrecht L, Blokzijl H, Faber KN, Moshage H, Aerts R, Van Steenbergen W, Jansen PL, Desmet VJ, Roskams TA. Diagnostic and pathogenetic implications of the expression of hepatic transporters in focal lesions occurring in normal liver. J Pathol. 2005 Dec;207(4):471–82.

Vander Borght S, van Pelt J, van Malenstein H, Cassiman D, Renard M, Verslype C, Libbrecht L, Roskams TA. Up-regulation of breast cancer resistance protein expression in hepatoblastoma following chemotherapy: A study in patients and in vitro. Hepatol Res. 2008 38(11):1112–21.

Vavricka SR, Jung D, Fried M, Grützner U, Meier PJ, Kullak-Ublick GA. The human organic anion transporting polypeptide 8 (SLCO1B3) gene is transcriptionally repressed by hepatocyte nuclear factor 3beta in hepatocellular carcinoma. J Hepatol. 2004 Feb;40(2):212–8.

Vee ML, Lecureur V, Stieger B, Fardel O. Regulation of drug transporter expression in human hepatocytes exposed to the proinflammatory cytokines tumor necrosis factor-alpha or interleukin-6. Drug Metab Dispos. 2009 37(3):685-693.

Vogel C, Marcotte EM. Insights into the regulation of protein abundance from proteomic and transcriptomic analyses. Nat Rev Genet. 2012 Mar 13;13(4):227-32.

Vogel, HG, Maas, J, Hock, FJ, Mayer, D. Drug Discovery and Evaluation: Safety and Pharmacokinetic Assays. Springer; 1 edition (October 10, 2006).

von Dippe P, Levy D. Expression of the bile acid transport protein during liver development and in hepatoma cells. J Biol Chem. 1990 Apr 15;265(11):5942–5.

Vredenburg MR, Ojima I, Veith J, Pera P, Kee K, Cabral F, Sharma A, Kanter P, Greco WR, Bernacki RJ. Effects of orally active taxanes on P-glycoprotein modulation and colon and breast carcinoma drug resistance. J Natl Cancer Inst. 2001 Aug 15;93(16):1234-45.

Vujic M, Heyer CM, Ars E, Hopp K, Markoff A, Orndal C, Rudenhed B, Nasr SH, Torres VE, Torra R, Bogdanova N, Harris PC. Incompletely penetrant PKD1 alleles mimic the renal manifestations of ARPKD. J Am Soc Nephrol. 2010;21:1097–102.

Wang H, Yan Z, Dong M, Zhu X, Wang H, Wang Z. Alteration in placental expression of bile acids transporters OATP1A2, OATP1B1, OATP1B3 in intrahepatic cholestasis of pregnancy. Arch Gynecol Obstet. 2012 Jun;285(6):1535-40.

Wang L, Collins C, Kelly EJ, Chu X, Ray AS, Salphati L, Xiao G, Lee C, Lai Y, Liao M, Mathias A, Evers R, Humphreys G, Hop CE, Kumer SC, Unadkat JD. Transporter expression in

liver tissue from subjects with alcoholic or hepatitis C cirrhosis quantified by targeted quantitative proteomics. Drug Metab Dispos. 2016 Aug 19.

Wang X, Gattone V 2nd, Harris PC, Torres VE. Effectiveness of vasopressin V2 receptor antagonists OPC-31260 and OPC-41061 on polycystic kidney disease development in the PCK rat. J Am Soc Nephrol. 2005 Apr;16(4):846-51.

Wang X, Ward CJ, Harris PC, Torres VE. Cyclic nucleotide signaling in polycystic kidney disease. Kidney Int. 2010; 77:129–140.

Ward CJ, Hogan MC, Rossetti S, Walker D, Sneddon T, Wang X, Kubly V, Cunningham JM, Bacallao R, Ishibashi M, Milliner DS, Torres VE, Harris PC. The gene mutated in autosomal recessive polycystic kidney disease encodes a large, receptor-like protein. Nat Genet. 2002;30:259–269

Watashi K, Urban S, Li W, Wakita T.. NTCP and Beyond: Opening the Door to Unveil Hepatitis B Virus Entry. Int J Mol Sci. 2014 February; 15(2): 2892–2905.

Watkins PB, Lewis JH, Kaplowitz N, Alpers DH, Blais JD, Smotzer DM, Krasa H, Ouyang J, Torres V.E, Czerwiec FS, Zimmer CA. (2015). Clinical pattern of tolvaptan-associated liver injury in subjects with autosomal dominant polycystic kidney disease: analysis of clinical trials database. Drug Saf. 38, 1103–1113.

Watkins PB. Biomarkers for the diagnosis and management of drug-induced liver injury. Semin Liver Dis. 2009 Nov;29(4):393-9.

Watnick T, He N, Wang K, Liang Y, Parfrey P, Hefferton D, St George-Hyslop P, Germino G, Pei Y. Mutations of PKD1 in ADPKD2 cysts suggest a pathogenic effect of trans-heterozygous mutations. Nat Genet. 2000;25:143–4.

Weiler S, Merz M2, Kullak-Ublick GA. Drug-induced liver injury: the dawn of biomarkers? F1000Prime Rep. 2015 Mar 3;7:34.

Weinman SA. Electrogenicity of Na(þ)-coupled bile acid transporters. Yale J Biol Med. 1997 Jul-Aug; 70(4): 331–340.

Wilson PD, Sherwood AC, Palla K, Du J, Watson R, Norman JT. Reversed polarity of Na(+) -K(+) -ATPase: mislocation to apical plasma membranes in polycystic kidney disease epithelia. Am J Physiol. 1991 Mar;260(3 Pt 2):F420-30.

Wlcek K, Svoboda M, Riha J, Zakaria S, Olszewski U, Dvorak Z, Sellner F, Ellinger I, Jäger W, Thalhammer T. The analysis of organic anion transporting polypeptide (OATP) mRNA and protein patterns in primary and metastatic liver cancer. Cancer Biol Ther. 2011 May 1;11(9):801–11.

Wolf P. Biochemical diagnosis of liver disease Indian J Clin Biochem. 1999 Jan; 14(1): 59–90.

Wong MH, Oelkers P, Craddock AL, Dawson PA. Expression cloning and characterization of the hamster ileal sodium-dependent bile acid transporter. J Biol Chem. 1994 Jan 14;269(2):1340-7.

Woo DD, Nguyen DK, Khatibi N, and Olsen P. Genetic identification of two major modifier loci of polycystic kidney disease progression in pcy mice. J Clin Invest 100: 1934–1940, 1997.

Woon C, Bielinski-Bradbury A2, O'Reilly K3, Robinson P4. A systematic review of the predictors of disease progression in patients with autosomal dominant polycystic kidney disease. BMC Nephrol. 2015 Aug 15;16:140.

Wu G, D'Agati V, Cai Y, Markowitz G, Park JH, Reynolds DM, Maeda Y, Le TC, Hou H, Kucherlapati R, Edelmann W, Somlo S. Somatic inactivation of Pkd2 results in polycystic kidney disease. Cell. 1998;93:177–88.

Wu Z, Martin KO, Javitt NB, Chiang JYL. Structure and functions of human oxysterol 7α-hydroxylase cDNAs and gene CYP7B1. J Lipid Res. 1999;40:2195–2203.

Xia X, Francis H, Glaser S, Alpini G, LeSage G. Bile acid interactions with cholangiocytes. World J Gastroenterol. 2006 Jun 14;12(22):3553-63.

Xiong H, Suzuki H, Sugiyama Y, Meier PJ, Pollack GM, Brouwer KL. Mechanisms of impaired biliary excretion of acetaminophen glucuronide after acute phenobarbital treatment or phenobarbital pretreatment. Drug Metab Dispos. 2002 Sep;30(9):962-9.

Xu J, Liu Y, Yang Y, Bates S, Zhang JT.Characterization of oligomeric human half-ABC transporter ATP-binding cassette G2. J Biol Chem. 2004 May 7;279(19):19781-9.

Xu N, Glockner J, Rossetti S et al. Autosomal dominant polycystic kidney disease coexisting with cystic fibrosis. J Nephrol. 2006;19, 529–534.

Yamaguchi T, Nagao S, Kasahara M, et al. Renal accumulation and excretion of cyclic adenosine monophosphate in a murine model of slowly progressive polycystic kidney disease. Am J Kidney Dis. 1997; 30:703–709.

Yamazaki M, Miyake M, Sato H, Masutomi N, Tsutsui N, Adam KP, Alexander DC, Lawton KA, Milburn MV, Ryals JA, Wulff JE, Guo L. Perturbation of bile acid homeostasis is an early pathogenesis event of drug induced liver injury in rats. Toxicol Appl Pharmacol. 2013 Apr 1;268(1):79-89.

Yamazaki M, Miyake M, Sato H, Masutomi N, Tsutsui N, Adam KP, Alexander DC, Lawton KA, Milburn MV, Ryals JA, Wulff JE, Guo L. Perturbation of bile acid homeostasis is an early pathogenesis event of drug induced liver injury in rats. Toxicol Appl Pharmacol. 2013 Apr 1;268(1):79-89.

Yan H, Zhong G, Xu G, He W, Jing Z, Gao Z, Huang Y, Qi Y, Peng B, Wang H, Fu L, Song M, Chen P, Gao W, Ren B, Sun Y, Cai T, Feng X, Sui J, Li W. Sodium taurocholate cotransporting polypeptide is a functional receptor for human hepatitis B and D virus. Elife. 2012 Nov 13;1:e00049.

Yang K, Woodhead JL, Watkins PB, Howell BA, Brouwer KL. Systems pharmacology modeling predicts delayed presentation and species differences in bile acid-mediated troglitazone hepatotoxicity. Clin Pharmacol Ther. 2014 Nov;96(5):589-98.

Yerushalmi B, Dahl R, Devereaux MW, Gumpricht E, Sokol RJ. Bile acid-induced rat hepatocyte apoptosis is inhibited by antioxidants and blockers of the mitochondrial permeability transition. Hepatology. 2001;33:616–626.

Younossi ZM, Koenig AB, Abdelatif D2, Fazel Y, Henry L, Wymer M. Global epidemiology of nonalcoholic fatty liver disease-Meta-analytic assessment of prevalence, incidence, and outcomes. Hepatology. 2016 Jul;64(1):73-84.

Zamek-Gliszczynski MJ, Hoffmaster KA, Nezasa K, Tallman MN, Brouwer KL. Integration of hepatic drug transporters and phase II metabolizing enzymes: mechanisms of hepatic excretion of sulfate, glucuronide, and glutathione metabolites. Eur J Pharm Sci 2006 27:447-86.

Zamek-Gliszczynski MJ, Xiong H, Patel NJ, Turncliff RZ, Pollack GM, Brouwer KL. Pharmacokinetics of 5 (and 6)-carboxy-2',7'-dichlorofluorescein and its diacetate promoiety in the liver. J Pharmacol Exp Ther. 2003 Feb;304(2):801-9.

Zelcer N, Reid G, Wielinga P, Kuil A, van der Heijden I, Schuetz JD, Borst P. Steroid and bile acid conjugates are substrates of human multidrug-resistance protein (MRP) 4 (ATP-binding cassette C4). Biochem J. 2003 Apr 15;371(Pt 2):361-7.

Zeng H, Chen ZS, Belinsky MG, Rea PA, Kruh GD. Transport of methotrexate (MTX) and folates by multidrug resistance protein (MRP) 3 and MRP1: effect of polyglutamylation on MTX transport. Cancer Res. 2001 Oct 1;61(19):7225-32.

Zerres K, Mucher G, Becker J, Steinkamm C, Rudnik-Schoneborn S, Heikkila P, Rapola J, Salonen R, Germino GG, Onuchic L, Somlo S, Avner ED, Harman LA, Stockwin JM, Guay-Woodford LM: Prenatal diagnosis of autosomal recessive polycystic kidney disease (ARPKD): Molecular genetics, clinical experience, and fetal morphology. Am J Med Genet 76: 137–144, 1998.

Zerres K, Rudnik-Schoneborn S, Deget F, Holtkamp U, Brodehl J, Geisert J, Scharer K: Autosomal recessive polycystic kidney disease in 115 children: Clinical presentation, course and influence of gender. Acta Paediatr 85: 437–445, 1996

Zhang M, Chiang JY. Transcriptional regulation of the human sterol 12alpha-hydroxylase gene (CYP8B1): roles of heaptocyte nuclear factor 4alpha in mediating bile acid repression. J Biol Chem 2001; 276: 41690-41699

Zhao J, Yu BY, Wang DY, Yang JE.Promoter polymorphism of MRP1 associated with reduced survival in hepatocellular carcinoma. World J Gastroenterol. 2010 Dec 28;16(48):6104-10.

Zhou J. Polycystins and primary cilia: primers for cell cycle progression. Annu Rev Physiol. 2009;71:83-113.

Zhou SF, Wang LL, Di YM, Xue CC, Duan W, Li CG, Li Y. Substrates and inhibitors of human multidrug resistance associated proteins and the implications in drug development. Curr. Med. Chem. 2008 15:1981–2039.

Zollner G, Fickert P, Silbert D, Fuchsbichler A, Marschall HU, Zatloukal K, Denk H, Trauner M. Adaptive changes in hepatobiliary transporter expression in primary biliary cirrhosis. J Hepatol. 2003 Jun;38(6):717–27.

Zollner G, Fickert P, Zenz R, Fuchsbichler A, Stumptner C, Kenner L, Ferenci P, Stauber RE, Krejs GJ, Denk H, Zatloukal K, Trauner M. Hepatobiliary transporter expression in percutaneous liver biopsies of patients with cholestatic liver diseases. Hepatology. 2001 Mar;33(3):633-46.

Zollner G, Wagner M, Fickert P, Silbert D, Fuchsbichler A, Zatloukal K, Denk H, Trauner M. Hepatobiliary transporter expression in human hepatocellular carcinoma. Liver Int. 2005 Apr;25(2):367–79.

Zollner G, Wagner M, Fickert P, Silbert D, Gumhold J, Zatloukal K, Denk H, Trauner M. Expression of bile acid synthesis and detoxification enzymes and the alternative bile acid efflux pump MRP4 in patients with primary biliary cirrhosis. Liver Int. 2007 Sep;27(7):920-9.

CHAPTER 2. Hepatic Disposition of ^{99m}Technetium–Mebrofenin is Altered in Patients with Non-Alcoholic Steatohepatitis (NASH)[2]

INTRODUCTION

Non-alcoholic fatty liver disease (NAFLD) is one of the most common forms of liver disease in western societies; it is estimated that 20-30% of adults in the general population have NAFLD (Bellentani et al., 2010; Younossi et al., 2016). However, for reasons not fully elucidated, some patients progress to an inflammatory form of NAFLD known as nonalcoholic steatohepatitis (NASH). NASH is an advanced form of NAFLD defined by the histological confirmation of hepatic steatosis, hepatocyte ballooning, and lobular inflammation (Chalasani et al., 2012). NASH is a significant health concern that can progress to advanced fibrosis, cirrhosis, hepatocellular carcinoma, and liver failure (Hasimoto et al., 2009; Hui et al., 2003; Powell et al., 1990). Several medications (e.g. sulfonylureas, statins, thiazolidinediones) have been evaluated to prevent fibrosis and reverse inflammation in this patient population, but studies thus far have indicated no or marginal efficacy (Nakahara et al., 2012; Sanyal et al., 20120; Torres et al., 2001). Hence, no Food and Drug Administration (FDA)-approved pharmacological interventions currently exist and diet/weight loss remains the only effective measure to resolve NASH (Chalasani et al., 2012; Promrat et al., 2010). Because the liver is the primary site of action of medications to treat NASH, it is imperative to understand how NASH alters hepatic drug disposition.

[2] This chapter will be submitted to *Journal of Hepatology*, and is presented in the style of that journal.

The significance of hepatic transport proteins in the regulation of systemic and hepatic exposure of drugs is well established. Perturbation(s) in these processes, especially when drugs are eliminated through a single pathway, have been shown to significantly alter the pharmacokinetics, and in some cases, the pharmacodynamics of drugs (Kalliokoski et al., 2008; Lau et al., 2007). The expression of important hepatic uptake and efflux transporters is dysregulated in patients with NASH. The organic anion transporting polypeptides (OATPs), hepatic uptake transporters, are downregulated, while multidrug resistance-associated protein (MRP)2, and MRP3, hepatic efflux transporters, appear to be upregulated in liver biopsies from patients with NASH compared to healthy controls (Clark et al., 2014; Hardwick et al., 2011). The functional impact of increased MRP3 expression has been evaluated in patients with NASH; however, the impact of altered OATP and/or MRP2 expression has yet to be determined (Canet et al., 2015; Ferslew et al., 2015). Furthermore, MRP2 appears to be mislocalized from the canalicular membrane into the pericanalicular cytoplasm, which makes the impact of NASH on MRP2 function unclear (Hardwick et al., 2011). The purpose of the present study was to evaluate the functional impact of altered hepatic transporter protein expression in patients with biopsy-confirmed NASH using non-invasive imaging techniques.

^{99m}Technetium–mebrofenin (^{99m}Tc-mebrofenin or MEB) is a radiodiagnostic used to diagnose or differentiate hepatobiliary abnormalities such as structural disorders, infantile jaundice, and biliary obstruction (Balon et al., 1997; Ben-Haim et al. 1995; Doo et al. 1991). MEB is highly extracted by the liver; ~98% of the dose taken up by the liver and excreted into bile with minimal urinary excretion (~1-2% up to 24 hrs) and negligible metabolism (Krishnamurthy et al., 1990; Choletec package insert). MEB was chosen as a phenotypic probe because the hepatobiliary transport pathways of this agent are well defined. MEB is primarily

taken up by OATP1B1/OATP1B3 and is rapidly excreted by the canalicular transporter MRP2 (de Graaf et al., 2011; Ghibellini et al., 2008; Swift et al., 2010). Altered function of OATP- and MRP2-mediated transport would be expected to impact the systemic and hepatic exposure of MEB; this is evidenced by increased systemic exposure of MEB due to drug inhibition of OATP and prolonged hepatic exposure of MEB and other iminodiacetic acid analogs due to genetic impairment of MRP2/Mrp2 in TR- rats and patients with Dubin-Johnson syndrome (Bhargava et al., 2009; Doo et al., 1991; Hendrikse et al., 2004; Pfeifer et al., 2013; Pinós et al., 1990; Pinós et al., 1991). MRP3, a basolateral efflux transporter, also has been shown to transport MEB, but MRP3-mediated clearance of MEB appears to be significantly lower compared to MRP2-mediated clearance (Ghibellini et al., 2008; Pfeifer et al., 2013). Therefore, we evaluated the systemic concentrations and liver activity of MEB to understand the functional impact of NASH-associated changes in OATPs, MRP2, and MRP3 on MEB systemic and hepatic disposition.

PATIENTS AND METHODS

Patients

Healthy subjects and patients with biopsy-confirmed NASH, between 18 and 65 years of age and of any race and ethnicity who reported drinking less than 20g/day of alcohol were eligible for the study. Any subject that had a history of gastrointestinal surgery, autoimmune disease, or other gastrointestinal/liver abnormality was excluded. Females were excluded if they were, or were trying to become, pregnant. All subjects exhibited normal values for serum creatinine, total bilirubin, nonreactive HIV, hepatitis B antigen, and hepatitis C antibody. Healthy subjects were eligible if all clinical lab values were within the normal range as determined by the University of North Carolina at Chapel Hill (UNC-CH) Hospitals McLendon

Laboratories for: sodium, potassium, chloride, bicarbonate, blood urea nitrogen (BUN), fasting glucose, calcium, magnesium, phosphorus, albumin, aspartate transaminase (AST), alanine transaminase (ALT), and alkaline phosphatase (ALP), coagulation panel (PT/PTT), homeostatic model assessment for insulin resistance (HOMA-IR) score <2.5, BMI ≤ 30 kg/m^2, not taking any concomitant medications other than birth control or a standard multivitamin. Patients with NASH were recruited from the UNC-CH Hepatology Clinic and were eligible for enrollment if all of the following applied: biopsy confirmed noncirrhotic NASH with nonalcoholic fatty liver disease activity score (NAS) >3, BMI ≤ 45 kg/m^2, no treatment for type 2 diabetes other than metformin, no milk thistle products or high-dose antioxidant treatment during the prior 30 days, and absence of prior treatment with NASH-associated drugs (i.e., tamoxifen, amiodarone, methotrexate, prednisone, tetracyclines, or valproic acid). Written informed consent was obtained from all subjects. This study was approved by the UNC-CH Biomedical Institutional Review Board and published on ClinicalTrials.gov (NCT2235233).

Study design

This single-center, comparative cohort study, evaluated the pharmacokinetics of MEB in healthy subjects and patients with NASH. Subjects and patients who met all inclusion/exclusion criteria were admitted to the Clinical and Translational Research Center at UNC-CH Hospitals after fasting overnight. Vital signs were assessed and an intravenous catheter was placed in one arm delivering a normal saline drip. Prior to MEB administration, a transmission-emission acquisition was performed using a cobalt-57 flood source (Isotope Products Laboratories, Burbank, CA) positioned posteriorly, and gamma rays were detected in the cobalt window (122 KeV±15%) for 5-10 min on the anterior detector in the absence and presence of the subject. A ~2.5 mCi intravenous bolus dose of MEB was administered via an indwelling catheter placed in

a contralateral forearm or hand vein, which was removed after drug administration. Blood samples (3 mL) were collected at baseline (0), 2.5, 5, 7.5, 10, 15, 20, 40, 60, 80, 100, 120, 140, 160, 180, 210, 240, 270, and 300 min after administration; urine samples were collected at baseline (0) and at 180 min after administration. Anterior and posterior scintigraphic images of the abdomen were acquired dynamically in the ^{99m}Tc window (140 KeV ± 15%) at 1-min intervals using a dual headed gamma camera up to 180 min after administration. Prior to discharge, vital signs were assessed and subjects were administered a safety questionnaire.

Sample processing and analysis

Blood and urine samples were analyzed for MEB radioactivity with a sodium iodide well counter and corrected for decay (^{99m}Tc t1/2 = 6.01 hr). A blood sample (3 mL) collected at 20 min post-dose was centrifuged to obtain serum and ultrafiltrate using the CentrifreeT ultrafiltration membrane system (Millipore Ireland Ltd, Tullagreen, Cork Ireland) according to the manufacturer's instructions to determine the unbound fraction of MEB in serum. A subject-specific correction matrix was obtained as described previously (Pfeifer et al., 2013) and multiplied by the geometric mean of the anterior and posterior ^{99m}Tc-mebrofenin gamma scintigraphy images to generate time-activity curves (excluding the gall bladder) using Syngo MI applications version 6.5.9.19 (Siemens, New York, NY).

Mathematical simulation for sample size calculation

A previously published semi-physiologically based pharmacokinetic model was used to describe the hepatobiliary disposition of MEB (Pfeifer et al., 2013) and simulate altered disposition of MEB in a virtual population of healthy subjects and patients with NASH. The difference in hepatic exposure ($AUC_{0\text{-}\infty,\ liver}$) was selected as the primary endpoint. Based on the

modeling output and estimates of variability from a previous study (Pfeifer et al., 2013), feasibility, timeliness, and patient availability, the number of subjects recruited (n=14 healthy subjects and n=7 NASH patients) was sufficient to reject the null hypothesis of no difference in $AUC_{0-\infty,\ liver}$ between subject groups.

Pharmacokinetic data analysis

The pharmacokinetics of MEB were evaluated using noncompartmental analysis (NCA) (Phoenix WinNonlin v. 6.3). Pharmacokinetic parameters were estimated using the blood concentration-time profile and the liver counts/sec-time profile. The area under the concentration-time curve or liver activity-time curve (AUC) from time zero to the last time point ($AUC_{0-300,blood}$ or $AUC_{0-180,liver}$) was determined using a linear-up log-down trapezoidal algorithm. Total AUC ($AUC_{0-\infty}$) was calculated as the sum of AUC_{0-last} and C_{last}/λ_z where λ_z was estimated using the terminal elimination phase. The terminal half-life ($t_{1/2}$) was calculated as $0.693/\lambda_z$. Blood clearance (CL_{blood}) of MEB was calculated as the ratio of administered dose to $AUC_{0-\infty,blood}$. The percentage of the dose excreted in urine was calculated by dividing the total mass of MEB in urine after 180 min (the product of urine concentration and total volume collected) by the administered dose. Renal clearance (CL_{renal}) was calculated as the mass of MEB excreted over 180 min divided by the blood AUC from 0 to 180 min.

Statistical analysis strategy

MEB blood and liver pharmacokinetics are presented as geometric mean and 95% confidence intervals (CIs) with the exception of $t_{max,liver}$, which is presented as median and range. A two-tailed t-test ($\alpha = 0.05$) was used to compare the log transformed pharmacokinetic parameters between groups; the Wilcoxon Mann-Whitney test was used to detect differences in

median the of $t_{max,liver}$. Linear regression was used to identify an association between NASH severity (defined as the sum of NAS and fibrosis biopsy scores) and blood and hepatic pharmacokinetics of MEB (GraphPad Prism, San Diego, CA).

RESULTS

Study Subjects

Twenty-one volunteers (14 healthy subjects and 7 patients with biopsy-confirmed NASH) were studied (Table 2.1). Every effort was made to select healthy subjects that were comparable to patients with NASH based on age, sex, race, and ethnicity. Albumin, total bilirubin, activated partial thromboplastin time (APTT), and creatinine was within normal limits for both groups (Table 2.2). ALP was within the normal range for both groups, indicating no underlying evidence of cholestasis. Patients with NASH had a higher body weight and body mass index (BMI). Additionally, patients with NASH had higher levels of serum aminotransferases (i.e. ALT, AST), triglycerides, and insulin resistance as evidenced by elevated levels of fasting glucose, insulin, and HOMA-IR scores. Based on biopsy results, patients with NASH had a NAFLD activity score (NAS) greater than 3, with a maximum of 5, and fibrosis (F0-F3) (Table 2.2).

Blood and urine MEB pharmacokinetics

After administration of a ~2.5 mCi intravenous dose of MEB, blood concentrations declined rapidly followed by a slower terminal elimination phase (Fig. 2.1A). The geometric mean of C_{max} and area under the MEB blood-concentration time curve ($AUC_{0-\infty,\ blood}$) was significantly increased by 1.9- and 1.7-fold in patients with NASH, respectively. Blood clearance (CL_{blood}) in healthy subjects was similar to values reported in healthy control subjects in

Ghibellini et al. (2004 and 2008) and Pfeifer et al. (2013); the geometric mean of CL_{blood} was significantly decreased by 60% in patients with NASH (Table 2.3). The terminal elimination half-life of MEB appeared to increase from 242 min to 314 min in patients with NASH, but there was no statistically significant difference in the elimination rate constant ($\lambda_{z,blood}$) (Table 2.3). Although albumin levels were similar between each group, the unbound fraction (f_u) of MEB in the plasma was evaluated to account for any potential difference in pharmacokinetics; as shown, there was no statistically significant difference in MEB f_u between healthy subjects and patients with NASH (Table 2.3). Urinary recovery of MEB was less than 1% and CL_{renal} was not different between healthy subjects and patients with NASH (Table 2.3).

Liver pharmacokinetics

Gamma scintigraphy of MEB over 180 min revealed rapid uptake of MEB by the liver. The time-to-maximal activity in the liver ($t_{max,\ liver}$) was 13 min and was comparable between both groups (Table 2.3). These results are consistent with previously reported values (Doo et al., 1991; Krishnamurthy et al., 1989; Pfeifer et al., 2013). The area under the MEB liver-activity time curve ($AUC_{0-\infty,\ liver}$) and maximal liver activity (X_{max}) was significantly increased by 2.0-fold and 1.4-fold in patients with NASH, respectively (Fig. 2.1B). The half-life of MEB in the liver ($t_{1/2,liver}$) also increased from 22.5 to 36.5 min, indicating impaired excretion of MEB compared to healthy subjects; the elimination rate constant of MEB in the liver ($\lambda_{z,30\text{-}80\ min,\ liver}$) was significantly decreased in patients with NASH (Table 2.3).

Linear Regression Analysis

Univariate linear regression detected a moderate association between NASH severity score (NAS+fibrosis) and blood exposure ($AUC_{0-\infty,\ blood}$) ($R^2 = 0.443$, p-value = 0.001) (Fig.

2A). Importantly, a strong correlation was detected between NASH severity score and blood C_{max} (R^2 = 0.683, p-value < 0.0001) as well as liver exposure ($AUC_{0-\infty, liver}$) (r^2 = 0.775, p-value < 0.0001) (Fig. 2.2B and 2.2C).

DISCUSSION

This is the first study to employ quantitative γ-scintigraphy techniques to assess the impact of NASH-associated alterations in hepatic uptake and efflux function in humans using a transporter probe substrate. This study demonstrated that patients with biopsy-confirmed NASH exhibited increased systemic and hepatic exposure of MEB, a hepatobiliary imaging agent, consistent with literature reports of disease-associated decreases in OATP expression, increases in MRP3 expression, and MRP2 mislocalization (Clark et al., 2014b; Dzierlenga et al., 2016; Hardwick et al., 2011; Hardwick et al., 2014).

Lake et al. (2011) first reported global gene expression changes associated with absorption, distribution, metabolism, and excretion (ADME) processes, including phase I and II drug metabolizing enzymes and hepatic transporters, in patients with NASH. These changes appear to be driven by an adaptive hepatoprotective response to prevent further injury. Due to the prevalence of comorbidities such as type 2 diabetes mellitus, hypertension, and dyslipidemia in this population, many of these patients are taking multiple medications (Portincasa et al., 2006). Hence, altered ADME processes may impact the disposition, efficacy, and/or safety of drugs in patients with NASH. Subsequent studies revealed increased protein expression of ATP-binding cassette (ABC) efflux transporters with NAFLD disease progression, including *ABCC2* (MRP2), although MRP2 appeared to be mislocalized from the canalicular membrane (Hardwick et al., 2011). Because MRP2-mediated transport is the rate-limiting step in canalicular efflux of MEB

(Araikum et al., 1996; Neyt et al., 2013), altered expression and/or localization of MRP2 would be expected to affect MEB liver exposure. Hepatic MEB exposure was significantly increased 2.0-fold compared to healthy age- and sex-matched subjects. This shift towards hepatic retention likely reflects mislocalization of MRP2 as evidenced by immunohistochemistry leading to reduced MRP2 function (Canet et al., 2015; Dzierlenga et al., 2015; Dzierlenga et al., 2016). The half-life of MEB in the liver increased from 22.5 to 36.5 min in patients with NASH, which supports our observations of increased hepatic retention. Linear regression analysis revealed the NASH severity score was able to predict hepatic exposure of MEB (Fig. 2.2C). Although Hardwick et al. (2011) reported increased MRP2 expression in patients with NASH, Okushin et al. (2015) recently reported that hepatic expression levels of MRP2 were inversely correlated with NAFLD progression in humans. Therefore, decreased expression of MRP2 cannot be dismissed as a contributing mechanism to our observations. Increased hepatic exposure of MEB is a novel finding, which is likely due to the functional impairment of MRP2. These data are consistent with human studies and experimental rodent models of NASH. For example, patients with Dubin-Johnson syndrome who lack functional MRP2 exhibit increased and prolonged exposure to MEB (Bar-Meir et al., 1982). In diet-induced rodent models of NASH, magnetic resonance imaging (MRI) of gadolinium-ethoxybenzyl-diethylenetriamine pentaacetic acid (Gd-EOB-DTPA), an OATP and MRP2 substrate, revealed that liver half-life was significantly increased in NASH animals (Tsuda et al., 2007; Tsuda et al. 2011). Enhanced hepatic exposure and increased half-life of Gd-EOB-DTPA in NASH rodents are consistent with our findings in patients with NASH using MEB.

Blood C_{max} and $AUC_{0\text{-}\infty,blood}$ were significantly increased by 1.9-fold and 1.7-fold in patients with NASH, respectively. This likely reflects decreased hepatic uptake of MEB by

OATPs, consistent with reports of OATP downregulation in NASH (Canet et al., 2014; Fisher et al., 2009). MEB is also a MRP3 substrate (Ghibellini et al., 2008; Pfeifer et al., 2013). Pharmacokinetic studies support increased MRP3-mediated efflux in patients with NASH; therefore, MRP3 may contribute to increased systemic concentrations observed in the present study (Canet et al., 2015b; Ferslew et al., 2015). Although OATPs and MRP3 mediate the basolateral uptake and efflux of MEB, respectively, pharmacokinetic modeling reveal that modest changes (i.e. < 5-fold) in these clearance pathways will have a negligible effect on hepatic exposure because MRP2-mediated excretion is the rate-limiting step in MEB clearance from the liver (Pfeifer et al., 2013). Likewise, systemic exposure is sensitive to alterations in OATPs and MRP3-mediated transport of MEB (Pfeifer et al., 2013); thus, increased systemic exposure likely reflects altered OATP and/or MRP3-mediated function.

Altered hepatic transporter function due to disease, genetic polymorphisms, or drug-drug interactions (DDIs) can contribute to interindividual variability in drug/metabolite systemic and hepatic disposition thereby affecting therapeutic efficacy and/or safety. OATPs (e.g. OATP1B1 and OATP1B3) have emerged as important determinants of hepatic uptake and consequently, systemic pharmacokinetics. For example, elevated concentrations of statins due to OATP inhibition are associated with increased prevalence of myopathy which can lead to life-threatening rhabdomyolysis (Ballantyne et al., 2003; Omar et al., 2001; Omar et al., 2002); increased simvastatin concentrations have been observed in a rodent model of NASH (Clarke et al., 2014b). Conversely, drugs whose site of action is the liver (e.g. statins) or rely on hepatic biotransformation to active metabolites (e.g. morphine) may display altered hepatic exposure thereby impacting pharmacodynamic response. Other clinically-relevant examples of OATP

substrates that may be impacted by altered OATP expression include repaglinide, enalapril, and olmesartan (Kalliokoski et al., 2009).

Biliary excretion is a major route of elimination for drugs and metabolites. Therefore, knowledge about hepatobiliary disposition and its relationship to clearance is essential to understanding drug pharmacokinetics .The notion that MRP2 function in NASH is impaired may have unintended consequences for drug disposition thereby placing a larger burden on the liver. For example, spiramycin has been associated with cholestatic hepatitis despite its favorable safety profile relative to other macrolide antibiotics (Denie et al., 1992). In vivo pharmacokinetics studies in Mrp2 knockout (KO) mice revealed a ~10-fold decrease in Mrp2-mediated biliary excretion, which suggests that patients with impaired MRP2 function, such as in NASH demonstrated in the current study, may be susceptible to spiramycin-induced liver injury (Tian et al., 2007). Interruption of the enterohepatic recirculation of mycophenolate and its glucuronide conjugate by the MRP2 inhibitor cyclosporine A unexpectedly decreased mycophenolic acid systemic exposure. Hence, it is conceivable that impaired MRP2 function could decrease systemic pharmacokinetics of drugs which may alter pharmacodynamic response (Pou et al., 2001). However, the dynamic interplay and overlapping substrate specificity between multiple uptake and efflux transporters (e.g. P-glycoprotein, breast cancer resistance protein) must be considered when predicting the clinical relevance of altered drug disposition (Varma et al., 2016).

Although a relatively low number of volunteers with NASH were enrolled in this study, the precision of pharmacokinetic parameters was increased by recruiting 2:1 healthy to NASH subjects. Ethical considerations precluded a biopsy to specifically quantify transporter expression, but OATP downregulation and MRP2 internalization are well documented in this

population. To define a homogenous population and confounding variables, subjects were excluded if they had evidence of cirrhosis, portal hypertension, or decompensated liver disease, a history of immune-related disease, bariatric surgery, a history of drugs associated with fatty liver disease or steatohepatitis, or were taking any type II diabetes medications other than metformin. Patients with a histological confirmation of NASH with an NAS score of >3 were enrolled because changes in transporter expression are expected after the onset of inflammation (Hardwick et al., 2011).

In conclusion, patients with biopsy-confirmed NASH displayed increased systemic and hepatic concentrations of MEB compared to age- and sex-matched healthy subjects. Specifically, these changes are consistent with NASH-associated downregulation of OATPs, upregulation of MRP3, and mislocalization of MRP2. Given the increasing prevalence of NAFLD and NASH, these data indicate that dysregulation of hepatic transporters may alter the systemic and hepatic exposure of drugs/metabolites. Further understanding how NASH affects hepatic and extrahepatic clearance mechanisms will improve the ability to predict drug disposition, efficacy, and safety of new and existing medications in this patient population.

REFERENCES

Araikum S, Mdaka T, Esser JD, Zuckerman M. Hepatobiliary kinetics of technetium-99m-IDA analogs: quantification by linear systems theory. Journal of Nuclear Medicine. 1996;37:1323–1330.

Ballantyne CM, Corsini A, Davidson MH, et al. Risk for myopathy with statin therapy in high-risk patients. Arch Intern Med. 2003;163(5):553–564.

Balon HR, Fink-Bennett DM, Brill DR, Fig LM, Freitas JE, Krishnamurthy GT, Klingensmith WC 3rd, Royal HD. Procedure guideline for hepatobiliary scintigraphy. Society of Nuclear Medicine. J Nucl Med. 1997 Oct;38(10):1654-7.

Bar-Meir S, Baron J, Seligson U, Gottesfeld F, Levy R, Gilat T. 99mTc-HIDA cholescintigraphy in Dubin-Johnson and Rotor syndromes. Radiology. 1982 Mar; 142(3):743-6.

Bhargava KK, Joseph B, Ananthanarayanan M, Balasubramaniyan N, Tronco GG, Palestro CJ, Gupta S. Adenosine triphosphate-binding cassette subfamily C member 2 is the major transporter of the hepatobiliary imaging agent (99m)Tc-mebrofenin. J Nucl Med. 2009 Jul;50(7):1140-6.

Bellentani S, Scaglioni F, Marino M, Bedogni G. Epidemiology of non-alcoholic fatty liver disease. Dig Dis. 2010;28(1):155-61.

Ben-Haim S, Seabold JE, Kao SC, Johnson J, Tran D, Brown BP. Utility of Tc-99m mebrofenin scintigraphy in the assessment of infantile jaundice. Clin Nucl Med. 1995 Feb;20(2):153-63.

Canet MJ, Merrell MD, Hardwick RN, Bataille AM, Campion SN, Ferreira DW, Xanthakos SA, Manautou JE, Hesham A-Kader H, Erickson RP, Cherrington NJ. Altered regulation of hepatic efflux transporters disrupts acetaminophen disposition in pediatric nonalcoholic steatohepatitis. Drug Metab Dispos. 2015 Jun;43(6):829-35.

Canet MJ, Hardwick RN, Lake AD, Dzierlenga AL, Clarke JD, Cherrington NJ. Modeling human nonalcoholic steatohepatitis-associated changes in drug transporter expression using experimental rodent models. Drug Metab Dispos. 2014 Apr;42(4):586-95.

Chalasani N, Younossi Z, Lavine JE, Diehl AM, Brunt EM, Cusi K, Charlton M, Sanyal AJ; American Association for the Study of Liver Diseases; American College of Gastroenterology; American Gastroenterological Association. The diagnosis and management of non-alcoholic fatty liver disease: Practice guideline by the American Association for the Study of Liver Diseases, American College of Gastroenterology, and the American Gastroenterological Association. Am J Gastroenterol. 2012 Jun;107(6):811-26.

Choletec® [package insert]. Bracco Diagnostics. Princeton, NJ; 2014.

Clarke JD, Hardwick RN, Lake AD, Lickteig AJ, Goedken MJ, Klaassen CD, Cherrington NJ. Synergistic interaction between genetics and disease on pravastatin disposition. JHepatol. 2014a 61,139–147.

Clarke JD, Hardwick RN, Lake AD, Canet MJ, Cherrington NJ. Experimental nonalcoholic steatohepatitis increases exposure to simvastatin hydroxy acid by decreasing hepatic organic anion transporting polypeptide expression. J Pharmacol Exp Ther. (2014b) Mar;348(3):452-8

Denie C, Henrion J, Schapira M, Schmitz A, Heller FR. Spiramycin-induced cholestatic hepatitis. J Hepatol. 1992 Nov;16(3):386.

Doo E, Krishnamurthy GT, Eklem MJ, Gilbert S, Brown PH. Quantification of hepatobiliary function as an integral part of imaging with technetium-99m-mebrofenin in health and disease. J Nucl Med. 1991 Jan;32(1):48-57.

de Graaf W, Häusler S, Heger M, van Ginhoven TM, van Cappellen G, Bennink RJ, Kullak-Ublick GA, Hesselmann R, van Gulik TM, Stieger B. Transporters involved in the hepatic uptake of (99m)Tc-mebrofenin and indocyanine green. J Hepatol. 2011 Apr;54(4):738-45.

Dzierlenga AL, Clarke JD, Hargraves TL, Ainslie GR, Vanderah TW, Paine MF, Cherrington NJ. Mechanistic basis of altered morphine disposition in nonalcoholic steatohepatitis. J Pharmacol Exp Ther. 2015 Mar;352(3):462-70.

Dzierlenga AL, Clarke JD, Klein DM, Anumol T, Snyder SA, Li H, Cherrington NJ. Biliary Elimination of Pemetrexed Is Dependent on Mrp2 in Rats: Potential Mechanism of Variable Response in Nonalcoholic Steatohepatitis. J Pharmacol Exp Ther. 2016 Aug;358(2):246-53.

Ferslew BC, Johnston CK, Tsakalozou E, Bridges AS, Paine MF, Jia W, Stewart PW, Barritt AS 4th, Brouwer KL. Altered morphine glucuronide and bile acid disposition in patients with nonalcoholic steatohepatitis. Clin Pharmacol Ther. 2015 Apr;97(4):419-27.

Fisher CD, Lickteig, AJ, Augustine, LM, Oude Elferink, RP, Besselsen DG, Erickson RP, Cherrington, NJ. Experimental non-alcoholic fatty liver disease results in decreased hepatic uptake transporter expression and function in rats. Eur J Pharmacol. 2009 Jun 24;613(1-3):119-27.

Ghibellini G, Leslie EM, Pollack GM, Brouwer KL. Use of tc-99m mebrofenin as a clinical probe to assess altered hepatobiliary transport: integration of in vitro, pharmacokinetic modeling, and simulation studies. Pharm Res. 2008 Aug;25(8):1851-60.

Ghibellini G, Johnson BM, Kowalsky RJ, Heizer WD, Brouwer KL. A novel method for the determination of biliary clearance in humans. AAPS J. 2004 Nov 23;6(4):e33.

Hardwick RN, Fisher CD, Canet MJ, Scheffer GL, Cherrington NJ. Variations in ATP-binding cassette transporter regulation during the progression of human nonalcoholic fatty liver disease. Drug Metab Dispos. 2011 Dec;39(12):2395-402.

Hardwick RN, Clarke JD, Lake AD, Canet MJ, Anumol T, Street SM, Merrell MD, Goedken MJ, Snyder SA, Cherrington NJ. Increased susceptibility to methotrexate-induced toxicity in nonalcoholic steatohepatitis. Toxicol Sci. 2014 Nov;142(1):45-55.

Hashimoto E, Satoru Yatsuji, Maki Tobari, Makiko Taniai, Nobuyuki Torii, Katsutoshi Tokushige, Keiko Shiratori. Hepatocellular carcinoma in patients with nonalcoholic steatohepatitis. J Gastroenterol. 2009 Jan;44 Suppl 19:89-95.

Hendrikse NH, Kuipers F, Meijer C, Havinga R, Bijleveld CM, van der Graaf WT, Vaalburg W, de Vries EG. In vivo imaging of hepatobiliary transport function mediated by multidrug resistance associated protein and P-glycoprotein. Cancer Chemother Pharmacol. 2004 Aug;54(2):131-8.

Hui JM, Kench JG, Chitturi S, Suda A, Farrell GC, Byth K, et al. Long-term outcomes of cirrhosis in nonalcoholic steatohepatitis compared with hepatitis C. Hepatology. 2003 Aug;38(2):420-7.

Kalliokoski A, Backman JT, Neuvonen PJ, Niemi M. Effects of the SLCO1B1*1B haplotype on the pharmacokinetics and pharmacodynamics of repaglinide and nateglinide. Pharmacogenet Genomics. 2008 Nov; 18(11):937-42.

Kalliokoski A, Niemi M. Impact of OATP transporters on pharmacokinetics. Br J Pharmacol. 2009 Oct; 158(3): 693–705.

Krishnamurthy GT, Turner FE. Pharmacokinetics and clinical application of technetium 99m-labeled hepatobiliary agents. Semin Nucl Med. 1990 Apr;20(2):130-49.

Lake AD, Novak P, Fisher CD, Jackson JP, Hardwick RN, Billheimer DD, Klimecki WT, Cherrington NJ. Analysis of global and absorption, distribution, metabolism, and elimination gene expression in the progressive stages of human nonalcoholic fatty liver disease. Drug Metab Dispos. 2011 Oct;39(10):1954-60.

Lau YY, Huang Y, Frassetto L, Benet LZ. Effect of OATP1B transporter inhibition on the pharmacokinetics of atorvastatin in healthy volunteers. Clin Pharmacol Ther. 2007 Feb;81(2):194-204.

Lee HY, Birkenfeld AL, Jornayvaz FR, Jurczak MJ, Kanda S, Popov V, Frederick DW, Zhang D, Guigni B, Bharadwaj KG, Choi CS, Goldberg IJ, Park JH, Petersen KF, Samuel VT, Shulman GI. Apolipoprotein CIII overexpressing mice are predisposed to diet-induced hepatic steatosis and hepatic insulin resistance. Hepatology. 2011 Nov;54(5):1650-60.

Lim S, Oh TJ, Koh KK. Mechanistic link between nonalcoholic fatty liver disease and cardiometabolic disorders. Int J Cardiol. 2015 Dec 15;201:408-14.

Nakahara T, Hyogo H, Kimura Y, Ishitobi T, Arihiro K, Aikata H, Takahashi S, Chayama K. Efficacy of rosuvastatin for the treatment of non-alcoholic steatohepatitis with dyslipidemia: An open-label, pilot study. Hepatol Res. 2012 Nov;42(11):1065-72.

Neyt S, Huisman MT, Vanhove C, De Man H, Vliegen M, Moerman L, Dumolyn C, Mannens G, De Vos F. In vivo visualization and quantification of (Disturbed) Oatp-mediated hepatic uptake and Mrp2-mediated biliary excretion of 99mTc-mebrofenin in mice. J Nucl Med. 2013 Apr;54(4):624-30.

Okushin K, Tsutsumi T, Enooku K, Fujinaga H, Kado A, Shibahara J, Fukayama M, Moriya K, Yotsuyanagi H, Koike K. The intrahepatic expression levels of bile acid transporters are inversely correlated with the histological progression of nonalcoholic fatty liver disease. J Gastroenterol. 2015 Nov 25 1-11.

Omar MA, Wilson JP, Cox TS. Rhabdomyolysis and HMG-CoA reductase inhibitors. Ann Pharmacother. 2001 Sep;35(9):1096-107.

Omar MA, Wilson JP. FDA adverse event reports on statin-associated rhabdomyolysis. Ann Pharmacother. 2002 Feb;36(2):288-95.

Pfeifer ND, Goss SL, Swift B, Ghibellini G, Ivanovic M, Heizer WD, Gangarosa LM, and Brouwer LR. Effect of Ritonavir on 99mTechnetium–Mebrofenin Disposition in Humans: A Semi-PBPK Modeling and In Vitro Approach to Predict Transporter-Mediated DDIs. CPT Pharmacometrics Syst Pharmacol. 2013 Jan; 2(1): e20.

Pinós, T., Figueras, C. & Herranz, R. Scintigraphic diagnosis of Dubin-Johnson syndrome: DISIDA is also useful. Am J Gastroenterol. 1991 Nov;86(11):1687-8.

Pinós, T., Constansa, J.M., Palacin, A. & Figueras, C. A new diagnostic approach to the Dubin-Johnson syndrome. Am J Gastroenterol. 1990 Jan;85(1):91-3.

Portincasa P, Grattagliano I, Palmieri VO, Palasciano G. Current pharmacological treatment of nonalcoholic fatty liver. Curr Med Chem. 2006;13(24):2889-900.

Pou L, Brunet M, Cantarell C, Vidal E, Oppenheimer F, Monforte V, Vilardell J, Roman A, Martorell J, Capdevila L. Mycophenolic acid plasma concentrations: influence of comedication. Ther Drug Monit. 2001 Feb;23(1):35-8.

Powell EE, Cooksley WGE, Hanson R, Searle J, Halliday JW, Powell LW. The natural history of nonalcoholic steatohepatitis: a follow-up study of forty-two patients for up to 21 years. Hepatology. 1990 Jan;11(1):74-80.

Promrat K, Kleiner DE, Niemeier HM, Jackvony E, Kearns M, Wands JR, Fava JL, Wing RR. Randomized controlled trial testing the effects of weight loss on nonalcoholic steatohepatitis. Hepatology. 2010 Jan;51(1):121-9.

Sanyal, AJ et al. Pioglitazone, vitamin E, or placebo for nonalcoholic steatohepatitis. N Engl J Med. 2010 May 6;362(18):1675-85.

Swift B, Yue W, Brouwer KL. Evaluation of (99m)technetium-mebrofenin and (99m)technetium-sestamibi as specific probes for hepatic transport protein function in rat and human hepatocytes. Pharm Res. 2010 Sep;27(9):1987-98.

Tian X, Li J, Zamek-Gliszczynski MJ, Bridges AS, Zhang P, Patel NJ, Raub TJ, Pollack GM, Brouwer KL. Roles of P-glycoprotein, Bcrp, and Mrp2 in biliary excretion of spiramycin in mice. Antimicrob Agents Chemother. 2007 Sep;51(9):3230-4.

Torres, DM, Jones, F., Shaw, JC, Williams, CD, Ward, JA, Harrison, SA. Rosiglitazone versus rosiglitazone and metformin versus rosiglitazone and losartan in the treatment of nonalcoholic stea-tohepatitis in humans: a 12-month randomized, prospective, open-label trial. Hepatology. 2011 Nov;54(5):1631-9.

Tsuda N, Okada M, Murakami T. Potential of gadolinium-ethoxybenzyl-diethylenetriamine pentaacetic acid (Gd-EOB-DTPA) for differential diagnosis of nonalcoholic steatohepatitis and fatty liver in rats using magnetic resonance imaging. Invest Radiol. 2007 Apr;42(4):242-7.

Varma MV, El-Kattan AF. Transporter-Enzyme Interplay: Deconvoluting Effects of Hepatic Transporters and Enzymes on Drug Disposition Using Static and Dynamic Mechanistic Models. J Clin Pharmacol. 2016 Jul;56 Suppl 7:S99-S109.

Younossi ZM, Koenig AB, Abdelatif D, Fazel Y, Henry L, Wymer M. Global epidemiology of nonalcoholic fatty liver disease-Meta-analytic assessment of prevalence, incidence, and outcomes. Hepatology. 2016 Jul;64(1):73-84.

Figure 2.1. ^{99m}Tc-mebrofenin (MEB) concentrations and liver activity in patients with NASH. MEB blood concentration vs. time curves (A); liver scintigraphy vs. time curves (B) in healthy subjects (black) and patients with NASH (grey) Data represent mean ± SD.

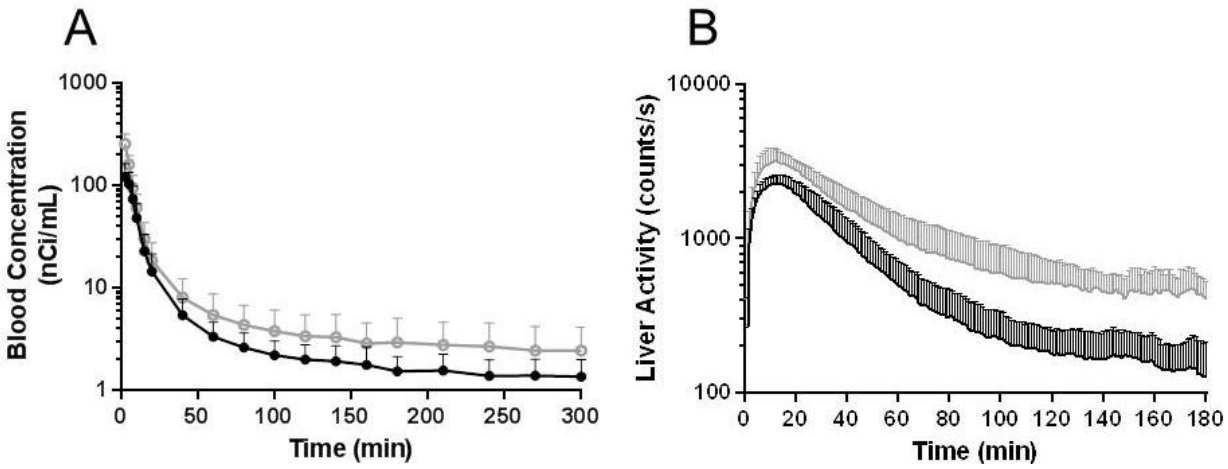

Figure 2.2 Association between NASH severity score and ^{99m}Tc-mebrofenin (MEB) pharmacokinetics. Association between NASH severity score (NAS+fibrosis) and ^{99m}Tc-mebrofenin (MEB) blood C_{max} (A), $AUC_{0\text{-}\infty,blood}$ (B), and $AUC_{0\text{-}\infty,liver}$ (C) in healthy subjects (black) and patients with NASH (grey). The best-fit line is represented by the solid black line while the 5th and 95th confidence intervals are represented by the lower and upper dashed lines, respectively. Results from linear regression are presented as the coefficient of determination (R^2), regression parameter estimate (β ± standard deviation of the parameter estimate), and the p-value.

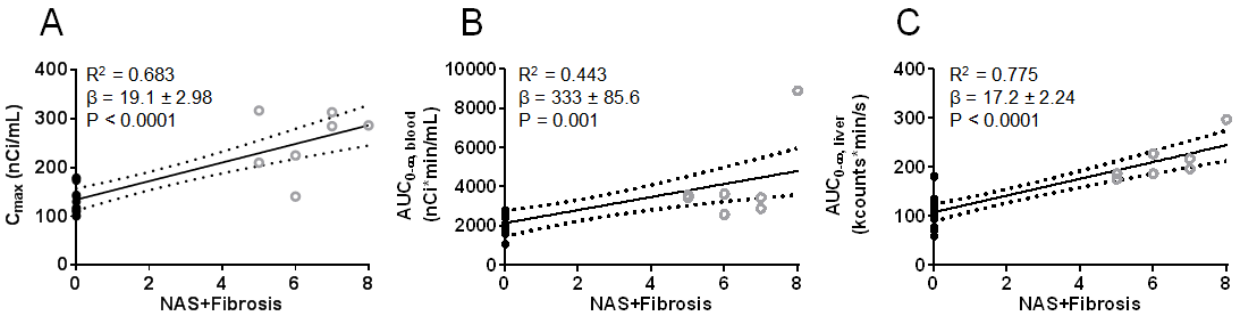

Table 2.1. Demographic characteristics of study participants

Parameter		Healthy (n=14)	NASH (n=7)
Sex			
	Men	8	4
	Women	6	3
Ethnicity	**Hispanic**	0	1
	Non-Hispanic	14	6
Race	**White**	11	5
	Hispanic	0	1
	Asian	1	1
	Black	3	0
Age (years)		38.9 (15.4)	37.4 (17.4)
Body weight (kg)		72.1 (12.1)	102 (16)*
Body mass index (kg/m^2)		24.4 (2.2)	33.3 (5.1)*
Waist circumference (cm)		81.9 (8.3)	111 (15)*
Hip circumference (cm)		89.3 (8.6)	119 (14)*
Waist-to-hip ratio	**All subjects**	0.90 (0.05)	1.00 (0.04)*
	Men	0.91 (0.06)	1.00 (0.04)*
	Women	0.88 (0.06)	1.01 (0.06)*

Data presented as mean (standard deviation); *$p < 0.05$ using two-tailed Student's t-test.

Table 2.2. Clinical chemistries and liver biopsy grade

Clinical parameter	Healthy	NASH
Creatinine (mg/dL)	0.86 (0.17)	0.83 (0.15)
Albumin (g/dL)	4.2 (0.2)	4.5 (0.4)
ALP (U/L)	56.3 (17.8)	68.1 (20.0)
ALT (U/L)	28.7 (9.8)	113 (60)*
AST (U/L)	25.2 (8.0)	72.9 (34.3)*
APTT (s)	31.3 (2.7)	33.7 (1.6)
Bilirubin, total (mg/dL)	0.7 (0.2)	1.0 (0.4)
Cholesterol (mg/dL)	153 (25)	133 (40)
Triglycerides (mg/dL)	73.2 (32.8)	146 (47)*
HDL (mg/dL)	57.4 (15.9)	42.2 (12.5)
LDL-direct (mg/dL)	86.1 (22.4)	72.5 (41.1)
Glucose, fasting (mg/dL)	86.6 (6.3)	142 (81)*
HOMA-IR	1.56 (0.53)	8.18 (4.56)*
Serum insulin (µIU/mL)	7.3 (2.8)	24.3 (8.6)*
Total NAS score	N/A	4 (4-5)
Steatosis	N/A	2 (2-3)
Hepatocyte ballooning	N/A	1 (0-1)
Inflammation	N/A	1 (1-2)
Fibrosis	N/A	2 (0-3)
NAS + Fibrosis	N/A	6 (5-8)

Data are presented as mean (standard deviation); biopsy scoring presented as median (range); *$p < 0.05$ using two-tailed Student's t-test. ALP, alkaline phosphatase; ALT, alanine aminotransferase; AST, aspartate aminotransferase; APPT; activated partial thromboplastin time; HDL, high-density lipoprotein; HOMA-IR, homeostasis model for assessing insulin resistance; LDL, low-density lipoprotein; NAS, nonalcoholic fatty liver disease activity score.

Table 2.3. Pharmacokinetics of ^{99m}Tc-mebrofenin in healthy subjects and patients with NASH

Parameter	Healthy	NASH
Administered dose[a] (mCi)	2.47 (0.16)	2.46 (0.23)
C_{max} (nCi/mL)	132 (117-148)	246* (188-322)
$AUC_{0\text{-}300,blood}$ (nCi*min/mL)	1700 (1440-2000)	2670* (1960-3640)
$AUC_{0\text{-}\infty,blood}$ (nCi*min/mL)	2150 (1840-2600)	3760* (2590-5450)
CL_{blood} (mL/min/kg)	16.1 (13.9-18.8)	6.49* (4.16-10.1)
$\lambda_{z,blood}$ (min)	0.00286 (0.00243-0.00337)	0.00221 (0.00161-0.00303)
Unbound fraction (f_u)[a]	0.0667 (0.0310)	0.0855 (0.0400)
Urinary recovery[b] (% of dose)	0.515 (0.390-0.681)	0.794 (0.557-1.13)
CL_{renal} (mL/min/kg)	0.117 (0.088-0.154)	0.082 (0.063-0.109)
$AUC_{0\text{-}180,liver}$ (kcounts*min/sec)	103 (87-122)	186* (157-219)
$AUC_{0\text{-}\infty,liver}$ (kcounts*min/sec)	105 (88-124)	210* (178-248)
$X_{max,liver}$ (counts/sec)	2350 (2180-2530)	3230* (2635-3970)
$t_{max,liver}$[c] (min)	13 (12-15)	13 (11-17)
$\lambda_{z,30\text{-}80\ min,\ liver}$ (min)	0.0309 (0.0275-0.0345)	.0190* (0.0127-0.0284)

Data presented as geometric mean (95% CI). [a]Mean (standard deviation). [b]Total mass excreted from 0-180 min. [c]Median (range). *$p < 0.05$, Student's two-tailed t-test of log transformed data comparing healthy subjects to patients with NASH. Maximal blood concentration (C_{max}), area under the blood-concentration time curve (AUC_{blood}), blood clearance (CL_{blood}), blood elimination rate constant ($\lambda_{z,blood}$), area under the liver activity-time curve (AUC_{liver}), maximal liver activity (X_{max}), renal clearance (CL_{renal}), time to maximum liver activity ($t_{max,liver}$), and liver elimination rate constant ($\lambda_{z,\ 30\text{-}80\ min,liver}$)

CHAPTER 3. Inhibition of Human Hepatic Bile Acid Transporters by Tolvaptan and Metabolites: Contributing Factors to Drug-Induced Liver Injury?[3]

INTRODUCTION

Autosomal Dominant Polycystic Kidney Disease (ADPKD) is a monogenic inheritable disease characterized by progressive renal cyst development, often leading to end-stage-renal-disease. Supportive care and surgical interventions represent the mainstay of ADPKD treatment because no Food and Drug Administration (FDA)-approved therapy currently exists (Patel et al., 2014; Torres et al., 2007). Tolvaptan, an orally available benzazepine derivative, is a selective vasopressin V2-receptor antagonist (Yamamura et al., 1998) used in the treatment of clinically significant hyponatremia (Schrier et al., 2006), volume overload in heart failure (Fukunami et al., 2011) and liver cirrhosis with edema (Sakaida, 2015). Tolvaptan recently has shown promise for delaying renal cyst progression in ADPKD (Boertien et al., 2015; Higashihara et al. 2011; Torres et al., 2012) with approvals in Canada and Europe for this indication. In the pivotal clinical trial, however, tolvaptan was associated with liver injury evident as increased liver enzymes and bilirubin in some patients. No signals of liver injury have been observed in patient populations treated with tolvaptan for other indications or in nonclinical studies (Oi et al., 2011; Watkins et al. 2015). The etiology and/or biological mechanism(s) underlying tolvaptan-associated liver injury in patients with ADPKD have yet to be elucidated.

[3] This chapter has been published in *Toxicological Sciences*, and is presented in the style of that journal: *Tox Sci* 2016 Jan;149(1):237-50

Drug-induced liver injury (DILI) is a frequent safety concern during drug development that has led to prescribing restrictions for some drugs (e.g. trovafloxacin) and market withdrawal for others (e.g. troglitazone) (Senior, 2014). Cholestatic and hepatocellular liver injury are two major forms of DILI, but despite extensive research, the underlying pathophysiological mechanism(s) remain ill-defined and are likely compound-specific. Inhibition of bile acid transport is one mechanism of DILI leading to intracellular accumulation of hydrophobic bile acids that can cause necrotic and/or apoptotic cell death (Marion et al., 2007; Perez and Briz, 2009; Wagner et al., 2009). The major transport proteins responsible for the basolateral uptake and biliary excretion of bile acids in humans are Na+-taurocholate cotransporting polypeptide (NTCP/SLC10A1) and the bile salt export pump (BSEP/ABCB11), respectively. Inhibition of BSEP-mediated bile acid transport has been implicated in DILI (Morgan et al., 2010; Woodhead et al., 2014). Additionally, multidrug resistance-associated proteins 2, 3 and 4 (MRP2/ABCC2, MRP3/ABCC3 andMRP4/ABCC4) also transport bile acids and may represent compensatory pathways for hepatic bile acid excretion under duress (Akita et al., 2001; Akita et al., 2002; Rius et al., 2006; Zelcer et al., 2003b). Recently, our group demonstrated that inhibition of MRP4, in addition to BSEP, may be a risk factor for the development of cholestatic DILI (Köck et al., 2014). Despite the association between bile acid inhibition and DILI, not all bile acid inhibitors cause DILI, suggesting that other mechanism(s) or patient-specific susceptibility factors may play a role in the development of DILI (Morgan et al., 2013).

In humans, tolvaptan exhibits dose-linear pharmacokinetics with an apparent elimination half-life ranging from 3 to 12 hours depending on the dose (Kim et al. 2011; Shoaf et al. 2007) and an oral bioavailability of ~50% following a 30 mg dose (Shoaf et al., 2012a). Tolvaptan is eliminated primarily by extensive CYP3A metabolism (Shoaf et al., 2012b) with several

metabolites detectable in the plasma including an oxybutyric acid metabolite (DM-4103) and a hydroxybutyric acid metabolite (DM-4107) (Fig. 3.1; Tammara et al., 1999; Sorbera et al., 2002). DM-4103 has a long half-life (~180 hours) in humans. Following a single, 60 mg oral dose of 14C-tolvaptan, plasma concentrations of DM-4103 are measurable for as long as 456 hours and account for ~52% of plasma radioactivity. While circulating concentrations of DM-4107 are lower than tolvaptan (which represents <3% of plasma radioactivity), approximately 20% of a tolvaptan dose is excreted in urine and feces as this metabolite (Tammara et al., 1999; Sorbera et al., 2002). In addition to the unknown etiology of tolvaptan-associated liver injury in ADPKD patients, it is also unclear whether DILI observed in ADPKD patients is due to the parent compound, a metabolite of tolvaptan, or some other specie(s).

These studies were designed to elucidate the interaction of tolvaptan and two metabolites, DM-4103 and DM-4107, with several proteins involved in the hepatic transport of bile acids. In addition, the accumulation and vectorial transport of selected bile acids in the absence and presence of tolvaptan was examined in sandwich-cultured human hepatocytes (SCHH). The results of this investigation, in combination with other ongoing research examining alternative potential mechanisms of hepatotoxicity (e.g., mitochondrial toxicity, adaptive immune response.), may provide important information to aid in determining the mechanism(s) underlying liver injury in tolvaptan-treated ADPKD patients.

MATERIALS AND METHODS

Materials.

[^{3}H]Taurocholic acid (TCA, 15.4 Ci/mmol), [^{3}H]estradiol-17β-glucuronide ($E_2$17G, 41.4 Ci/mmol), and [^{3}H]dehydroepiandrosterone sulfate (DHEAS, 60 Ci/mmol) were purchased from

PerkinElmer (Schwerzenbach, Switzerland). Unlabeled substrates (TCA, $E_2$17G, and DHEAS) were purchased from Cayman Chemicals (Ann Arbor, MI) or Sigma-Aldrich (St. Louis, MO). Stable-labeled taurocholic acid (d_8-TCA) and chenodeoxycholic acid (d_5-CDCA) were purchased from Martex Inc. (Minnetonka, MN). GCDCA (glycochenodeoxycholic acid), TCDCA (taurochenodeoxycholic acid), and erythromycin-estolate were purchased from Sigma-Aldrich (St. Louis, MO). MK-571 was purchased from Cayman Chemicals (Ann Arbor, MI). A/E Type glass filters (25mm) used in membrane vesicle studies were purchased from Pall Life Sciences (Ann Arbor, MI). Supplements added to culture NTCP-CHO cells were purchased from Invitrogen (Zug, Switzerland). Tolvaptan, DM-4103, and DM-4107 were provided by Otsuka Pharmaceutical Co. Ltd (Tokyo, Japan). The purity of these compounds was >99%.

Cell Culture

Chinese Hamster Ovary (CHO) cells.

CHO cells expressing human NTCP seeded in a 96-well format were obtained from Solvo Biotechnology (Szeged, Hungary). Cells were stored in a humidity-controlled incubator (37°C, 5% CO_2) until used. If possible, studies were completed on the day CHO cells arrived. In the event that experiments were not conducted on the arrival day, the media was replaced according to the supplier's protocol and the experiment was conducted within 24 hours.

Sandwich-Cultured Human Hepatocytes (SCHH).

SCHH were prepared by Qualyst Transporter Solutions (Durham, NC) using Transporter Certified^{TM} cryopreserved human hepatocytes from donor S-1099 (Kaly-Cell, Plobsheim, France) or donor HUM4059 (Triangle Research Laboratories, Durham, NC). Cryopreserved hepatocytes were thawed following the supplier's thawing instructions. SCHH were prepared by

plating hepatocytes suspended in propriety hepatocyte QualGro™ Seeding Medium (Qualyst Transporter Solutions, Durham, NC) at a density of $0.7x10^6$ viable cells/mL onto BioCoat® 24-well cell culture plates (BD Biosciences, San Jose, CA). Following plating, cells were allowed to attach for 2-4 hours, rinsed and fed with warm (37^oC) seeding medium. Eighteen to 24 hours later, cells were fed and over-laid with the appropriate species-specific propriety culture medium (Qualyst Transporter Solutions, Durham, NC) supplemented with the extracellular matrix (ECM) Matrigel® (BD Biosciences, San Jose, CA). Cells were maintained in culture medium in a humidity-controlled incubator (37°C, 5% CO_2) until experiments were conducted on day 5 of culture.

Assays

Membrane Vesicle Assay.

BSEP, MRP2, and MRP4 membrane vesicles were obtained from GenoMembrane (Kanagawa, Japan) and MRP3 membrane vesicles were obtained from Solvo Biotechnology (Szeged, Hungary). Membrane vesicles (10 µg BSEP, 5 µg MRP2, 10 µg MRP3, 5 µg MRP4, or control vesicles) were incubated at 37°C with the substrate [^{3}H]TCA, [^{3}H] $E_2$17G, or [^{3}H]DHEAS (2 µCi/mL) supplemented with the unlabeled substrate to achieve a concentration of 2 µM TCA (for BSEP), 50 µM $E_2$17G (for MRP2), 10 µM $E_2$17G (for MRP3), or 2 µM DHEAS (for MRP4) in transport buffer (10 mM Hepes-Tris for BSEP; 40 mM MOPS-Tris for MRP2 and MRP4; 10 mM Tris-HCl for MRP3) containing $MgCl_2$ (10 mM), sucrose (50 mM for BSEP or 250 mM for MRP3) and adenosine triphosphate (ATP) or adenosine monophosphate (AMP) (4 mM) in a final volume of 50 µL. Dimethyl sulfoxide (DMSO) was used to solubilize tolvaptan, DM-4103, and DM-4107; the final concentration of DMSO was < 1% v/v. After incubation for 2

min (for BSEP and MRP4), 3 min (for MRP2), or 5 min (for MRP3) with vehicle or increasing concentrations of tolvaptan, DM-4103, or DM-4107, the reaction was stopped by the addition of 800 µL ice-cold transport buffer and immediately filtered using A/E glass fiber filters presoaked in transport buffer overnight. The tested concentrations and incubation time points were determined by the limit of solubility for each compound and from preliminary data (data not shown). For the BSEP uptake studies, the filters were presoaked with 1 mM TCA solution to minimize nonspecific binding. For the MRP2, MRP3, and MRP4 uptake studies, the filters were presoaked with 3 mM reduced glutathione and 10mM dithiothreitol solution to minimize nonspecific binding. The filters were washed three times with ice-cold transport buffer using a vacuum filtration system. The filters were transferred to glass vials, and 10 mL liquid scintillation cocktail was added and mixed by vortex before analysis using the Tri-Carb 3100 TR liquid scintillation analyzer (PerkinElmer, Waltham, MA). The ATP-dependent uptake of substrate was calculated by subtracting substrate uptake in the presence of AMP from substrate uptake in the presence of ATP. The assays were performed in triplicate in three separate experiments.

CHO Transport Studies.

CHO cells were rinsed twice with 100 µL of prewarmed (37°C) Krebs-Henseleit uptake buffer with or without Na^+. A third aliquot of 100 µL transport buffer was left on the cells and incubated at 37°C for 15 min. The media was then aspirated and discarded. Uptake was initiated by the addition of prewarmed (37°C) uptake buffer containing the substrate [^{3}H]TCA (2 µCi/mL) supplemented with unlabeled TCA to achieve a concentration of 1 µM. Increasing concentrations of tolvaptan (0-50 µM), DM-4103 (0-75 µM), and DM-4107 (0-200 µM) were added to the substrate solution; the highest concentrations approached the limit of solubility for each

compound. DMSO was used to solubilize tolvaptan, DM-4103, and DM-4107; the final concentration of DMSO was < 1% v/v. The cells were incubated for 5 min at 37°C. Transport was stopped by quick aspiration of the radiolabeled solution; the cells were rinsed three times with 100 µL of ice-cold uptake buffer to stop the reaction. The cells were solubilized by adding 100 µL of 100 mM NaOH and left at room temperature for 2 min; 80 µL of the cell suspension was mixed with 5 mL scintillation fluid for radioactivity counting using the Tri-Carb 3100 TR liquid scintillation analyzer (PerkinElmer, Waltham, MA). NTCP-mediated uptake of TCA was calculated by subtracting substrate uptake in the absence of sodium from substrate uptake in the presence of sodium. The assays were performed in three separate experiments in triplicate.

Sandwich-Cultured Human Hepatocyte Studies.

Time-, Temperature-, and Na^+-Dependent Uptake of Tolvaptan in SCHH.

On day 5 of culture, media was aspirated and the SCHH were rinsed with 0.5 mL/well of standard or Ca^{2+}-free Hank's Balanced Salt Solution (HBSS). For Na^+-dependent uptake studies, Na^+-containing or Na^+- free (choline) HBSS buffers were used instead. After the second rinse, HBSS buffers were aspirated completely and SCHH were incubated with 0.5 mL of standard or Ca^{2+}-free HBSS buffers for 10 min (or Na^+-containing or Na^+- free HBSS buffers for the NTCP-mediated uptake studies). After 10 min, HBSS buffers were aspirated and then incubated with standard HBSS buffer containing tolvaptan (15 µM) at 37ºC for 5, 10, or 20 min, or 4ºC for 10 min. DMSO was used to solubilize tolvaptan; the final concentration of DMSO was 0.2% v/v. For the Na^+-dependent uptake studies, tolvaptan was incubated at 37ºC for 10 min. A tolvaptan concentration of 15 µM was selected because it was the highest concentration in the linear range for tolvaptan uptake (data not shown). After incubation, the HBSS buffer was aspirated from all

wells and rinsed three times with ice-cold standard HBSS buffer. Plates were sealed and stored at -80ºC until analysis.

Hepatobiliary Disposition of Taurocholic Acid (TCA), Chenodeoxycholic Acid (CDCA), Taurochenodeoxycholic Acid (TCDCA), and Glycochenodeoxycholic Acid (GCDCA) in the Presence of Tolvaptan.

On day 7 of culture, culture media was aspirated completely and SCHH were rinsed with 0.5 mL/well of standard or Ca^{2+}-free HBSS buffers. After the second rinse, HBSS buffers were aspirated completely and SCHH were incubated with 0.5 ml of standard or Ca^{2+}-free HBSS buffers for 10 min. After 10 min, HBSS buffers were aspirated completely and then incubated with the standard HBSS containing 2.5 µM of the probe substrate (d_8-TCA, d_5-CDCA, TCDCA, or GCDCA) with or without tolvaptan (15µM) for 10 min. After incubation, the incubation solutions were aspirated from all wells and rinsed three times with ice-cold standard HBSS buffer. Plates were sealed and stored at -80ºC until analysis.

Analysis of Tolvaptan, DM-4103, and DM-4107 in SCHH and Media by Liquid Chromatography-Tandem Mass Spectrometry (LC-MS/MS).

A volume of 500 µL of lysis solution (70:30 methanol:water (v:v) containing 27.5 nM internal standard) was added to each well of previously frozen 24-well plates containing study samples. Plates were shaken for approximately 15 min and the cell lysate solution was transferred to a Whatman® 96-well Unifilter® 25 µm MBPP / 0.45 µm PP filter plate (Maidstone, England) stacked on a 96-well deepwell plate. Lysate was filtered into the deepwell plate by centrifugation (2000 x g for 5 min). The sample filtrate was evaporated to dryness and the samples were reconstituted in 200 µL sample diluent (70:30 methanol:water containing 0.1%

formic acid) and mixed for 15 min on a plate shaker. The reconstituted samples were transferred to a 0.45 µm filter plate (Millipore, Billerica, MA) and filtered into a 96-well plate by centrifugation (2000 x g for 2 min) and sealed with a silicone capmat prior to LC-MS/MS analysis. Analytical controls for tolvaptan, DM-4103, and DM-4107 were measured using standard curves. Analytical standards were prepared over a range of concentrations to deliver, with the addition of a 10 µL volume per well, the range of mass 0.5 – 5000 pmoles/well for tolvaptan, DM-4103, and DM-4107. Cell lysates from SCHH were utilized for the generation of standard curves and related quality control (QC) samples. QC lysate samples were prepared at the lower limit of quantitation (LLQ) and the upper limit of quantitation (ULQ). These lysate controls were further processed as described above. A binary HPLC system (Shimadzu, Columbia, MD) composed of LC-10ADvp pumps, a CTO-10Avp oven, and an HTc – 96-well autosampler was used. The chromatographic column was a Hypersil Gold™ C18 (100 x 1.0 mm, 3 µm) with matching guard (5 µm) and pre-column filter (Thermo Scientific, Bellefont, PA). Column temperature was maintained at 35°C. A mobile phase gradient composed of A = 50% methanol with 0.1% formic acid and B = 90% methanol with 0.01% formic acid was used at a flow rate of 50 µL/min and a total run time of 10 min. All test compounds were chromatographically resolved. The gradient profile was: initial 25% B for 2.0 minutes; from 2.0 – 5.0 minutes ramp to 100% B and hold for 0.9 minute; step back to 25% B at 6.0 minutes and re-equilibrate for 4.0 minutes. An injection volume of 5 µL was used. Tandem mass spectrometry with positive ion electrospray ionization was conducted with a Thermo Electron TSQ® Quantum Discovery MAX™ (Thermo Fisher, Waltham, MA) with an Ion Max ESI source. The transitions monitored (parent m/z > product m/z) at unit resolution for tolvaptan, the internal standard, DM-4103, and DM-4107 were 449.2 > 252.0, 463.2 > 266.0, 479.0 > 252.0

and 481.0 > 252.0, respectively. The analytical run was typically conducted with a standard curve at the beginning of the run. A ULQ QC and a LLQ QC sample were placed in the middle of the run and at the end of the run. Analyte and internal standard peak area responses were determined for the standards, QC's, and unknown samples, and the unknown and QC samples (pmoles/well) were calculated utilizing the standard curve. Analytical run ruggedness was evaluated based on percent accuracy of the back calculated values for the standards and QC's. Acceptance criteria for percent accuracy of back calculated values were typically 15 - 20%.

Analysis of TCA, CDCA, TCDCA, and GCDCA.

Analysis of d_8-TCA, d_5-CDCA, TCDCA and GCDCA was performed using LC-MS/MS as described previously (Marion et al., 2012). Assay acceptance criteria were similar to those defined above. For the analysis of TCDCA and GCDCA only, the relative amounts (no standard curve) were determined by measuring the peak area ratios from the unknown LC-MS/MS peak area and the area of the corresponding internal standard. Relative changes were determined for individual treatments.

Data Analysis and Statistics.

Membrane Vesicle and CHO Cell Assays.

Transporter-mediated uptake was normalized to vehicle control values (without inhibitor). IC_{50} values were determined by nonlinear regression techniques using the following equation in GraphPad Prism 6 (San Diego, CA):

$Y=100/[1+10\text{^}((X-LogIC_{50}))]$

where X represents the log concentration of inhibitor and Y represents the percentage of control

activity. Data are reported as the point estimate and 95% confidence interval (CI). If the inhibitor did not reduce substrate transport by >50% at the highest tested concentration, nonlinear regression to estimate an IC_{50} value was not conducted. The type of inhibition and inhibition constant (K_i) for BSEP-mediated TCA transporter was determined by fitting competitive, noncompetitive, and uncompetitive models to the untransformed data by nonlinear regression analysis using GraphPad Prism 6 (San Diego, CA). The best-fit model was assessed based on visual inspection of the observed versus predicted data and the Akaike Information Criteria (Akaike, 1974). Equations used for each inhibition model were as follows:

$$\text{Competitive: } v = \frac{V_{max} \times \mathrm{S}}{K_m \times \left(1 + \frac{I}{K_i}\right) + \mathrm{S}}$$

$$\text{Noncompetitive: } v = \frac{V_{max} \times \mathrm{S}}{K_m \times \left(1 + \frac{I}{K_i}\right) + \mathrm{S} \times \left(1 + \frac{I}{K_i}\right)}$$

$$\text{Uncompetitive: } v = \frac{V_{max} \times \mathrm{S}}{K_m + \mathrm{S} \times \left(1 + \frac{I}{K_i}\right)}$$

Where S represents the concentration of TCA, I represents the concentration of tolvaptan or DM-4103, ν represents the rate of TCA transport, ν_{max} represents the maximal rate of TCA transport, K_m represents the TCA concentration that yields half maximal TCA transport, and K_i represents the dissociation constant for the BSEP-inhibitor complex. Data are from n=3 independent experiments in triplicate.

Sandwich-Cultured Hepatocyte Studies.

All mass values were normalized to the mean protein (mg) content per well from SCHH. Protein content was determined using the Pierce BCA protein assay kit. Cellular accumulation determined in Ca^{2+}-free HBSS buffer was assumed to represent the total mass of analyte inside

the hepatocyte at the end of the incubation time period. Total accumulation determined in standard HBSS buffer represents the total mass of compound taken up and excreted (cells + bile). The biliary excretion index (BEI) was calculated according to the following equation (Liu et al., 1999a):

$$\text{BEI (\%)} = \frac{\text{Accumulation}_{\text{Standard HBSS}} - \text{Accumulation}_{\text{Ca}^{2+}\text{-free HBSS}}}{\text{Accumulation}_{\text{Standard HBSS}}} \times 100$$

The *in vitro* biliary clearance ($Cl_{biliary}$) was determined using the following equation (Ghibellini et al. 2007; Liu et al., 1999b) and was scaled to body weight using scaling factors (Qualyst Transporter Solutions Technical Application Bulletin, 2011).

$$Cl_{biliary} = \frac{Accumulation_{Standard\ HBSS} - Accumulation_{Ca^{2+}-free\ HBSS}}{time \times concentration_{media}}$$

The biliary clearance for DM-4103 and DM-4107 could not be determined because the metabolites were generated endogenously. The intracellular concentration of each test compound was calculated by dividing the mass of compound in cells by the respective hepatocyte intracellular fluid volume for human hepatocytes (7.69 µl/mg protein; Qualyst Transporter Solutions Technical Application Bulletin, 2011). All calculations were performed using Microsoft Excel (Redmond, Washington).

RESULTS

NTCP- and BSEP-Mediated TCA Transport.

TCA was used as a substrate to study the interaction of tolvaptan, DM-4103, and DM-4107 with the basolateral uptake transporter NTCP. TCDCA (100 µM) was used as a positive control and inhibited NTCP-mediated uptake by >98% (data not shown). The estimated IC50 values for tolvaptan, DM-4103 and DM-4107 were ~41.5, 16.3 and 95.6 µM, respectively (Fig. 3.2A-C; Table 3.1). TCA was used as a substrate to study the interaction of tolvaptan, DM-4103,

and DM-4107 with the canalicular efflux transporter BSEP. Rifampicin (50 μM) was used as a positive control and inhibited BSEP-mediated uptake by >50% (data not shown; Byrne et al., 2002). BSEP-mediated TCA uptake was reduced to 16.4% of control when incubated with 50 μM tolvaptan; the estimated IC_{50} value was 31.6 μM (Fig. 3.2D; Table 3.1). DM-4103 inhibited BSEP-mediated TCA uptake with an IC_{50} value of 4.15 μM, while the IC50 value for DM-4107 was 119 μM (Fig. 3.2E-F). The K_i was estimated using nonlinear regression by incubating BSEP membrane vesicles with TCA (2-30 μM) and designated concentrations of tolvaptan (0-50 μM) or DM-4103 (0-20 μM). A K_i for DM-4107 was not determined because it was a less potent inhibitor of BSEP-mediated TCA transport based on the estimated IC_{50} value compared to tolvaptan and DM-4103. Nonlinear regression analysis of the data revealed that tolvaptan was best described by a noncompetitive inhibition model (K_i=34.2 μM), while DM-4103 was best described by a competitive inhibition model (K_i=3.77 μM) (Fig. 3.3).

MRP2- and MRP3-Mediated E217G Transport, and MRP4-Mediated DHEAS Transport.

E217G and DHEAS were used as substrates to study the interaction of tolvaptan, DM-4103, and DM4107 with the efflux transporters MRP2, MRP3, and MRP4. MK-571 (50 μM) was used as a positive control and inhibited MRP2-, MRP3- and MRP4-mediated transport by >95%, >50%, and >90%, respectively (data not shown). If transporter-mediated uptake of a probe substrate was not inhibited by >50%, nonlinear regression analysis was not conducted (Fig. 3.4C, D, and G). At the highest concentration of tolvaptan, MRP2-mediated E217G uptake was 115% of control, indicating that tolvaptan did not inhibit MRP2 transport (Fig. 3.4A). The estimated IC_{50} value for DM-4103 was ~51.0 μM (Fig. 4B). The estimated IC_{50} values for DM-4103 and DM-4107 mediated MRP3 inhibition were ~44.6 and 61.2 μM, respectively (Fig. 3.4E and F; Table 3.1). DHEAS was used as a substrate to study the interaction of tolvaptan, DM-

4103 and DM4107 with the basolateral efflux transporter MRP4. At the highest concentration of tolvaptan (50 μM), MRP4-mediated DHEAS uptake was 88.0% of control, indicating that tolvaptan had minimal impact on MRP4 transport (Fig. 3.4G). The estimated IC_{50} values for DM-4103 and DM-4107 were 4.26 and 37.9 μM, respectively (Fig. 3.4H-I; Table 3.1). DM-4103 inhibited MRP2-mediated E217G uptake by >50% only at the highest tested concentration (Fig. 3.4B). Although a curve was fit to these data to estimate an IC_{50} of ~51.0 μM, caution must be exercised when interpreting this value. The limits of solubility precluded testing higher concentrations of DM-4103. Such was the case with MRP3-mediated inhibition by DM-4103 as well as NTCP-mediated inhibition by tolvaptan (Fig. 3.2A and 4E).

Time- and Temperature-Dependent Uptake of Tolvaptan in Sandwich-Cultured Human Hepatocytes (SCHH).

SCHH were incubated with tolvaptan (15 μM) for 5, 10, or 20 min at 37ºC or for 10 min at 4ºC. Tolvaptan accumulated in SCHH reaching a concentration of ~500 μM after 10 min, assuming that binding to the hepatocyte surface was negligible and that accumulation represented the mass of tolvaptan in the cell. Temperature-dependent uptake suggested that both active and passive components are involved in tolvaptan uptake (Fig. 3.5A). The biliary excretion index (BEI) for tolvaptan was < 10%, indicating a low potential for biliary excretion of tolvaptan. In separate SCHH studies, formation of both DM-4103 and DM-4107 was observed during a 10-min incubation with tolvaptan (15 μM) at 37ºC (Fig. 3.5B); the mean total (bound+unbound) cellular concentrations of tolvaptan, DM-4103 and DM-4107 were 530, 1.71, and 35.6 μM, respectively.

Sodium-Dependent (NTCP) Uptake of Tolvaptan in SCHH.

To determine the sodium-dependent uptake of tolvaptan in SCHH, hepatocytes were incubated in the presence or absence of sodium. The total accumulation of tolvaptan and the accumulation of generated DM-4103 and DM-4107 were unaffected by the absence of sodium (Table 3.2).

Hepatobiliary Disposition of TCA, CDCA, TCDCA and GCDCA in the Presence of Tolvaptan in SCHH.

The effect of tolvaptan on the hepatobiliary disposition of four model bile acids (TCA, CDCA, TCDCA, and GCDCA) was evaluated in SCHH. When co-incubated with 15 µM tolvaptan, the total accumulation of TCA was decreased by 32.6% and the BEI was decreased by 15.7% compared to control (Table 3.3). The combined effect of the inhibition of both uptake and efflux by tolvaptan decreased the biliary clearance of TCA by 0.57-fold to control (Table 3.3; Fig. 3.6A). In contrast to TCA, the cellular accumulation of CDCA tended to increase by 1.30-fold relative to control. Tolvaptan-mediated changes in the biliary clearance and BEI of CDCA were 0.39 and 0.45-fold of control (Table 3.3). Erythromycin estolate (100 µM), a broad-spectrum efflux transport inhibitor, was used as a positive control and had no effect on the total accumulation (cell + bile) of CDCA, but inhibited the biliary excretion of CDCA (data not shown). Similar to CDCA, tolvaptan had no effect on the total accumulation of TCDCA or GCDCA, but did appear to increase the cellular accumulation (cells) of TCDCA and GCDCA by 1.68 and 2.16-fold, respectively compared to control when co-incubated with tolvaptan (Table 3.3; Fig. 3.6B).

DISCUSSION

In the present study, the inhibitory effect of tolvaptan, DM-4103, and DM-4107 on human hepatic bile acid transporters was investigated. This work was undertaken because tolvaptan was associated with liver injury in some patients with ADPKD during clinical investigation. Liver injury had not been reported previously for other patient populations, e.g., patients treated for hyponatremia, or cardiac and hepatic edema. In the ADPKD pivotal trials and the subsequent ongoing open-label safety study (NCT01214421), 4.9% of patients treated with tolvaptan had elevated alanine aminotransferase levels compared to 1.2% of those receiving the placebo (Torres et al., 2012). Fewer patients treated with tolvaptan than those receiving the placebo (0.9% vs. 1.9%) had increased bilirubin levels. However, two cases of Hy's Law were observed in tolvaptan-treated ADPKD patients, while no Hy's Law cases were reported in placebo-treated patients (Torres et al., 2012). A third case of Hy's Law was observed in a tolvaptan-treated ADPKD patient in an open-label follow on trial (Watkins et al., 2015). Furthermore, these observations did not appear to be associated with dose or exposure and generally occurred after three months or more of treatment (Watkins et al., 2015).

Idiosyncratic DILI is, by definition, a rare event. There was no apparent correlation between renal impairment, apparent hepatorenal cyst burden or stage of ADPKD and occurrence of hepatic events. Because of the low number of events, a definitive conclusion about an association between cyst burden and DILI cannot be made at this time. These data were described at the FDA Advisory Committee meeting for tolvaptan (August 2013; www.fda.gov) but have not been published yet. Interestingly, systemic tolvaptan exposure based on AUC was greater in patients with reduced creatinine clearance (<30 mL/min) than in patients with preserved renal function (Shoaf et al., 2014). Thus, prolonged renal impairment may alter

excretory mechanisms thereby placing a larger burden on the liver. With renal impairment in this population, an increase in systemic exposure does occur compared to non-ADPKD patients, although the differences are minimal since patients with severe renal impairment were excluded from the pivotal clinical trial (Torres et al., 2012). It is worth noting, however, that the liver is the primary elimination pathway for tolvaptan/metabolites (metabolism and fecal excretion) and not urinary excretion (Shoaf et al., 2012a). Hence, increasing the hepatic burden could alter hepatic exposure to tolvaptan/metabolites and may be associated with bile acid transporter inhibition, as shown in the present experiments.

BSEP inhibition has been implicated as one mechanism of DILI, although inhibition of other efflux transporters such as MRP2 and MRP4 also have been shown to exhibit an association with DILI (Köck et al., 2014; Mennone et al., 2006; Morgan et al., 2013). Under normal physiological conditions in humans, bile acids, primarily the conjugated bile acids taurodeoxycholic acid (TDCA), glycodeoxycholic acid (GDCA), TCDCA, and GCDCA, are transported across the canalicular membrane into bile and stored in the gallbladder until released into the duodenum (Hofmann et al., 2008; Rodrigues et al., 2013). Bile acids concentrate in the bile ducts relative to hepatocytes; active canalicular transport via BSEP is the rate-limiting step in bile acid transport and an important determinant of bile flow (Kullak-Ublick et al., 2004; Meier et al., 2004). Inhibition of BSEP may lead to accumulation of bile acids within hepatocytes and subsequently induce cytotoxicity.

Cholestatic DILI is a subset of liver disease that can result from direct damage to hepatic parenchyma (e.g. hepatocytes, bile ducts) through toxic or immunogenic mechanisms, and/or by impairment of biliary excretory function. Apart from genetic defects [e.g., progressive familial intrahepatic cholestasis type 2 (PFIC2)], numerous drugs have been implicated in cholestasis

(Padda et al., 2011). Cyclosporine, a prototypical drug that can induce cholestatic liver injury, alters bile acid transport function, intrahepatic vesicle transport, canalicular membrane fluidity and bile-acid independent bile flow (Böhme et al., 1994; Bramow et al., 2001; Román et al., 2003; Yasumiba et al., 2001). No cases of hepatotoxicity were reported during the development of troglitazone. However, this thiazolidinedione was removed from the market due to idiosyncratic liver injury. Subsequent studies, after market withdrawal, revealed that troglitazone and the sulfate conjugate of troglitazone inhibit BSEP. Further, studies with troglitazone revealed that cholestasis was more prevalent in male rats presumably due to sex-dependent differences in the toxic sulfate-conjugated species (Funk et al., 2001; Kostrubsky et al., 2001). These examples highlight the potential multi-mechanistic nature of DILI as well as the interplay between the formation and excretion of drug metabolites.

These present experiments were designed to test the hypothesis that bile acid transporter interference could be a biologically plausible mechanism to explain DILI in tolvaptan-treated patients with ADPKD. As shown, DM-4103 was a ~7.5-fold and a ~29-fold more potent inhibitor of BSEP (IC_{50}: 4.15 μM) compared to tolvaptan and DM-4107, respectively, based on IC_{50} data (Table 3.1). The ratio between the concentration at steady state (C_{ss}) or maximal plasma concentration (C_{max}) and the inhibitory potency (IC_{50}) is used commonly to understand the relationship between drug or metabolite exposure and inhibition (Zhang, 2012; Morgan et al., 2013). According to FDA guidance, when the estimated $[I]/K_i$ or $[I]/IC_{50}$ ratio is greater than 0.1, where [I] represents the total (bound plus unbound) mean steady-state C_{max} after administration of the highest proposed clinical dose, an *in vivo* drug interaction study may be warranted (Huang et al., 2008). For BSEP, both tolvaptan and DM-4107 exhibited (total) C_{max}/IC_{50} values < 0.1 while DM-4103 exhibited a value of 3.78 (Table 3.1), which suggests that DM-4103 may be a

relevant inhibitor of BSEP at the therapeutic dose of 90 mg tolvaptan. However, cellular rather than plasma concentrations of tolvaptan, DM-4103 and DM-4107 would be more relevant for predictions of efflux inhibition.

To further understand BSEP inhibition, the mechanism of inhibition was interrogated for tolvaptan and DM-4103. Inhibition of BSEP by tolvaptan was best described by a noncompetitive inhibition model (K_i=34.2 μM) while DM-4103 was best described by a competitive inhibition model (K_i=3.77 μM). Unlike competitive inhibition, noncompetitive inhibition reduces the rate of transport (e.g. of bile acids) and the resulting effects of depressed bile acid transport may lead to accumulation of bile acids, impaired bile flow, and hepatotoxicity. This principle is supported by Woodhead et al. (2014) who showed that in a simulated patient population treated with CP-724,714, an anti-cancer agent terminated from further development due to hepatotoxicity thought to be due, in part, to BSEP inhibition (Guo et al., 2008), clinically-relevant ALT elevations developed more frequently when BSEP inhibition was noncompetitive in nature. Mitochondrial toxicity also was implicated as a mechanism of CP-724,714 toxicity (Feng et al., 2009) and clinical findings suggest that CP-724,714 exerted both hepatocellular and hepatobiliary cholestatic injury (Guo et al., 2008; Munster et al., 2007).

As noted earlier, inhibition of BSEP alone cannot always predict or explain DILI. This may be due, in part, to the adaptive abilities of the liver. When bile acids accumulate in hepatocytes, compensatory or salvage pathways are transcriptionally upregulated/downregulated that function as hepatoprotective mechanisms (Wagner et al., 2005). MRP4, a sinusoidal bile acid efflux transporter, is normally expressed at low levels in human hepatocytes but protein expression can be increased significantly during cholestasis (Chai et al., 2012; Teng et al., 2007, Wagner et al., 2009; Zollner et al., 2006). Alterations in other bile acid efflux transporter

expression/function have been reported including MRP2, MRP3 and organic solute transporters (OSTα/OSTβ), indicating a complex adaptive response to cholestasis and/or bile acid-mediated toxicity (Boyer et al., 2006; Trauner et al., 1997; Zollner et al., 2001). Because of these potential adaptive responses, Morgan et al. (2013) developed decision criteria for bile acid transporter-mediated hazard identification, which includes evaluating the inhibition of important bile acid efflux transporters (i.e. MRP2, MRP3, and MRP4) in addition to BSEP. All evaluated compounds that exhibited a BSEP C_{ss}/IC_{50} ratio ≥ 0.1 and either a MRP2, MRP3 or MRP4 C_{ss}/IC_{50} ratio ≥ 0.1 were associated with some form of liver injury. These findings highlight the potential importance of compensatory mechanisms of bile acid transport when BSEP is impaired. Because inhibition of MRP-mediated transport function, in addition to BSEP, is associated with DILI, we sought to determine the inhibitory potency of tolvaptan, DM-4103 and DM-4107 on MRP2-, MRP3- and MRP4-mediated transport function.

As shown, tolvaptan and DM-4107 showed no or marginal MRP2 inhibition, respectively (Fig. 3.4A-C). Although DM-4103 inhibited MRP2-mediated transport by >50% at the highest tested concentration, caution should be exercised when interpreting the IC_{50} of DM-4103 (~51.0 μM) because limits of solubility precluded testing the effects of higher tolvaptan concentrations on MRP2-mediated transport. Such was the case with DM-4103 on MRP3-mediated transport. Tolvaptan showed no effect on MRP3-mediated transport and although the IC_{50} for DM-4107 was estimated to be 61.2 μM, the C_{max}/IC_{50} value was 0.04, indicating that DM-4107 may not be a relevant inhibitor of MRP3 (Table 3.1). In contrast, the C_{max}/IC_{50} value for DM-4103 was 0.35 for MRP3-mediated transport. DM-4103 was a ~9-fold more potent inhibitor of MRP4-mediated transport based on IC_{50} when compared to DM-4107 (IC_{50} of 4.26 vs. 37.9 μM, respectively), while tolvaptan exhibited minimal inhibition of MRP4-mediated transport (Fig. 3.4G-I). When

taking into account plasma concentrations, DM-4103 exhibited a C_{max}/IC_{50} value of 3.69 for MRP4 (Table 3.1), indicating that DM-4103 may be a relevant inhibitor of the basolateral efflux transporter MRP4 since this ratio was >0.1. The effects of tolvaptan on BSEP, MRP2 and MRP4 transport were similar to the IC_{50} values reported by Morgan et al. (2013) (9.99, >133 and >133 μM, respectively).

Although over-expressing cell lines and inside-out membrane vesicles are used commonly to screen for interactions at the transporter level, such systems may not be entirely predictive of the interactions that may or may not occur in complex cellular systems (e.g., hepatocytes) or *in vivo* (Byrne et al., 2002; Colombo et al., 2013; Xia et al., 2007). SCHH are a promising tool to study drug disposition and hepatotoxicity (Marion et al. 2007; Swift et al., 2010). Therefore, to further explore the interaction of tolvaptan with hepatocellular bile acid transporters, the disposition of tolvaptan and bile acids was evaluated in SCHH. Tolvaptan accumulation in SCHH was rapid and appeared to consist of both passive and active uptake processes (Fig. 3.5). After a 10-min incubation with 15 μM tolvaptan, the total cellular concentration was ~500 μM, assuming that all tolvaptan was localized intracellularly. In SCHH, approximately 30% of the tolvaptan dose was metabolized over 10 min, with ~1% and 10% representing DM-4103 and DM-4107, respectively. The cellular concentrations of DM-4103 and DM-4107 after a 10-min incubation with 15 μM tolvaptan were ~1.73 and ~23.8 μM, respectively. Although DM-4107 is formed preferentially compared to DM-4103 in about a 10:1 ratio (DM-4107:DM4103) after 10 min in SCHH, DM-4103 is the main circulating metabolite *in vivo* (Tammara et al., 1999; Sorbera et al., 2002). This apparent discrepancy may be due to differences in metabolite formation rates, i.e., DM-4103 and DM-4107 are downstream metabolites of tolvaptan (Tammara et al., 1999). Furthmore, intracellular metabolite

concentrations in culture may not be similar to metabolite concentrations circulating in human plasma.

Four bile acids (TCA, CDCA, TCDCA and GCDCA) were used as probes to determine the inhibitory potential of tolvaptan on hepatocellular bile acid transport in SCHH. CDCA, TCDCA, and GCDCA are among the most common circulating bile acids in humans and alterations in their disposition have been implicated in cholestatic liver injury (Greim et al., 1973; Ijare et al., 2009; Perwaiz et al., 2001; Roda et al., 1998; Tagliacozzi et al., 2003). Both the BEI and $Cl_{biliary}$ of TCA and CDCA in human SCHH appeared to decrease (0.84- and 0.57-fold of control, respectively for TCA and 0.39 and 0.45-fold of control, respectively for CDCA) when incubated with tolvaptan (Table 3.3). The cellular accumulation of TCA was not altered by tolvaptan, indicating that cellular basolateral efflux may be able to compensate for TCA accumulation even though TCA $Cl_{biliary}$ was decreased; TCA $Cl_{biliary}$ is approximately 3-fold greater than basolateral clearance in SCHH (Yang et al., 2015). Similarly, both the BEI and $Cl_{biliary}$ of CDCA in SCHH were modestly decreased (Table 3.3). Unlike TCA, CDCA appeared to accumulate intracellularly when co-incubated with tolvaptan (increased by 1.3-fold relative to control) (Fig. 3.6A). The cellular accumulation of TCDCA and GCDCA also appeared to increase when co-incubated with tolvaptan (increased by 1.68 and 2.16-fold relative to control, respectively), which indicates the potential for these bile acids to accumulate, possibly due to inhibition of biliary and/or basolateral efflux (Fig. 3.6B). The BEI for TCDCA and GCDCA also appeared to be lower when co-incubated with tolvaptan (Table 3.3). Inhibition of bile acid transport in SCHH is consistent with the observations from the membrane vesicle studies. These data support the hypothesis that accumulation of tolvaptan in hepatocytes may play a role in the mechanism(s) of DILI.

Although the cellular accumulation of bile acids such as TCDCA has been shown to experimentally induce liver injury *in vivo* (Sokol et al., 1998), the biological importance of such changes in bile acid biliary clearance and hepatocyte accumulation in humans is not well defined. In sandwich-cultured hepatocytes, Marion et al. (2007) and Griffin et al. (2013) demonstrated that some hepatotoxic drugs were associated with impaired bile acid biliary clearance and/or increased cellular accumulation of bile acids and subsequent toxicity, similar to the present findings. Furthermore, the current study examined bile acid disposition in short-term incubations, which may be exacerbated in long-term exposures as shown by the delayed presentation of bile acid-mediated toxicity of troglitazone (Yang et al., 2014).

As described earlier, inhibition of hepatic bile acid transporters may not be the sole mechanism of DILI noted in the ADPKD population. Alternative mechanisms of hepatotoxicity currently are being explored. Wu et al. (2015) recently demonstrated that tolvaptan induces *in vitro* cellular apoptosis in HepG2 cells, potentially through several mechanisms including mitochondrial dysfunction. However, considering clinically relevant concentrations of tolvaptan and the fact that hepatotoxicity has not been reported in non-ADPKD populations, the clinical relevance of these studies remains uncertain. In addition to direct drug-induced mitochondrial dysfunction and oxidative stress, bile acids can cause hepatocellular damage by inducing swelling and abnormal mitochondrial cristae, disruption of cellular membranes, and generation of reactive oxygen species (Billington et al., 1980; Philips et al., 1987; Sokol et al., 1993). As described by Watkins et al. (2015), the signature pattern of hepatic events occurred after approximately 3-4 months of treatment, and resolved over a prolonged period of time following discontinuation of tolvaptan. The signature pattern of hepatotoxicity suggested an adaptive immune-mediated hepatic event, which continues to be explored in patients. However, multiple

mechanisms of DILI cannot be ruled out including the inhibition of bile acid transport, as shown here, and mitochondrial toxicity (Feng et al. 2009). The results of studies focused on these alternative mechanism(s) will be reported subsequently. As noted at the outset of this paper, the purpose of the current investigation was to test the hypothesis that inhibition of human hepatic bile acid transporters by tolvaptan and metabolites could play a role in tolvaptan-associated DILI.

It has been suggested that inhibition of NTCP-mediated bile acid uptake may provide some cellular protection from hepatic accumulation of bile acids, such as shown with bosentan (Leslie et al. 2007). However, the NTCP IC_{50} value for tolvaptan (~41.5 μM) was >2-fold higher than the dose concentration in the SCHH studies, indicating that tolvaptan would have little impact on TCA uptake in hepatocytes; this is consistent with the data obtained in SCHH (Fig. 3.6A). DM-4103 and DM-4107 concentrations in the media were negligible after a 10-min incubation (data not shown); these metabolites likely had little impact on TCA uptake in the present study. Based on C_{max} concentrations achieved with therapeutic doses of tolvaptan, only DM-4103 exhibited an $I/IC_{50} > 0.1$ for NTCP (Table 3.1). However, when taking into account the unbound fraction (assuming f_u ~1%, similar to that of tolvaptan, Shoaf et al., 2014), an interaction at the level of NTCP would not be expected. Tolvaptan did not appear to be a substrate of NTCP (Table 3.2). While NTCP is considered the primary hepatic bile acid transporter in humans, OATPs also may transport endogenous anions including bile acids and bilirubin (Cui et al., 2001; Meier et al., 1997; Tamai et al., 2000). Although inhibition of OATPs is a concern for the interaction of concomitantly administered drugs (Zhang et al., 2012), inhibition of OATPs has not been associated with DILI and thus, may not be relevant to

understanding bile acid-mediated toxicity/disposition. Furthermore, OATP drug-drug interactions with tolvaptan have not been reported in humans (Bhatt et al., 2014).

In conclusion, results of the present studies demonstrate that tolvaptan and metabolites inhibited multiple human hepatic proteins involved in bile acid transport (i.e. NTCP, BSEP, MRP2, MRP3 and MRP4). Impaired bile acid transport by tolvaptan and/or its metabolites may negatively impact bile acid homeostasis, which may explain, in part, the mechanism(s) behind liver injury in tolvaptan-treated ADPKD patients. However, the fact that liver injury has been observed only in patients with ADPKD, and that no evidence of cholestasis (i.e., no clinically significant increases in alkaline phosphatase) was observed in the ADPKD clinical trial (Torres et al., 2012), suggests that other mechanisms may predispose this patient population to DILI. Research into other genetic and non-genetic mechanisms of tolvaptan-induced DILI is on-going.

REFERENCES

Akaike, H. (1974). A new look at the statistical model identification. *IEEE Trans. Auto. Ctrl.* AC-19, 716-723.

Akita, H., Suzuki, H., Hirohashi, T., Takikawa, H., Sugiyama, Y. (2002). Transport activity of human MRP3 expressed in Sf9 cells: comparative studies with rat MRP3. *Pharm. Res.* 19, 34-41.

Bhatt, P.R., McNeely, E.B., Lin, T.E., Adams, K.F., Patterson, J.H. (2014). Review of tolvaptan's pharmacokinetic and pharmacodynamic properties and drug interactions. *J Clin Med*. 3, 1276-1290.

Billington, D., Evans, C.E., Godfrey, P.P., Coleman, R. (1980). Effects of bile salts on the plasma membranes of isolated rat hepatocytes. *Biochem J*, 188, 321-327.

Bramow, S., Ott, P., Thomsen Nielsen, F., Bangert, K., Tygstrup, N., Dalhoff, K. (2001). Cholestasis and regulation of genes related to drug metabolism and biliary transport in rat liver following treatment with cyclosporine A and sirolimus (Rapamycin). *Pharmacol Toxicol.* 89, 133-139.

Boertien, W.E., Meijer, E., de Jong PE, Ter., Horst, G.J., Renken, R.J., van der Jagt, E.J., Kappert, P., Ouyang, J., Engels, G.E., van Oeveren, W., Struck, J., Czerwiec, F.S., Oberdhan, D., Krasa, H.B., Gansevoort, R.T. (2015). Short-term effects of tolvaptan in individuals with autosomal dominant polycystic kidney disease at various levels of kidney function. *Amer. J. Kidney Dis.* 65, 833-841.

Boyer, J.L., Trauner, M., Mennone, A., Soroka, C.J., Cai, S.Y., Moustafa, T., Zollner, G., Lee, J.Y., Ballatori, N. (2006). Upregulation of a basolateral FXR-dependent bile acid efflux transporter OSTalpha-OSTbeta in cholestasis in humans and rodents. *Am J Physiol Gastrointest Liver Physiol.* 290, G1124–G1130.

Böhme, M., Müller, M., Leier, I., Jedlitschky, G., Keppler, D. (1994). Cholestasis caused by inhibition of the adenosine triphosphate-dependent bile salt transport in rat liver. *Gastroenterol.* 107, 255-265.

Byrne, J.A., Strautnieks, S.S., Mieli-Vergani, G., Higgins, C.F., Linton, K.J., Thompson, R.J. (2002). The human bile salt export pump: characterization of substrate specificity and identification of inhibitors. *Gastroenterol.* 123, 1649-1658.

Chai, J., H.e, Y., Cai, S.Y., Jiang, Z., Wang, H., Li, Q., Chen, L., Peng, Z., He, X., Wu, X., Xiao, T., Wang, R., Boyer, J.L., Chen, W. (2012). Elevated hepatic multidrug resistance-associated protein 3/ATP-binding cassette subfamily C 3 expression in human obstructive cholestasis is mediated through tumor necrosis factor alpha and c-Jun NH2-terminal kinase/stress-activated protein kinase-signaling pathway. *Hepatol.* 55, 1485-1494.

Colombo, F., Poirier, H., Rioux, N., Montecillo, M.A., Duan, J., Ribadeneira, M.D. (2013). A

membrane vesicle-based assay to enable prediction of human biliary excretion. *Xenobiotica.* 43, 915-919.

Cui, Y., König, J., Leier, I., Buchholz, U., Keppler, D. (2001) Hepatic uptake of bilirubin and its conjugates by the human organic anion transporter SLC21A6. *J Biol Chem*. 276, 9626-9630.

Feng, B., Xu, J.J., Bi, Y.A., Mireles, R., Davidson, R., Duignan, D.B., Campbell,S., Kostrubsky, V.E., Dunn, M.C., Smith, A.R., Wang, H.F. (2013). Role of hepatic transporters in the disposition and hepatotoxicity of a HER2 tyrosine kinase inhibitor CP-724,714. *Toxicol Sci*. 108, 492-500.

Fukunami, M., Matsuzaki, M., Hori, M., Izumi, T., Tolvaptan Investigators. (2011). Efficacy and safety of tolvaptan in heart failure patients with sustained volume overload despite the use of conventional diuretics: a phase III open-label study. *Cardiovas Drugs Ther*. 25, S47-56.

Funk, C., Pantze, M., Jehle, L., Ponelle, C., Scheuermann, G., Lazendic, M., Gasser, R. (2001). Troglitazone-induced intrahepatic cholestasis by an interference with the hepatobiliary export of bile acids in male and female rats. Correlation with the gender difference in troglitazone sulfate formation and the inhibition of the canalicular bile salt export pump (BSEP) by troglitazone and troglitazone sulfate. *Toxicol.* 167, 83-98.

Ghibellini, G., Vasist, L.S., Leslie, E.M., Heizer, W.D., Kowalsky, R.J., Calvo, B.F., Brouwer, K.L. (2007). In vitro-in vivo correlation of hepatobiliary drug clearance in humans. *Clin Pharmacol Ther.* 81, 406-413.

Greim, H., Czygan, P., Schaffner, F., Popper, H. (1973). Determination of bile acids in needle biopsies of human liver. *Biochem. Med.* 8, 280–286.

Griffin, L.M., Watkins, P.B., Perry, C.H., St Claire, R.L. 3rd, Brouwer, K.L. (2013). Combination lopinavir and ritonavir alter exogenous and endogenous bile acid disposition in sandwich-cultured rat hepatocytes. *Drug Metab Dispos*. 41, 188-196.

Guo, F., Letrent, S. P., Munster, P. N., Britten, C. D., Gelmon, K., Tolcher, A. W., Sharma A. (2008). Pharmacokinetics of a HER2 tyrosine kinase inhibitor CP-724,714 in patients with advanced malignant HER2 positive solid tumors: correlations with clinical characteristics and safety. *Cancer Chemother. Pharmacol*. 62, 97–109.

Higashihara, E., Torres, V.E., Chapman, A.B., Grantham, J.J., Bae, K., Watnick, T.J., Horie, S., Nutahara, K., Ouyang, J., Krasa, H.B., Czerwiec, F.S. (2011). TEMPO Formula and 156-05-002 study investigators. Tolvaptan in autosomal dominant polycystic kidney disease: three years' experience. *Clin. J. Amer. Soc. Nephrol.* 6, 2499-2507.

Hofmann A.F., Hagey L.R. (2008). Bile Acids: Chemistry, Pathochemistry, Biology, Pathobiology, and Therapeutics. *Cell Mol Life Sci.* 65, 2461-2483.

Huang S.M., Strong, J.M., Zhang, L., Reynolds, K.S., Nallani, S., Temple, R., Abraham, S.,

Habet, S.A., Baweja, R.K., Burckart, G.J., Chung, S., Colangelo, P., Frucht, D., Green, M.D., Hepp, P., Karnaukhova, E., Ko, H.S., Lee, J.I., Marroum, P.J., Norden, J.M., Qiu, W., Rahman, A., Sobel, S., Stifano, T., Thummel, K., Wei, XX., Yasuda, S., Zheng, J.H., Zhao, H., Lesko, L.J. (2008). New era in drug interaction evaluation: US Food and Drug Administration update on CYP enzymes, transporters, and the guidance process. J *Clin Pharmacol.* 48, 662-670.

Ijare, O.B., Bezabeh, T., Albiin, N., Arnelo, U., Bergquist, A., Lindberg, B., Smith, I.C. (2009). Absence of glycochenodeoxycholic acid (GCDCA) in human bile is an indication of cholestasis: a 1H MRS study. Absence of glycochenodeoxycholic acid (GCDCA) in human bile is an indication of cholestasis: a 1H MRS study. *NMR Biomed.* 22, 471-479.

Kim, S.R., Hasunuma, T., Sato, O., Okada, T., Kondo, M., Azuma, J. (2011). Pharmacokinetics, pharmacodynamics and safety of tolvaptan, a novel, oral, selective nonpeptide AVP V2-receptor antagonist: results of single- and multiple-dose studies in healthy Japanese male volunteers. *Cardiovasc Drugs Ther.* 25, S5-17.

Köck, K., Ferslew, B.C., Netterberg, I., Yang, K., Urban, T.J., Swaan, P.W., Stewart, P.W., Brouwer, K.L. (2014). Risk factors for development of cholestatic drug-induced liver injury: inhibition of hepatic basolateral bile acid transporters multidrug resistance-associated proteins 3 and 4. *Drug Metab Dispos.* 42, 665-674.

Kostrubsky, V.E., Vore, M., Kindt, E., Burliegh, J., Rogers, K., Peter, G., Altrogge, D., Sinz, M.W. (2001). The effect of troglitazone biliary excretion on metabolite distribution and cholestasis in transporter-deficient rats. *Drug Metab Dispos.* 29, 1561-1566.

Kullak-Ublick, G.A., Stieger, B., Meier, P.J. (2004). Enterohepatic bile salt transporters in normal physiology and liver disease. *Gastroenterology.* 126, 322-342.

Leslie, E.M., Watkins, P.B., Kim, R.B., Brouwer, K.L. (2007). Differential inhibition of rat and human Na+-dependent taurocholate cotransporting polypeptide (NTCP/SLC10A1)by bosentan: a mechanism for species differences in hepatotoxicity. *J Pharmacol Exp Ther.* 321, 1170-1178.

Liu, X., LeCluyse, E.L., Brouwer, K.R., Gan, L.S., Lemasters, J.J., Stieger, B., Meier, P.J., Brouwer, K.L. (1999a). Biliary excretion in primary rat hepatocytes cultured in a collagen-sandwich configuration. *Am J Physiol.* 277, G12-G21.

Liu, X., Chism, J.P., LeCluyse, E.L., Brouwer, K.R., Brouwer, K.L. (1999b). Correlation of biliary excretion in sandwich-culture rat hepatocytes and in vivo in rats, *Drug Metab. Dispos.* 27, 637-644.

Marion, T.L., Leslie, E.M., Brouwer, K.L. (2007). Use of sandwich-cultured hepatocytes to evaluate impaired bile acid transport as a mechanism of drug-induced hepatotoxicity. *Mol. Pharm.* 4, 911-918.

Marion TL, Perry CH, St Claire RL 3rd, Brouwer KL. (2012). Endogenous bile acid disposition in rat and human sandwich-cultured hepatocytes. *Toxicol Appl Pharmacol*. 261, 1-9.

Meier, P.J., Eckhardt, U., Schroeder, A., Hagenbuch, B., Stieger, B. (1997). Substrate specificity of sinusoidal bile acid and organic anion uptake systems in rat and human liver. *Hepatol*. 26, 1667-1677.

Meier, P.J., Stieger, B. (2002). Bile salt transporters. *Annu Rev Physiol.* 64, 635-661.

Mennone, A., Soroka, C.J., Cai, S.Y., Harry, K., Adachi, M., Hagey, L., Schuetz, J.D., Boyer, J.L. (2006). Mrp4$^{-/-}$ mice have an impaired cytoprotective response in obstructive cholestasis. *Hepatol.* 43, 1013-1021.

Morgan, R.E., Trauner, M., van Staden, C.J., Lee, P.H., Ramachandran, B., Eschenberg, M., Afshari, C.A., Qualls, C.W. Jr., Lightfoot-Dunn, R., Hamadeh, H.K. (2010). Interference with bile salt export pump function is a susceptibility factor for human liver injury in drug development. *Toxicol. Sci.* 118, 485-500.

Morgan, R.E., van Staden, C.J., Chen, Y., Kalyanaraman, N., Kalanzi, J., Dunn, R.T., Afshari, C.A., Hamadeh, H.K. (2013). A multifactorial approach to hepatobiliary transporter assessment enables improved therapeutic compound development. *Toxicol Sci.* 136, 216-2141.

Munster, P. N., Britten, C. D., Mita, M., Gelmon, K., Minton, S. E., Moulder, S., Slamon, D. J., Guo, F., Letrent, S. P., Denis, L., et al. (2007). First study of the safety, tolerability, and pharmacokinetics of CP-724,714 in patients with advanced malignant solid HER2-expressing tumors. *Clin. Cancer Res*. 13, 1238–1245.

Oi, A., Morishita, K., Awogi, T., Ozaki, A., Umezato, M., Fujita, S., Hosoki, E., Morimoto, H., Ishiharada, N., Ishiyama, H., Uesugi, T., Miyatake, M., Senba, T., Shiragiku, T., Nakagiri, N., Ito, N. (2011). Nonclinical safety profile of tolvaptan. *Cardiovasc Drugs Ther.* 1, S91-S99.

Padda, M.S., Sanchez, M., Akhtar, A.J., Boyer, J.L. (2011). Drug-induced cholestasis. *Hepatol.* 53, 1377-1387.

Patel, M.S., Kandula, P., Wojciechowski, D., Markmann, J.F., Vagefi, P.A. (2014). Trends in the management and outcomes of kidney transplantation for autosomal dominant polycystic kidney disease. *J. Transplant.* 2014, 675-697.

Perez, M.J., Briz, O. (2009). Bile-acid-induced cell injury and protection. *World J. Gastroenterol. 14* 15, 1677-1689.

Perwaiz, S., Tuchweber, B., Mignault, D., Gilat, T., Yousef, I.M. (2001). Determination of bile acids in biological fluids by liquid chromatography-electrospray tandem mass spectrometry. *J Lipid Res.* 42, 114-119.

Phillips, M.J., Poucell, S., Patterson, J., Valencia, P. Cholestasis. In: Phillips, M.J., Poucell, S., Patterson, J., Valencia, P. (1987). The liver: an atlas and text of ultrastructural pathology. *New York: Raven Press*, 101-158.

Qualyst Transporter Solutions Technical Application Bulletin TAB Biol 005. (2011). *TAB Biol* 005v2.

Rius, M., Hummel-Eisenbeiss, J., Hofmann, A.F., Keppler, D. (2006). Substrate specificity of human ABCC4 (MRP4)-mediated co-transport of bile acids and reduced glutathione. *Amer. J. Physiol. Gastrointest. Liver Physiol.* 290, G640-G649.

Roda, A., Piazza, F., Baraldini, M., Speroni, E., Guerra, M.C., Cerré, C., Cantelli Forti, G. (1998). Taurohyodeoxycholic acid protects against taurochenodeoxycholic acid-induced cholestasis in the rat. *Hepatol.* 27, 520-525.

Rodrigues, A.D., Lai, Y., Cvijic, M.E., Elkin, L.L., Zvyaga, T., Soars, M.G. (2014). Drug-induced perturbations of the bile acid pool, cholestasis, and hepatotoxicity: mechanistic considerations beyond the direct inhibition of the bile salt export pump. *Drug Metab Dispos.* 42, 566-74.

Román, I.D., Fernández-Moreno, M.D., Fueyo, J.A., Roma, M.G. (2003). Coleman R Cyclosporin A induced internalization of the bile salt export pump in isolated rat hepatocyte couplets. *Toxicol Sci.* 71, 76-81.

Sakaida, I. (2014). Tolvaptan for the treatment of liver cirrhosis oedema. *Expert Rev Gastroenterol Hepatol*. 8, 461-70.

Schrier, R.W., Gross, P., Gheorghiade, M., Berl, T., Verbalis, J.G., Czerwiec, F.S., Orlandi, C. (2006). SALT Investigators. Tolvaptan, a selective oral vasopressin V2-receptor antagonist, for hyponatremia. *N. Engl. J. Med.* 355, 2099-2112.

Senior, J.R. (2014). Evolution of the Food and Drug Administration approach to liver safety assessment for new drugs: current status and challenges. *Drug Saf. 37 Suppl* 1, S9-S17.

Shoaf, S.E., Wang, Z., Bricmont, P., Mallikaarjun, S. (2007). Pharmacokinetics, pharmacodynamics, and safety of tolvaptan, a nonpeptide AVP antagonist, during ascending single-dose studies in healthy subjects. *J. Clin. Pharmacol.* 47, 1498-1507.

Shoaf, S.E., Bricmont, P., Mallikaarjun, S. (2012a). Absolute bioavailability of tolvaptan and determination of minimally effective concentrations in healthy subjects. Int. J. Clin. Pharmacol. Ther. 50, 150-156.

Shoaf, S.E., Bricmont, P., Mallikaarjun, S. (2012b). Effects of CYP3A4 inhibition and induction on the pharmacokinetics and pharmacodynamics of tolvaptan, a non-peptide AVP antagonist in healthy subjects. Br. J. Clin. Pharmacol. 73, 579-587.

Shoaf, S.E., Bricmont, P., Mallikaarjun, S. (2014). Pharmacokinetics and pharmacodynamics of oral tolvaptan in patients with varying degrees of renal function. *Kidney Int.* 85, 953-61.

Sokol RJ.., Devereaux M., Khandwala R., O'Brien K. (1993). Evidence for involvement of oxygen free radicals in bile acid toxicity to isolated rat hepatocytes. *Hepatol*, 17, 869-881.

Sokol R.J., McKim J.M. Jr., Goff M.C., Ruyle S.Z., Devereaux M.W., Han D., Packer L.,

Everson G. (1998). Vitamin E reduces oxidant injury to mitochondria and the hepatotoxicity of taurochenodeoxycholic acid in the rat. *Gastroenterol*. 114, 164-74.

Sorbera, L.A., Castaner, J., Bayes, M., Silvestre, J. (2002). Tolvaptan: Treatment for heart failure Vasopressin V_2 antagonist. *Drugs of the Future.* 27, 350-357.

Swift, B., Pfeifer, N.D., Brouwer, K.L. (2010). Sandwich-cultured hepatocytes: an in vitro model to evaluate hepatobiliary transporter-based drug interactions and hepatotoxicity. *Drug Metab Rev.* 42, 446-471.

Tagliacozzi, D., Mozzi, A.F., Casetta. B., Bertucci, P., Bernardini, S., Di Ilio, C., Urbani, A., Federici, G. (2003). Quantitative analysis of bile acids in human plasma by liquid chromatography-electrospray tandem mass spectrometry: a simple and rapid one-step method. *Clin Chem Lab Med.* 41, 1633-1641.

Tamai, I., Nezu, J., Uchino, H., Sai, Y., Oku, A., Shimane, M., Tsuji, A. 2000. Molecular identification and characterization of novel members of the human organic anion transporter (OATP) family. Biochem *Biophys Res Commun*. 273, 251-60.

Tammara, B.K., Sekar, K.S., Brumer, S.L. (1999). The disposition of a single dose of ^{14}C OPC-41061 in healthy male volunteers. *Ann. Meeting Amer. Assoc. Pharm. Sci.* Abstract 2025.

Teng, S., Piquette-Miller, M. (2007). Hepatoprotective role of PXR activation and MRP3 in cholic acid-induced cholestasis. *Br J Pharmacol.* 151, 367-376.

Torres, V.E., Harris, P.C., Pirson, Y. (2007). Autosomal dominant polycystic kidney disease. *Lancet*. 369, 1287-1301.

Torres, V.E., Chapman, A.B., Devuyst, O., Gansevoort, R.T., Grantham, J.J., Higashihara, E., Perrone, R.D., Krasa, H.B., Ouyang, J., Czerwiec, F.S. (2012). TEMPO 3:4 trial investigators. Tolvaptan in patients with autosomal dominant polycystic kidney disease. *N. Engl. J. Med.* 367, 2407-2418.

Trauner, M., Arrese, M., Soroka, C.J, Ananthanarayanan M., Koeppel T.A., Schlosser S.F., Suchy F.J., Keppler D., Boyer J.L. (1997). The rat canalicular conjugate export pump (Mrp2) is down-regulated in intrahepatic and obstructive cholestasis. *Gastroenterology*. 113, 255-64.

Wagner, M., Trauner, M. (2005). Transcriptional regulation of hepatobiliary transport systems in health and disease: implications for a rationale approach to the treatment of intrahepatic cholestasis. *Ann Hepatol.* 4, 77–99.

Wagner, M., Zollner, G., Trauner, M. (2009). New molecular insights into the mechanisms of cholestasis. *J Hepatol.* 51, 565-580.

Watkins, P.B., Lewis, J.H., Kaplowitz, N., Alpers, D.H., Blais, J.D., Smotzer, D.M., Krasa, H., Ouyang, J., Torres, V.E., Czerwiec, F.S., Zimmer, C.A. (2015). Clinical Pattern of Tolvaptan-

Associated Liver Injury in Subjects with Autosomal Dominant Polycystic Kidney Disease: Analysis of Clinical Trials Database. *Drug Saf.* 2015 Jul 19. [Epub ahead of print]

Woodhead, J.L., Yang, K., Siler, S.Q., Watkins, P.B., Brouwer, K.L., Barton, H.A., Howell, B.A. (2014). Exploring BSEP inhibition-mediated toxicity with a mechanistic model of drug-induced liver injury. *Front Pharmacol.* 7, 5-240.

Wu, Y., Beland, F.A., Chen, S., Liu, F., Guo, L., Fang, J-L. (2015). Mechanisms of tolvaptan-induced toxicity in HepG2 cells. *Biochem. Pharmacol.* 95, 324-336.

Xia, C.Q., Milton, M.N., Gan, L.S. (2007). Evaluation of drug-transporter interactions using in vitro and in vivo models. *Curr Drug Metab.* 8, 341-363.

Yamamura, Y., Nakamura, S., Itoh, S., Hirano, T., Onogawa, T., Yamashita, T., Yamada, Y., Tsujimae, K., Aoyama, M., Kotosai, K., Ogawa, H., Yamashita, H., Kondo, K., Tominaga, M., Tsujimoto, G., Mori, T. (1998). OPC-41061, a highly potent human vasopressin V2-receptor antagonist: pharmacological profile and aquaretic effect by single and multiple oral dosing in rats. *J. Pharmacol. Exp. Ther.* 287, 860-867.

Yang K., Woodhead J.L., Watkins P.B., Howell B.A., Brouwer K.L. (2014). Systems pharmacology modeling predicts delayed presentation and species differences in bile acid-mediated troglitazone hepatotoxicity. *Clin Pharmacol Ther*. 96, 589-598.

Yang, K., Pfeifer, N.D., Kock, K., Brouwer, K.L. (2015). Species differences in hepatobiliary disposition of taurocholic acid in human and rat sandwich-cultured hepatocytes: Implications for drug-induced liver injury. *J Pharmacol Exp Ther.* 353, 415-423.

Yasumiba, S., Tazuma, S., Ochi, H., Chayama, K., Kajiyama, G. (2001). Cyclosporin A reduces canalicular membrane fluidity and regulates transporter function in rats. *Biochem J.* 2001 354, 591-596.

Zelcer, N., Reid, G., Wielinga, P., Kuil, A., van der Heijden, I., Schuetz, J.D., Borst, P. (2003). Steroid and bile acid conjugates are substrates of human multidrug-resistance protein (MRP) 4 (ATP-binding cassette C4). *Biochem. J.* 71, 361-367.

Zhang, L. (2012). Guidance for Industry: Drug Interaction Studies – Study Design, Data Analysis, Implications for Dosing, and Labeling Recommendations. *Silver Spring, MD: Office of Clinical Pharmacology, Food and Drug Administration.*

Zollner, G., Fickert, P., Zenz, R., Fuchsbichler, A., Stumptner, C., Kenner, L., Ferenci, P., Stauber, R.E., Krejs, G.J., Denk, H., Zatloukal, K., Trauner, M. (2001). Hepatobiliary transporter expression in percutaneous liver biopsies of patients with cholestatic liver diseases. *Hepatology*. 33, 633-46.

Zollner, G., Marschall, H.U., Wagner, M., Trauner, M. (2006). Role of nuclear receptors in the

adaptive response to bile acids and cholestasis: pathogenetic and therapeutic considerations. *Mol Pharm* 3, 231–251.

Figure 3.1. Chemical structures of tolvaptan, DM-4103, and DM-4107.

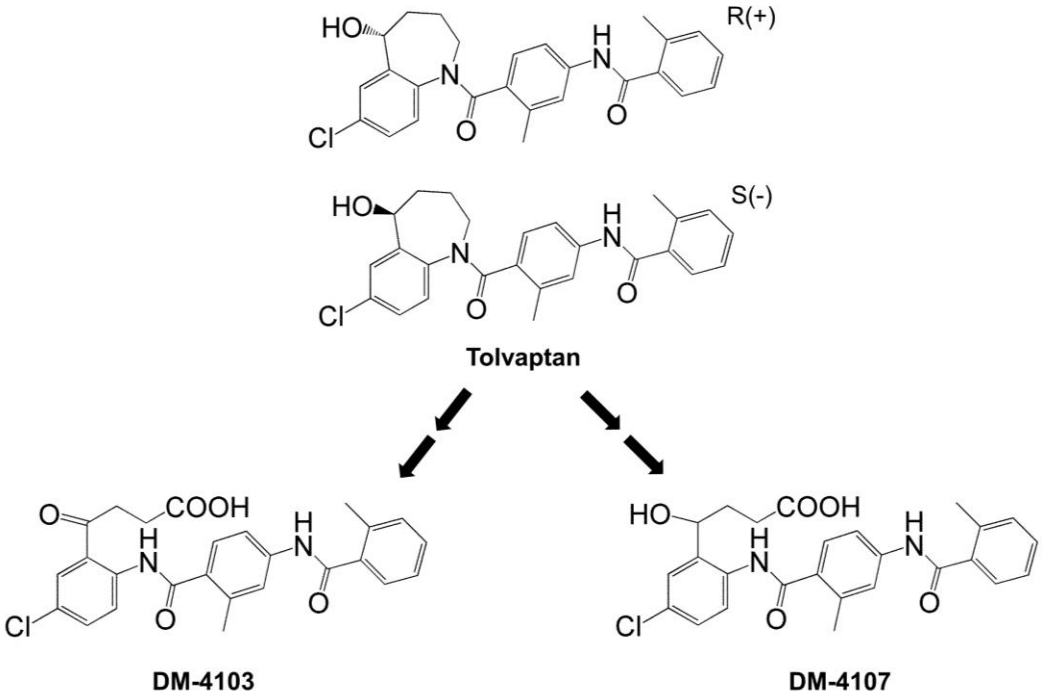

Figure 3.2. Inhibition of NTCP- and BSEP-mediated uptake by tolvaptan, DM-4103, and DM4107. NTCP-overexpressing cells were co-incubated with tolvaptan (0-50 μM), DM-4103 (0-75 μM), or DM4107 (0-200 μM) and [^{3}H]TCA (2 μCi/ml; 1 μM) for 5 min at 37°C (A-C); BSEP vesicles were co-incubated with tolvaptan (0-50 μM), DM-4103 (0-75 μM), or DM4107 (0-200 μM) and [^{3}H]TCA (2 μCi/ml; 2 μM) for 2 min at 37°C (D-F). NTCP-mediated uptake of TCA was calculated by subtracting substrate uptake in the absence of sodium from substrate uptake in the presence of sodium. BSEP-mediated transport was calculated by subtracting TCA uptake in the presence of AMP from TCA uptake in the presence of ATP. Values are expressed as percentage of vehicle control; each value represents the mean ± SD from three independent experiments. The curve represents the best fit line using nonlinear regression techniques. See *Materials and Methods* for further details.

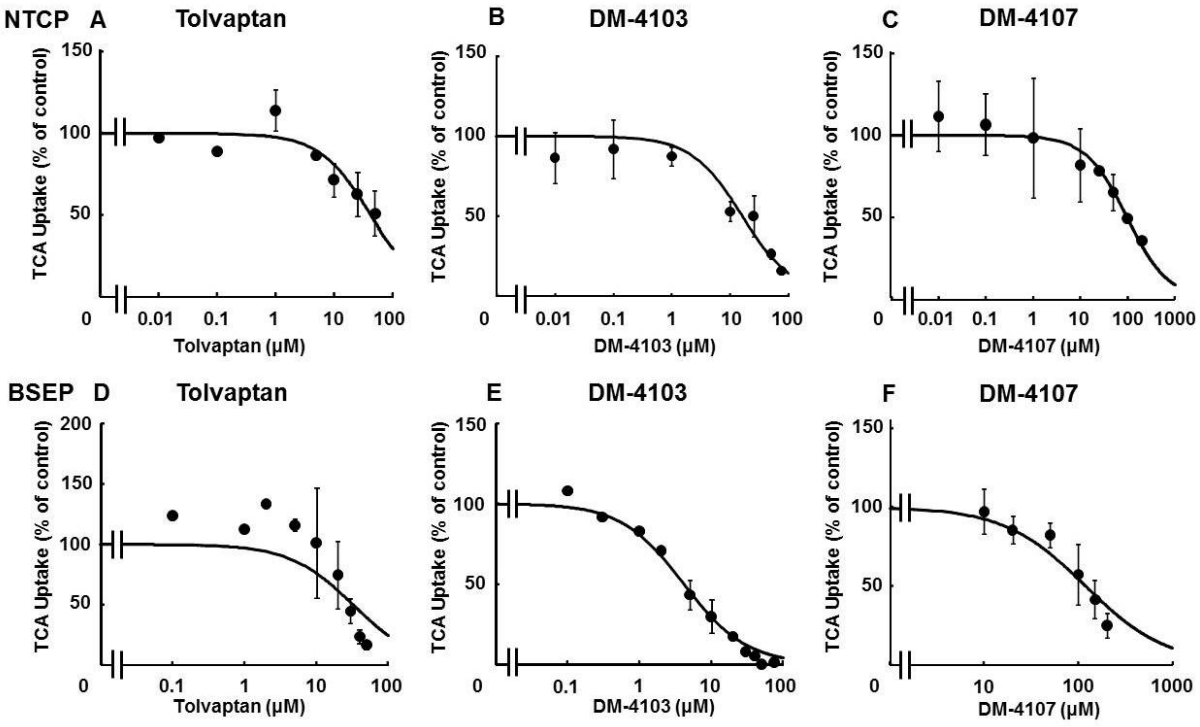

Figure 3.3. BSEP K_i determination. Uptake of TCA (2, 5, 10, 20, or 30 µM) was determined in the presence of 0 µM (●), 10 µM (○), 25 µM (▲), or 50 µM (Δ) tolvaptan (A) or 0 µM (●), 2 µM(○), 5 µM (▲), or 20 µM (Δ) of DM-4103 (B). TCA uptake was measured after an incubation of 2 min at 37ºC in the presence or absence of inhibitor. BSEP-mediated transport was calculated by subtracting TCA uptake in the presence of AMP from TCA uptake in the presence of ATP; each value represents the mean ± SD from three independent experiments. The curves represent the best fit model using nonlinear regression techniques. See *Materials and Methods* for further details.

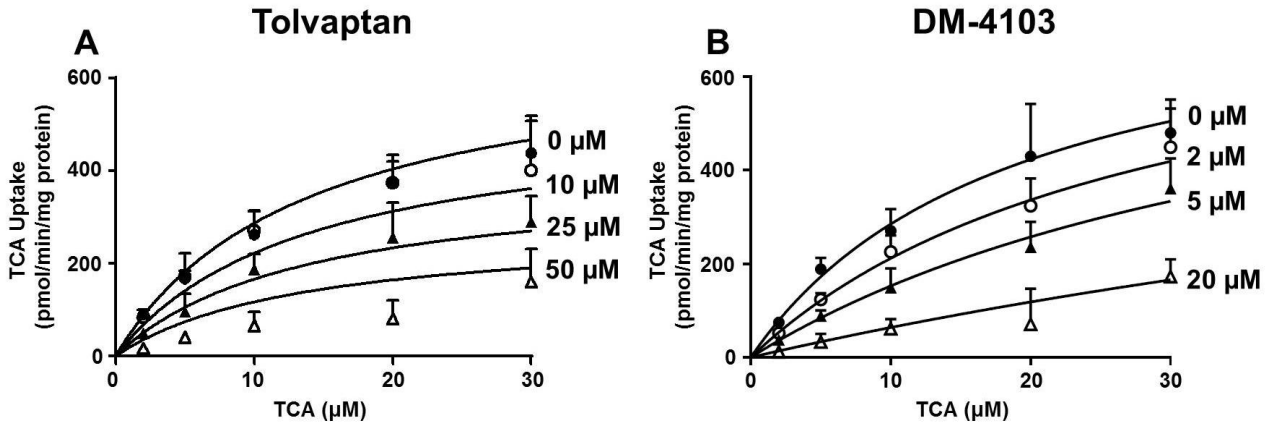

Figure 3.4. Inhibition of MRP2-, MRP3-, and MRP4-mediated uptake by tolvaptan, DM-4103, and DM4107. MRP2 (A-C), MRP3 (D-F) or MRP4 (G-I) vesicles were co-incubated with tolvaptan (0-50 μM), DM-4103 (0-50 μM for MRP2 and MPR3, and 0-20 μM for MRP4), or DM-4107 (0-200 μM) and [^{3}H]$E_2$17G (2 μCi/ml; 50 μM) (A-C) for 2 min, [^{3}H]$E_2$17G (2 μCi/ml; 10 μM) (D-F) for 5 min, or [^{3}H]DHEAS (2 μCi/ml; 2 μM) (G-I) for 2 min at 37°C. MRP-mediated transport was calculated by subtracting substrate uptake in the presence of AMP from substrate uptake in the presence of ATP. Values are expressed as percentage of vehicle control; each value represents the mean ± SD from three independent experiments. If the inhibitor did not reduce substrate transport by >50% at the highest tested concentration, nonlinear regression to estimate an IC_{50} value was not conducted. The curve represents the best fit line using nonlinear regression techniques. See *Materials and Methods* for further details.

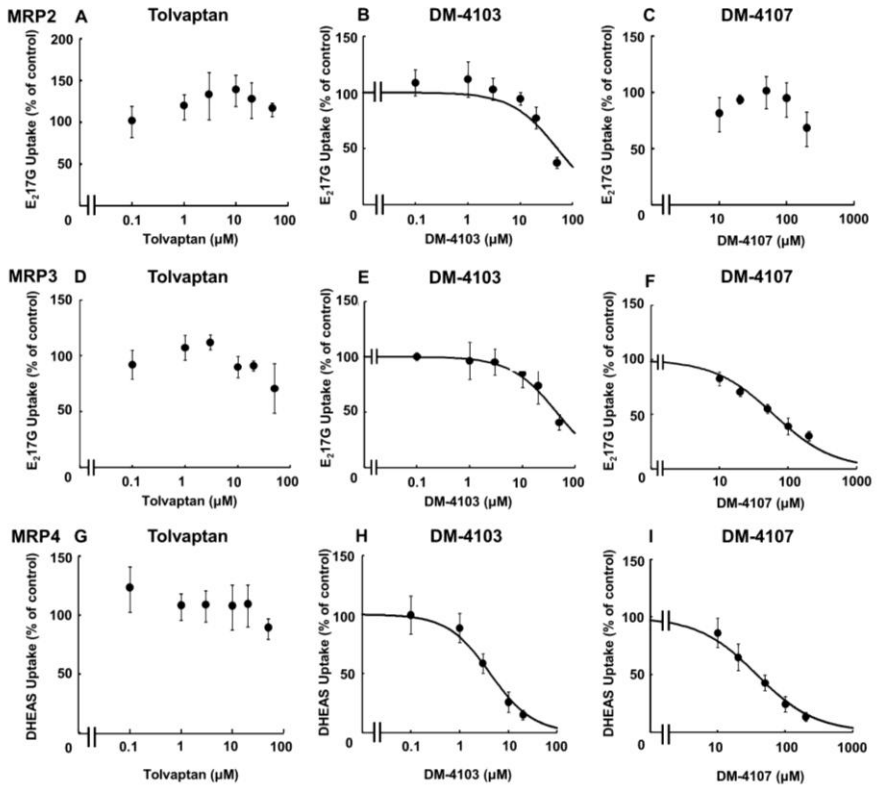

Figure 3.5. Time- and temperature-dependent accumulation of tolvaptan in sandwich-cultured human hepatocytes (SCHH). Accumulation of tolvaptan in cells + bile (black bars) and cells (white bars) was measured by incubating SCHH with 15 µM of tolvaptan for 5, 10, or 20 min at 37ºC, or for 10 min at 4 ºC (A). Accumulation of tolvaptan, and the generated metabolites DM-4103 and DM-4107 in cells+bile (black bars) and cells (white bars) was measured by incubating SCHH with 15 µM of tolvaptan for 10 min at 37ºC (B). *Cellular concentrations were calculated using the total mass of tolvaptan, DM-4103, or DM-4107 in cells (white bars) and hepatocyte fluid volume as described in *Materials and Methods*; each value represents the mean ± SD from n= 1 liver in triplicate.

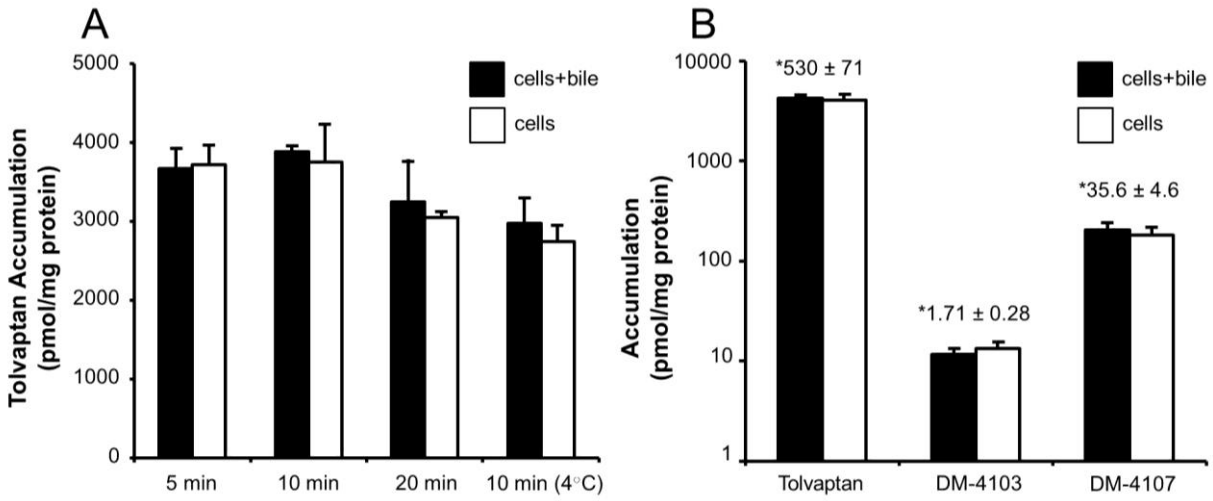

Figure 3.6. Accumulation of TCA, CDCA, TCDCA, and GCDCA after incubation in the presence or absence of tolvaptan in sandwich-cultured human hepatocytes (SCHH). Accumulation of d_8-TCA (2.5 µM) and d_5-CDCA (2.5 µM) (A), or TCDCA (2.5 µM) and GCDCA (2.5 µM) (B) in cells+bile (black bars) and cells (white bars) was measured after incubating SCHH with designated bile acids in the presence or absence of tolvaptan (15 µM) for 10 min at 37ºC; each value represents the mean ± SD from n= 1 liver in triplicate.

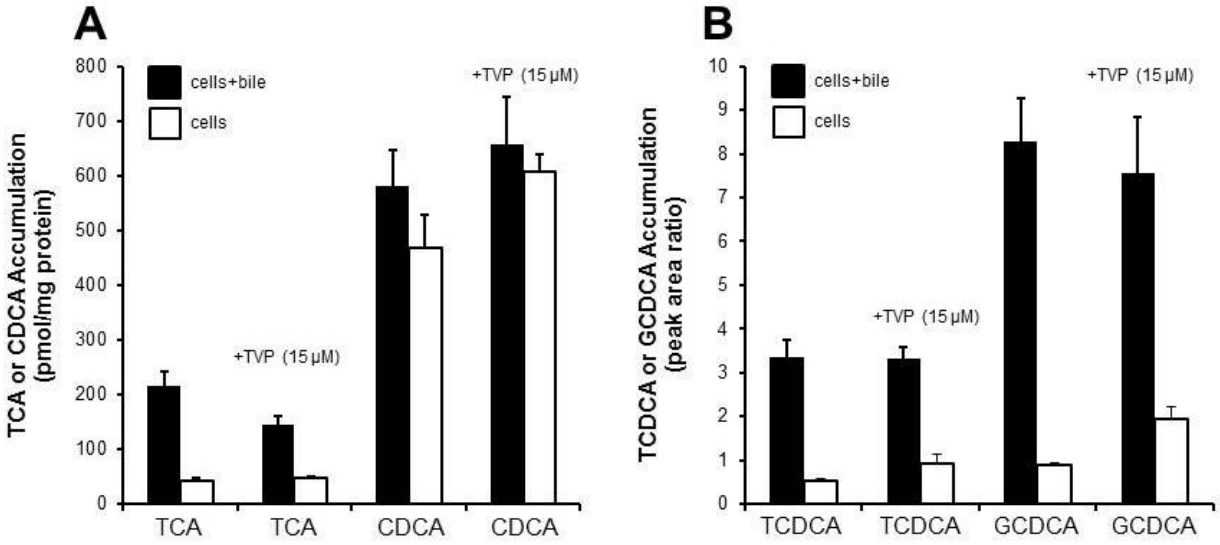

Table 3.1. Inhibitory potency of tolvaptan, DM-4103, and DM-4107 on transporter-mediated uptake.

Transporter	Inhibitor	IC_{50} (μM)	95% CI (μM)	C_{max}/IC_{50}
NTCP	Tolvaptan	~41.5	26.0-66.3	0.03
	DM-4103	16.3	11.1-24.0	0.96*
	DM-4107	95.6	58.7-156	0.02
BSEP	Tolvaptan	31.6	16.5-60.3	0.04
	DM-4103	4.15	3.45-4.99	3.78*
	DM-4107	119	86.2-163	0.02
MRP2	Tolvaptan	>50	NC	NC
	DM-4103	~51.0	32.0-81.3	0.31*
	DM-4107	>200	NC	NC
MRP3	Tolvaptan	>50	NC	NC
	DM-4103	~44.6	30.9-64.5	0.35*
	DM-4107	61.2	51.5-72.8	0.04
MRP4	Tolvaptan	>50	NC	NC
	DM-4103	4.26	3.32-5.47	3.69*
	DM-4107	37.9	32.1-44.7	0.06

CI: confidence interval; mean C_{max} following a 90 mg dose in humans. In cases where substrate uptake was inhibited by >50% only at the highest tested inhibitor concentration, the data were curve fit in the usual manner, but the estimated IC_{50} value was designated as an approximation (~). If the inhibitor did not reduce substrate transport by >50% at the highest tested concentration, nonlinear regression to estimate an IC_{50} value was not conducted and the value was reported as greater than the highest tested concentration. *C_{max} values were not determined in clinical trials therefore, concentrations at steady-state were used instead.

Table 3.2. Sodium-dependent uptake of tolvaptan, DM-4103 and DM-4107 in sandwich-cultured human hepatocytes (SCHH).

		Tolvaptan	DM-4103	DM-4107
Tolvaptan Dose Concentration	**Buffer**	**Total Accumulation (pmol/mg)**	**Total Accumulation (pmol/mg)**	**Total Accumulation (pmol/mg)**
15 µM	Sodium	2730 ± 397	7.82 ± 0.84	121 ± 19
	Choline	3460 ± 684	8.35 ± 0.83	136 ± 16

Data represent mean ± SD (n= 1 liver in triplicate)

Table 3.3. Hepatobiliary disposition of bile acids in the absence or presence of tolvaptan in sandwich-cultured human hepatocytes (SCHH). Hepatobiliary disposition of 2.5 µM taurocholic acid (TCA), chenodeoxytaurocholic acid (CDCA), taurochenodeoxycholic acid (TCDCA) or glycochenodeoxycholic acid (GCDCA) in the absence or presence of tolvaptan (15 µM) in sandwich-cultured human hepatocytes (SCHH).

Probe	Inhibitor	Total Accumulation[#]	Cellular Accumulation[#]	$Cl_{biliary}$ (mL/min/kg)	BEI (%)
TCA	Vehicle Control	215 ± 27	43.3 ± 4.4	20.3	79.8
	Tolvaptan	145 ± 16	47.5 ± 2.1	11.6	67.3
CDCA	Vehicle Control	580 ± 67	469 ± 60	13.1	19.1
	Tolvaptan	658 ± 86	608 ± 31	5.86	7.52
TCDCA	Vehicle Control	3.37 ±0.55	0.545 ± 0.049	NC*	83.8
	Tolvaptan	3.32 ± 0.27	0.915 ± 0.22	NC*	71.0
GCDCA	Vehicle Control	8.82 ± 0.98	0.892 ± 0.065	NC*	89.2
	Tolvaptan	7.55 ± 1.28	1.93 ± 0.28	NC*	74.5

[#]Accumulation of TCA and CDCA is expressed as pmol/mg protein; accumulation of TCDCA and GCDCA is expressed as peak area ratio; BEI=biliary excretion index; Data represent mean ± SD (n=1 liver in triplicate); *NC: not calculable, see *Materials and Methods*.

CHAPTER 4. Bile Acids as Potential Biomarkers to Assess Liver Impairment in Polycystic Kidney Disease [4]

INTRODUCTION

Polycystic kidney disease (PKD) is a class of ciliopathic disorders that arise from abnormalities in the primary cilium in many epithelial organs that lead to the development of fluid-filled cysts (Igarashi et al., 2007). These inheritable diseases are genetically transmitted in either a dominant form (autosomal dominant polycystic kidney disease; ADPKD) or a recessive form (autosomal recessive polycystic kidney disease; ARPKD) from mutations in the PKD1/2 or PKDH1 gene, respectively (Torres et al., 2007; Ward et al., 2002). ADPKD is the most common form of PKD and occurs between 1 in 400 and 1 in 1000 live births (Ecder et al., 2006; Torres et al., 1998). The destruction/displacement of renal tubules as a result of cystic growth and subsequent decline in renal function is central to the morbidity and mortality in patients with ADPKD. However, cysts occur in other epithelial organs such as the spleen, pancreas, lungs, and liver (Danaci et al., 1998; Levine et al., 1985, Perrone, 1997; Torra et al., 1997).

The liver is the most frequently affected extrarenal organ in ADPKD. A recent study by Hogan et al. (2015) reported that ~70% of men and ~80% of women with ADPKD have liver cysts. Although increases in serum γ-glutamyl transferase (GGT) or alkaline phosphatase (ALP) of ~2-5 times the upper limit of normal have been observed in some patients, typical biochemical measures of liver impairment, as with many liver diseases, are not sensitive or specific to detect

[4] This chapter was submitted to *Toxicology and Applied Pharmacology* and is presented in the style of that journal.

liver injury (Alempijevic et al. 2009; Giannini et al. 2005; Mofrad et al. 2003; Pohl et al. 2001). Therefore, there is value in establishing more sensitive and/or specific molecular biomarker(s) that may be useful in staging, diagnosis/prognosis, and/or clinical response to intervention(s) in ADPKD and related polycystic liver diseases (PLD). Several rodent models of PKD have been described with some animal models displaying isolated renal disease whereas others exhibit isolated hepatic abnormalities (McDonald et al., 2006; Schieren et al., 1996). In 2000, a spontaneous mutation in a colony of Sprague-Dawley rats displaying bilateral renal and hepatic cysts, now known as the polycystic kidney (PCK) rat, was described by Katsuyama et al. (2000). Although the inheritance of PKD in PCK rats is autosomal recessive, the renal and hepatic histopathological features resemble human ADPKD (Lager et al., 2001). For example, the kidney in PCK rats and human ADPKD are normal at birth but exhibit slow, progressive renal cyst growth. Furthermore, liver ductal plate abnormalities, biliary dysgenesis, and hepatic cyst development in PCK rats are consistent with the natural history of human ADPKD (Lager et al., 2001; Mason, et al. 2010; Masyuk et al., 2004). Hence, the PCK rat has been a valuable tool to understand the progression of ADPKD as well as to evaluate therapeutic interventions (Blazer-Yost et al., 2010; Lager et al., 2001; Sabbatini et al., 2014). Therefore, the PCK rat model was selected in the present study to evaluate the association between potential biomarkers and liver impairment in ADPKD.

Bile acids are a diverse, but structurally similar group of cholesterol-derived acidic steroids important in digestion/absorption and normal hepatic function. They also act as signaling molecules and play a critical role in the regulation of lipid metabolism and inflammation (Marin et al., 2015). Bile acids have been evaluated as biomarkers in various liver diseases such as cirrhosis, hepatocellular carcinoma, and nonalcoholic steatohepatitis (Chen et

al., 2011; Ferslew et al., 2015; Mannes et al., 1986). However, the association between bile acids and severity of liver impairment in ADPKD has yet to be established. Thus, this study was designed to investigate the association between liver impairment and bile acid concentrations in an established rodent model of ADPKD. These data may provide justification for future research in ADPKD patients.

MATERIALS AND METHODS

Materials.

All bile acid standards were obtained from Steraloids Inc. (Newport, RI) and TRC Chemicals (Toronto, ON, Canada). Nine stable isotope- labeled standards were obtained from C/D/N Isotopes Inc. (Quebec, Canada) and Steraloids Inc. (Newport, RI). Methanol (Optima LC-MS), acetonitrile (Optima LC-MS) and formic acid (Optima LC-MS) were purchased from Thermo-Fisher Scientific (FairLawn, NJ). Ultrapure water was produced by a Mill-Q Reference system equipped with a LC-MS Pak filter (Millipore, Billerica, MA).

Animals.

Male Sprague-Dawley (SD) or polycystic kidney disease (PCK/Crlj Crl-Pkhd1pck/Cr) rats were purchased from Charles River Laboratories (Wilmington, MA). Rats were housed in a constant alternating 12-hr light/dark cycle and allowed water and food ad libitum and acclimated for a minimum of 1 week prior to experimentation. All animal procedures complied with the guidelines of the Institutional Animal Care and Use Committee (University of North Carolina, Chapel Hill, NC).

Magnetic resonance imaging.

Magnetic resonance images (MRI) were acquired with a 9.4T Bruker Biospec 94/30USR (Bruker BioSpin, Billerica, MA) controlled with ParaVision software (v5.1. Billerica, MA). Rats

were anesthetized with 2% isoflurane in an air/oxygen mix. Respiratory-gated axial images were acquired with a 2D FLASH sequence with a repetition time of 533ms and an echo time of 10ms. Axial slices covered a 6x6 cm^2 field of view with a 256x256 matrix at a separation of 2mm and utilized two averages. The region of interest was multiplied by the slice thickness to estimate the volume of the liver tissue or cysts using the following equation:

V_{liver} or V_{cyst} = (A_{liver} or A_{cyst} in slice 1)●(Thickness) + (A_{liver} or A_{cyst} in slice 2)●(Thickness) + (A_{liver} or A_{cyst} in slice 3)●(Thickness) +…+ (A_{liver} or A_{cyst} in slice n)●(Thickness)

Where V_{liver} is the volume of the liver, V_{cyst} is the volume of cysts; A_{liver} is the area of the liver MRI slice; A_{cyst} is the area of cyst in the MRI slice and the thickness is the thickness of each slice (2mm). Cyst segmentation and volume were measured using ImageJ 1.48v (National Institutes of Health, USA).

Sample collection.

After 72 hrs following MRI, rats were fasted overnight and anesthetized with ketamine:xylazine (60:12 mg/kg IP). Bile was collected by cannulating the bile duct using PE-10 tubing; urine was collected from the bladder by cystocentesis; liver samples were excised from the median lobe; whole blood was collected and spun down at 1500g for 10 min to collect serum. All samples were immediately frozen at -80°C until bioanalysis.

Sample preparation and bioanalysis.

Sample preparation and bile acid quantification methodology were adapted from Xie et al. (2015). Briefly, an internal standard solution containing nine internal standards (100 nM for d4-GCA, d4-TCA, d9-TCDCA, d4-UDCA, d4- CA, d4-GCDCA, d4-GDCA, d4-DCA, and 200

nM for d4-LCA) was added to serum, urine, bile, liver homogenate, or standard solution and centrifuged. Liver tissue was homogenized with 100 µL of 50% methanol using a Bullet Blender Tissue Homogenizer (Next Advance, Inc., Averill Park, NY). After centrifugation, the supernatant was evaporated to dryness using a freeze dryer system (Labconco, Kansas City, MO). The residue was reconstituted in 1:1 (v/v) mobile phase B (acetonitrile / methanol =95:5, v/v) and mobile phase A (water with formic acid, pH=3.25), and centrifuged at 13,500g (4°C) for 20 min. The supernatant was transferred to a 96-well plate for analysis. An ultra-performance liquid chromatography coupled to tandem mass spectrometry (UPLC-MS/MS) system (ACQUITY UPLC-Xevo TQ-S, Waters Corp., Milford, MA) was used to quantify bile acids in the rat bile, serum, urine, and liver homogenate samples. Calibration solutions containing all analytes prepared at a series of concentrations in pooled naïve serum and urine depleted of bile acids using activated charcoal were used to generate standard curves using TargetLynx application manager (Waters Corp, Milford, MA). The limit of quantification was 1.024 nM for all bile acid species, except for a limit of 2.56 nM for cholic acid (CA), murocholic acid (MCA), glycodeoxycholic acid (GDCA), glycochenodeoxycholic acid (GCDCA), ursodeoxycholic acid (UDCA), α-hyodeoxycholic acid (HDCA), 6-ketolithocholic acid (6-keto-LCA), tauroursodeoxycholic acid (TUDCA), taurohyodeoxycholic acid (THDCA), and chenodeoxycholic acid 24-acyl-β-D-glucuronide (CDCA-24G); the limit of quantification for tauro-ω-muricholic acid, tauro-α-muricholic acid, tauro-β-muricholic acid, and taurocholic acid was 12.8 nM.

Immunohistochemistry (IHC).

Liver samples from the median lobe were excised and immediately placed in 4% paraformaldehyde for 48 h, processed, embedded in paraffin, serially sectioned at 4 µm thickness

and placed on coated glass slides. Sectioned slides were used for IHC immediately or unstained slides were stored in the nitrogen gas chamber if staining was not done immediately. Goat polyclonal anti-BSEP antibody sc-17292 was purchased from Santa Cruz Biotechnology (Dallas, TX). IHC was carried out in the Bond fully automated immunostainer (Leica Biosystems Inc., Vista, CA). Slides were dewaxed in Bond Dewax solution (AR9222) and hydrated in Bond Wash solution (AR9590). Antigen retrieval was performed for 30 min at 100ºC in Bond-Epitope Retrieval Solution 1 pH-6.0 (AR9961). The antigen retrieval was followed with 5 min Bond peroxide blocking (DS9800) and 10 min protein blocking (PV6122, Leica) steps. After pretreatment, slides were incubated with the antibody (1:50) for 4 hrs. Bond polymer was supplemented with ImmPRESS HRP anti-Goat secondary antibody (MP-7405-15, Vector Labs; Burlingame, CA Bond™) and detected using the Polymer Refine Detection system (DS9800). Stained slides were dehydrated and covered with a coverslip. Positive and negative controls (no primary antibody) were evaluated.

Data and statistical analysis.

The molar sum of all measured bile acids is reported as total bile acids. Total unconjugated and glycine- and taurine-conjugated bile acids were calculated as the sum of all unconjugated or glycine- or taurine-conjugated species of CA, CDCA, hyocholic acid (HCA), HDCA, MCA, deoxycholic acid (DCA), lithocholic acid (LCA), and UDCA. The relative abundance of each group of bile acid species was calculated as the total molar mass for that particular species divided by the total bile acid molar mass. Measured bile acid concentrations below the limit of quantification, but above the limit of detection, were imputed as one-half of the limit of quantification; concentrations measured below the limit of detection were imputed as zero. Statistical significance was determined using the nonparametric Mann-Whitney test, with

α=0.05 using GraphPad Prism (v.6.0 GraphPad Software, La Jolla, CA) to compare PCK versus wild-type rats. Given the number, complexity, and potential intercorrelation(s) between data in large metabolomic data sets, a multivariate statistical approach was utilized to reduce the dimensionality of the bile acid data to detect differences in the bile acid metabolome between wild-type and PCK rats. Without multivariate analysis, this may lead to false positives if traditional methods of statistical hypothesis testing are used alone (e.g. t-tests, ANOVAs) (Ringnér et al., 2008) Therefore, Principal component analysis (PCA) was performed to visualize the bile acid metabolome in PCK compared to wild-type rats (SIMCA 14, Umetrics, Umea, Sweden). Spearman correlation coefficients (two-tailed) were determined using GraphPad Prism (v.6.0 GraphPad Software, La Jolla, CA) where p-values ≤ 0.05 were considered statistically significant. Multiple analysis of variance (MANOVA) was conducted using R package (v. 3.3.1).

RESULTS

Rat Characteristics.

Hepatic cyst volume was measured at 12, 16, and 20 weeks in PCK rats to monitor the progression of cystic volume. Cystic disease is progressive and these time frames are consistent with the presentation of hepatic cysts and liver dysfunction in PCK rats (Lager et al., 2001; Katsuyama et al., 2000). Furthermore the mortality in PCK rats is high after 20 weeks of age (Katsuyama et al., 2000). The cystic volume (mean ± standard deviation) in PCK rats increased from 2.83 ± 1.42 to 3.92 ± 1.98 to 5.20 ± 2.61 at 12, 16 and 20 weeks, respectively. Representative magnetic resonance images are shown in Fig. 4.1. At 20 weeks, liver and total kidney weights were significantly increased in PCK rats compared to wild-type rats (Table 4.1).

Bile Acid Composition.

Under fasting conditions, 42 bile acids were measured in the liver, bile, serum, and urine of wild-type and PCK rats. Total liver and serum bile acids were significantly increased in PCK rats by 13.2- and 5.5-fold compared to wild-type rats, respectively ($p < 0.05$; Fig. 4.2A and 4.2C). Total urine bile acids also were increased 3.0-fold in PCK rats but differences did not reach statistical significance (Fig. 4.2D). There was no apparent different in total biliary bile acids (Fig. 4.2B). As shown, the difference in liver bile acids was driven by similar fold increases in unconjugated, taurine- and glycine-conjugated bile acids ($p < 0.05$; Fig. 4.3A). In contrast, unconjugated bile acids were significantly increased ($p < 0.05$) and appeared to increase to a greater extent (6.6-fold) compared to taurine conjugates (3.8-fold) in the serum of PCK rats (Fig. 4.3C). In urine, taurine and glycine conjugates increased by 7.4- and 5.1-fold compared to a 2.8-fold increase of unconjugated bile acids in PCK rats (Fig. 4.3D), although these differences did not reach statistical significance. No apparent differences in unconjugated or glycine or taurine-conjugated bile acids were observed in the bile between wild-type and PCK rats. Hepatic sulfate (i.e. lithocholic acid -3-sulfate) and glucuronide (i.e. CDCA 24-acyl-β-D-glucuronide and CDCA 3-acyl-β-D-glucuronide) bile acid conjugates also were significantly increased in PCK rats by 5.1-fold and 6.9-fold, respectively ($p < 0.05$; Supplement Table 4.1). Serum and urine glucuronide conjugates also were significantly increased by 15.5-fold and 12.2-fold ($p < 0.05$), respectively, in PCK rats. Serum and urine sulfate conjugates appeared to increase in PCK rats but differences did not reach statistical significance; no differences were apparent in biliary sulfate or glucuronide bile acid conjugates.

To determine whether the relative abundance of bile acid species was different between wild-type and PCK rats, the relative amounts (expressed as a % of the total molar sum) of total

unconjugated and glycine- and taurine-conjugated species of CDCA, CA, DCA, LCA, and UDCA were evaluated in each matrix. Few notable differences between wild-type and PCK rats were observed. For example, LCA species decreased in the liver of PCK rats ($p < 0.05$; Table 4.2). In contrast, the relative abundance of DCA (serum and urine) and LCA (liver) species increased in PCK rats ($p < 0.05$). The remaining species in each matrix appeared to be unchanged. Secondary bile acids (e.g. glycohyodeoxycholic acid (GHDCA), HDCA, and MCA were among bile acids species that displayed the greatest-fold change in PCK compared to wild-type rats (Supplement Table 4.2).

Bile Acids Associated with Hepatotoxicity.

Due to their detergent-like effects, bile acid hydrophobicity is positively associated with liver injury (Attili et al., 1986). Generally recognized hepatotoxic bile acids include the glycine and taurine conjugates of DCA and CDCA (Perez et al., 2009). When bile acids associated with hepatotoxicity (i.e. TDCA, TCDCA, GDCA, and GCDCA) were analyzed separately, total toxic bile acids were significantly increased in PCK rat liver and serum by 8.4-fold and 3.3-fold, respectively (Fig.4.4A and 4C). GCDCA was increased as much as 22.8-fold in the liver of PCK rats, whereas in serum, TDCA, TCDCA, GDCA, and GCDCA were increased to a similar extent (i.e. ~2-5-fold). Total toxic bile acids tended to increase in the urine (2.8-fold) but differences failed to reach statistical significance (Fig. 4.4D). No notable differences were observed in biliary bile acids (Fig. 4.4B). LCA, one of the most hydrophobic bile acids, was significantly increased by ~2.5-fold in the liver and serum, but not in the urine or bile of PCK rats (Supplementary Table 4.3). DCA concentrations did not reach statistically significant differences in the liver; however, DCA was significantly increased by 5.2 and 30.5-fold in the serum and urine of PCK rats, respectively (Supplementary Table 4.3).

Principal Component Analysis.

Separate PCA score plots for bile acids in each matrix were used to evaluate differences in the profile of individual bile acid species in wild-type and PCK rats. PCA score plots indicated that PCK rats clearly separated from wild-type rats (liver cumulative $r^2 = 0.874$; bile cumulative $r^2 = 0.707$; serum cumulative $r^2 = 0.804$; urine cumulative $r^2 = 0.652$) under fasting conditions (Fig. 4.5).

Correlation Analysis and Multivariate Analysis of Variance (MANOVA)

Correlation analysis was used first to evaluate the correlation between serum bile acids and markers of liver impairment (i.e. liver weight, total liver bile acids, total toxic liver bile acids, and cystic volume) to test the hypothesis that serum bile acids correlated with markers of liver impairment ($\alpha = 0.05$). Serum bile acids positively correlated with liver weight ($r = 0.919$, 95% CI = 0.650-0.985), total liver bile acids ($r = 0.976$; 95% CI = 0.869-0.995), total toxic liver bile acids ($r = 0.950$; 95% CI = 0.743-0.991), and cystic volume ($r = 0.939$; 95% CI = 0.693-0.989) (Fig. 4.6); p-values were < 0.01. After adjusting using the Bonferroni correction, p-values remained statistically significant. As a follow-on assessment, a MANOVA model was used to: (1) obtain the point and interval estimates of the mean levels, (2) estimate correlations among the five variables, and (3) perform a test of the overall multi-dimensional null hypothesis that the two strains (i.e. wild-type and PCK) do not differ based on mean values for any of the five variables (i.e. serum bile acids, total liver weight, total liver bile acids, total toxic liver bile acids, and cystic volume) of interest. Wild-type and PCK rats were different for all five variables and a statistically significant MANOVA effect was obtained, Pillais Trace = 0.977 $F(32.1, 4)$ $p < 0.001$. Subsequently, a series of one-way analysis of variances (ANOVAs) on each of the four

dependent variables was conducted as follow-up tests to the MANOVA. The ANOVA values for liver weight (F-value = 32.5; p = 0.00126), total liver bile acids (F-value = 34.4; p = 0.00109), total hepatotoxic liver bile acids (F-value = 15.1; p = 0.0081), and cyst volume (F-value = 43.9; p = 0.000570) were statistically significant.

Immunohistochemistry (IHC).

Visualization of Bsep in wild-type and PCK rats using immunohistochemical techniques revealed similar expression and distribution of Bsep throughout the liver acinus (Fig. 4.7).

DISCUSSION

Serum bile acids have been used as a clinical index of liver pathology. To our knowledge, this is the first study to examine the relationship between serum bile acids and markers of liver impairment in a rodent model of ADPKD, which may provide justification for future research in ADPKD patients. As shown, total liver bile acids were increased by 13.2-fold compared to wild-type rats (Fig. 4.2A). During the analysis of these data, Munoz-Garrido et al. (2015) reported that hepatic bile acids were elevated in PCK rats, a finding that is in agreement with the current data presented. Elevated hepatic bile acids are consistent with cholestasis in PCK rats; in addition, total serum and urine bile acids were increased by 5.5- and 3.0-fold, respectively, in PCK rats (Fig. 4.2C and 2D).

A functional alteration in Bsep, the rate-limiting step in the translocation of bile acids from hepatocytes to the bile canaliculus, is one mechanism of impaired biliary secretion that can lead to bile acid accumulation, acute liver toxicity, and fibrosis (Kisseleva et al., 2011). Bsep was internalized and transport function was impaired in a taurolithocholate-induced model of cholestasis (Crocenzi et al., 2003). In the present study, taurolithocholate was increased by 27.3

and 22.4-fold in the liver and serum, respectively, of PCK rats (Supplementary Table 4.3), which suggests that elevated concentrations of taurolithocholate (and other bile acids) could decrease bile acid transport through internalization and/or downregulation of Bsep. Therefore, we hypothesized that Bsep expression and/or localization may be impaired in PCK rats, which may, in part, explain elevated liver bile acid concentrations. However, IHC analysis failed to detect any apparent difference in Bsep expression and/or localization (Fig. 4.7). Although mechanisms of bile acid-mediated internalization of Bsep have been demonstrated *in vitro*, Bsep expression is maintained in models of chronic cholestasis in the rat (Buscher et al., 1989; Lee et al., 2000), consistent with the current data. Moreover, we did not observe significant differences in biliary bile acid concentrations, which further support the relative preservation of Bsep function (Fig. 4.2B).

Although the purpose of this study was not to elucidate the mechanisms underlying altered bile acid homeostasis, the data generated raise several questions. Using gene expression analysis, Ruh et al. (2013) first reported down-regulation of primary bile acid synthesis pathways, a compensatory mechanism aimed at reducing hepatic bile acid concentrations. However, this would not explain increased hepatic taurocholic acid concentrations reported by Ruh et al. (2013) as well as increased concentrations of most bile acid species in the liver, as observed in the present study and reported by Munoz-Garrido et al. (2015). Furthermore, Cyp7a1, the rate-limiting step in bile acid synthesis, was not altered in PCK rats (Munoz-Garrido et al., 2015). These data suggest that increased bile acid synthesis may not account for elevated hepatic bile acid concentrations, although other enzymes are involved in bile acid metabolism and should be considered (e.g. Cyp27A1, Cyp8B1, and bile acid– coenzyme A:amino acid N-acyltransferase) (Chiang et al., 2009; Pellicoro et al., 2007). Altered function of other

hepatobiliary bile acid transporters may explain the observations reported here. For example, NTCP/Ntcp and OATP/Oatp are responsible for the sinusoidal uptake of bile acids from the blood to hepatocytes, and are downregulated in obstructive cholestasis, which may explain elevated serum bile acid concentrations observed in the present study (Geier, et al. 2007; Lee et al., 2000; Moseley et al. 1996; Trauner et al. 1997). In addition, MRP3/Mrp3 is upregulated in cholestasis to provide an additional compensatory route for hepatic bile acid efflux (Chai et al., 2012; Donner et al., 2001). IHC analysis revealed that Mrp3 appears to be upregulated in PCK rats consistent with a cholestatic state (Slizgi et al., manuscript in preparation) and further work quantifying the protein expression of relevant transporters in PCK rats is currently underway. It must be noted that canalicular membrane fluidity and cholesterol content can affect Bsep function without affecting localization or expression, which could contribute to the observations reported here and should be explored in future mechanistic studies (Kanno et al., 2003; Kis et al., 2009).

High concentrations of bile acids can be cytotoxic, which may lead to hepatocellular damage and acute liver injury (Alnouti 2008; Hoffman et al., 2009). Because of the positive relationship between hydrophobicity and detergent effects, hydrophobic bile acid (e.g. LCA, DCA, CDCA and their glycine and taurine conjugates) are considered the most cytotoxic (Attili et al., 1986). Mechanistic studies indicate that hydrophobic bile acids can disrupt cell membranes, promote the generation of reactive oxygen species, and cause mitochondrial and endoplasmic reticulum stress triggering hepatocyte apoptosis and necrosis (Perez et al., 2009). Therefore, the disposition of hepatotoxic bile acids in PCK rats that may contribute to liver dysfunction was evaluated. Although the relative abundance of bile acid species was generally similar between wild-type and PCK rats (Table 4.2), concentrations of total bile acids associated

with hepatotoxicity (i.e. GDCA, GCDCA, TDCA, and GCDCA) were increased by 8.3- and 3.3-fold in the liver and serum of PCK rats, respectively. Secondary bile acids associated with hepatotoxicity (i.e. LCA and DCA), also were increased in the serum of PCK rats, albeit to a lesser extent relative to the glycine and taurine conjugates of DCA and CDCA (Supplementary Table 4.3). Studies have shown that accumulation of bile acids in the systemic circulation can promote endothelial cell injury, such as in the kidney (Bomzon et al., 1997; Hofmann et al., 2002). In accordance with increased hepatotoxic bile acids, liver biochemical abnormalities are generally observed in PCK rats. For example, GGT and glutamate dehydrogenase (GLDH), markers for hepatocellular damage, were increased in PCK rats (Ruh et al., 2013). Additionally, elevated levels of bilirubin and transaminases also may indicate hepatocellular damage (Mason et al., 2010; Shimomura et al., 2015). Contrasting observations of increased or unchanged levels of ALP, a marker of bile duct obstruction and cholestasis, have been reported (Munoz-Garrido et al., 2015; Mason et al., 2010; Shimomura et al., 2015).

Although liver tests (e.g. transaminases, bilirubin, ALP) are used routinely in clinical practice, these measures are generally not sensitive, specific, and/or may display large interindividual variability in the presence of liver impairment, thus making diagnoses challenging. Therefore, we sought to determine whether serum bile acids were associated with markers of liver impairment to justify their evaluation as biomarkers in PKD. Total liver bile acids and total toxic liver bile acids were chosen as markers of liver impairment because elevated bile acids are associated with hepatotoxicity. Liver weight was chosen as a marker of liver impairment because hepatomegaly may indicate vascular swelling, inflammation, and portal hypertension, which can lead to cirrhosis (Dooley et al., 2011). Finally, cystic volume was used as a marker of liver impairment because cysts are associated with infection, hemorrhaging, liver

cancer, and in some cases, cholangitis (Chauveau et al., 1997; Chauveau et al., 2000; Dooley et al., 2011; Suwabe et al., 2012; Yazdanpanah et al., 2013).

As shown, serum bile acids correlated with liver weight, total liver bile acids, total toxic liver bile acids, and cystic volume ($r > 0.9$; $p < 0.01$; Fig. 4.6). Because there are potential intercorrelation(s) between markers of liver impairment (e.g. liver weight would be expected to increase with an increase in cystic volume), subsequent MANOVA revealed a statistically significant effect ($p < 0.0085$). Follow-on ANOVAs also revealed a statistically significant effect, indicating that markers of liver impairment independently associated with total serum bile acids. An association between serum bile acids and hepatic cyst bile acid concentrations was reported in patients with ADPKD (Garrido-Munoz et al., 2015). The present data indicate that total toxic bile acids are increased in the livers of PCK rats and that elevated serum bile acids are associated with elevated liver bile acids. Given the similar hepatorenal abnormalities observed between PCK rats and human ADPKD, hepatotoxic bile acids also may be increased in ADPKD patients; thus, metabolomic profiling in ADPKD patients is warranted to test this hypothesis.

In a recent clinical trial, some patients with ADPKD experienced drug-induced liver injury (DILI) while being treated with tolvaptan, a vasopressin V_2-receptor antagonist (Watkins et al., 2015). Inhibition of bile acid transporters by tolvaptan/metabolites leading to intrahepatic accumulation of bile acids and subsequent hepatotoxicity has been explored as a biologically plausible mechanism underlying tolvaptan-associated DILI (Slizgi et al., 2016). However, tolvaptan was not associated with hepatotoxicity in other patient populations, which suggests that patients with ADPKD may be more susceptible to liver injury (Watkins et al., 2015). It is possible that elevated concentrations of hepatic bile acids in ADPKD due to liver pathology (e.g. hepatic cyst burden) may predispose some patients to bile acid-mediated hepatotoxicity. In the

context of tolvaptan-associated liver injury, the present data suggest that some ADPKD patients may be susceptible to bile acid-mediated hepatotoxicity if their hepatic bile acid load is characteristically elevated. Inhibition of bile acid transporter function by tolvaptan and/or metabolites, as reported in Slizgi et al. (2016), may further increase hepatic bile acid concentrations and lead to hepatotoxicity. It must be noted, however, that no evidence of cholestasis (e.g. no clinically significant increases in ALP) was apparent in ADPKD trials, which may suggest that alternative and/or contributing mechanism(s) may predispose this patient population to tolvaptan-associated DILI (Torres et al., 2012).

In conclusion, the results of these studies indicate that bile acids are increased in the liver and the serum of PCK rats, including bile acids associated with hepatotoxicity. Total serum bile acids are correlated with markers of liver impairment, which suggests that serum bile acids may be useful biomarkers of hepatic impairment in ADPKD.

REFERENCES

Alempijevic T, Krstic M, Jesic R, Jovanovic I, Sokic Milutinovic A, Kovacevic N, Krstic S, Popovic D. Biochemical markers for non-invasive assessment of disease stage in patients with primary biliary cirrhosis. World J Gastroenterol. 2009 Feb 7;15(5):591-4.

Alnouti Y. Bile Acid sulfation: a pathway of bile acid elimination and detoxification. Toxicol Sci. 2009 Apr;108(2):225-46.

Attili AF, Angelico M, Cantafora A, Alvaro D, Capocaccia L. Bile acid-induced liver toxicity: relation to the hydrophobic-hydrophilic balance of bile acids. Med Hypotheses. 1986 Jan;19(1):57-69.

Blazer-Yost BL, Haydon J, Eggleston-Gulyas T, Chen JH, Wang X, Gattone V, Torres VE. Pioglitazone Attenuates Cystic Burden in the PCK Rodent Model of Polycystic Kidney Disease. PPAR Res. 2010; 2010:274376.

Bomzon A, Holt S, Moore K. Bile acids, oxidative stress, and renal function in biliary obstruction. Semin Nephrol. 1997 Nov;17(6):549-62.

Buscher HP, Miltenberger C, Macnelly S, Gerok W. The histoautoradiographic localization of taurocholate in rat liver after bile ductligation. J Hepatol. 1989 Mar;8(2):181-91.

Chai J, He Y, Cai SY, Jiang Z, Wang H, Li Q, Chen L, Peng Z, He X, Wu X, Xiao T, Wang R, Boyer JL, Chen W. Elevated hepatic multidrug resistance-associated protein 3/ATP-binding cassette subfamily C 3 expression in human obstructive cholestasis is mediated through tumor necrosis factor alpha and c-Jun NH2-terminal kinase/stress-activated protein kinase-signaling pathway. Hepatology. 2012 May;55(5):1485-94.

Chauveau D, Fakhouri F, Grunfeld JP. Liver Involvement in Autosomal-Dominant Polycystic Kidney Disease: Therapeutic Dilemma. J Am Soc Nephrol. 2000 Sep;11(9):1767-75.

Chauveau D, Pirson Y, Le Moine A, Franco D, Belghiti J, Grünfeld JP. Extrarenal manifestations in autosomal dominant polycystic kidney disease. Adv Nephrol Necker Hosp. 1997;26:265-89.

Chen T, Xie G, Wang X, Fan J, Qiu Y, Zheng X, Qi X, Cao Y, Su M, Wang X, Xu LX, Yen Y, Liu P, Jia W. Serum and urine metabolite profiling reveals potential biomarkers of human hepatocellular carcinoma. Mol Cell Proteomics. 2011 Jul;10(7):M110.004945.

Chiang J. Bile acids: regulation of synthesis. J Lipid Res. 2009 Oct;50(10):1955-66.

Crocenzi FA, Mottino AD, Sánchez Pozzi EJ, Pellegrino JM, Rodríguez EA, Garay, Milkiewicz P, Vore M, Coleman R, and Roma MG. Impaired localisation and transport function of canalicular Bsep in taurolithocholate induced cholestasis in the rat. Gut. 2003 Aug; 52(8): 1170–1177.

Danaci M, Akpolat T, Baştemir M, Sarikaya S, Akan H, Selçuk MB, Cengiz K. The prevalence of seminal vesicle cysts in autosomal dominant polycystic kidney disease. Nephrol Dial Transplant. 1998 Nov;13(11):2825-8.

Donner MG, Keppler D. Up-regulation of basolateral multidrug resistance protein 3 (Mrp3) in cholestatic rat liver. Hepatology. 2001 Aug;34(2):351-9.

Dooley J, Lok A, Andrew K. Burroughs AK, Jenny Heathcote J. Sherlock's Diseases of the Liver and Biliary System, 12th Edition. 2011 Blackwell Publishing Ltd.

Ecder T, Fick-Brosnahan G, Schrier RW. Polycystic kidney disease: diseases of the kidney and urinary tract. Philadelphia, PA: Lippincott Williams & Wilkins; 2006.

Ferslew BC, Xie G, Johnston CK, Su M, Stewart PW, Jia W, Brouwer KL, Sidney Barritt A 4th. Altered Bile Acid Metabolome in Patients with Nonalcoholic Steatohepatitis. Dig Dis Sci. 2015 Nov;60(11):3318-28.

Giannini E, Testa R, Savarino V. Liver enzyme alteration: a guide for clinicians. CMAJ. 2005 Feb 1; 172(3): 367–379.

Geier A, Wagner M, Dietrich CG, Trauner M. Principles of hepatic organic anion transporter regulation during cholestasis, inflammation and liver regeneration. Biochim Biophys Acta. 2007 Mar;1773(3):283-308.

Hofmann AF. Cholestatic liver disease: pathophysiology and therapeutic options. Liver. 2002;22 Suppl 2:14–19.

Hogan MC, Abebe K, Torres VE, Chapman AB, Bae KT, Tao C, Sun H, Perrone RD, Steinman TI, Braun W, Winklhofer FT, Miskulin DC, Rahbari-Oskoui F, Brosnahan G, Masoumi A, Karpov IO, Spillane S, Flessner M, Moore CG, Schrier RW. Liver involvement in early autosomal-dominant polycystic kidney disease. Clin Gastroenterol Hepatol. 2015 Jan;13(1):155-64.

Igarashi P, Somlo S. Polycystic Kidney Disease. JASN. 2007 vol. 18 no. 5 1371-1373.

Kanno K, Tazuma S, Niida S, Chayama K. Unique reciprocal changes of hepatocellular membrane transporter expression and fluidity in rats with selective biliary obstruction. Hepatol Res. 2003 Jun;26(2):157-163.

Katsuyama M, Masuyama T, Komura I, Hibino T, Takahashi H. Characterization of a novel polycystic kidney rat model with accompanying polycystic liver. Exp Anim. 2000 Jan;49(1):51-5.

Kis E, Ioja E, Nagy T, Szente L, Herédi-Szabó K, Krajcsi P. Effect of membrane cholesterol on BSEP/Bsep activity: species specificity studies for substrates and inhibitors. Drug Metab Dispos. 2009 Sep;37(9):1878-86.

Kisseleva T, Brenner DA. Anti-fibrogenic strategies and the regression of fibrosis. Best Pract Res Clin Gastroenterol. 2011;25:305–317. Aquaporins: their role in cholestatic liver disease. World J Gastroenterol. 2008 Dec 14;14(46):7059-67.

Lager DJ, Qian Q, Bengal RJ, Ishibashi M, Torres VE. The pck rat: a new model that resembles human autosomal dominant polycystic kidney and liver disease. Kidney Int. 2001 Jan;59(1):126-36.

Lee JM, Trauner M, Soroka CJ, Stieger B, Meier PJ, Boyer JL. Expression of the bile salt export pump is maintained after chronic cholestasis in the rat. Gastroenterology. 2000 Jan;118(1):163-72.

Levine E, Cook LT, Grantham JJ. Liver cysts in autosomal-dominant polycystic kidney disease: clinical and computed tomographic study. AJR Am J Roentgenol. 1985 Aug;145(2):229-33.

Mannes GA, Thieme C, Stellaard F, Wang T, Sauerbruch T, Paumgartner G. Prognostic significance of serum bile acids in cirrhosis. Hepatology. 1986 Jan-Feb;6(1):50-3.

Marin JJ, Macias RI, Briz O, Banales JM, Monte MJ. Bile Acids in Physiology, Pathology and Pharmacology. Curr Drug Metab. 2015;17(1):4-29.

Mason SB, Liang Y, Sinders RM, Miller CA, Eggleston-Gulyas T, Crisler-Roberts R, Harris PC, Gattone VH 2nd. Disease stage characterization of hepatorenal fibrocystic pathology in the PCK rat model of ARPKD. Anat Rec (Hoboken). 2010 Aug;293(8):1279-88.

Masyuk TV, Huang BQ, Masyuk AI, Ritman EL, Torres VE, Wang X, Harris PC, Larusso NF. Biliary dysgenesis in the PCK rat, an orthologous model of autosomal recessive polycystic kidney disease. Am J Pathol. 2004 Nov;165(5):1719-30.

McDonald RA, Avner ED. Watson ML, editor. New York: Oxford University Press; Mouse Models of Polycystic Kidney Disease. 1996:pp 63–87.

Mofrad P, Contos MJ, Haque M, et al. Clinical and histologic spectrum of nonalcoholic fatty liver disease associated with normal ALT values. Hepatology. 2003;37:1286–1292.

Moseley RH, Wang W, Takeda H, Lown K, Shick L, Ananthanaray anan M, Suchy FJ. Effect of endotoxin on bile acid transport in rat liver: a potential model for sepsis-associated cholestasis. Am J Physiol 1996;271:G137–G146.

Munoz-Garrido P, Marin JJ, Perugorria MJ, Urribarri AD, Erice O, Sáez E, Úriz M, Sarvide S, Portu A, Concepcion AR, Romero MR, Monte MJ, Santos-Laso Á, Hijona E, Jimenez-Agüero R, Marzioni M, Beuers U, Masyuk TV, LaRusso NF, Prieto J, Bujanda L, Drenth JP, Banales JM.

Ursodeoxycholic acid inhibits hepatic cystogenesis in experimental models of polycystic liver disease. J Hepatol. 2015 Oct;63(4):952-61.

Pellicoro A, van den Heuvel FA, Geuken M, Moshage H, Jansen PL, Faber KN. Human and rat bile acid-CoA:amino acid N-acyltransferase are liver-specific peroxisomal enzymes: implications for intracellular bile salt transport. Hepatology. 2007 Feb;45(2):340-8.

Perez MJ, Briz O. Bile-acid-induced cell injury and protection. World J Gastroenterol. 2009 Apr 14;15(14):1677-89.

Perrone RD. Extra-renal manifestations of autosomal dominant polycystic kidney disease. Kidney Int 1997:51:2022-36

Pohl A, Behling C, Oliver D, Kilani M, Monson P, Hassanein T. Serum aminotransferase levels and platelet counts as predictors of degree of fibrosis in chronic hepatitis C virus infection. Am J Gastroenterol. 2001 Nov;96(11):3142-6.

Ringnér M. What is principal component analysis? Nature Biotechnology. 2008 26, 303–304.

Ruh H, Salonikios T, Fuchser J, Schwartz M, Sticht C, Hochheim C, Wirnitzer B, Gretz N, Hopf C. MALDI imaging MS reveals candidate lipid markers of polycystic kidney disease. J Lipid Res. 2013 Oct;54(10):2785-94.

Sabbatini M, Russo L, Cappellaio F, Troncone G, Bellevicine C, De Falco V, Buonocore P, Riccio E, Bisesti V, Federico S, Pisani A. Effects of combined administration of rapamycin, tolvaptan, and AEZ-131 on the progression of polycystic disease in PCK rats. Am J Physiol Renal Physiol. 2014 May 15;306(10):F1243-50.

Schieren G, Pey R, Bach J, Hafner M, Gretz N. Murine models of polycystic kidney disease. Nephrol Dial Transplant. 1996;11 Suppl 6:38-45.

Shimomura Y, Brock WJ, Ito Y, Morishita K. Age-Related Alterations in Blood Biochemical Characterization of Hepatorenal Function in the PCK Rat: A Model of Polycystic Kidney Disease. Int J Toxicol. 2015 Nov-Dec;34(6):479-90.

Slizgi JR, Lu Y, Brouwer KR, St Claire RL, Freeman KM, Pan M, Brock WJ, Brouwer KL. Inhibition of Human Hepatic Bile Acid Transporters by Tolvaptan and Metabolites: Contributing Factors to Drug-Induced Liver Injury? Toxicol Sci. 2016 Jan;149(1):237-50.

Suwabe T, Ubara Y, Sumida K, Hayami N, Hiramatsu R, Yamanouchi M, Hasegawa E, Hoshino J, Sawa N, Saitoh S, Okuda I, Takaichi K. Clinical features of cyst infection and hemorrhage in ADPKD: new diagnostic criteria. Clin Exp Nephrol. 2012 Dec;16(6):892-902.

Torra R, Nicolau C, Badenas C, Navarro S, Pérez L, Estivill X, Darnell A. Ultrasonographic study of pancreatic cysts in autosomal dominant polycystic kidney disease. Clin Nephrol. 1997 Jan;47(1):19-22.

Torres VE, Chapman AB, Devuyst, O, Gansevoort RT, Grantham JJ, Higashihara, E, Perrone, RD, Krasa HB, Ouyang J, and Czerwiec, FS. TEMPO 3:4 trial investigators. Tolvaptan in patients with autosomal dominant polycystic kidney disease. N.Engl.J.Med. 2012 367,2407–2418.

Torres VE, Harris PC, Pirson Y. Autosomal dominant polycystic kidney disease. Lancet. 2007 Apr 14;369(9569):1287-301.

Torres VE. New insights into polycystic kidney disease and its treatment. Curr Opin Nephrol Hypertens. 1998 Mar;7(2):159-69.

Trauner M, Arrese M, Soroka C, Ananthanarayanan M, Koeppel TA, Schlosser SF, Suchy FJ, Keppler D, Boyer JL. The rat canalicular conjugate export pump (mrp 2) is down-regulated in intrahepatic and obstructive cholestasis. Gastroenterology. 1997 Jul;113(1):255-64.

Ward CJ, Hogan MC, Rossetti S, Walker D, Sneddon T, Wang X, Kubly V, Cunningham JM, Bacallao R, Ishibashi M, Milliner DS, Torres VE, Harris PC. 2002. The gene mutated in autosomal recessive polycystic kidney disease encodes a large, receptor-like protein. Nat Genet. 2002 Mar;30(3):259-69.

Watkins PB, Lewis JH, Kaplowitz N, Alpers DH, Blais JD, Smotzer DM, Krasa H, Ouyang J, Torres VE, Czerwiec FS, Zimmer CA. Clinical Pattern of Tolvaptan-Associated Liver Injury in Subjects with Autosomal Dominant Polycystic Kidney Disease: Analysis of Clinical Trials Database. Drug Saf. 2015 Nov;38(11):1103-13.

Xie G, Wang Y, Wang X, Zhao A, Chen T, Ni Y, Wong L, Zhang H, Zhang J, Liu C, Liu P, Jia W. Profiling of serum bile acids in a healthy Chinese population using UPLC-MS/MS. J Proteome Res. 2015 Feb 6;14(2):850-9.

Yazdanpanah K, Manouchehri N, Hosseinzadeh E, Emami MH, Mehdi Karami, Sarrami AH. Recurrent Acute Pancreatitis and Cholangitis in a Patient with Autosomal Dominant Polycystic Kidney Disease. Int J Prev Med. 2013 February; 4(2): 233–236.

Figure 4.1. Magnetic resonance images of the hepatic parenchyma and cystic regions in wild-type and three different PCK rats at 20 weeks of age. Representative magnetic resonance images of the hepatic parenchyma and cystic regions in wild-type (A) and three different PCK (B-D) rats at 20 weeks of age.

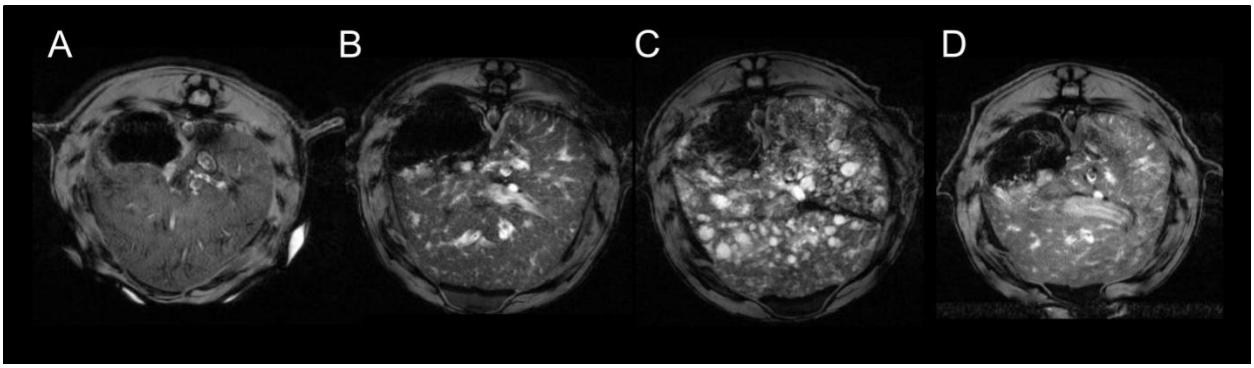

Figure 4.2. Total bile acid concentrations in the liver, bile, serum, and urine in wild-type and PCK rats. Total bile acid concentrations in the liver (A), bile (B), serum (C), and urine (D) in wild-type (white) and PCK (grey) rats. Data represent the mean, first and third quartiles, and the maximum and minimum values (n=4/cohort except n=3 in bile of wild-type). Individual values are shown (black circles); ** $p < 0.05$ comparing wild-type versus PCK rats.

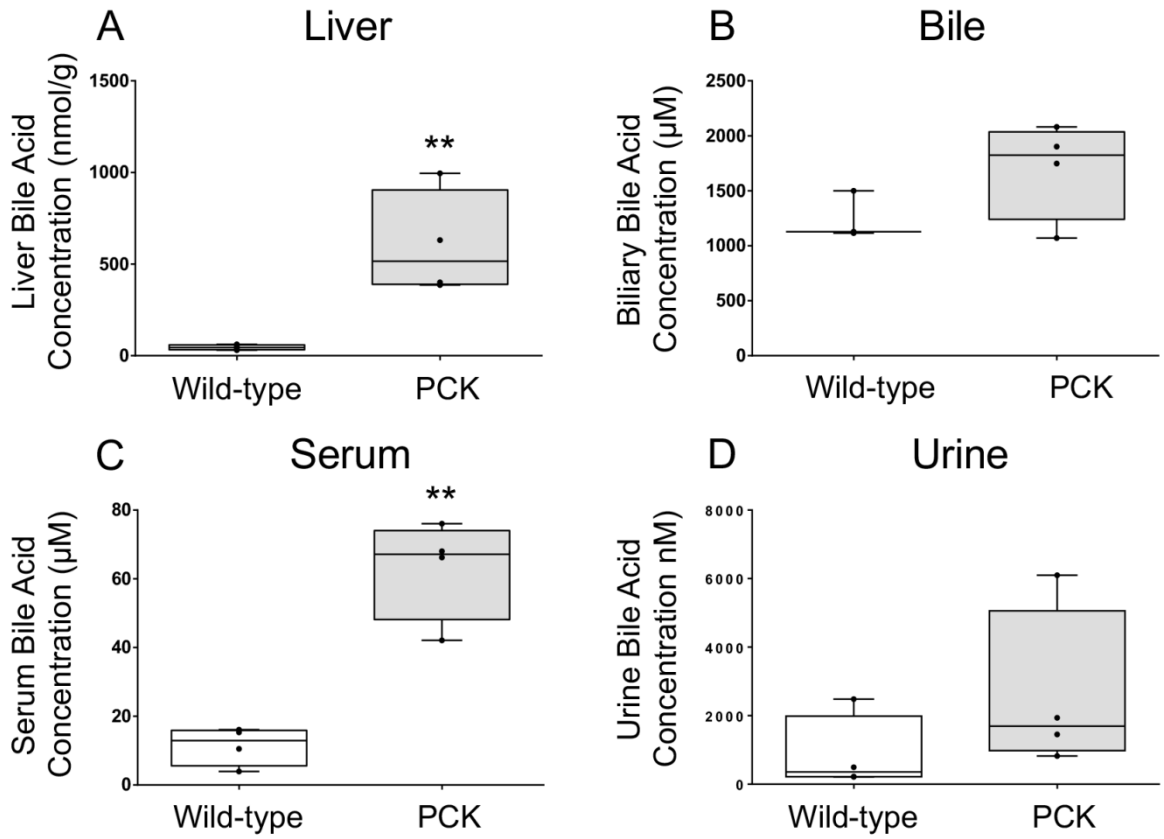

Figure 4.3. Unconjugated and conjugated bile acids in the liver, bile, serum, and urine in wild-type and PCK rats. Unconjugated and conjugated bile acids in the liver (A), bile (B), serum (C), and urine (D) in wild-type (white) and PCK (grey) rats. Data represent the mean, first and third quartiles, and the maximum and minimum values (n=4/cohort except n=3 in bile of wild-type). Individual values are shown (black circles); ** $p < 0.05$, wild-type vs. PCK rats.

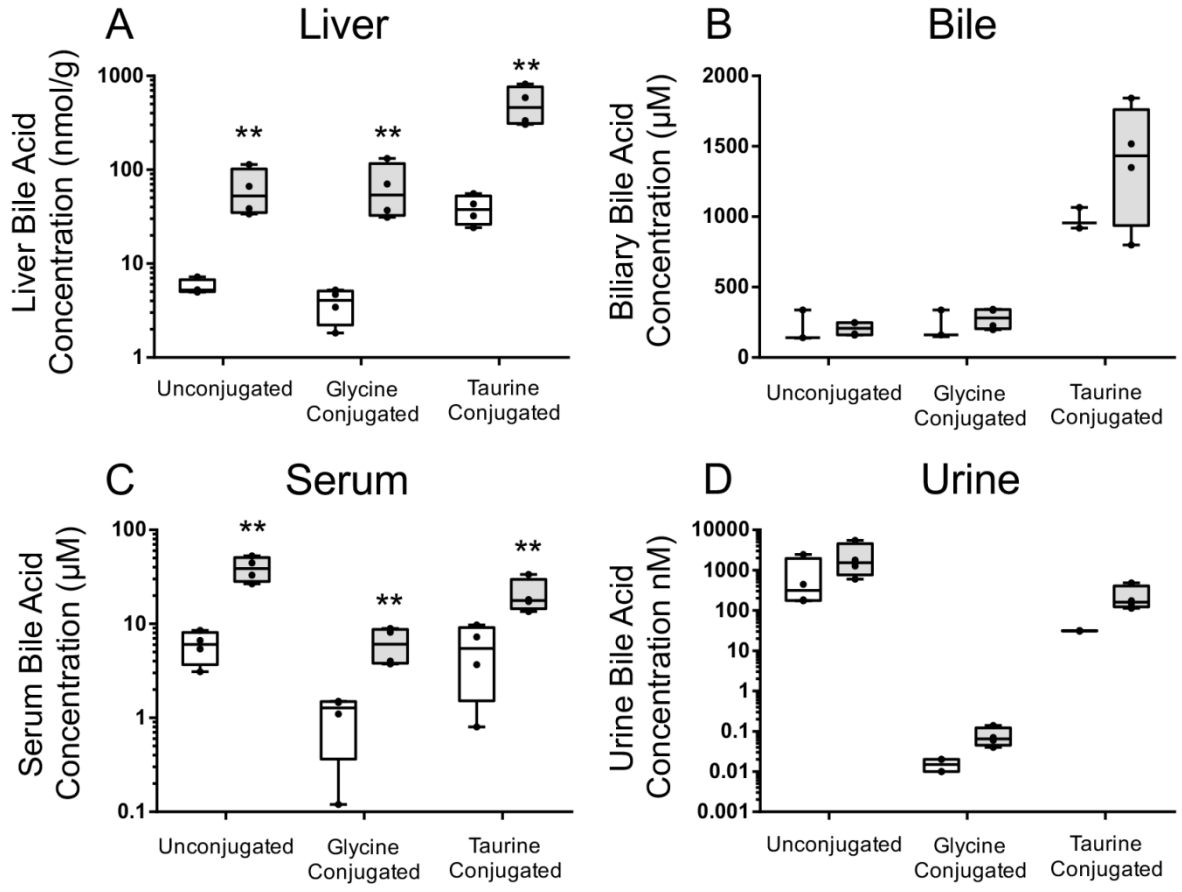

Figure 4.4. Bile acids associated with hepatotoxicity in the liver, bile, serum, and urine in wild-type and PCK rats. Bile acids associated with hepatotoxicity (i.e. glycochenodeoxycholic acid (GCDCA), glycodeoxycholic acid (GDCA), taurochenodeoxycholic acid (TCDCA), taurodeoxycholic acid (TDCA)) in the liver (A), bile (B), serum (C), and urine (D) in wild-type (white) and PCK (grey) rats. Data represent the mean, first and third quartiles, and the maximum and minimum values (n=4/cohort except n=3 in bile of wild-type). Individual values are shown (black circles); ** $p < 0.05$, wild-type vs. PCK rats.

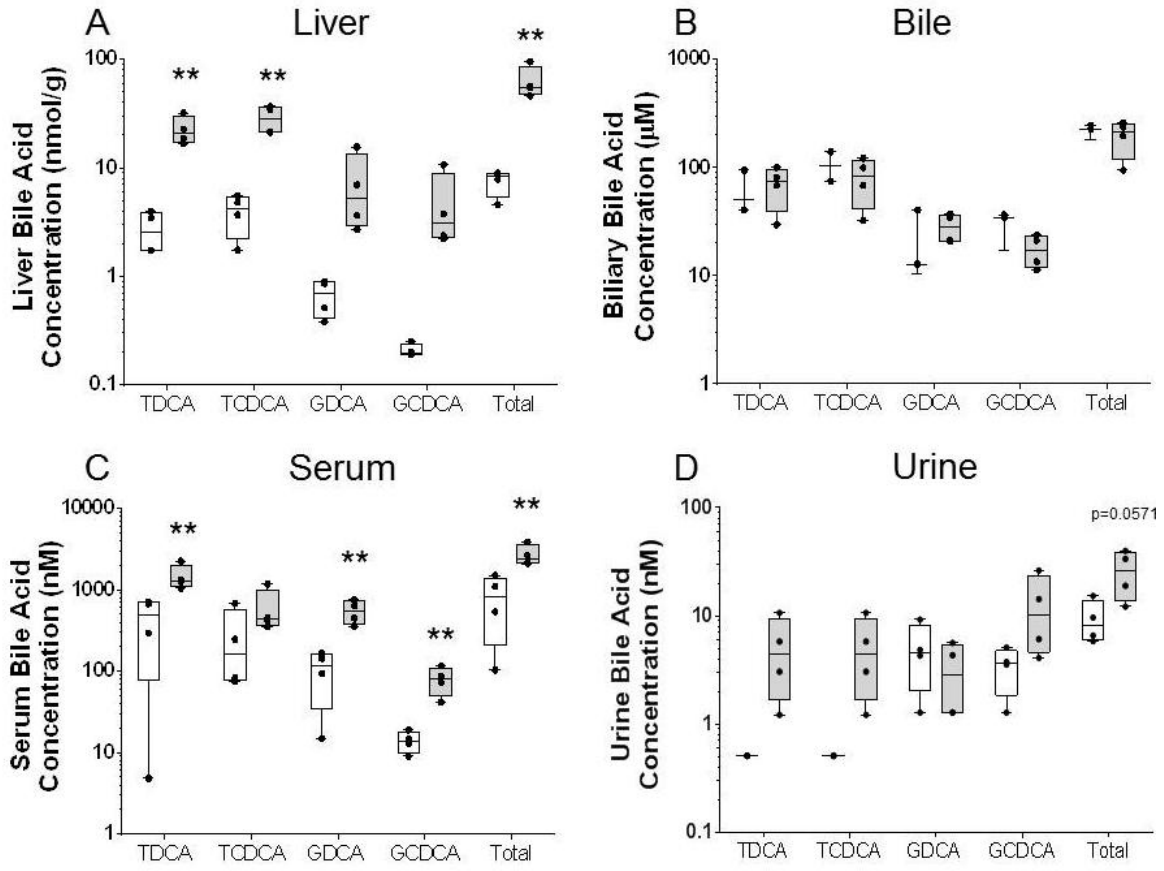

Figure 4.5. Principle component analysis (PCA) score plots. Score plots of the PCA models of bile acid profiles in the liver (A), bile (B), serum (C), and urine (D) of wild-type (black circles) and PCK (open circles) rats.

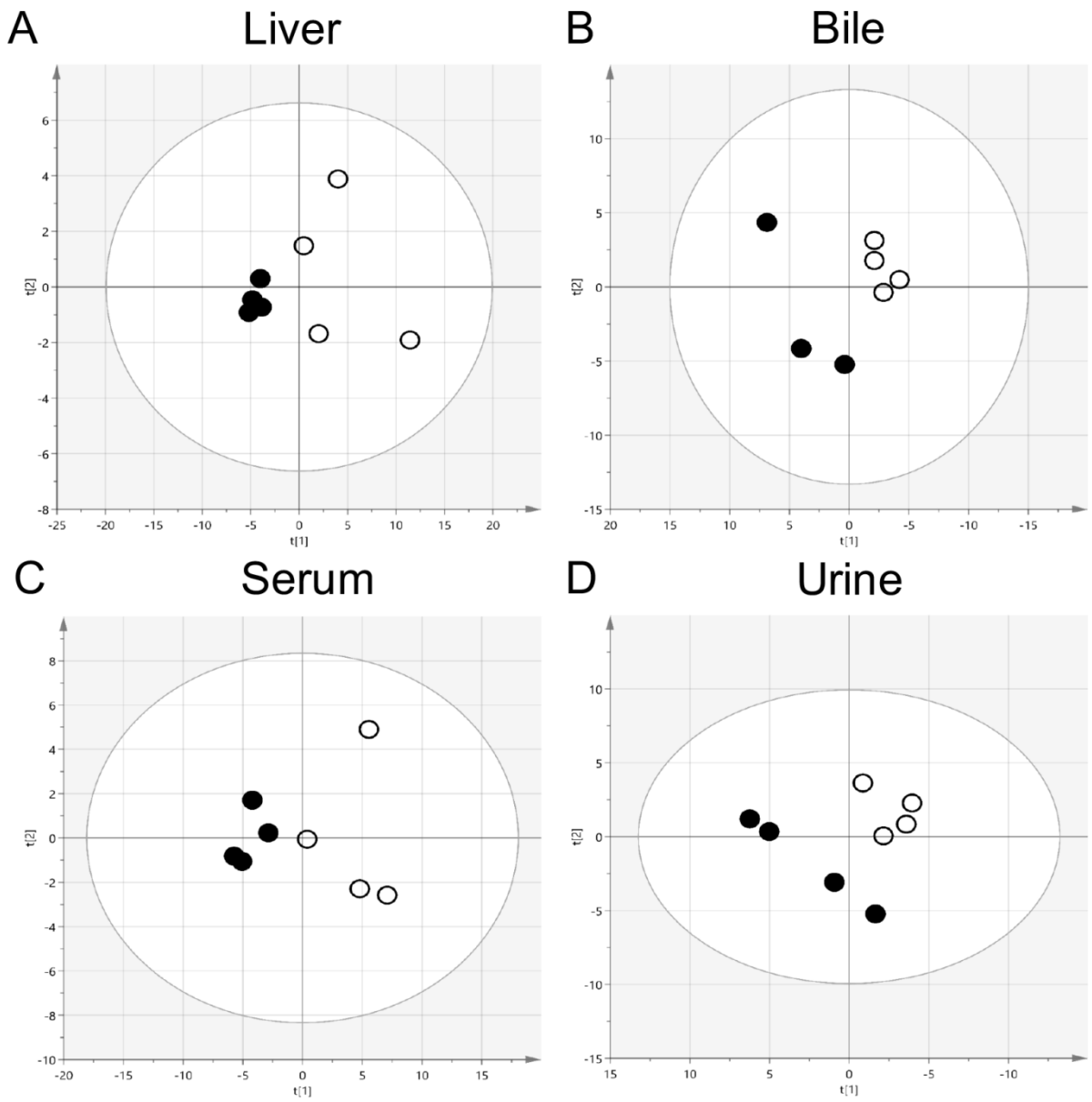

Figure 4.6. Correlation between serum bile acids and markers of liver impairment.

Correlation between liver weight (A), total liver bile acids (B), total liver bile acids associated with hepatotoxicity (C), cystic volume (D) and total serum bile acids in wild-type (black circles) and PCK (open circles) (n=4/cohort). The best-fit line is represented by the solid black line. Cystic volume was assumed to be zero in wild-type rats.

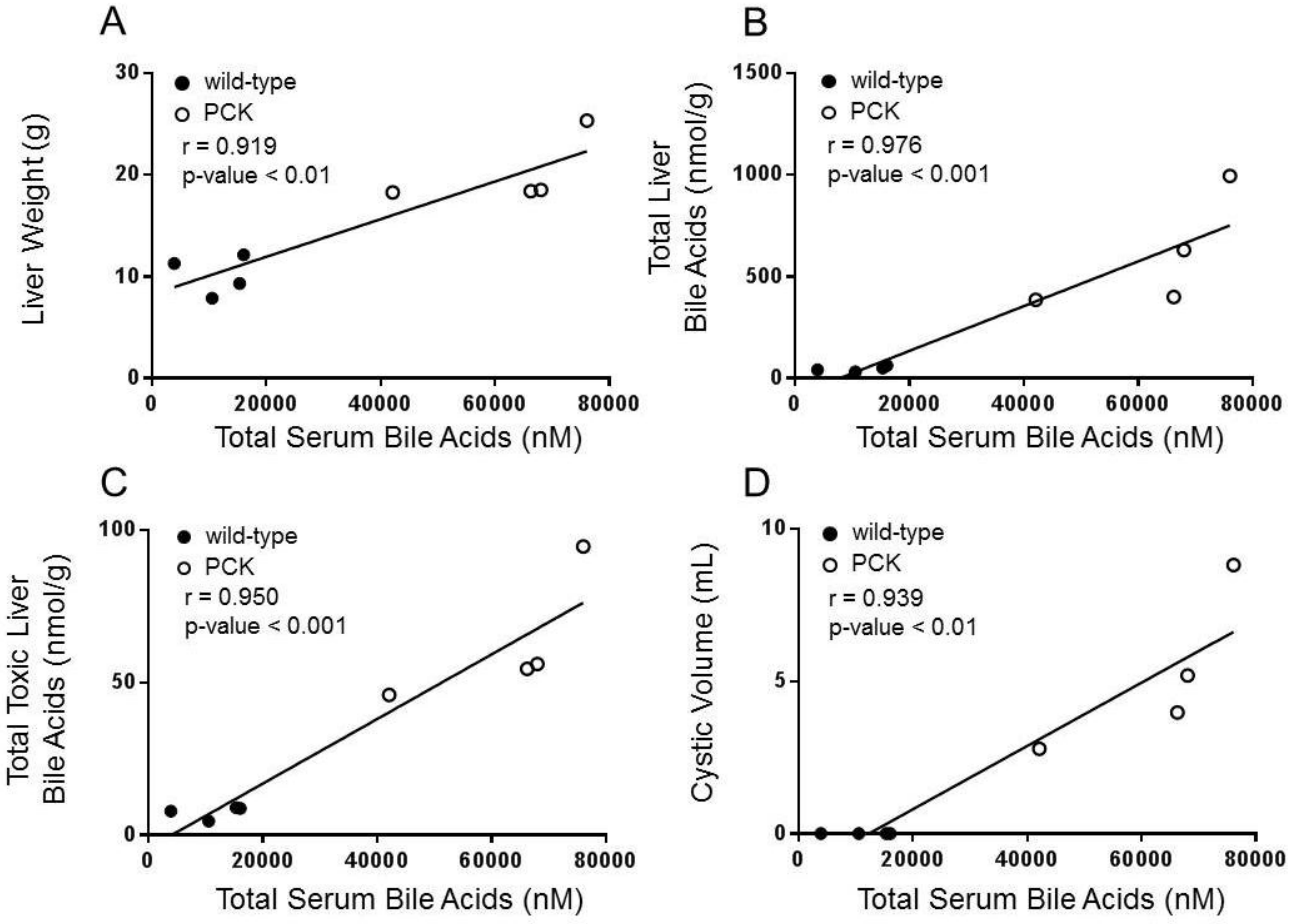

Figure 4.7. Immunohistochemical (IHC) staining of Bsep in wild-type and PCK rats.

Representative immunohistochemical staining of Bsep in liver tissue from male wild-type (A) and PCK (B) rats (20X magnification).

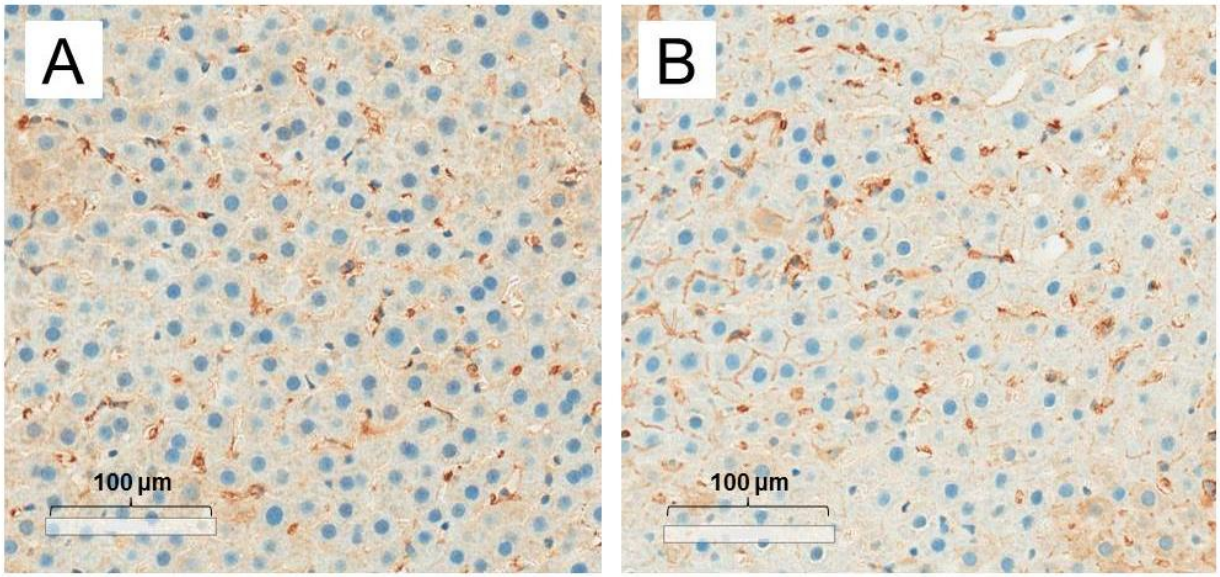

Table 4.1. Body weight, organ weight, and estimated cyst volume in wild-type and PCK rats at 20 weeks of age.

Parameter	Wild-type	PCK
Body weight (g)	409 ± 87	501 ± 21
Liver weight (g)	10.1 ± 1.9	20.2 ± 3.5**
Liver weight/ body weight (%)	2.49 ± 0.17	4.16 ± 0.74**
Total kidney weight (g)	2.50 ± 0.30	6.97 ± 0.45**
Total kidney weight/ body weight (%)	0.620 ± 0.069	1.29 ± 0.18**
Estimated cyst volume (mL)[a]	N/A	5.20 ± 2.61

Data represent the mean ± SD (n=4/cohort); ** $p < 0.05$, wild-type vs. PCK rats; N/A: no liver cysts were apparent in wild-type rats. [a]Estimated using MRI as described in *Materials and Methods* .

Table 4.2. Relative abundance of bile acids in wild-type and PCK rats as a percentage of total bile acid concentrations in each matrix.

Matrix	Bile Acid Species	Wild-type (% of total)	PCK (% of total)
Liver	CDCA species	0.272 ± 0.169	0.0746 ± 0.0303
	CA species	77.6 ± 8.3	84.8 ± 3.61
	DCA species	18.7 ± 8.3	13.3 ± 3.6
	LCA species	1.90 ± 0.24	0.816 ± 0.179**
	UDCA species	1.46 ± 0.59	1.01 ± 0.17
Bile	CDCA species	0.200 ± .207	0.376 ± 0.090
	CA species	81.5 ± 3.03	84.6 ± 1.45
	DCA species	16.6 ± 2.76	13.8 ± 1.4
	LCA species	0.660 ± 0.131	0.374 ± 0.062
	UDCA species	0.986 ± 0.387	0.823 ± 0.044
Serum	CDCA species	8.72 ± 9.30	2.03 ± 0.44
	CA species	80.9 ± 9.5	65.9 ± 6.2
	DCA species	7.73 ± 1.94	27.0 ± 5.8**
	LCA species	1.10 ± 0.63	3.75 ± 0.65**
	UDCA species	1.53 ± 0.52	1.28 ± 0.11
Urine	CDCA species	1.30 ± 0.82	1.56 ± 0.89
	CA species	83.7 ± 11.7	77.3 ± 5.1
	DCA species	5.96 ± 4.19	18.3 ± 4.3**
	LCA species	7.36 ± 5.62	1.98 ± 0.63
	UDCA species	1.63 ± 1.38	0.857 ± 0.203

Data are presented as mean ± SD (n=4/cohort except n=3 in bile of wild-type rats); ** $p < 0.05$, wild-type vs. PCK rats.

Supplementary Materials

Supplementary Table 4.1. Sulfate and glucuronide conjugates in wild-type and PCK rats. Data are presented as mean ± SD (n=4/cohort except n=3 in bile of wild-type rats); * $p < 0.05$, wild-type vs. PCK rats.

Matrix	BA species	Wild-type	PCK
Liver (pmol/g)	Sulfate conjugates[a]	0.645 ± 0.265	3.26 ± 1.27*
	Glucuronide conjugates[b]	25.1 ± 8.6	174 ± 53*
Bile (μM)	Sulfate conjugates[a]	12.7 ± 8.7	8.00 ± 6.11
	Glucuronide conjugates[b]	2.55 ± 3.30	6.15 ± 1.54
Serum (nM)	Sulfate conjugates[a]	0.651 ± 0.278	10.1 ± 14.6
	Glucuronide conjugates[b]	9.66 ± 4.66	118 ± 68*
Urine (nM)	Sulfate conjugates[a]	0.512 ± 0.0	1.29 ± 0.75
	Glucuronide conjugates[b]	1.45 ± 0.21	7.01 ± 2.70*

[a]Lithocholic acid-3-sulfate (LCA-S); [b]sum of chenodeoxycholic acid-3-β-D-glucuronide (CDCA-3G); chenodeoxycholic acid 24-acyl-β-D-glucuronide (CDCA-24G)

Supplementary Table 4.2. Bile acids exhibiting the greatest fold-increase compared to wild-type rats. The relative fold-change was calculated by dividing the mean bile acid concentration in PCK rats by the mean bile acid concentration in wild-type rats.

Matrix	Bile acid species	Relative fold change
Liver	GHDCA	317
	HDCA	213
	THDCA	185
	MCA	47.3
Bile	6-ketoLCA	53.9
	HDCA	43.2
	THDCA	20.9
	MCA	16.0
Serum	HDCA	1710
	GHDCA	154
	6-ketoLCA	122
	THDCA	52.9
Urine	DCA	30.5
	β-MCA	26.5
	MCA	25.0
	HDCA	24.9

6-ketolithocholic acid (6-ketoLCA), deoxycholic acid (DCA), glycohyodeoxycholic acid (GHDCA), hyodeoxycholic acid (HDCA), muricholic acid (MCA), taurohyodeoxycholic acid (THDCA).

Supplementary Table 4.3. Bile acid concentrations in liver (nmol/g), bile (μM), serum (nM), and urine (nM) of fasting wild-type and PCK rats. Data are presented as mean ± standard deviation (n=4/cohort except n=3 in bile of wild-type rats).

BA species	Matrix	Wild-type	PCK
ACA	Liver	0.217 ± 0.005	0.360 ± 0.308
	Bile	1.29 ± 1.36	1.01 ± 0.19
	Serum	81.0 ± 35.2	474 ± 102
	Urine	23.5 ± 23.7	45.9 ± 34.5
CA	Liver	0.420 ± 0.204	7.77 ± 6.63
	Bile	33.3 ± 29.5	24.3 ± 5.2
	Serum	2170 ± 970	9660 ± 1340
	Urine	198 ± 211	651 ± 681
3β-CA	Liver	0.0174 ±0.0004	0.0677 ± 0.0344
	Bile	0.413 ± 0.179	0.274 ± 0.057
	Serum	11.1 ± 8.3	47.2 ± 20.5
	Urine	BQL	BQL
norCA	Liver	0.0251 ± 0.0142	0.0636 ± 0.0224
	Bile	0.757 ± 0.282	0.294 ± 0.150
	Serum	2.88 ± 2.17	4.52 ± 2.97
	Urine	9.90 ± 11.2	6.15 ± 2.68
muroCA	Liver	0.0573 ± 0.0253	2.71 ± 1.16
	Bile	0.0786 ± 0.0432	1.26 ± 0.34
	Serum	36.9 ± 22.1	1170 ± 550
	Urine	1.81 ± 1.05	45.2 ± 48.3
CDCA	Liver	0.0961 ±0.0741	0.217 ± 0.061
	Bile	0.218 ± 0.105	0.0622 ± 0.0197
	Serum	647 ± 224	1120 ± 170
	Urine	4.63 ± 3.73	37.0 ± 42.1
CDCA-3G	Liver	0.00517 ±0.00133	0.110 ± 0.0326
	Bile	2.55 ± 3.30	6.15 ± 1.54
	Serum	7.16 ± 3.97	117 ± 68
	Urine	1.45 ± 0.21	7.01 ± 2.73
CDCA-24G	Liver	0.0199 ± 0.0092	0.0639 ± 0.0217
	Bile	BQL	BQL
	Serum	2.50 ± 0.86	1.28 ± 0.00
	Urine	BQL	BQL
DCA	Liver	1.37 ± 2.27	0.707 ± 0.268
	Bile	0.187 ± 0.106	0.205 ± 0.055
	Serum	212 ± 68	1100 ± 230
	Urine	1.13 ± 1.24	34.5 ± 40.1

BA species	Matrix	Wild-type	PCK
norDCA	Liver	0.00188 ±0.00165	0.0146 ± 0.0030
	Bile	0.00240 ± 0.00296	0.000828 ± 0.000632
	Serum	BQL	BQL
	Urine	BQL	BQL
3-DHCA	Liver	0.00774 ± 0.00130	0.0475 ± 0.0316
	Bile	0.222 ± 0.228	0.0900 ± 0.0388
	Serum	30.7 ± 13.3	58.9 ± 11.2
	Urine	20.0 ± 16.5	45.5 ± 46.6
7-DHCA	Liver	0.0411 ± 0.0238	0.229 ± 0.259
	Bile	2.72 ± 2.19	0.919 ± 0.145
	Serum	165 ± 198	92.1 ± 37.5
	Urine	20.1 ± 26.4	21.1 ± 13.3
GCA	Liver	2.79 ± 1.23	39.6 ± 23.7
	Bile	156 ± 79	164 ± 44
	Serum	900 ± 560	3200 ± 1240
	Urine	5.88 ± 3.75	32.8 ± 16.2
GCDCA	Liver	0.207 ± 0.026	4.73 ± 3.98
	Bile	29.2 ± 10.5	17.3 ± 5.9
	Serum	13.9 ± 4.1	79.3 ± 30.8
	Urine	3.42 ± 1.58	12.7 ± 10.1
GDCA	Liver	0.659 ± 0.256	7.19 ± 5.83
	Bile	21.1 ± 16.6	28.3 ± 8.7
	Serum	104 ± 67	548 ± 177
	Urine	4.92 ± 3.29	3.14 ± 2.21
GHCA	Liver	0.00863 ± 0.00479	0.127 ± 0.131
	Bile	0.310 ± 0.0530	0.0815 ± 0.0636
	Serum	0.844 ± 1.03	3.59 ± 2.16
	Urine	BQL	BQL
GHDCA	Liver	0.0489 ± 0.0201	15.5 ± 12.2
	Bile	4.69 ± 2.92	62.5 ± 17.8
	Serum	15.4 ± 11.3	2360 ± 1450
	Urine	BQL	29.7 ± 23.8
GLCA	Liver	0.0235 ± 0.0041	0.183 ± 0.199
	Bile	0.812 ± 0.484	0.500 ± 0.166
	Serum	2.89 ± 2.14	10.5 ± 3.3
	Urine	BQL	BQL
GUDCA	Liver	0.0654 ± 0.0203	39.6 ± 23.7
	Bile	3.01 ± 0.97	3.42 ± 1.21
	Serum	6.37 ± 5.37	26.2 ± 8.9
	Urine	BQL	BQL
HCA	Liver	0.00716 ± 0.00249	0.0317 ± 0.0248
	Bile	0.119 ± 0.100	0.0763 ± 0.0393
	Serum	24.1 ± 12.3	33.7 ± 17.9
	Urine	1.59 ± 2.15	4.46 ± 5.36

BA species	Matrix	Wild-type	PCK
HDCA	Liver	0.0163 ± 0.0148	3.47 ± 1.68
	Bile	0.0492 ± 0.0778	2.12 ± 0.45
	Serum	6.77 ± 7.49	11600 ± 5000
	Urine	15.5 ± 1.44	386 ± 360
LCA	Liver	0.0149 ± 0.0037	0.0399 ± 0.0104
	Bile	0.0306 ± 0.0090	0.0282 ± 0.0019
	Serum	18.5 ± 7.7	43.9 ± 8.4
	Urine	3.90 ± 1.51	13.0 ± 14.7
LCA-S	Liver	0.000645 ± 0.000265	0.00326 ± 0.00127
	Bile	0.0127 ± 0.0087	0.00972 ± 0.00354
	Serum	0.641 ± 0.277	10.1 ± 14.6
	Urine	0.512 ± 0.00	1.28 ± 0.75
6-ketoLCA	Liver	0.0515 ± 0.0156	2.41 ± 1.19
	Bile	0.0351 ± 0.0187	1.89 ± 0.65
	Serum	17.3 ± 3.6	2110 ± 840
	Urine	16.3 ± 5.0	22.6 ± 7.8
7-ketoLCA	Liver	BQL	0.0124 ± 0.0077
	Bile	0.00716 ± 0.00070	0.0147 ± 0.0082
	Serum	24.3 ± 26.2	116 ± 36
	Urine	0.512 ± 0.00	1.25 ± 0.88
12-ketoLCA	Liver	BQL	0.125 ± 0.061
	Bile	0.00903 ± 0.00274	0.0388 ± 0.0251
	Serum	13.3 ± 13.2	67.8 ± 10.8
	Urine	2.25 ± 0.79	1.30 ± 0.76
alloLCA	Liver	0.00573 ± 0.00202	0.0132 ± 0.0068
	Bile	0.00515 ± 0.00243	0.00358 ± 0.00088
	Serum	1.57 ± 2.12	8.40 ± 5.29
	Urine	BQL	0.563 ± NC
dehydroLCA	Liver	0.00193 ±0.00058	0.00356 ± 0.00059
	Bile	0.00247 ± 0.00081	0.00215 ± 0.00125
	Serum	3.55 ± 2.14	3.89 ± 0.33
	Urine	0.778 ± 0.532	0.901 ± 0.459
αMCA	Liver	0.108 ± 0.037	0.388 ± 0.229
	Bile	4.30 ± 2.81	2.63 ± 0.18
	Serum	523 ± 199	1728 ± 230
	Urine	27.7 ± 38.9	133 ± 111
βMCA	Liver	0.380 ± 0.134	4.13 ± 2.75
	Bile	2.20 ± 1.87	4.91 ± 1.72
	Serum	349 ± 146	4590 ± 2860
	Urine	10.4 ± 11.1	275 ± 310
tαMCA	Liver	4.99 ± 2.32	28.8 ± 14.9
	Bile	126 ± 41	85.5 ± 32.7
	Serum	787 ± 535	1490 ± 650
	Urine	6.40 ± 0.00	12.7 ± 12.6

BA species	Matrix	Wild-type	PCK
tβMCA	Liver	2.52 ± 0.86	117 ± 95
	Bile	29.8 ± 3.2	233 ± 95
	Serum	244 ± 146	3570 ± 2050
	Urine	6.40 ± 0.00	32.7 ± 17.9
tωMCA	Liver	1.12 ± 1.09	14.2 ± 9.7
	Bile	7.95 ± 5.98	26.8 ± 8.0
	Serum	80.4 ± 80.7	518 ± 244
	Urine	6.40 ± 0.00	6.40 ± 0.00
ωMCA	Liver	0.145 ± 0.085	0.429 ± 0.300
	Bile	1.39 ± 1.12	0.975 ± 0.174
	Serum	499 ± 364	1420 ± 624
	Urine	234 ± 413	468 ± 452
TCA	Liver	21.7 ± 8.1	212 ± 72
	Bile	621 ± 114	651 ± 250
	Serum	3380 ± 2480	8210 ± 4000
	Urine	6.40 ± 0.00	108 ± 18
TCDCA	Liver	3.94 ± 1.65	28.4 ± 8.3
	Bile	106 ± 32	80.1 ± 38.6
	Serum	270 ± 282	598 ± 386
	Urine	0.512 ± 0.000	5.18 ± 4.11
TDCA	Liver	2.71 ± 1.16	22.5 ± 6.7
	Bile	61.7 ± 28.4	69.4 ± 29.7
	Serum	421 ± 335	1470 ± 530
	Urine	0.512 ± 0.000	5.18 ± 4.11
THDCA	Liver	0.442 ± 0.145	81.5 ± 42.2
	Bile	10.2 ± 0.8	213 ± 44
	Serum	86.7 ± 65.3	4590 ± 1430
	Urine	2.41 ± 1.31	56.6 ± 58.5
TLCA	Liver	0.771 ± 0.255	1.95 ± 0.58
	Bile	7.24 ± 1.12	4.02 ± 1.57
	Serum	22.4 ± 19.2	27.3 ± 7.5
	Urine	BQL	BQL
TUDCA	Liver	0.588 ± 0.448	6.13 ± 3.83
	Bile	11.7 ± 3.2	14.0 ± 4.2
	Serum	94.9 ± 77.8	180 ± 83
	Urine	2.09 ± 0.94	3.47 ± 1.71
UCA	Liver	0.0529 ± 0.0492	0.0893 ± 0.0786
	Bile	1.45 ± 0.31	0.136 ± 0.116
	Serum	114 ± 142	86.6 ± 21.9
	Urine	211 ± 377	50.6 ± 43.3
UDCA	Liver	0.0346 ± 0.0154	0.264 ± 0.182
	Bile	0.0621 ± 0.0367	0.0933 ± 0.0255
	Serum	81.2 ± 57.1	627 ± 220
	Urine	4.14 ± 2.61	18.5 ± 19.2

Allocholic acid (ACA); below quantitation limit (BQL); cholic acid (CA); 23-norcholic acid (norCA); murocholic acid (muroCA); chenodeoxycholic acid (CDCA); chenodeoxycholic acid-3-β-D-glucuronide (CDCA-3G); chenodeoxycholic acid 24-acyl-β-D-glucuronide (CDCA-24G); deoxycholic acid (DCA); 23-nordeoxycholic acid (norDCA); 3-dehydrocholic acid (3-DHCA); 7-ketodeoxycholic acid (7-DHCA); glycocholic acid (GCA); glycochenodeoxychol ic acid (GCDCA); glycodeoxycholic acid (GDCA); glycohyocholic acid (GHCA); glycohyodeoxychol ic acid (GHDCA); glycolithocholic acid (GLCA); glycoursodeoxycholic acid (GUDCA); hyocholic acid (HCA); α-hyodeoxycholic acid (HDCA); lithocholic acid (LCA); lithocholic acid-3-sulfate (LCA-S); 6-ketolithocholic acid (6-ketoLCA); 7-ketolithocholic acid (7-ketoLCA); 12-ketolithocholic acid (12-ketoLCA); allolithocholic acid (alloLCA); dehydrolithocholic acid (dehydroLCA); α-muricholic acid (αMCA); β-muricholic acid (βMCA); tauro- α-muricholic acid (tαMCA); tauro-β-muricholic acid (tβMCA); tauro-ω-muricholic acid (tωMCA); ω-muricholic acid (ωMCA); not calculable (NC); taurocholic acid (TCA); taurochenodeoxycholic acid (TCDCA); taurodeoxycholic acid (TDCA); taurohyodeoxycholic acid (THDCA); taurolithocholic acid (TLCA); tauroursodeoxycholic acid (TUDCA); ursocholic acid (UCA); ursodeoxycholic acid (UDCA). The limit of quantification was 1.024 nM for all bile acid species, except for a limit of 2.56 nM for cholic acid, murocholic acid, glycodeoxycholic acid, glycochenodeoxycholic acid, ursodeoxycholic acid, α-hyodeoxycholic acid, 6-ketolithocholic acid, tauroursodeoxycholic acid, taurohyodeoxycholic acid, and chenodeoxycholic acid 24-acyl-β-D-glucuronide; the limit of quantification for tauro-ω-muricholic acid, tauro-α-muricholic acid, tauro-β-muricholic acid, and taurocholic acid was 12.8 nM.

CHAPTER 5. Altered Hepatobiliary Disposition of the Mrp2 Probe Substrate Carboxydichlorofluorescein in Isolated Perfused Livers from a Rat Model of Polycystic Kidney Disease[5]

INTRODUCTION

Polycystic kidney disease (PKD) is the most common class of inheritable genetic diseases characterized by the progressive development of kidney cysts and subsequent decline in renal function (Harris et al., 2009). Autosomal dominant polycystic kidney disease (ADPKD) is the most common form of PKD. ADPKD is primarily due to a germline mutation in the polycystin-1 (PKD1) or polycystin-2 (PKD2) gene located on the arm of chromosome 16 and 4, respectively, while autosomal recessive polycystic kidney disease (ARPKD) is due to a mutation in the polycystic kidney and hepatic disease 1 (PKHD1) gene located on chromosome 6 (Igarashi et al., 2002). Despite the clinical and genetic heterogeneity of ADPKD and ARPKD, both these ciliopathies manifest themselves in the formation and progression of fluid-filled cysts that alter and destroy renal nephrons. While it is clear that the decline in renal function is central to morbidity and mortality of PKD, this disease is a multisystem disorder that affects other epithelial organs (Danaci et al., 1998; Levine et al., 1985, Torra et al., 1997).

The liver is the most common extrarenal organ affected in patients with ADPKD. One study showed that the prevalence of hepatic cysts increased with age and was as high as 94% in 35- to 46-year-old patients with ADPKD (Bae et al., 2006). While hepatic biochemical abnormalities have been reported, liver synthetic function typically is preserved, and the presence of liver cysts is generally considered benign (Everson et al., 1999; Hogan et al., 2015,

[5] This chapter will be submitted to *Molecular Pharmacology* and is presented in the style of that journal.

Qian et al., 2003). This is likely due to the fact that hepatic parenchymal volume is maintained (Everson et al., 1999), although a recent report by Hogan et al. (2015) showed that parenchymal volume may contribute to hepatomegaly in humans. However, in some patients, particularly with severe hepatomegaly, increases in serum γ-glutamyl transferase or alkaline phosphatase ~2-5 times the upper limit of normal have been reported (Chauveau et al., 1997).

Although renal cyst progression and functional decline have been associated with decreased elimination of renally-cleared drugs, the same observation has not been established for drugs that undergo hepatic elimination – despite the prevalence of cysts, and in some cases, the burden of cysts in the liver. Surprisingly, the impact of PKD on the hepatobiliary disposition of drugs has not been evaluated. Bile acids were reported to be increased in serum, and decreased in bile, of rats with polycystic kidney disease (i.e., PCK rats), a rodent model that resembles human ADPKD (Lager et al., 2001; Munoz-Garrido et al. 2015; Ruh et al. 2013). Although the exact mechanism of altered bile acid disposition in PCK rats has yet to be determined, studies so far have excluded any difference in the rate and/or extent of bile acid metabolism, suggesting that altered bile acid transporter function may be involved.

Hepatocyte uptake of bile acids is mediated primarily by the Na^+-taurocholate co-transporting polypeptide (NTCP) and the organic anion transporting polypeptide (OATP) family of transporters. Bile acids are efficiently secreted into bile by the ATP-dependent bile salt export pump (BSEP). Bile acid conjugates also are excreted into bile by the multidrug resistance–associated protein (MRP) 2. Additionally, bile acids can undergo transport from hepatocytes into sinusoidal blood by the basolateral efflux transporters MRP3, MRP4, and the heteromeric organic solute transporter (OST)α-OSTβ (Boyer et al., 2006). To this end, this study was designed to examine the effect of PKD on the hepatobiliary disposition of 5(6)-carboxy-2',7'-

dichlorofluorescein (CDF), a fluorescent MRP2/Mrp2 probe, in isolated perfused livers from PCK rats compared to healthy Sprague Dawley (SD) rats (Heredi-Szabo et al., 2008; Myint et al., 2015; Zamek-Gliszczynski et al., 2003). CDF was chosen because it is excreted unchanged into bile by Mrp2 in rats (Zamek-Gliszczynski et al., 2003); CDF is also a substrate for Oatps and the basolateral efflux transporter Mrp3 (Chandra et al., 2005).

The isolated perfused rat liver is an established ex vivo model that has been used to investigate the physiology and function of the liver including the assessment of ischemia-reperfusion injury, synthesis of proteins, oxygen consumption, and metabolism and transport of drugs and metabolites (Dahn et al., 1999; Haussinger et al., 1986; Khezrian et al., 2015; Lindell et al., 1994; Pfeifer et al., 2013) . The primary advantages of the isolated perfused rat liver model are the retention of normal hepatic architecture, microcirculation, and bile production in a system that approaches normal physiology (Bessems et al., 2006; Brouwer and Thurman, 1996). Given the accompanying pathological changes that are expected in PCK rats, the isolated perfused liver model was chosen to test the effect of PKD on hepatic organic anion transporter function.

MATERIALS AND METHODS

Materials.

CDF was obtained from Sigma-Aldrich (St. Louis, MO). All other chemicals and reagents were of analytical grade or higher and were readily available from commercial sources.

Animals.

Male Sprague-Dawley (SD) or polycystic kidney disease (PCK/Crlj Crl-Pkhd1pck/Cr) rats were purchased from Charles River Laboratories (Wilmington, MA). Rats were housed in a constant alternating 12-h light/dark cycle and allowed water and food ad libitum and acclimated for a minimum of 1 week prior to experimentation. All animal procedures complied with the

guidelines of the Institutional Animal Care and Use Committee (University of North Carolina, Chapel Hill, NC). Isolated perfused liver procedures and liver tissue samples were collected at 16 weeks of age because the expected pathological changes (e.g., hepatic cysts) in PCK rats are well defined at this age (Lager et al., 2001, Mason et al., 2010).

Isolated perfused liver experiments.

Wild-type and PCK rat livers were perfused in a single-pass manner as described previously (Brouwer and Thurman, 1996; Chandra et al., 2005). Briefly, animals were anesthetized with ketamine:xylazine (60:12 mg/kg i.p.) and the portal vein and bile duct were cannulated. Following cannulation, the liver was removed from the carcass and transferred to a humidified 37ºC perfusion chamber, and perfused with oxygenated Krebs-Ringer bicarbonate buffer containing 15 μM taurocholate for ~10 min at a flow rate of 38 mL/min. Following the ~10-min equilibration period, the perfusate was switched to 1 μM CDF-containing buffer for 30 min (approximately steady-state). The perfusate was then switched to CDF-free buffer for a 30-min washout phase. Liver viability was assessed by monitoring inflow perfusion pressure (< 15 cm H_2O), gross morphology, and maintenance of bile flow. Bile volume was determined gravimetrically in pre-weighed tubes. Bile and perfusate samples were collected from 0 to 60 min and frozen at -80ºC until analysis. A blank perfusion (without liver) was performed to assess adsorption to the tubing and apparatus; adsorption was negligible (data not shown). A liver was perfused with 0.1% triton-X and served as a positive control for the viability assessment.

Lactate dehydrogenase (LDH) assay.

Leakage of LDH into the outflow perfusate during perfusions was determined using the LDH cytotoxicity detection kit (Thermo Fisher Scientific, Waltham, MA). Briefly, outflow perfusate samples were thawed and aliquots were dispensed into a 96-well format. LDH

substrate mixture was prepared per the manufacturer's protocol and incubated for 30 min. LDH released from hepatocytes into the perfusate reduced the tetrazolium salt 2-(4-iodophenyl)-3-(4-nitrophenyl)-5-phenyl-2H-tetrazolium chloride (INT) to formazan by a coupled enzymatic reaction. After incubation, formazan was measured by using the Fluoroskan Ascent FL Fluorometer (Thermo Scientific, Waltham, MA) at wavelengths of 492 nm per the manufacturer's protocol. Data were converted to percentage of positive control from a liver perfused with 0.1% triton-X.

CDF sample preparation.

Perfusate and bile samples were thawed and appropriately diluted with buffer and analyzed for CDF by fluorescence spectroscopy using the Fluoroskan Ascent FL Fluorometer (Thermo Scientific, Waltham, MA) at wavelengths of 485 nm (excitation) and 518 nm (emission). Standard curves were prepared daily by diluting CDF in buffer. The linear range was determined to be 1.95-125 nM; the lower limit of quantitation was 1.95 nM.

Pharmacokinetic analyses.

Pharmacokinetic models were developed to describe the disposition of CDF in wild-type and PCK rat livers. Various models were evaluated to simultaneously fit the outflow perfusate rate and biliary excretion rate vs. time data by nonlinear least-squares regression using a $1/Y_{predicted}^2$ weighting scheme (Phoenix WinNonlin 4.3, Pharsight, Mountain View, CA). Selection criteria included coefficients of variation on the estimated parameters, distribution of residuals, and Akaike's information criterion (Akaike, 1976). Model structures describing the hepatocellular space as one or two compartments (Fig. 5.1) were compared. Based on the goodness-of-fit criteria, the model scheme presented in Fig. 5.1B best described the data. The differential equations used to describe the disposition of CDF are provided below:

$$(1)\ \frac{dX_{sin}}{dt} = (Q \bullet C_{in}) - (Q \bullet C_{out}) + (k_{perfusate} \bullet X_{L1}) - (CL_{up} \bullet C_{out}) \qquad X°_{sin} = 0$$

$$(2)\ \frac{dX_{L1}}{dt} = (CL_{up} \bullet C_{out}) - (k_{perfusate} \bullet X_{L1}) - (k_{12} \bullet X_{L1}) + (k_{21} \bullet X_{L2}) \quad t \leq 30\ \text{min} \quad X°_{sin} = 0$$

$$(3)\ \frac{dX_{L1}}{dt} = (k_{21} \bullet X_{L2}) - (k_{perfusate} \bullet X_{L1}) - (k_{12} \bullet X_{L1}) \qquad t > 30\ min \quad X°_{sin} = 0$$

$$(4)\ \frac{dX_{L2}}{dt} = (k_{12} \bullet X_{L1}) - (k_{21} \bullet X_{L2}) - (k_{bile} \bullet X_{L2}) \qquad X°_{sin} = 0$$

$$(5)\ \frac{dX_{bile}}{dt} = (k_{bile} \bullet X_{L2}) \qquad X°_{sin} = 0$$

where C_{in} is the concentration of CDF in the inflow perfusate, C_{out} is the concentration of CDF in the outflow perfusate, Q is the flow rate (38 mL/min), X_{sin} is the amount of CDF in the sinusoidal space, CL_{up} is the uptake clearance into the liver, $k_{perfusate}$ is the first-order rate constant for basolateral excretion, X_{L1} and X_{L2} are the amounts of CDF in the two compartments representing the hepatocellular space of the liver, k_{12} is the first-order rate constant for movement from liver compartment 1 to liver compartment 2, k_{21} is the first-order rate constant for movement from liver compartment 2 to liver compartment 1, and k_{bile} is the first-order rate constant for biliary excretion. The model was constructed assuming that CDF was not metabolized, and that all processes were linear and were represented by either an uptake clearance (i.e., CL_{up}) or a first-order rate constant (i.e., $k_{perfusate}$, k_{12}, k_{21}, and k_{bile}). The perfusate outflow rate was calculated as the product of the flow rate and the outflow perfusate concentration at each designated time point; similarly, the biliary excretion rate was calculated as the product of bile flow during the specified collection interval and the biliary concentration at each designated time point. The extraction ratio was calculated by subtracting C_{in} from C_{out} and

then dividing by C_{in}. The area under the concentration-time curve (AUC) was determined using a linear-up log-down trapezoidal algorithm (Phoenix WinNonlin 4.3, Pharsight, Mountain View, CA). Simulations were performed to evaluate the effects of perturbations in CL_{up} and $k_{perfusate}$ on the extent of CDF biliary excretion using the final model structure (Fig. 5.1B) and equations (1)-(5) listed above. Simulations were conducted assuming a constant infusion rate of CDF into the liver (1 μM at 38 mL/min for 30 min) by modulating parameter estimates based on the mean values from wild-type rats (Table 5.1) using Phoenix WinNonlin (v. 4.3 Pharsight, Mountain View, CA).

Immunoblot analysis.

Liver samples from the median lobe were excised, snap frozen, and immediately placed in -80 ºC. Liver samples were thawed in 2 mL protease-containing radioimmunoprecipitation assay (RIPA) buffer (Santa Cruz Biotechnology, Inc. Dallas, TX) and sonicated for 30 sec on ice. Homogenates were centrifuged at 1500g for 10 min at 4ºC; the supernatant was removed and subsequently centrifuged at 100,000g for 30 min, and the remaining pellet was suspended in protease-containing RIPA buffer and stored at -80 ºC until use. Protein concentration was determined using the bicinchoninic acid method (Smith et al., 1985). Samples for Western blots were prepared according to the manufacturer's instructions (Invitrogen, Carlsbad, CA); 40 μg (for MRP2) or 30 μg (for MRP3) was loaded onto 4-12% Bis-Tris gels. After electrophoresis, proteins were transferred to polyvinylidene fluoride membranes according to standard procedures. The membranes were probed with anti-MRP2 antibody (MC-206, 1:100, Kamiya Biochemical Company, Seattle, WA) or anti-MRP3 antibody (sc-5776, 1:200, Santa Cruz Biotechnology, Dallas, TX) overnight in diluted 5% (w/v) milk- tris-buffered saline tween 20 (TBS-T). After washing three times in TBS-T for 10 min, the blots were probed with horseradish

peroxidate-conjugated anti-mouse or anti-goat IgG secondary antibody (Santa Cruz Biotechnology, Dallas, TX) for 2 hr at room temperature. Detection was enhanced using chemiluminescence reagents (SuperSignal/West Dura; Pierce Chemical, Rockford IL). Actin was used as the loading control (sc-1615, Santa Cruz Biotechnology, Dallas, TX). The data were normalized to loading control (actin) using densitometric analysis to compare protein expression between wild-type and PCK rats with ImageLab software version 4.1 (Bio-Rad, Hercules, CA).

Immunohistochemical (IHC) staining.

Liver samples from the median lobe were excised and immediately placed in 4% paraformaldehyde for 48 hr, processed, embedded in paraffin, serially sectioned at 4 µm thickness, and placed on coated glass slides. Sectioned slides were used for IHC immediately or unstained slides were stored in the nitrogen gas chamber if staining was not done immediately. Mouse monoclonal anti-MRP2 (MC-206, Kamiya Biochemical Company, Seattle, WA) and goat polyclonal anti-MRP3 (sc-5776, Santa Cruz Biotechnologies, Dallas, TX) antibodies were used for IHC. IHC was carried out in the Bond fully automated immunostainer (Leica Biosystems Inc., Vista, CA). Slides were dewaxed in Bond Dewax solution (AR9222) and hydrated in Bond Wash solution (AR9590). Antigen retrieval was performed for 30 min at 100ºC in Bond-Epitope Retrieval solution 1 pH-6.0 (AR9961). Antigen retrieval was followed with 5 min Bond peroxide blocking (DS9800) step; for MRP3 protein blocking reagent (PV6122, Leica) was added for 10 min. After pretreatment, slides were incubated with anti-MRP2 (1:50) and anti-MRP3 (1:100) antibodies for 30 min and 4 hr, respectively. Bond™ Polymer Refine Detection system (DS9800) was used to detect both antibodies; for MRP3, Bond polymer was supplemented with ImmPRESS HRP anti-goat secondary antibody (MP-7405-15, Vector Labs; Burlingame, CA).

Stained slides were dehydrated and covered with a coverslip. Positive and negative controls (no primary antibody) were evaluated.

Statistical analysis.

The data were reported as the mean ± SD. Five rat livers per cohort were used in the isolated perfused liver experiments; three rat livers per cohort were used in western blot and IHC analysis. Statistically significant differences between the generated parameters for each cohort were determined by the nonparametric two-tailed Wilcoxon rank sum test using GraphPad Prism 6 (San Diego, CA). Statistical significance was determined at the $\alpha = 0.05$ level.

RESULTS

Isolated-perfused liver experiments.

The body weight of wild-type and PCK rats was similar although the liver weight was significantly increased in PCK rats (Table 5.1). Liver viability was maintained as evidenced by negligible LDH release (< 0.1% toxicity; data not shown) and constant bile flow throughout the 60-min perfusion (Fig. 5.2). Bile flow was ~0.9 µL/min/g liver in wild-type rat livers, which is similar to previously reported values (Beckh, et al., 1991; Beckh et al., 1994). Although bile flow appeared to be increased in PCK rat livers, when normalized by liver weight, bile flow was lower in PCK rat livers (~0.5-0.7 µL/min/g) (Fig. 5.2). The outflow perfusate excretion rate vs. time data were similar between both cohorts (Fig. 5.3A); notably, the biliary excretion rate vs. time data were lower in PCK rat livers (Fig. 5.3B). The total dose of CDF perfused (mean ± SD) was similar between wild-type (1140 ± 30 nmol) and PCK (1130 ± 30 nmol) rat livers. The extraction ratio (mean ± SD) of CDF in PCK rat livers appeared to decrease (0.0672 ± 0.0203) compared to wild-type rat livers (0.0965 ± 0.0143) but this difference was not statistically significant. The

total mass of CDF recovered in bile (mean ± SD) was significantly higher in wild-type (33.5 ± 8.8 nmol) compared to PCK (0.108 ± 0.171 nmol) perfused rat livers. The mass in the perfusate washout phase (30-60 min) (mean ± SD) was significantly increased in PCK (25.2 ± 9.0 nmol) compared to wild-type (11.1 ± 6.0 nmol) rat livers. The total mass of CDF collected in the perfusate (mean ± SD) throughout the 60-min perfusion was similar between wild-type (1040 ± 30 nmol) and PCK (1070 ± 40 nmol) rat livers.

Pharmacokinetic modeling.

Pharmacokinetic parameters estimated based on a model with either one or two compartments representing the hepatocellular space (Fig. 5.1) were compared. In wild-type and PCK perfused rat livers, the CV% of the parameter estimates tended to be smaller using a two-compartment liver model (Table 5.2). The weighted residuals for the outflow perfusate excretion rate vs. time data were similar for both model structures and both cohorts (data not shown). Representative weighted residuals for the biliary excretion rate vs. time data using the model with two compartments to describe the hepatocellular space tended to be evenly distributed and centered around zero (Fig. 5.5D) more so than for the one-compartment model for PCK rat livers (Fig. 5.5B). This observation was consistent for all PCK rats (data not shown). Furthermore, AIC values were lower using the two-compartment model (AIC = -22.3) compared to the one-compartment model (AIC = -12.3) in PCK rat livers. Therefore, the pharmacokinetic model with two compartments representing the hepatocellular space was selected as the final model structure (Fig. 5.1B) to describe the CDF perfusate outflow rate- and biliary excretion rate-time data. A representative fit of the final model scheme is shown in Fig. 5.4 and the final parameter estimates are summarized in Table 5.1. PCK rat liver #3 and wild-type rat liver #1 were used as representative data in Fig. 5.4 and Fig. 5.5. The uptake clearance of CDF (CL_{up}) (mean ± SD)

appeared to decrease in PCK rat livers (2.64 ± 0.51 mL/min) compared to wild-type rat livers (3.23 ± 0.23 mL/min). The rate constant for biliary excretion (k_{bile}) (mean ± SD) was significantly decreased in PCK (0.00146 ± 0.00223 min^{-1}) compared to wild-type (0.176 ± 0.012 min^{-1}) rat livers. Conversely, the basolateral excretion rate constant of CDF ($k_{perfusate}$) (mean ± SD) was significantly increased in PCK (0.0538 ± 0.0112 min^{-1}) compared to wild-type (0.0184 ± 0.0012 min^{-1}) rat livers. Intercompartmental rate constants between wild-type and PCK rat livers were similar for both k_{12} and k_{21}.

Simulations were performed to evaluate the effects of perturbations in CL_{up} and $k_{perfusate}$, reflecting Oatp-mediated uptake and Mrp3-mediated basolateral efflux, respectively, on the extent of CDF biliary excretion using the model structure in Fig. 5.1B. Simulations were conducted assuming a constant infusion rate of CDF into the liver for 30 min (1 μM; 38 mL/min) using parameter estimates based on the mean values from wild-type isolated perfused rat livers (Table 5.1). Simulations revealed that the basolateral efflux rate constant would need to be increased by more than 100-fold to account for the observed decrease in CDF biliary excretion (Table 5.3; Supplementary Table 5.1). Although CL_{up} was not statistically different between PCK and wild-type rat livers, it is possible that CL_{up} was decreased in some PCK rat livers, which might explain the decreased biliary excretion of CDF in PCK isolated perfused rat livers. Based on simulations, a 2-fold decrease in CL_{up} combined with a 10-fold increase in $k_{perfusate}$ would not reduce the biliary excretion of CDF in PCK rat livers to the negligible levels observed in the present study (Table 5.3; Supplementary Table 5.1). A 10-fold increase in $k_{perfusate}$ was chosen for this simulation because Mrp3 protein expression has been reported to be induced by as much as ~5-10-fold in rodents (Ogawa et al., 2000; Xiong et al., 2000).

Protein expression and immunohistochemical analysis (IHC).

To address the molecular basis for decreased biliary excretion of CDF in the livers of PCK rats, the expression of hepatic Mrp2 and Mrp3 was quantified. Immunoblots did not detect a significant difference between Mrp2 expression in wild-type and PCK rat liver tissue using densitometric analysis (Fig. 5.6A and Fig. 5.6C). IHC indicated proper localization of Mrp2 to the canalicular membrane in wild-type (Fig. 5.7A) and PCK rat livers (Fig. 5.7B). Interestingly, immunoblots revealed that Mrp3 was significantly increased by 2.7-fold in PCK rat liver tissue using densitometric analysis (Fig. 5.6B and Fig. 5.6D). IHC also indicated an increase in Mrp3 expression in PCK (Fig.5.7D) compared to wild-type (Fig. 5.7C) rat livers, although Mrp3 did not appear to be predominantly localized to the basolateral membrane.

DISCUSSION

Liver cysts are a common liver pathology observed in human ADPKD. The effect of hepatic impairment (e.g., liver cysts) on hepatobiliary drug disposition in ADPKD, however, has not been studied. To address this knowledge gap, hepatic transporter function was evaluated in PCK rats using the isolated perfused rat liver model. The PCK rat was chosen because it displays hepatorenal abnormalities that are phenotypically consistent with human ADPKD (Chauveau et al., 2000; Hogan et al., 2010; Lager et al., 2001; Masyuk et al., 2004; Mason et al., 2010). Similar to human ADPKD, the PCK rat is characterized by remodeling of the biliary tree and formation of multiple biliary microhamartomas that progress to form distinct cysts with advancing age. The effect of these hepatic pathological findings on drug disposition, to date, is unknown.

CDF is a fluorescent anionic probe used to study the excretory function of Mrp2, a hepatic transporter localized on the canalicular membrane of hepatocytes. CDF is not

metabolized and is transported from hepatocytes to the bile via Mrp2, as evidenced by impaired CDF excretion in perfused livers from Mrp2-deficient TR^- rats (Jansen et al., 1987; Swift et al., 2010; Zamek-Gliszczynski et al., 2003). In the present study, PCK rat livers displayed a significant decrease in the biliary excretion rate vs. time data of CDF compared to wild-type rat livers (Fig. 5.3B). Weight-normalized bile flow was lower in PCK rat livers (Fig. 5.2), although absolute bile flow was higher in PCK rat livers, consistent with reports of enhanced bile secretion in PCK rats (Mason et al., 2010; Masyuk et al., 2004).

A pharmacokinetic model with either one or two compartments representing the hepatocellular space was evaluated to describe the hepatobiliary disposition of CDF. The precision of the parameter estimates tended to increase (i.e., lower CV%) using the two-compartment model structure compared to the model structure with one compartment (Table 5.2). CV% values < 30% are generally desirable when modeling pharmacokinetic data (Mould et al., 2013). Furthermore, weighted residuals using the two compartment model in PCK rats were randomly distributed around the mean (and centered around zero) (Fig. 5.5D), whereas the weighted residuals did not appear to be randomly distributed using the one-compartment model structure in PCK perfused rat livers (Fig. 5.5B). Hence, the model structure with two compartments representing the hepatocellular space was used as the final model structure (Fig. 5.1B).

To prevent further hepatic injury, decreased expression of hepatic bile acid uptake transporters in rats (e.g., Ntcp and Oatp) has been documented in cholestasis (Pauli-Magnus et al., 2006). Serum and hepatic bile acids were increased in PCK rats (Munoz-Garrido et al. 2015), consistent with a cholestatic-like state. A decrease in Oatp-mediated CDF uptake could explain, in part, decreased biliary excretion of CDF in PCK rats (Zamek-Gliszczynski et al., 2003).

Although uptake clearance (CL_{up}) of CDF tended to be lower in PCK rat livers, the differences were not statistically significant (Table 5.1). Furthermore, while Oatp1a1 is decreased during cholestatic-like conditions in rodents, Oatp1a4 and Oatp1b2 expression are maintained (Dumont et al., 1997; Geier et al., 2001); hence, it is possible that overlapping substrate specificity of CDF for multiple Oatps may explain why differences in the CDF CL_{up} values in PCK rat livers failed to reach statistical significance. It should be noted that CL_{up} values for CDF were higher in the single-pass isolated perfused rat liver study reported by Chandra et al. (2005). Differences in the strain of rats (i.e., Wistar vs. Sprague-Dawley), pre-treatment with vehicle (e.g., 90% propylene glycol/10% ethanol for up to four days by Chandra et al., (2005)) prior to liver perfusion, or age/liver weight-related alterations in transporter function may account for the ~2.5-fold higher Cl_{up} values reported by Chandra et al. (2005). Decreased hepatic transporter expression (e.g. Oatp1a1) has been reported in aging rodents (Fu et al., 2012).

To understand the mechanism(s) responsible for the decreased biliary excretion rate of CDF in PCK rat livers, the expression of Mrp2 was quantified. Immunblot and densitometric analysis did not detect a difference in the expression of Mrp2 between PCK and wild-type rat livers (Fig. 5.6A and 5.6C). Furthermore, IHC analysis corroborated these findings and indicated that Mrp2 appeared to be properly localized to the canalicular membrane of hepatocytes in both wild-type and PCK rat livers (Fig. 5.7A and 5.7B). When biliary excretion is compromised, basolateral efflux can play an important role in the egress of compounds from hepatocytes (Pfeifer et al., 2014). The basolateral organic anion transporter Mrp3 is a compensatory transporter involved in the efflux of bile acids and drug conjugates; Mrp3 also transports CDF (Nezasa et al. 2006; Xiong et al., 2000; Zelcer et al. 2003; Zamek-Gliszczynski et al., 2003). Pharmacokinetic modeling revealed that the basolateral efflux rate constant ($k_{perfusate}$) was

increased ~3-fold in isolated perfused PCK rat livers (Table 5.1). Furthermore, the mass of CDF recovered during the washout phase was ~2-fold greater from PCK perfused rat livers, consistent with increased basolateral efflux. These data are also consistent with increased basolateral efflux of CDF in Mrp2-knockout rodents that exhibit increased Mrp3 expression (Nezasa et al., 2006). Correspondingly, immunoblot analysis indicated a strong upregulation of Mrp3 in PCK rat livers (Fig. 5.6B and 5.6D), which is consistent with the inducible nature of Mrp3 under a cholestatic-like state and increased basolateral efflux ($k_{perfusate}$) of CDF (Donner et al., 2001; Soroka et al. 2001). IHC staining corroborated these findings and indicated that Mrp3 expression was increased in PCK (Fig. 5.7D) compared to wild-type (Fig. 5.7C) rat livers.

Increased $k_{perfusate}$ and/or decreased CL_{up} may contribute to decreased CDF biliary excretion. Simulations were performed to test the hypothesis that impaired biliary excretion of CDF was due solely to increased $k_{perfusate}$ and/or decreased CL_{up}. Simulations revealed that a ~200-fold increase in $k_{perfusate}$ would be required to decrease the amount of CDF excreted into bile to values measured in isolated perfused PCK rat livers (Table 5.3; Supplementary Table 5.1). Mrp3 protein expression has been reported to be induced by as much as ~5-10-fold in rodents (Ogawa et al., 2000; Xiong et al., 2000). Based on these reports, it may not be biologically plausible for Mrp3-mediated $k_{perfusate}$ to increase ~200-fold to account alone for the decrease in CDF biliary excretion observed in isolated perfused PCK rat livers. Although there was no statistically significant difference in CL_{up} between wild-type and PCK rat livers, the effect of a decrease in CL_{up} and an increase in $k_{perfusate}$ on CDF biliary excretion also was simulated. A 50% decrease in CL_{up} and a 10-fold increase in $k_{perfusate}$ reduced the amount of CDF in the bile to 2.09 nmol (Table 5.3), suggesting that alterations in these parameters can contribute to the decreased biliary excretion of CDF in PCK rat livers, but changes in these parameters

alone cannot account for the marked decrease in CDF biliary excretion observed (Supplementary Table 5.1). Therefore, a decrease in k_{bile} is necessary to explain the decreased CDF biliary excretion in isolated perfused PCK rat livers.

The mechanism(s) responsible for decreased biliary excretion of CDF in PCK rat livers, despite the apparent preservation of Mrp2 expression and localization, is unclear. Cholangiocytes also express Mrp3 (Donner et al., 2001; Konig et al., 1999; Soroka et al., 2001). Because liver cysts in PCK rats are derived from the biliary epithelium, it is conceivable that CDF may be actively transported into cysts, thereby decreasing the apparent biliary excretion. However, focal hepatic lesions, such as liver cysts and biliary hamartomas, are hypointense and do not accumulate contrast agent when using magnetic resonance imaging-based contrast agents such as gadolinium-ethoxibenzyl-diethylenetriamine pentaacetic acid (Gd-EOB-DTPA), an established Mrp2 and Mrp3 substrate (Campos et al., 2012; Kitao et al., 2010). Alternatively, increased cholangiocyte uptake could decrease CDF accumulation in the common bile duct. Carrier-mediated transport of Mrp2/Mrp3 substrates (i.e. conjugated bile acids) has been demonstrated using fluorescent assays in biliary epithelial cell culture (Bendedetti et al., 1997). In fact, cholangiocyte-mediated bile acid transport is increased in bile duct ligated rodents, a model of chronic cholestasis (Alpini et al., 2001). Interestingly, this observation was not attributable to marked increases in transporter expression per cholangiocyte, but rather to increased intrahepatic bile duct surface area (e.g., increased number of cholangiocytes). Masyuk et al. (2004) reported extensive remodeling of the biliary tree in PCK rats that increased the intrahepatic biliary volume ~20-40-fold. It should be noted that CDF was not measurable in the liver homogenate due to high background fluorescence. Based on the mass of CDF not recovered in either the perfusate or bile, the estimated CDF remaining in the liver was similar between wild-type and PCK rat livers

(66.6 vs. 53.0 nmol, respectively; Supplementary Table 5.1). Although Mrp2 has been extensively studied in the context of biliary excretion of drugs, Mrp2 also transports endogenous substances such as bilirubin-glucuronide and conjugated bile acids (Akita et al., 2001; Keppler, 2014). Increased concentrations of serum bilirubin have been reported in PCK rats, suggestive of impaired Mrp2 function (Mason et al., 2010; Shimomura et al. 2015). Furthermore, recent literature reports indicate that hepatocellular concentrations of bile acids are significantly increased in PCK rats, consistent with a cholestatic-like state and with our finding of increased Mrp3 in the present study (Munoz-Garrido et al., 2015). It is possible that elevated concentrations of hepatic bile acids in PCK rats directly compete for Mrp2-mediated transport of CDF. The current study provides mechanistic data to support this hypothesis. For example, the sulfate conjugates of taurochenodeoxycholate and taurolithocholate are actively transported in an ATP-dependent manner in Mrp2-overexpressing membrane vesicles and have been shown to inhibit bile acid transport (Akita et al., 2001). Furthermore, inhibition of bile acid transport was potentiated when vesicles were pre-incubated with sulfated bile acids, indicating that these conjugates may trans-inhibit bile acid transport. Taurolithocholate also inhibits canalicular secretion of sodium fluorescein and sulfobromophthalein, both Mrp2 substrates, in *in vivo* studies (Roma et al., 1994; Ryan et al., 2014). Studies by Gerk et al. (2007; 2004) also revealed that tauroursodeoxycholate, glycoursodeoxycholate, and estrogen glucuronides associated with cholestasis (i.e., β-estradiol 3-β-d-glucuronide and β-estradiol 17-β-d-glucuronide) inhibit MRP2-mediated transport. Hence, increased bile acid concentrations in PCK rats may play a role in the apparent decrease in Mrp2-mediated CDF excretion as reported in the present study.

Evidence of cholestasis in ADPKD patients is rare and biliary stenosis is usually associated with a physical stricture by overlaying cyst(s) (Kolodziejski et al., 2004; Lerner et al.,

1992). Interestingly, Salam et al. (1989) reported prolonged hepatic retention of ^{99m}Tc–mebrofenin, a clinical hepatobiliary diagnostic agent and MRP2 substrate in a patient with ADPKD, which suggests that MRP2-mediated biliary excretion is impaired, consistent with our findings in PCK rats (Ghibellini et al., 2008; Pfeifer et al., 2013). Delayed visualization or inability to visualize the gallbladder using λ-scintigraphy has been reported in patients with choledochal cysts of various or unknown origin (Gad et al., 1992; Huang et al., 1982).

The impact of pathophysiological disease states, such as the presence of hepatic cysts, on transporter-mediated drug disposition is under recognized. Negligible biliary excretion of the Mrp2 substrate CDF in PCK rat livers was an unexpected and novel finding. Impaired Mrp2 function may impact the hepatobiliary disposition of Mrp2 substrates that have pharmacologic and/or toxicological effects. For example, the biliary excretion of spiramycin, an antibiotic associated with cholestatic hepatitis, was decreased ~10-fold in Mrp2-deficient rats, which suggests that elevated hepatic concentrations of spiramycin may increase the susceptibility to liver injury when Mrp2 function is impaired (Denie et al., 1992; Tian et al., 2007). Further investigations are warranted to evaluate the impact of altered MRP2/Mrp2 function on drug efficacy and/or safety in polycystic kidney diseases with hepatic involvement.

REFERENCES

Akaike H. An information criterion. Math Sci. 1976 14:5–9.

Akita H, Suzuki H, Ito K, Kinoshita S, Sato N, Takikawa H, Sugiyama Y. Characterization of bile acid transport mediated by multidrug resistance associated protein 2 and bile salt export pump. Biochim Biophys Acta. 2001 Mar 9;1511(1):7-16.

G Alpini SG, Phinizy JL, Kanno N. et al. Regulation of cholangiocyte apical bile acid transporter (ABAT) activity by biliary bile acids: Different potential compensatory changes for intrahepatic and extrahepatic cholestasis. Gastroenterology. 2001;120:A6.

Bae KT, Zhu F, Chapman AB, Torres VE, Grantham JJ, Guay-Woodford LM, Baumgarten DA, King BF Jr, Wetzel LH, Kenney PJ, Brummer ME, Bennett WM, Klahr S, Meyers CM, Zhang X, Thompson PA, Miller JP; Consortium for Radiologic Imaging Studies of Polycystic Kidney Disease (CRISP). Magnetic resonance imaging evaluation of hepatic cysts in early autosomal-dominant polycystic kidney disease: the Consortium for Radiologic Imaging Studies of Polycystic Kidney Disease cohort. Clin J Am Soc Nephrol. 2006 Jan;1(1):64-9. Epub 2005 Oct 26.

Beckh K, Kneip S, Arnold R. Direct regulation of bile secretion by prostaglandins in perfused rat liver. Hepatology. 1994 May;19(5):1208-13.

Beckh K, Arnold R. Regulation of bile secretion by sympathetic nerves in perfused rat liver. Am J Physiol. 1991 Nov;261(5 Pt 1):G775-80.

Benedetti A, Di Sario A, Marucci L. et al. Carrier-mediated transport of conjugated bile acids across the basolateral membrane of biliary epithelial cells. Am J Physiol. 1997 Jun;272(6 Pt 1):G1416-24.

Bessems M, 't Hart NA, Tolba R, Doorschodt BM, Leuvenink HG, Ploeg RJ, Minor T, van Gulik TM. The isolated perfused rat liver: standardization of a time-honoured model. Lab Anim. 2006 Jul;40(3):236-46.

Boyer JL, Trauner M, Mennone A, Soroka CJ, Cai SY, Moustafa T, Zollner G, Lee JY, Ballatori N. Upregulation of a basolateral FXR-dependent bile acid efflux transporter OSTalpha-OSTbeta in cholestasis in humans and rodents. Am J Physiol Gastrointest Liver Physiol. 2006 Jun;290(6):G1124-30.

Brouwer KLR and Thurman RG.Isolated perfused liver.Pharm Biotechnol. 1996; 8:161–192

Campos JT, SirlinCB, Choi JY Focal hepatic lesions in Gd-EOB-DTPA enhanced MRI: the atlas. Insights Imaging. 2012 Oct; 3(5): 451–474.

Chandra P, Johnson BM, Zhang P, Pollack GM, and Brouwer KLR. Modulation of hepatic canalicular or basolateral transport proteins alters hepatobiliary disposition of a model organic

anion in the isolated perfused rat liver. Drug Metab Dispos. 2005 33:1238–1243

Chauveau D, Pirson Y, Le Moine A, Franco D, Belghiti J, Grünfeld JP. Extrarenal manifestations in autosomal dominant polycystic kidney disease. Adv Nephrol Necker Hosp. 1997;26:265-89.

Chauveau D, Fakhouri F, Grünfeld JP. Liver involvement in autosomal-dominant polycystic kidney disease: therapeutic dilemma. J Am Soc Nephrol. 2000 Sep;11(9):1767-75.

Dahn MS, Lange MP, Benn S. The influence of hepatic venous oxygen saturation on the liver's synthetic response to metabolic stress. Proc Soc Exp Biol Med. 1999 May;221(1):39-45.

Danaci M, Akpolat T, Baştemir M, Sarikaya S, Akan H, Selçuk MB, Cengiz K. The prevalence of seminal vesicle cysts in autosomal dominant polycystic kidney disease. Nephrol Dial Transplant. 1998 Nov;13(11):2825-8.

Denie C, Henrion J, Schapira M, Schmitz A, Heller FR. Spiramycin-induced cholestatic hepatitis. J Hepatol. 1992 Nov;16(3):386.

Donner MG, Keppler D. Up-regulation of basolateral multidrug resistance protein 3 (Mrp3) in cholestatic rat liver. Hepatology. 2001 Aug;34(2):351-9.

Dumont M, Jacquemin E, D'Hont C, Descout C, Cresteil D, Haouzi D, Desrochers M, Stieger B, Hadchouel M, Erlinger S. Expression of the liver Na+-independent organic anion transporting polypeptide (oatp-1) in rats with bile duct ligation. J Hepatol. 1997 Dec;27(6):1051-6.

Everson GT, Scherzinger A, Berger-Leff N, Reichen J, Lezotte D, Manco-Johnson M, Gabow P. Polycystic liver disease: quantitation of parenchymal and cyst volumes from computed tomography images and clinical correlates of hepatic cysts. Hepatology. 1988 Nov-Dec;8(6):1627-34.

Fu ZD, Csanaky IL, Klaassen CD. Effects of aging on mRNA profiles for drug-metabolizing enzymes and transporters in livers of male and female mice. Drug Metab Dispos. 2012 Jun;40(6):1216-25.

Gad MA, Krishnamurthy GT, Glowniak JV. Identification and differentiation of congenital gallbladder abnormality by quantitative technetium-99m IDA cholescintigraphy. J Nucl Med. 1992 Mar;33(3):431-4.

Geier A, Matern S., Gartung C. Regulation of sinusoidal transporters in cholestasis and liver regeneration. Hepatobiliary Transport: From Bench to Bedside, Kluwer Academic Publishers, Dordrecht. 2001, pp. 32–36.

Gerk PM, Li W, Megaraj V, Vore M. Human multidrug resistance protein 2 transports the therapeutic bile salt tauroursodeoxycholate. J Pharmacol Exp Ther. 2007 Feb;320(2):893-9.

Gerk PM, Li W, Vore M. Estradiol 3-glucuronide is transported by the multidrug resistance-associated protein 2 but does not activate the allosteric site bound by estradiol 17-glucuronide. Drug Metab Dispos. 2004 Oct;32(10):1139-45.

Ghibellini G, Leslie EM, Pollack GM, Brouwer KL. Use of tc-99m mebrofenin as a clinical probe to assess altered hepatobiliary transport: integration of in vitro, pharmacokinetic modeling, and simulation studies. Pharm Res. 2008 Aug;25(8):1851-60.

Haussinger D, Gerok W, Sies H. The effect of urea synthesis on extracellular pH in isolated perfused rat liver. Biochem J. 1986 May 15; 236(1): 261–265.

Harris PC, Torres VE. Polycystic kidney disease. Annu Rev Med. 2009;60:321-37.

Heredi-Szabo K, Kis E, Molnar E, Gyorfi A, Krajcsi P. Characterization of 5(6)-carboxy-2,'7'-dichlorofluorescein transport by MRP2 and utilization of this substrate as a fluorescent surrogate for LTC4. J Biomol Screen. 2008 Apr;13(4):295-301.

Hogan MC, Abebe K, Torres VE, Chapman AB, Bae KT, Tao C, Sun H, Perrone RD, Steinman TI, Braun W, Winklhofer FT, Miskulin DC, Rahbari-Oskoui F, Brosnahan G, Masoumi A, Karpov IO, Spillane S, Flessner M, Moore CG, Schrier RW. Liver involvement in early autosomal-dominant polycystic kidney disease. Clin Gastroenterol Hepatol. 2015 Jan;13(1):155-64.e6.

Huang MJ, Liaw TF. Intravenous cholescintigraphy using Tc-99m-Labeled agents in the diagnosis of choledochalcyst. J Nucl Med. 1982 Feb;23(2):113-6.

Igarashi P, Somlo S. Genetics and pathogenesis of polycystic kidney disease. J Am Soc Nephrol. 2002 Sep;13(9):2384-98.

Jansen PL, Groothuis GM, Peters WH, and Meijer DF. Selective hepatobiliary transport defect for organic anions and neutral steroids in mutant rats with hereditary-conjugated hyperbilirubinemia. Hepatology. 1987 Jan-Feb;7(1):71-6.

Keppler D. The roles of MRP2, MRP3, OATP1B1, and OATP1B3 in conjugated hyperbilirubinemia. Drug Metab Dispos. 2014 Apr;42(4):561-5.

Khezrian M, Sheikholeslami B, Dadashzadeh S, Lavasani H, Rouini M.Effects of cyclosporine A on the hepatobiliary disposition and hepatic uptake of etoposide in an isolated perfused rat liver model. Cancer Chemother Pharmacol. 2015 May;75(5):961-8.

Kitao A, Zen Y, Matsui O, Gabata T, Kobayashi S, Koda W, Kozaka K, Yoneda N, Yamashita T, Kaneko S, Nakanuma Y.. Hepatocellular carcinoma: signal intensity at gadoxetic acid-enhanced MR Imaging--correlation with molecular transporters and histopathologic features. Radiology. 2010 Sep;256(3):817-26.

Kolodziejski TR, Safadi BY, Nakanuma Y, Milkes DE, Soetikno RM. Bile duct cysts in a patient with autosomal dominant polycystic kidney disease. Gastrointest Endosc. 2004 Jan;59(1):140-2.

Konig J, Rost D, Cui Y, Keppler D. Characterization of the human multidrug resistance protein isoform MRP3 localized to the basolateral hepatocyte membrane. Hepatology. 1999 Apr;29(4):1156-63.

Lager DJ, Qian Q, Bengal RJ, Ishibashi M, Torres VE. The pck rat: a new model that resembles human autosomal dominant polycystic kidney and liver disease. Kidney Int. 2001 Jan;59(1):126-36.

Lerner ME, Roshkow JE, Smithline A, Ng C. Polycystic liver disease with obstructive jaundice: treatment with ultrasound-guided cyst aspiration. Gastrointest Radiol. 1992 Winter;17(1):46-8.

Levine E, Cook LT, Grantham JJ. Liver cysts in autosomal-dominant polycystic kidney disease: clinical and computed tomographic study. AJR Am J Roentgenol. 1985 Aug;145(2):229-33.

Lindell SL, Southard JH, Vreugdenhil P, Belzer FO. Kupffer cells depress hepatocyte protein synthesis on cold storage of the rat liver. Transplantation. 1994 Oct 27;58(8):869-74.

Pauli-Magnus C, Meier PJ. Hepatobiliary transporters and drug-induced cholestasis. Hepatology. 2006 Oct;44(4):778-87.

Mason SB, Liang Y, Sinders RM, Miller CA, Eggleston-Gulyas T, Crisler-Roberts R, Harris PC, Gattone VH 2nd. Disease stage characterization of hepatorenal fibrocystic pathology in the PCK rat model of ARPKD. Anat Rec (Hoboken). 2010 Aug;293(8):1279-88.

McCarty KS Jr, Miller LS, Cox EB, Konrath J, McCarty KS Sr. Estrogen receptor analyses. Correlation of biochemical and immunohistochemical methods using monoclonal antireceptor antibodies. Arch Pathol Lab Med. 1985 Aug;109(8):716-21.

Masyuk TV, Huang BQ, Masyuk AI, Ritman EL, Torres VE, Wang X, Harris PC, Larusso NF. Biliary dysgenesis in the PCK rat, an orthologous model of autosomal recessive polycystic kidney disease.Am J Pathol. 2004 Nov;165(5):1719-30.

Mould DR, Upton RN. Basic concepts in population modeling, simulation, and model-based drug development-part 2: introduction to pharmacokinetic modeling methods. CPT Pharmacometrics Syst Pharmacol. 2013 Apr 17;2:e38.

Munoz-Garrido P, Marin JJ, Perugorria MJ, Urribarri AD, Erice O, Sáez E, Úriz M, Sarvide S, Portu A, Concepcion AR, Romero MR, Monte MJ, Santos-Laso Á, Hijona E, Jimenez-Agüero R, Marzioni M, Beuers U, Masyuk TV, LaRusso NF, Prieto J, Bujanda L, Drenth JP, Banales JM. Ursodeoxycholic acid inhibits hepatic cystogenesis in experimental models of polycystic liver disease. J Hepatol. 2015 Oct;63(4):952-61.

Myint K, Li Y, Paxton J, McKeage M. Multidrug Resistance-Associated Protein 2 (MRP2) Mediated Transport of Oxaliplatin-Derived Platinum in Membrane Vesicles. PLoS One. 2015 Jul 1;10(7):e0130727.

Nezasa K, Tian X, Zamek-Gliszczynski MJ, Patel NJ, Raub TJ, Brouwer KL. Altered hepatobiliary disposition of 5 (and 6)-carboxy-2',7'-dichlorofluorescein in Abcg2 (Bcrp1) and Abcc2 (Mrp2) knockout mice. Drug Metab Dispos. 2006 Apr;34(4):718-23.

Ogawa K, Suzuki H, Hirohashi T, Ishikawa T, Meier PJ, Hirose K, Akizawa T, Yoshioka M, Sugiyama Y. Characterization of inducible nature of MRP3 in rat liver. Am J Physiol Gastrointest Liver Physiol. 2000 Mar;278(3):G438-46.

Roma MG, Penalva GL, Agüero RM, Rodríguez Garay EA. Hepatic transport of organic anions in taurolithocholate-induced cholestasis in rats. J Hepatol. 1994 May;20(5):603-10.

Ryan JC, Dunn KW, Decker BS. Effects of chronic kidney disease on liver transport: quantitative intravital microscopy of fluorescein transport in the rat liver. Am J Physiol Regul Integr Comp Physiol. 2014 Dec 15;307(12):R1488-92.

Pfeifer ND, Hardwick RN, Brouwer KL. Role of hepatic efflux transporters in regulating systemic and hepatocyte exposure to xenobiotics. Annu Rev Pharmacol Toxicol. 2014;54:509-35.

Pfeifer ND, Bridges AS, Ferslew BC, Hardwick RN, Brouwer KL. Hepatic basolateral efflux contributes significantly to rosuvastatin disposition II: characterization of hepatic elimination by basolateral, biliary, and metabolic clearance pathways in rat isolated perfused liver. J Pharmacol Exp Ther. 2013 Dec;347(3):737-45.

Pfeifer ND, Goss SL, Swift B, Ghibellini G, Ivanovic M, Heizer WD, Gangarosa LM, and Brouwer LR. Effect of Ritonavir on 99mTechnetium–Mebrofenin Disposition in Humans: A Semi-PBPK Modeling and In Vitro Approach to Predict Transporter-Mediated DDIs. CPT Pharmacometrics Syst Pharmacol. 2013 Jan 2;2:e20.

Qian Q, Li A, King BF, Kamath PS, Lager DJ, Huston J 3rd, Shub C, Davila S, Somlo S, Torres VE. Clinical profile of autosomal dominant polycystic liver disease. Hepatology. 2003 Jan;37(1):164-71.

Ruh H, Salonikios T, Fuchser J, Schwartz M, Sticht C, Hochheim C, Wirnitzer B, Gretz N, Hopf C. MALDI imaging MS reveals candidate lipid markers of polycystic kidney disease. J Lipid Res. 2013 Oct;54(10):2785-94.

Salam M, Keeffe EB. Liver cysts associated with polycystic kidney disease: role of Tc-99m hepatobiliary imaging. Clin Nucl Med. 1989 Nov;14(11):803-7.

Shimomura Y, Brock WJ, Ito Y, Morishita K. Age-Related Alterations in Blood Biochemical Characterization of Hepatorenal Function in the PCK Rat: A Model of Polycystic Kidney Disease. Int J Toxicol. 2015 Nov-Dec;34(6):479-90.

Smith PK, Krohn RI, Hermanson GT, Mallia AK, Gartner FH, Provenzano MD, Fujimoto EK, Goeke NM, Olson BJ, Klenk DC. Measurement of protein using bicinchoninic acid. Anal Biochem. 1985 Oct;150(1):76-85.

Soroka CJ, Lee JM, Azzaroli F, Boyer JL. Cellular localization and up-regulation of multidrug resistance-associated protein 3 in hepatocytes and cholangiocytes during obstructive cholestasis in rat liver. Hepatology. 2001 Apr;33(4):783-91.

Swift B, Pfeifer ND, Brouwer KL. Sandwich-cultured hepatocytes: an in vitro model to evaluate hepatobiliary transporter-based drug interactions and hepatotoxicity. Drug Metab Rev. 2010 Aug;42(3):446-71.

Tian X, Li J, Zamek-Gliszczynski MJ, Bridges AS, Zhang P, Patel NJ, Raub TJ, Pollack GM, Brouwer KL. Roles of P-glycoprotein, Bcrp, and Mrp2 in biliary excretion of spiramycin in mice. Antimicrob Agents Chemother. 2007 Sep;51(9):3230-4.

Torra R, Nicolau C, Badenas C, Navarro S, Pérez L, Estivill X, Darnell A. Ultrasonographic study of pancreatic cysts in autosomal dominant polycystic kidney disease. Clin Nephrol. 1997 Jan;47(1):19-22.

Verbeeck RK. Pharmacokinetics and dosage adjustment in patients with hepatic dysfunction. Eur J Clin Pharmacol. 2008 Dec;64(12):1147-61.

Xiong H, Turner KC, Ward ES, Jansen PL, and Brouwer KLR. Altered hepatobiliary disposition of acetaminophen glucuronide in isolated perfused livers from multidrug resistance-associated protein 2-deficient TR rats. J Pharmacol Exp Ther. 2000 Nov;295(2):512-8.

Zamek-Gliszczynski MJ, Xiong H, Patel NJ, Turncliff RZ, Pollack GM, Brouwer KL. Pharmacokinetics of 5 (and 6)-carboxy-2',7'-dichlorofluorescein and its diacetate promoiety in the liver. J Pharmacol Exp Ther. 2003 Feb;304(2):801-9.

Zelcer N, Saeki T, Bot I, Kuil A, Borst P. Transport of bile acids in multidrug-resistance-protein 3-overexpressing cells co-transfected with the ileal Na+-dependent bile-acid transporter. Biochem J. 2003 Jan 1;369(Pt 1):23-30.

Figure Legends

Figure 5.1. Model schemes of CDF disposition in the isolated perfused rat liver.

Compartmental model scheme of CDF disposition in rat isolated perfused livers. Q, flow; X_{sin}, amount of CDF in sinusoidal space; C_{in}, concentration of CDF in inflow perfusate; C_{out}, concentration of CDF in outflow perfusate; CL_{up}, uptake clearance of CDF from the sinusoidal space into the liver compartment; first-order rate constant for basolateral excretion, $k_{perfusate}$; X_{L1} and X_{L2}, amount of CDF in liver compartments 1 and 2, respectively; k_{12}, first-order rate constant for movement from X_{L1} to X_{L2}; k_{21}, first-order rate constant for movement from X_{L2} to X_{L1}; k_{bile}, first-order rate constant for biliary excretion; X_{bile}, amount of CDF in bile. The model scheme with two compartments representing the hepatocellular space (B) was selected as the final model.

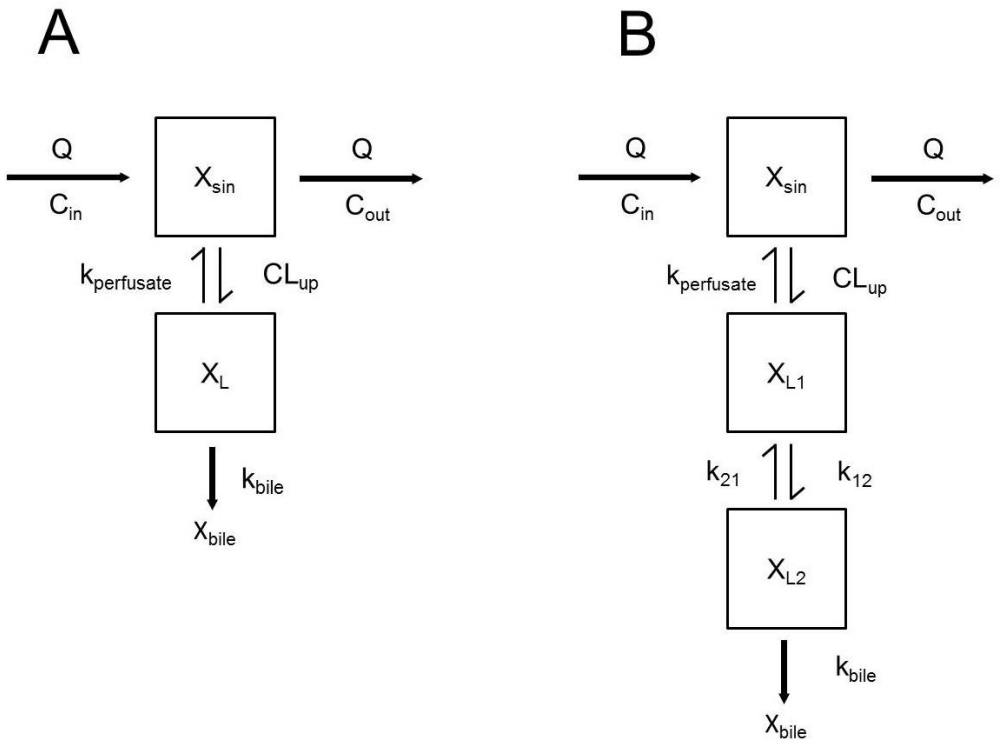

Figure 5.2. Bile flow in isolated perfused livers from wild-type and PCK rats. Bile flow rate in wild-type (closed circles, solid black line) and PCK (open circles, long dashed line) rat livers (n=5 per cohort, mean ± SD). Livers were perfused with 1 µM CDF-containing perfusate for 30 min and then switched to CDF-free perfusate for an additional 30 min as described in *Materials and Methods*.

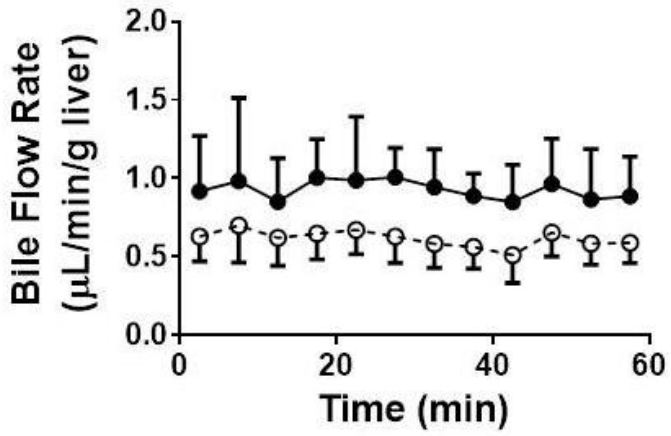

Figure 5.3. CDF outflow perfusate rate and biliary excretion rate vs. time data. CDF outflow perfusate rate (A) and CDF biliary excretion rate (B) in wild-type (closed circles) and PCK (open circles) rat livers (n=5 per cohort, mean ± SD). Livers were perfused with 1 µM CDF-containing perfusate for 30 min and then switched to CDF-free perfusate for an additional 30 min as described in *Materials and Methods*.

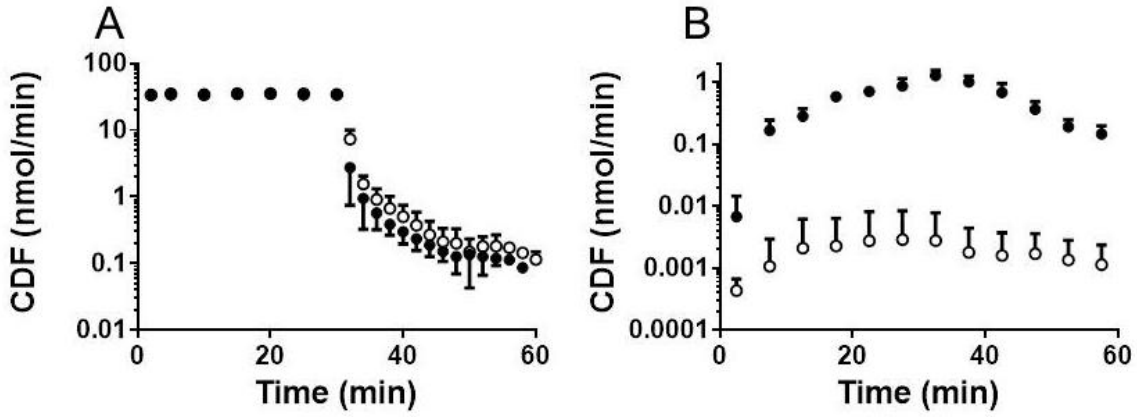

Figure 5.4. Model fit of the outflow perfusate rate and biliary excretion rate vs. time data. Representative fit of the 2-compartment liver model (scheme depicted in Fig. 5.1B) to outflow perfusate rate (circles) or biliary excretion rate (triangles) vs. time data in a wild-type (A) and PCK (B) rat liver.

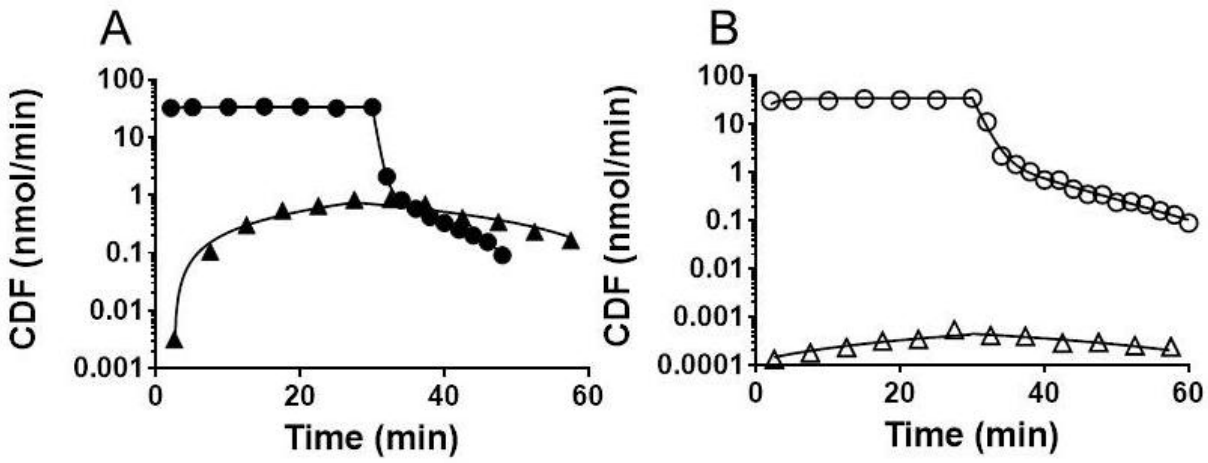

Figure 5.5. Weighted residuals of the model fit to the biliary excretion rate vs. time data depicted in Fig. 5.4 comparing one- and two-compartment model structures representing the hepatocellular space. Weighted residuals of the biliary excretion rate vs. time data using a model structure with one compartment representing the hepatocellular space (A and B) and two compartments representing the hepatocellular space (C and D) in wild-type (A and C) and PCK (B and D) isolated perfused rat livers.

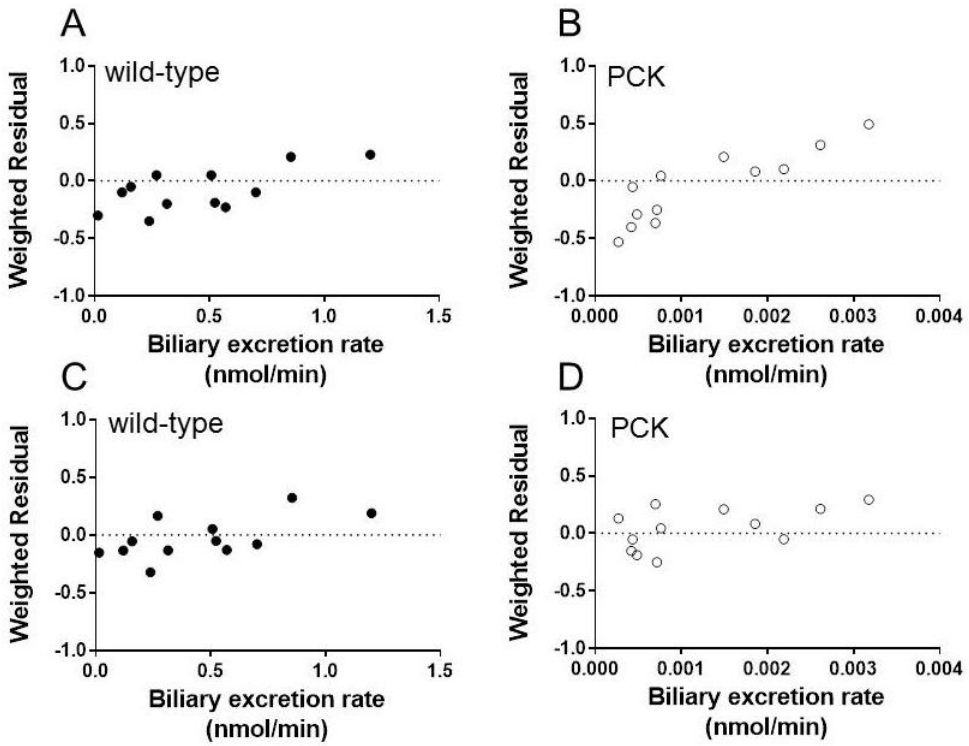

Figure 5.6. Western blots of Mrp2 and Mrp3. Western blot of Mrp2 in wild-type and PCK (A), and Mrp3 in wild-type and PCK (B) rat liver tissue, and relative optical density (OD) of Mrp2 (C) and Mrp3 (D) using densitometric analysis as described in *Materials and Methods*.; **p < 0.05, wild-type vs. PCK (n=3 per cohort, mean ± SD).

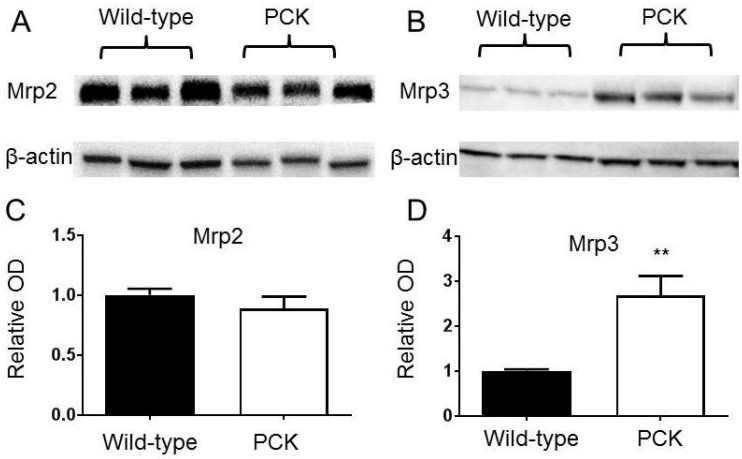

Figure 5.7. Immunohistochemical staining of Mrp2 and Mrp3. Representative expression of Mrp2 in wild-type (A) and PCK (B), and Mrp3 in wild-type (C) and PCK (D) rat liver tissue using immunohistochemical staining as described in *Materials and Methods*

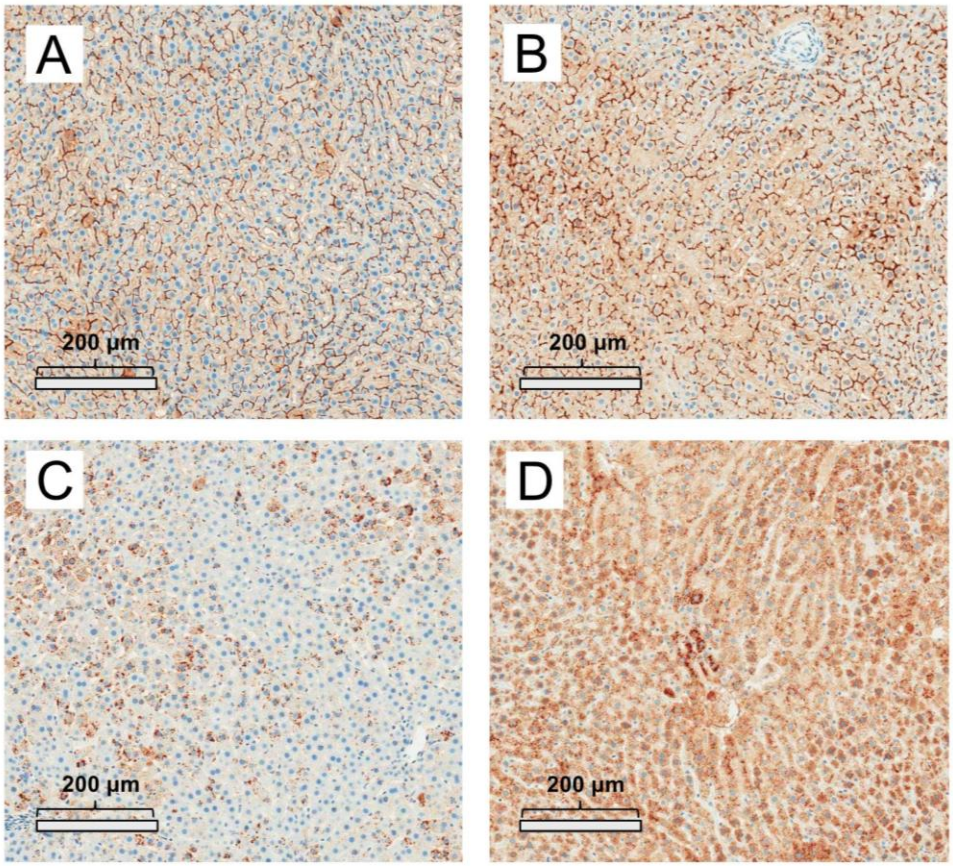

Tables

Table 5.1. Physiological parameters and compartmental modeling parameter estimates. Physiological and pharmacokinetic parameters describing CDF disposition in single-pass isolated perfused livers from wild-type and PCK rats. Pharmacokinetic parameters were estimated using nonlinear regression analysis with the two-compartment hepatocellular model shown in Fig. 5.1B.

Parameter	Wild-Type	PCK
Body weight (g)	539 ± 15	536 ± 34
Liver weight (g/kg)	33.6 ± 5.7	75.2 ± 27.6**
Cl_{up} (mL/min)	3.23 ± 0.23	2.64 ± 0.51
$k_{perfusate}$ (min^{-1})	0.0184 ± 0.0012	0.0538 ± 0.0112*
k_{12} (min^{-1})	0.0509 ± .0062	0.0628 ± 0.0077
k_{21} (min^{-1})	0.0555 ± 0.0192	0.0350 ± 0.0104
k_{bile} (min^{-1})	0.176 ± 0.012	0.00146 ± 0.00223**

Data represent mean ± SD (n=5); *p < 0.05; **p < 0.01, wild-type vs. PCK

Table 5.2. Pharmacokinetic parameter estimates determined based on one- or two-compartment models representing the hepatocellular space in PCK rat livers.

		PCK (animal number)				
		1	2	3	4	5
		Estimate (CV%)	Estimate (CV%)	Estimate (CV%)	Estimate (CV%)	Estimate (CV%)
1 liver compartment	Cl_{up} (mL/min)	3.22 (8.21)	2.67 (9.53)	2.80 (12.2)	2.64 (13.6)	2.48 (13.7)
	$k_{perfusate}$ (min^{-1})	0.0854 (29.5)	0.0784 (22.3)	0.0809 (18.1)	0.0890 (38.6)	0.103 (28.0)
	k_{12} (min^{-1})	n/a	n/a	n/a	n/a	n/a
	k_{21} (min^{-1})	n/a	n/a	n/a	n/a	n/a
	k_{bile} (min^{-1})	0.000744 (49.1)	0.000632 (59.1)	0.00079 (45.2)	0.00865 (62.5)	0.000967 (42.0)
2 liver compartments	Cl_{up} (mL/min)	3.42 (5.39)	2.34 (6.65)	2.56 (8.52)	2.78 (9.53)	2.10 (9.60)
	$k_{perfusate}$ (min^{-1})	0.0524 (19.4)	0.0421 (15.6)	0.0498 (12.7)	0.0523 (27.0)	0.0723 (19.6)
	k_{12} (min^{-1})	0.0562 (31.4)	0.0668 (40.0)	0.0739 (22.9)	0.0558 (31.5)	0.0613 (30.2)
	k_{21} (min^{-1})	0.0329 (24.8)	0.0509 (31.5)	0.0220 (18.0)	0.0262 (24.8)	0.0330 (23.8)
	k_{bile} (min^{-1})	0.000488 (25.5)	0.000327 (32.5)	0.000487 (18.6)	0.00545 (25.6)	0.000539 (24.6)

		Wild-type (animal number)				
		1	2	3	4	5
		Estimate (CV%)	Estimate (CV%)	Estimate (CV%)	Estimate (CV%)	Estimate (CV%)
1 liver compartment	Cl_{up} (mL/min)	2.95 (5.53)	3.28 (6.51)	3.10 (5.08)	3.12 (9.40)	2.66 (6.53)
	$k_{perfusate}$ (min^{-1})	0.0137 (14.7)	0.0152 (17.9)	0.0141 (26.6)	0.0133 (22.3)	0.0122 (17.9)
	k_{12} (min^{-1})	n/a	n/a	n/a	n/a	n/a
	k_{21} (min^{-1})	n/a	n/a	n/a	n/a	n/a
	k_{bile} (min^{-1})	0.160 (29.7)	0.161 (31.5)	0.180 (33.5)	0.177 (29.0)	0.179 (31.5)
2 liver compartments	Cl_{up} (mL/min)	3.09 (3.36)	3.59 (4.55)	3.19 (3.55)	3.30 (6.56)	2.98 (12.5)
	$k_{perfusate}$ (min^{-1})	0.0189 (19.0)	0.0187 (12.5)	0.0198 (18.6)	0.0168 (15.5)	0.0176 (12.5)
	k_{12} (min^{-1})	0.0455 (15.0)	0.0542 (15.9)	0.0600 (22.0)	0.0452 (19.6)	0.0497 (21.6)
	k_{21} (min^{-1})	0.0756 (15.4)	0.0342 (12.6)	0.0541 (17.4)	0.0741 (15.5)	0.0392 (17.0)
	k_{bile} (min^{-1})	0.161 (15.4)	0.167 (12.9)	0.183 (11.9)	0.187 (10.9)	0.182 (11.6)

n/a: not applicable (i.e., parameter not in the model structure); PCK rat liver #3 was selected as the representative data for Fig. 5.4 and Fig. 5.5.

Table 5.3. Effect of Modulating $k_{perfusate}$ or CL_{up} on CDF excretion into the bile.

Parameter	Fold-change in parameter	CDF in bile after a 30-min infusion (nmol)
$k_{perfusate}$	3	11.9
	5	9.50
	10	4.18
	100	0.161
	200	0.0532
CL_{up} and $k_{perfusate}$	CL_{up}: 0.5 $k_{perfusate}$: 3	5.94
	CL_{up}: 0.5 $k_{perfusate}$: 10	2.09

Simulations using the final model structure (Fig. 5.1B) were conducted assuming a constant infusion rate of CDF into the liver (1 μM at 38 mL/min for 30 min) by modulating parameter estimates based on the mean values from wild-type rats (Table 5.1) using Phoenix WinNonlin (v. 4.3 Pharsight, Mountain View, CA). The mass in bile was calculated by multiplying the rate of CDF in bile (nmol/min) by the time interval.

Supplementary Data

Table 5.1. Model Independent Parameter Estimates

Parameter	Wild-Type	PCK
Dose (nmol)	1140 ± 30	1130 ± 30
Total mass in outflow perfusate through 60 min (nmol)	1040 ± 30	1070 ± 40
Mass in perfusate during 30 min washout (nmol)	11.1 ± 6.0	25.2 ± 9.0*
Mass in bile through 30 min (nmol)	13.3 ± 0.9	0.0576 ± 0.104**
Mass in bile through 60 min (nmol)	33.5 ± 8.8	0.108 ± 0.171**
Mass not collected in perfusate or bile through 60 min (nmol)	66.6 ± 27.5	53.0 ± 41.1
CL_H (mL/min)	3.67 ± 0.54	2.55 ± 0.77
$AUC_{0\rightarrow last}$ (nM*min)	27400 ± 1000	28300 ±1300

Data represent mean ± SD (n=5); total mass in the outflow perfusate was calculated throughout the 60-min perfusion, including the mass during the 30-min washout; CL_H was calculated as the product of the flow rate (38 mL/min) and extraction ratio. Mass not collected in the perfusate or bile through 60 min was calculated as the difference between the administered dose and the mass collected in the perfusate and bile through 60 min; *$p < 0.05$; **$p < 0.01$, wild-type vs. PCK

CHAPTER 6. Summary and Future Directions

This dissertation has focused on the application of preclinical and clinical tools to study hepatic transporter function in liver disease. The impact of liver disease-associated alterations in hepatic transporter function on the pharmacokinetics and hepatobiliary disposition of drugs and endogenous substances is poorly understood. To address this knowledge gap, a multiexperimental, translational approach was employed including *in vitro* studies in human transporter expression systems, rat *in vivo* and isolated perfused liver studies, metabolomic profiling, imaging, and a clinical study. The liver plays a central role in the metabolism, hepatobiliary transport, and pharmacokinetics of drugs and endogenous substances. Consequently, the disposition of such substances may be altered in patients with liver dysfunction, which may contribute to the pathophysiology of hepatic and extrahepatic disease, require dose adjustments, or impact the safety of medications (Morgan et al., 1995; Palatini et ak, 2016; Rodighiero et al. 1999). Two types of liver disease were studied: non-alcoholic steatohepatitis (NASH) and autosomal dominant polycystic kidney disease (ADPKD).

NASH is an advanced form of non-alcoholic fatty liver disease (NAFLD) driven by the prevailing obesity epidemic; it is estimated that ~25% and ~2-3% of the general population have NAFLD and NASH, respectively (Younossi et al., 2016; Bellentani et al., 2010). Due to NASH-associated oxidative and inflammatory stress, increasing evidence suggests that absorption, distribution, metabolism, and excretion (ADME) genes are dysregulated in this patient population (Canet et al., 2014a). For example, uptake transporters (e.g. sodium-dependent

taurocholate cotransporting polypeptide (NTCP) and organic anion transporting polypeptide (OATPs)) are generally downregulated whereas efflux transporters [e.g. multidrug resistance-associated protein (MRP)2, MRP3] are generally upregulated in what appears to be a hepatoprotective response to liver injury/inflammation in NASH (Canet et al., 2014a Canet et al., 2014b; Clarke et al., 2014; Hardwick et al., 2011). However, functional studies in humans to evaluate altered transporter expression are limited. In **Chapter 2**, technetium-99m mebrofenin (MEB) was used as a clinical probe to assess the function of OATP, MRP2, and MRP3 in patients with biopsy-confirmed NASH. MEB is a metabolically stable imaging agent used to diagnose dysfunctions associated with the gallbladder and hepatobiliary network, although broader applications include the evaluation of hepatocyte viability as well as hepatic transporter function (Gencoglu et al., 2002; Ghibellini et al., 2008; Koruk et al., 2003; Pfeifer et al., 2013). Given that MEB is predominantly taken up by OATPs and excreted from the hepatocyte by MRP2 and MRP3, NASH-associated changes in OATP, MRP2, and MRP3 would be expected to alter the systemic and hepatic concentrations of MEB (de Graaf et al., 2011; Neyt et al., 2013).

Tolvaptan is a competitive vasopressin V_2-receptor antagonist that has shown promise in treating ADPKD, a monogenetic inheritable disease for which no treatment is currently approved by the Food and Drug Administration (FDA) (Torres et al., 2012). During clinical development, however, elevated levels of transaminases (i.e. alanine aminotransferase) were disproportionately reported in patients taking tolvaptan compared to placebo-controlled patients (Torres et al., 2012; Watkins et al., 2015). Furthermore, two patients met the definition of Hy's Law while an additional Hy's Law case was reported in the TEMPO 4:4 trial while on tolvaptan therapy. Hence, the FDA has not granted approval for this indication in the U.S. due, in part, to reports of hepatotoxicity in tolvaptan-treated ADPKD patients (Watkins et al., 2015). The mechanistic

etiology of these clinical observations are currently unknown. The studies outlined in **Chapter 3**, **4**, and **5** were designed to evaluate the biological plausibility of bile acid-mediated liver injury as a contributing mechanism to tolvaptan-associated hepatotoxicity. Knowledge of the effect of tolvaptan and/or metabolites on transporter-mediated bile acid uptake/efflux (**Chapter 3**) as well as disease-contributing alterations in bile acid homeostasis (**Chapter 4 and Chapter 5**) may help implicate bile acid-mediated hepatotoxicity as a mechanism of liver injury. Furthermore, these data may identify biomarkers (e.g. bile acids), which may help identify patients susceptible to hepatotoxicity.

This dissertation research has provided valuable contributions to the knowledge of hepatic transporter function in NASH and ADPKD, which may enhance our ability to predict hepatobiliary bile acid and drug disposition in these patient populations in order to optimize pharmacotherapy and minimize toxicity. The following is a summary of the contributions of this dissertation research as well as a perspective on opportunities for further investigations.

Altered Hepatic Disposition of the Transporter Probe ^{99m}Technetium–Mebrofenin in Patients with Non-Alcoholic Steatohepatitis (NASH) (Chapter 2)

Hepatobiliary transporters are important determinants of drug disposition and response. Many factors contribute to the variability of hepatic transporter expression and function including concurrent disease(s), physiological or life-style factors, concomitant medications, or genetics (Ho et al., 2005; König et al., 2013). Therefore, significant effort has been directed towards quantifying hepatic transporter expression and function, which may aid in predicting drug disposition and efficacy. Although animal studies or in vitro studies are valuable research tools used to understand hepatobiliary transporter function, clinical probe substrates are highly

sought after tools to assess transporter function in humans. This work evaluated the impact of altered basolateral uptake and efflux as well as canalicular efflux on the systemic and hepatic disposition of the clinical imaging agent MEB. MEB is an OATP, MRP2, and MRP3 substrate that has been used as a tool to evaluate impaired hepatobiliary uptake and efflux. (de Graaf et al., 2011; Geisel et al., 2015; Ghibellini et al., 2008; Pfeifer et al., 2013; Swift et al., 2010). MRP2 is the rate-limiting step in biliary excretion of MEB as evidenced by a prolonged half-life and increased hepatic exposure in Mrp2-knockout (KO) mice and in patients with Dubin-Johnson syndrome (Bar-Meir et al., 1982; Neyt et al., 2013). The objective of using MEB as a probe for OATP, MRP2, and MRP3 function was to assess whether reports of dysregulation of OATP, MRP2, and MRP3 expression/localization in patients with NASH would lead to altered systemic and/or hepatic pharmacokinetics of MEB. By leveraging protein expression data from human liver biopsies and modeling and simulation techniques, a comparative cohort study was designed to compare the systemic and hepatic disposition of MEB in healthy volunteers and patients with NASH (Canet et al., 2014b; Fisher et al., 2009; Geisel et al., 2015; Hardwick et al., 2011).

A previously published semiphysiologically-based pharmacokinetic (PBPK) model describing the disposition of MEB was used to estimate basolateral uptake/efflux and canalicular efflux of MEB in healthy human volunteers (Pfeifer et al., 2013). The difference in hepatic exposure ($AUC_{0\text{-}\infty,liver}$) was selected as the primary endpoint and sample size was estimated. Computer-based modeling and simulation, as utilized here, can provide tremendous value to predict the effect of altered ADME processes on drug pharmacokinetics. Such mechanistic models can explore the impact of biological parameters, drug-drug interactions, and population variability, among others, that may improve rationally guided decision making in drug discovery and development. This may be of particular use in the design of Phase I and early Phase II trials

where *in vitro* or functional data may be implemented to guide sample size considerations and/or dose selection.

Although systemic concentrations are routinely measured to estimate drug exposure, it has become increasingly evident that drug exposure in a particular compartment or tissue may be altered without significantly affecting systemic concentrations (Mennone et al., 2006; Swift et al., 2009). To address this limitation, quantitative imaging techniques can provide noninvasive estimation of drug concentrations and/or pharmacokinetic parameters in organ(s) of interest. Altered function of OATP, MRP2, and/or MRP3 in patients with NASH has significant implications for drug therapy and safety. Several medications (e.g. sulfonylureas, statins, thiazolidinediones) have been evaluated to prevent fibrosis and reverse inflammation in this patient population, but studies thus far have indicated no or marginal efficacy (Nakahara et al., 2012; Sanyal et al., 2010; Torres et al., 2011). Because the liver is the primary site of action of medications to treat NASH, it is imperative to understand how NASH alters hepatic drug disposition. The notion that MRP2 function in NASH is impaired may have unintended consequences for drug disposition thereby placing a larger burden on the liver. For example, Mrp2-mediated biliary excretion of spiramycin, an antibiotic been associated with cholestatic hepatitis, was impaired in Mrp2-knockout mice (Denie et al., 1992; Tian et al., 2007). These data suggest that hepatic exposure to spiramycin may increase in patients with impaired MRP2 function (e.g. patients with NASH) and that such individuals may be more susceptible to spiramycin-induced liver injury. To date, a link between NASH and susceptibility to liver injury has not been established. Additionally, the MRP2 inhibitor cyclosporine A unexpectedly decreased mycophenolic acid systemic exposure, presumably by interrupting the enterohepatic recirculation of mycophenolate and its glucuronide conjugate (Pou, et al., 2001). Hence, it is

conceivable that impaired MRP2 function could decrease systemic exposure to drugs (e.g. mycophenolate) and alter pharmacodynamic response, which may have clinical significance since NASH is projected to become a leading indication for liver transplant in addition to the reoccurrence of NASH post-transplant (Patil et al., 20120). Because the efficacy of pharmacotherapeutic interventions to treat NASH (e.g. metformin) have been disappointing, it is tempting to attribute these failures to altered pharmacokinetics as described by the current study. However, metformin is an organic cation transporter (OCT) substrate and it is unknown if the expression of OCTs in NASH is altered (Han et al., 2015; Kimuara et al., 2005). Pharmacokinetic-pharmacodynamic modeling may be required to extrapolate the findings from the current study to clinical efficacy in NASH.

Gamma scintigraphy is a well-established noninvasive functional imaging technique used in nuclear medicine to quantify the distribution of a radiotracer over time. Several probes for drug transporters have been developed for the pharmacokinetic analysis of transporter function in tissues such as the liver and the blood-brain-barrier (Mairinger et al., 2011). Advantages of γ-imaging include low costs, commercial availability of clinical probes, and the potential for imaging with two different radioisotopes simultaneously (e.g. technetium-99m, iodine-123), among others. However, some limitations do exist. For example, γ-scintigraphy has lower sensitivity and spatial resolution compared to positron emission tomography (PET), which can lead to images of poor quality. Although corrections for body mass attenuation can be applied, such as in the current study, attenuation effects in patients with severe obesity (e.g. body mass index (BMI) > 45 kg/m^2) may introduce uncertainty in the estimation of attenuation-corrected drug concentrations and therefore, may limit the utility of two-dimensional (2D) planar imaging (Lee et al., 2001; Pitcairn et al., 1997). To address this limitation, single photon emission

computed tomography (SPECT) imaging can be employed, which allows 360° rotation of γ-cameras thereby facilitating three-dimensional (3D) imaging. This increases imaging precision compared to 2D planar imaging. When SPECT is combined with high-resolution computed tomography (HRCT), anatomical information can be aligned to reconstruct a 3D image of the organ(s) of interest (e.g. the liver) to provide more accurate quantification of drug distribution (Fleming et al., 2011). Furthermore, this technique may be useful when overlying structures can obscure and/or confound quantification in an organ (e.g. the gallbladder in the liver). It must also be noted that γ-scintigraphy requires the administration of ionizing radiation. The International Commission of Radiological Protection (ICRP) recommends a whole body radiation dose of 5 rem/yr (Radiation Protection Procedures 1978). Although the total radiation dose throughout the current study is ~0.2 rem, even low amounts of exposure to ionizing radiation are considered a risk and therefore, should be carefully considered when designing studies involving radiation exposure in humans.

Alternative imaging techniques are available that may help overcome quantification limitations of organ-specific drug concentrations using γ-scintigraphy. PET imaging has emerged as a powerful tool to study the molecular mechanisms of drug distribution and transport (Testa et al., 2015). The advantages of PET are its remarkable sensitivity and spatial resolution and low tissue attenuation. PET typically requires microdoses (which are less likely to have pharmacological or toxic effects), and it exposes subjects to negligible amounts of radiation (Rahmim et al., 2008). In the context of drug development, SPECT radiotracers require the introduction of chelating moieties, which may significantly affect the physiochemical properties, and hence the biodistribution of a radio-labeled drug, whereas chemical structures or properties of drugs are less likely to be altered when a PET radioisotope is introduced (Bergstrom et al.,

2003; Matthews et al., 2012). To avoid ionizing radiation exposure altogether, magnetic resonance imaging (MRI) can be employed. It must be noted that the use of noninvasive imaging techniques currently lacks the ability to discriminate between an active drug (or probe) and formed metabolites. Therefore, in situations involving the dynamic interplay between metabolism and transport, alternative sampling techniques may be used to evaluate drug/metabolite disposition (e.g. microdialysis).

Given the heterogeneity of the NASH patient population, more robust studies including a larger sample size are warranted to corroborate these findings. Including patients with a dynamic range of fibrosis and NAFLD activity score (NAS) may help establish a robust correlation between these clinical variables and MEB pharmacokinetics. Association analysis found a statistically significant association between NASH severity score and liver exposure, suggesting that as disease severity progresses, MRP2-mediated function becomes progressively impaired. These data likely implicate inflammation has a key mediator of altered MEB pharmacokinetics. Therefore, validated inflammatory markers (e.g. tumor necrosis factor-α, cytokeratin-18, interleukin (IL)-6) should be measured to determine if there is an association between serum markers of inflammation and altered MEB pharmacokinetics. NASH generally progresses with age but there does not appear to be any effect of age on hepatic transporter expression in healthy adults (i.e. 18-65 yrs old); therefore, it is not clear if age-related changes in transporter expression may independently correlate with NASH progression or altered MEB pharmacokinetics. However, differences in expression and function have been reported in pediatric and geriatric populations (Badée et al., 2015; Bennink et al., 2016; Mooij et al., 2014). Given the increasing prevalence of NAFLD/NASH in adolescents, the effect of age on transporter

expression/function in this special population may contribute to altered drug disposition and warrants further investigation (Loomba et al., 2009).

Dynamic SPECT/CT imaging, as mentioned previously, could aid in the precision of quantifying MEB concentrations in the liver. The experimental paradigm described herein could be applied to more clinically relevant drugs to estimate the impact of NASH on drug pharmacokinetics and pharmacodynamics. For example, a novel pravastatin derivative recently was synthesized as a PET probe for noninvasive measurement of hepatobiliary transporter kinetics (Shingaki et al., 2013). Administration of rifampicin, an Oatp and Mrp2 inhibitor, revealed impaired systemic clearance of the pravastatin derivative and decreased canalicular efflux clearance consistent with Oatp and Mrp2 inhibition, respectively, although metabolism of the pravastatin derivative in rats may confound the interpretation of these results (Shingaki et al., 2013). Similar findings were observed in rats using the novel tracer ^{11}C-rosuvastatin (He et al., 2014). The data generated in the current study indicate that OATP, MRP2, and MRP3 function are altered in patients with NASH. These data could be applied to pharmacokinetic models of other drugs/probe substrates if OATP-, MRP2-, and MRP3-mediated clearance values are known. Given the multiplicity of substrate selectivity, careful consideration should be given to multiple transporters/efflux pathways when selecting a suitable probe substrate. For example, MEB is both an OATP1B1 and OATP1B3 substrate; therefore, the current study is unable to deconvolute the relative reduction of OATP1B1 or OATP1B3 function in patients with NASH, but rather suggests that OATP1B function is decreased. When noninvasive imaging techniques prove technically challenging and/or are unavailable, pharmacodynamic measurements may be useful surrogate endpoints for hepatic exposure.

Studies in humans can be difficult; therefore, it would be advantageous to develop preclinical model(s) that recapitulate the pathophysiological changes that occur in human NASH. Although several murine models exist, rodents given a diet deficient in both methionine and choline (MCD) are one of the most commonly used models of NASH due to the rapid development of steatosis, inflammation, oxidative stress, and fibrosis (Morales et al., 2010; Takahashi et al., 2012). However, MCD-deficient animals generally do not gain weight or develop insulin resistance, which are common comorbidities in patients with NASH, which may limit their translational value (Morales et al., 2010). In vitro NASH models using human hepatocyte cultures are promising, however, require further characterization and validation to establish their usefulness in translational NASH research (Di Mauro et al., 2016; Neuman et al., 2016).

The results of this clinical study evaluated the effect of NASH on OATP, MRP2, and MRP3 function using quantitative γ-scintigraphy. Future studies should focus on NASH-mediated alterations in other clinically-relevant hepatic transporters that may impact drug disposition and therapy (Guidance for Industry, 2016).

Inhibition of Human Hepatic Bile Acid Transporters by Tolvaptan and Metabolites: Contributing Factors to Drug-Induced Liver Injury? (Chapter 3)

Bile acids are a family of cholesterol-derived amphipathic molecules synthesized in the liver that contribute to numerous physiological functions such intestinal absorption, cholesterol elimination, and normal hepatic function (Monte et al., 2009). The bile salt export pump (BSEP) is a transport protein located on the canalicular domain of hepatocytes that translocates bile acids from hepatocytes to the bile canaliculi, and is a major determinant of bile flow. Due to their

detergent-like properties, bile acids can accumulate in the liver when BSEP is inhibited, thus leading to cholestasis and bile acid-induced hepatotoxicity. Increasing evidence indicates that drugs can inhibit BSEP and other compensatory bile acid transporters (e.g. MRPs) leading to liver toxicity (Köck et al., 2014; Morgan et al., 2010; Morgan et al., 2013). Therefore, the purpose of **Chapter 3** was to evaluate the effect of tolvaptan on bile acid-mediated transporter function. It is also unclear whether drug induced liver injury (DILI) observed in ADPKD patients is due to the parent compound and/or metabolite(s) of tolvaptan. Thus, tolvaptan, and two major tolvaptan metabolites, DM-4103 and DM-4107, were evaluated as inhibitors of bile acid transport.

The current work suggests that tolvaptan and metabolites have the potential to inhibit BSEP function using BSEP-overexpressing membrane vesicles (**Fig. 3.2**). Multifactorial approaches incorporating the inhibitory effect of inhibitors on compensatory bile acid transporters such as MRP2, MRP3, and MRP4 increase the correlation between bile acid inhibition and evidence of liver injury in humans (Dawson et al., 2014; Morgan et al., 2010; Morgan et al., 2013). Accordingly, the inhibitory effect of tolvaptan and metabolites on MRP2-, MRP3-, and MRP4-mediated transporter revealed the potential for additional cholestatic liability (**Fig. 3.4**). It must be noted that the half maximal inhibitory concentration (IC_{50}) values generated could translate to clinical risk; however, exposure levels (e.g. serum concentrations) of the drug must be considered. The ratio of the maximal concentration (C_{max}) or the concentration at steady state (C_{ss}) and the inhibitory potency (i.e. IC_{50}) has been proposed as a relevant parameter (i.e. C_{max} or C_{ss}/IC_{50} >0.1) to establish the potential for a drug interaction (Chu et al., 2013; Huang et al., 2008; Morgan et al., 2013. Interestingly, DM-4103 exhibited a C_{max}/IC_{50} >0.1 for all

evaluated transporters, which may specifically implicate this metabolite as having a role in tolvaptan-induced DILI (**Table 3.1**).

Although transporter panels are becoming rapidly adopted by pharmaceutical companies, extrapolating BSEP and MRP inhibition data to clinical risk is challenging. For example, BSEP inhibition by metabolite(s) may not be evaluated routinely; hence, the observation that a metabolite of tolvaptan (i.e. DM-4103) appears to be a potent inhibitor of bile acid transporters supports the need to evaluate the inhibitory potential of metabolite(s). From a technical perspective, apparent IC_{50} values also assume that added drug is available in solution. True concentrations of insoluble compounds, or compounds that display nonspecific binding (e.g. to plastic tubes), may be lower than expected and thus, may under estimate the inhibitory potency of perpetrators (i.e. predict an IC_{50} value that is greater than its true IC_{50} value). Additionally, the generation of IC_{50} values does not provide any information on the mechanism of inhibition. Alternative modes of inhibition, such as noncompetitive inhibition of BSEP-mediated taurocholate uptake by tolvaptan revealed in the current work (**Fig. 3.3**), could increase the risk of toxicity due to the fact that noncompetitive inhibition reduces the rate of transport (e.g., of bile acids), which cannot be overcome by accumulating bile acid concentrations, whereas a competitive mechanism of inhibition does not affect V_{max} (Strelow et al., 2012). Therefore, the mechanism of inhibition should be considered when extrapolating inhibition data to clinical risk. Furthermore, membrane vesicle studies cannot address time dependent, irreversible, or trans inhibition.

Perhaps as a result of these limitations, among others, it is unclear what extent of *in vitro* BSEP inhibition is functionally significant in vivo. Because the pore complex of BSEP and MRPs face the hepatocyte cytosol, hepatocyte concentrations may be more relevant in contrast to

plasma concentrations. Thus, incorporating hepatocellular drug/metabolite concentrations may improve the extrapolation of information generated from membrane vesicle studies to its *in vivo* relevance.

Sandwich-cultured human hepatocytes (SCHH) are a promising tool to study drug disposition and hepatotoxicity due the preservation of cellular architecture and relevant ADME genes (Marion et al., 2007; Swift et al., 2010). When tolvaptan was incubated in SCHH, the total (bound + unbound) cellular concentrations were ~40-fold higher relative to the dosing concentration, suggesting that tolvaptan accumulates within hepatocytes. If this correction factor is applied to the inhibitory potency of tolvaptan, the C_{max}/IC_{50} ratio for BSEP is >0.1, which may indicate a relevant interaction. However, according to the free drug hypothesis, unbound concentrations should be most relevant for the disposition and efficacy of drugs. Therefore, unbound concentrations of tolvaptan (and metabolites) should be measured in the future to translate these findings (Chu et al., 2013; Mariappan et al., 2013). The impact of tolvaptan and metabolites revealed an increase in the cellular accumulation of taurocholic acid (TCA), as well as bile acids associated with hepatotoxicity (e.g. chenodeoxycholic acid, taurochenodeoxycholic acid, and glycochenodeoxycholic acid) in SCHH studies (**Table 3.3**), which indicates that impaired transporter function established in membrane vesicles studies translated to a functional impact in a human hepatocyte system. The extrapolation of these data to clinical findings is unknown. However, the principle of altered bile acid disposition in SCHH studies has been demonstrated with drugs associated with liver injury such as troglitazone, cyclosporine A, and glyburide (Ansede et al., 2010). Thus, the data generated in the current experiments provide the first evidence of altered bile acid disposition due to tolvaptan administration, which should be explored in future mechanistic studies.

Although there does not appear to be a dose- and/or exposure-relationship with liver injury in patients with ADPKD, the low frequency of elevated transaminases makes it difficult to establish a link (Watkins et al., 2015). Furthermore, the novel implication that DM-4103 is a potent inhibitor of bile acid transporters should be taken into consideration when evaluating the causality of liver injury. Tolvaptan is primarily eliminated by CYP3A to several metabolites, mostly notably the oxybutyric acid metabolite (DM-4103) and the hydroxybutyric acid metabolite (DM-4107) (Shoaf et al., 2012). Interestingly, DM-4103 has a long half-life (~180 h) and accounts for ~52% of plasma radioactivity following a single 60-mg oral dose of ^{14}C-tolvaptan in humans (Shoaf et al., 2012; Tammara et al., 1999). The mechanism underlying the extensive half-life of DM-4103 is not known, although enterohepatic recirculation may play a role and could increase hepatic exposure over time. Enterohepatic recirculation has been implicated as a mechanism for toxicity of drugs in several examples such as damage to the gastrointestinal tract by NSAID-containing carboxylic acid moieties (Davies et al., 1997; Dobrinska et al., 1989; Ghanem et al., 2009). Although the data generated herein attempts to quantify the inhibitory potency and relevant concentrations of tolvaptan/metabolites, *in vitro* systems have limitations that make it difficult to predict *in vivo* organ exposure and toxicity.

Physiologically-based pharmacokinetic (PBPK) modeling and systems pharmacology approaches are useful *in silico* tools to address the complex mechanisms governing drug disposition, efficacy, and safety in humans (Sager et al., 2015; Schotland et al., 2016; Zhao et al., 2012). PBPK models mathematically integrate drug characteristics (e.g. molecular weight, logP, tissue partitioning, metabolism etc.) and physiological characteristics (e.g. organ weights, blood flow etc.) to describe the time-course of drug disposition. Although PBPK models typically require extensive data that describe drug and physiological characteristics, an advantage of this

approach is that it provides a quantitative framework to leverage *in vitro* data to estimate drug/metabolite exposure levels under various scenarios, which may be further linked to pharmacodynamic and/or toxicological endpoints. One key question generated from this work is: what are the steady-state hepatocellular concentrations of tolvaptan and metabolites in patients with ADPKD? Although SCHH data indicate that tolvaptan rapidly accumulates in hepatocytes, cellular concentrations of DM-4103 and DM-4107 were low relative to tolvaptan concentrations and negligible when measured in the media. The most likely explanation for these observations is that tolvaptan was incubated in SCHH for only 10 minutes. Because DM-4103 and DM-4107 are downstream metabolites, as opposed to direct metabolites, this suggests that the study design may not have captured the time course of tolvaptan uptake and subsequent metabolism. Therefore, extrapolating concentrations of DM-4103 and DM-4107 from the current studies may not represent true hepatocellular concentrations at steady-state. To address this limitation, a PBPK modeling approach could be implemented to estimate relevant hepatic concentrations after long term dosing, which may then be compared to IC_{50} values generated in the current work. Alternatively, long-term dosing experiments in SCHH could be employed to estimate hepatocellular drug/metabolite concentrations but clinical data do not exist to validate these findings.

Data discussed in **Chapter 3** consider the role of direct inhibition of BSEP in the context of tolvaptan-associated DILI. However, considering the complexity of the bile acid pool and the dynamic interplay between the formation and excretion of bile acids, alternative and contributing bile acid-related mechanisms to DILI must be considered. For example, disruption of nuclear hormone receptor function can impair the adaptive ability of the liver to handle increased hepatocellular bile acids. Ketoconazole, an antifungal associated with DILI, has been shown to

inhibit the activation of pregnane X receptor (Huang et al., 2007). Other mechanisms that can impair bile acid homeostasis, such as the modulation of kinases (which can impact transport trafficking), maintenance of membrane integrity and phospholipid flux (by transporters such as multidrug resistance protein 3 and ATPase phospholipid transporting 8B1), and perturbations in gut bacteria, by tolvaptan and/or metabolite(s) should be considered when determining the causality of tolvaptan-associated DILI (Rodrigues et al., 2014).

Wu et al. (2015) demonstrated that tolvaptan was able to inhibit cell growth and induce apoptosis through the generation of reactive oxygen species and mitochondrial dysfunction in HepG2 cells. Concentrations of tolvaptan greater than 60 μM were required to induce a cytotoxic response. However, total maximal concentrations (C_{max}) of tolvaptan are ~1 μM after a single 60 mg dose in humans; hence, the clinical relevance of these findings from Wu et al. (2015) are unknown, but cannot be dismissed as a contributing mechanism of toxicity (Shoaf et al., 2012). In fact, impaired mitochondrial activity has been proposed as a source of oxidative stress due to hepatotoxic bile acids, which may imply that direct effects and bile acid-mediated dysfunction of mitochondrial respiration due to tolvaptan/metabolite(s) can contribute to liver injury (Perez et al., 2009; Rolo et al., 2000). Systems pharmacology approaches demonstrated that a synergy between multiple mechanisms is conceivable (Woodhead et al., 2016).

The results from **Chapter 3** demonstrated, for the first time, that tolvaptan and metabolites can inhibit multiple human hepatic proteins involved in bile acid transport (i.e. NTCP, BSEP, MRP2, MRP3, and MRP4). Impaired bile acid transport by tolvaptan and/or its metabolites may negatively impact bile acid homeostasis, which may explain, in part, the mechanism(s) behind liver injury in tolvaptan-treated ADPKD patients.

Bile Acids as Potential Biomarkers to Assess Liver Impairment in Polycystic Kidney Disease (Chapter 4)

In **Chapter 3**, tolvaptan and metabolites (i.e. DM-4103 and DM-4107) were identified as inhibitors of major bile acid transporters. Hepatotoxic liability within a drug class indicates that physiochemical properties, such as inhibition of bile acid transporters, may play a role in DILI. For example, troglitazone was associated with irreversible liver injury in patients whereas rosiglitazone and pioglitazone are less harmful and still used in clinical practice today (Jaeschke et al., 2007). Although the incidence of DILI is linked to the administration of certain drugs, the idiosyncratic nature of some DILI cases suggests that patient-specific factors play an important role in the development and/or the pathogenesis of hepatotoxicity (Fontana et al., 2014). No hepatic events were observed in tolvaptan-treated patients with hyponatremia, heart failure, or cirrhosis, which may indicate that ADPKD patients may be particularly susceptible to liver injury (Watkins et al., 2015). It must be noted that patients with hyponatremia typically receive lower doses (single daily dose up to 60 mg/day) compared to patients with ADPKD (split daily dose up to 120 mg/day), although there does not appear to be a link between exposure and hepatotoxicity (Watkins et al., 2015). Given the rarity of hepatotoxic signals, tolvaptan-associated liver injury has been adjudicated as idiosyncratic in nature.

It is interesting that patients with cirrhosis do not appear to display signals of liver injury compared to patients with ADPKD, which may suggest that underlying liver pathology may contribute to tolvaptan-associated liver injury in the ADPKD patient population. Although clinical manifestations of ADPKD are typically related to kidney dysfunction (e.g. hypertension, urinary tract infection, hematuria, renal functional decline), the liver is the most commonly affected extrarenal organ (Hogan et al., 2015; Milutinovic et al., 1990). Hogan et al. (2015)

reported that ~70% of men and ~80% of women have liver cysts. Biliary microhamartomas arise from the cholangiocyte epithelium and remodeling of the ductal plate. Altered fluid secretion and proliferative activity of the cystic epithelium contributes to cystogenesis and hepatomegaly over time (Feranchak et al., 2001). The incidence of bile duct dilatation is common in patients with ADPKD and obstructive jaundice has been reported (Chauveau et al., 2000; Ishikawa et al., 1996). Hence, it is conceivable that biliary dysmorphogenesis and progressive cyst development impair normal bile formation and/or flow thereby increasing hepatic exposure to cytotoxic bile acids.

The polycystic kidney (PCK) rat, a rodent model of human ADPKD, was used to investigate bile acid homeostasis. Total liver bile acids, including bile acids associated with hepatotoxicity, were significantly increased in PCK rats compared to wild-type rats (**Fig. 4.2** and **Fig. 4.3**). Elevated hepatic bile acids are consistent with cholestasis and further evidenced by increased serum and urine bile acids in PCK rats (**Fig. 4.2**). The retention and accumulation of bile acids, particularly hydrophobic (i.e. toxic) bile acids such as DCA, CDCA and their taurine and glycine conjugates, is a key feature underlying cholestatic hepatotoxicity. Although the cellular biology underlying toxicity continues to be investigated, bile acid-mediated hepatotoxicity has been experimentally established using cultured hepatocytes and animal models (Perez et al., 2009). These data demonstrate that hepatic accumulation of toxic bile acids, independent of tolvaptan treatment, is possible in patients with ADPKD. Therefore, metabolomic profiling of bile acids in liver biopsies of patients with ADPKD is warranted.

Given the number and complexity between data in large metabolomic data sets, a multivariate statistical approach was utilized (Ringnér et al., 2008). As shown in **Fig. 4.5**, wild-type and PCK rats separated from each other (e.g. did not overlap) in each matrix, indicating that

the bile acid metabolome between wild-type and PCK rats are distinctly different from one another. Furthermore, the cumulative r^2 for each matrix was > 0.65, indicating that a two principle component model was sufficient to explain the data; a cumulative $r^2 > 0.3$ is generally considered ideal ((Ringnér et al., 2008).

Impaired localization and transport function of Bsep in a rodent model of cholestasis has been reported (Crocenzi et al., 2003). These data suggest that elevated levels of bile acids could decrease bile acid transport through internalization and/or downregulation of Bsep and thereby provide an explanation for altered bile acid homeostasis observed in the current study. However, immunohistochemical analysis did not detect any apparent difference in Bsep expression and/or localization (**Fig. 4.7**). Moreover, significant differences in biliary bile acids were not observed, which further supports the relative preservation of Bsep function (**Fig. 4.2**). The mechanism(s) underlying increased hepatic accumulation of bile acids remains to be fully elucidated. Cyp7a1, the rate limiting step in bile acid synthesis, was unaltered in PCK rats, suggesting that increased bile acid synthesis may not account for elevated hepatic bile acid concentrations, although functional studies may be needed to corroborate these findings (Munoz-Garrido et al., 2015). The alternative (acidic) pathway is initiated by Cyp27A1 and Cyp7B1, which may contribute to total bile acid synthesis and could explain alterations in bile acid homeostasis (Chiang et al., 2009). Thus, full characterization of proteins/enzymes involved in bile acid synthesis, transport (e.g. Ntcp, Oatp), and enterohepatic recirculation are needed. It should be noted that bile flow appears to be increased in PCK rats (Mason et al., 2010). Although the exact mechanism has not been defined, this is likely due to enhanced cyclic adenosine monophosphate (cAMP)-induced expression of cystic fibrosis transmembrane conductance regulator (CFTR) and aquaporin (AQP1) that account for increased ion-driven water transport and bile flow (Banales et al., 2008).

Given the similar hepatorenal abnormalities observed in PCK rats and human ADPKD, these data demonstrate that hepatic bile acids may be elevated in this patient population, which could implicate ADPKD as a susceptibility factor for bile acid-mediated liver injury. However, the rarity of hepatic events indicates the risk of tolvaptan-associated liver injury is low in a majority of patients. Why do some ADPKD patients display evidence of liver injury while others do not? Because of the positive relationship between intracellular bile acid concentrations and toxicity, it is possible that some patients may be more susceptible to liver injury if their hepatic bile acid load is characteristically elevated compared to the general ADPKD population (Palmeira et al., 2004; Shoda et al., 2014; Yang et al., 2015). The current study demonstrated a correlation between total serum bile acids and markers of liver impairment (e.g. total liver weight, total liver bile acids, total liver bile acids associated with hepatotoxicity, and cystic volume) in PCK rats (**Fig. 4.6**). If these findings translate to human ADPKD, these data support the concept that characteristically elevated bile acid concentrations may be a contributing factor to DILI observed in this population. Therefore, evaluation of serum bile acids in tolvaptan-treated patients at baseline and during a tolvaptan-associated hepatic event (e.g. during increased ALT elevations) compared to ADPKD patients that did not display drug-induced hepatotoxicity, should be compared.

The onset of hepatocellular injury, which occurred between 3 and 18 months after tolvaptan therapy, indicates that an adaptive immune response may be involved in tolvaptan-associated hepatotoxicity. One-half of the subjects experienced no ALT elevations whereas one-half of the subjects experienced rapid ALT elevations when re-challenged with tolvaptan and were permanently withdrawn from therapy (Watkins et al., 2015). Altered bile acid homeostasis can result in delayed presentation of hepatocellular injury. For example, delayed ALT elevations

of troglitazone were attributed to delayed build-up of toxic hepatic bile acids driven by (1) competitive inhibition of biliary bile acid excretion and (2) the inability for FXR-mediated regulation of bile acid synthesis/transport to compensate for altered bile acid homeostasis over time (Yang et al., 2014). Therefore, it is possible that ADPKD patients are susceptible to tolvaptan-associated liver injury related to time on tolvaptan therapy.

It should be noted that all three Hy's law cases, and 60% of cases adjudicated as probably or highly associated with tolvaptan therapy, occurred in women (Watkins et al., 2015). True sex differences in the susceptibility of tolvaptan-associated liver injury cannot be made at this time. However, hepatic cysts occur more frequently and in greater size in women; similar findings are observed in PCK rats (Hogan et al., 2015; Mason et al., 2010). This observation may be due to hormonal differences in women. Postmenopausal estrogen therapy was shown to stimulate hepatic cyst enlargement in women; hence, clinicians recommend avoiding hormonal therapy or hormone-containing oral contraceptive therapy when symptomatic liver cystic disease presents (Chapman et al., 2015; Sherstha et al., 1997). Furthermore, sulfate conjugates of certain hormones, such as progesterone for example, are known to inhibit FXR, which can repress the expression of BSEP and could contribute to decreased BSEP function and consequently, increased concentrations of hepatic bile acids (Chen et al., 2013; Abu-Hayyeh et al., 2013). Therefore, sex-differences in hepatic bile acid concentrations in ADPKD patients should be evaluated.

Altered Hepatobiliary Disposition of the Mrp2 Probe Substrate Carboxydichlorofluorescein in Isolated Perfused Livers from a Rat Model of Polycystic Kidney Disease (Chapter 5)

In **Chapter 4**, altered bile acid homeostasis was established in PCK rats. However, these data do not provide any mechanistic explanations for altered bile acid homeostasis. Furthermore, the impact of ADPKD on the hepatobiliary disposition of drugs from a pharmacokinetic or pharmacologic standpoint has not been addressed, which may aid in understanding the apparent susceptibility of ADPKD patients to tolvaptan-associated hepatotoxicity. Therefore, the study described in **Chapter 5** was designed to examine the effect of PKD on the hepatobiliary disposition of 5(6)-carboxy-2',7'-dichlorofluorescein (CDF), a fluorescent OATP/Oatp, MRP2/Mrp2, and MRP3/Mrp3 probe in isolated perfused livers from PCK rats compared to healthy Sprague-Dawley (wild-type) rats (Zamek-Gliszczynski et al., 2003).

The isolated perfused rat liver (IPRL) is an *ex vivo* model used to investigate the physiology and function of the liver. It has been used in the assessment of ischemia-reperfusion injury, synthesis of proteins, oxygen consumption, and metabolism and transport of drugs (Dahn et al., 1999; Haussinger et al., 1996; Khezrian et al., 2015; Lindell et al., 1994). Although hepatocyte cultures and liver slices are useful whole-cell models, the primary advantages of the IPRL are the retention of normal hepatic architecture, microcirculation, and bile production in a system that approaches normal physiology (Bessems et al., 2006). Wild-type and PCK rats were perfused with CDF in a single-pass manner for a 30-min loading phase followed by a 30-min washout phase to evaluate the hepatic and biliary clearance of CDF. The extraction ratio was not different between the two cohorts but interestingly, the biliary excretion rate was significantly decreased in PCK rats. The most logical explanation for decreased biliary excretion of CDF is

decreased Mrp2 expression and function. Indeed, Mrp2 expression is decreased in models of cholestasis and in some cases, appears to be removed from the canalicular membrane into the pericanalicular cytoplasm (Ban et al., 2009; Trauner et al., 1997). However, western blot analysis failed to detect a difference in Mrp2 expression in the present studies. Immunohistochemical (IHC) analysis corroborated these findings and also indicated proper localization of Mrp2 on the canalicular membrane. Although we established a cholestatic-like state in PCK rats as evidenced by significantly increased hepatic bile acids in **Chapter 4,** cyclic adenosine monophosphate (cAMP), which has been shown to induce the translocation of Mrp2 to the canalicular membrane, is significantly increased in PCK rats (Chebib et al., 2015; Schonhoff et al., 2010). Hence, it is possible that enhanced cAMP activity counteracts bile acid-mediated effects (i.e. downregulation) on Mrp2, which accounts for our observations of preserved Mrp2 expression and localization in PCK rats.

CDF can also be transported back into the perfusate by Mrp3 (Zamek-Gliszczynski et al., 2003). Increased basolateral excretion by Mrp3 in PCK rats is evidenced by increased CDF in the dose recovered during the washout phase . Compensatory bile acid transporters (e.g. MRP3/Mrp3, MRP4/Mrp4) can be upregulated during hepatocellular stress and cholestasis, which could explain these observations (Chai et al., 2012; Donner et al., 2001; Gradhand et al., 2008; Mennone et al., 2006). Indeed, western blot analysis detected a ~3-fold increase in Mrp3 protein expression, which was corroborated using IHC analysis. Although decreased hepatic uptake and a shift from biliary to basolateral excretion could help explain decreased biliary excretion, the observation that Mrp2 expression and localization is preserved despite negligible biliary excretion is paradoxical and unexplained by the data generated herein.

In **Chapter 4**, increased hepatocellular bile acid concentrations were observed in PCK rats. It is possible that increased concentrations of bile acids in PCK rats inhibit Mrp2-mediated transport of CDF. The current study provides mechanistic data to support this hypothesis. For example, the sulfate conjugates of taurochenodeoxycholate and taurolithocholate are actively transported in an ATP-dependent manner in Mrp2-overexpressing membrane vesicles and have been shown to inhibit bile acid transport (Akita et al., 2001). Furthermore, bile acid inhibition was potentiated when vesicles were pre-incubated with sulfated bile acids, indicating that these conjugates may trans-inhibit Mrp2-mediated transport. Studies by Gerk et al. (2007) and Gerk et al. (2004) also revealed that tauroursodeoxycholate, glycoursodeoxycholate, and estrogen glucuronides associated with cholestasis (i.e. β-estradiol 3-β-d-glucuronide and β-estradiol 17-β-d-glucuronide) are able to inhibit MRP2-mediated transport. Hence, increased bile acid concentrations in PCK rats may play a role in the apparent decrease in Mrp2-mediated biliary clearance of CDF. Mechanistic studies (e.g. using membrane vesicles) should be evaluated to determine if this mechanism can explain these observations. Other hepatocellular mechanisms that could explain decreased biliary clearance of CDF include enhanced cellular sequestration mediated by PCK-related alterations in intracellular binding to cytosolic proteins, organelles, or vesicles (e.g. mitochondria, microsomes, and nuclei). Quantitative intravital microscopy and digital analysis could be employed to specifically monitor the transport of fluorescent substrates from the hepatocyte into the bile canaliculi (Ryan et al., 2014). In addition, other substrates (e.g. fluorescent bile acids) could be evaluated in PCK rats to corroborate the findings generated in **Chapter 5** (Holzinger et al., 1998).

Considering the significant remodeling of the biliary tree and biliary dysgenesis in PCK rats, extrahepatocellular mechanism(s) may contribute to decreased biliary clearance of CDF.

Much like hepatocytes themselves, cholangiocytes interact with bile acids and anionic compounds in many ways. *In vitro* studies indicate the bile acids are vectorially transported into the peribiliary vascular plexus in an apical-to-basolateral manner by several transporters including the apical sodium dependent bile acid transporter (ASBT), MRP3, multidrug resistance transporter 3 (MDR3), and organic solute transporter (OST) alpha and OST beta (Ballatori et al., 2005; Ballatori et al., 2009; Benedetti et al., 1997; Hirohashi et al., 2000; Lazaridis et al., 2000; Tabibian et al., 2013). The exchange of bile acids between hepatocytes and cholangiocytes is known as the cholehepatic shunt pathway, first proposed by Hoffman et al. (1989) to explain the hypercholeretic effects of some bile acids. Because cysts are derived from the biliary epithelium, it is conceivable that CDF may diffuse or be actively transported into cysts, thereby decreasing biliary excretion. However, focal hepatic lesions, such as liver cysts and biliary hamartomas, are hypointense (i.e. do not accumulate contrast agents) when using magnetic resonance imaging (MRI)-based contrast agents such as gadolinium-ethoxibenzyl-diethylenetriamine pentaacetic acid (Gd-EOB-DTPA), a known Mrp2 and Mrp3 substrate (Campos et al., 2012; Kitao et al., 2010).

Alternatively, enhanced cholangiocyte uptake by increased Mrp3 expression and/or other unidentified CDF transporters (e.g. organic solute transporter Ost alpha-Ost beta, Mrp4) could decrease CDF excretion into the common bile duct. Carrier mediated transport of Mrp2/Mrp3 substrates (i.e. conjugated bile acids) have been demonstrated using fluorescent assays in biliary epithelial cell culture (Benedetti et al., 1997). The cholehepatic shunt pathway may provide a mechanism to enhance bile acid-dependent secretion from cholangiocytes back to hepatocytes in an adaptive response to cholestasis and/or liver injury and thus provide an alternative route of bile acid efflux. This hypothetical mechanism is supported by observations of increased

hepatocellular bile acids, described in **Chapter 4** and increased Mrp3 in the current study. In fact, cholangiocyte-mediated bile acid transport is increased in bile duct ligated rodents, a model of chronic cholestasis (Alpini et al., 2001). Interestingly, this observation was not attributable to marked increases in transporter expression per cholangiocyte, but rather to increased intrahepatic bile duct surface area (e.g. increased number of cholangiocytes). Masyuk et al. (2004) reported extensive remodeling of the biliary tree in PCK rats that results in an up to ~40-fold increase in biliary volume. Hence, significant increases in the cholangiocyte epithelial surface area may contribute to enhanced transport of CDF from the biliary lumen.

The clinical significance of these findings is uncertain. Evidence of cholestasis in ADPKD patients is rare and biliary stenosis is usually associated with a physical stricture by overlaying cyst(s) (Kolodziejski et al., 2004; Lerner et al., 1992). Interestingly, Salam et al. (1989) reported prolonged hepatic retention of MEB, the clinical diagnostic agent and MRP2 substrate used in **Chapter 2**, in a patient with ADPKD. This report suggests that MRP2-mediated biliary excretion is impaired, similar to the findings in PCK rats reported in **Chapter 5**. Delayed or nonvisualization of the gallbladder using λ-scintigraphy also has been reported in patients with choledochal cysts of various or unknown origin (Gad et al., 1992; Huang et al., 1982).

The relevance of PCK rats to evaluate the potential of bile acid-mediated toxicity while on tolvaptan therapy is unknown, but may have limitations. Liver abnormalities in tolvaptan-treated wild-type or PCK rats were not reported during nonclinical testing (Oi et al., 2011; Wang et al., 2005). Furthermore, preclinical animals are less sensitive to bile acid-mediated injury compared to humans (Leslie et al., 2007; Watkins et al., 2005). This is likely due to differential bile acid composition. For example, rats have a more hydrophilic (i.e. less toxic) bile acid pool

whereas chenodeoxycholic acid, a bile acid implicated in cholestatic liver disease, is a dominant bile acid species in humans (Garcia-Canaveras et al., 2012; Greim et al., 1972; Trottier et al., 2011). Retrospective analysis of nonclinical data has yet to provide sufficient evidence that idiosyncratic DILI, such as observed in tolvaptan-treated ADPKD patients, can be reliably predicted from nonclinical toxicity studies (Kaplowitz et al., 2005; Ong et al., 2007; Peters et al., 2005). Therefore, clinically relevant *in vitro* assays (e.g. human hepatocyte models) and mechanistic modeling may have better predictive power for rare DILI at this time.

The impact of pathophysiological disease state(s) on drug disposition, such as in ADPKD, is under recognized. This study demonstrates that the biliary excretion of the Oatp, Mrp2 and Mrp3 substrate CDF is impaired in PCK rats. This novel finding may have clinical relevance. In the context of tolvaptan-associated livery injury, these data suggest that altered hepatobiliary disposition, combined with impaired renal function, may increase hepatic exposure to tolvaptan and/or metabolite(s) in patients with ADPKD and place undue burden on the liver leading to hepatotoxicity in some patients.

Concluding Remarks

This dissertation project focused on two types of liver disease: NASH and ADPKD. Data generated herein have resulted in novel contributions to the field of pharmacokinetics and DILI. The use of clinical and preclinical tools has advanced the study of drug transport, particularly in the context of ADPKD, where data characterizing hepatic transporter expression and function has not been evaluated to date. The results of these studies enhance existing knowledge about drug disposition in NASH and ADPKD, which may improve the efficacy and safety of drugs administered in these patient populations.

REFERENCES

Abu-Hayyeh S, Papacleovoulou G, Lövgren-Sandblom A, Tahir M, Oduwole O, Jamaludin NA, Ravat S, Nikolova V, Chambers J, Selden C, Rees M, Marschall HU, Parker MG, Williamson C. Intrahepatic cholestasis of pregnancy levels of sulfated progesterone metabolites inhibit farnesoid X receptor resulting in a cholestatic phenotype. Hepatology. 2013 Feb;57(2):716-26.

Akita H, Suzuki H, Ito K, Kinoshita S, Sato N, Takikawa H, Sugiyama Y. Characterization of bile acid transport mediated by multidrug resistance associated protein 2 and bile salt export pump. Biochim Biophys Acta. 2001 Mar 9;1511(1):7-16.

Alpini SG, Phinizy JL, Kanno N. et al. Regulation of cholangiocyte apical bile acid transporter (ABAT) activity by biliary bile acids: Different potential compensatory changes for intrahepatic and extrahepatic cholestasis. Gastroenterology. 2001;120:A6.

Ansede JH, Smith WR, Perry CH, St Claire RL 3rd, Brouwer KR. An in vitro assay to assess transporter-based cholestatic hepatotoxicity using sandwich-cultured rat hepatocytes. Drug Metab Dispos. 2010 Feb;38(2):276-80.

Badée J, Achour B, Rostami-Hodjegan A, Galetin A. Meta-analysis of expression of hepatic organic anion-transporting polypeptide (OATP) transporters in cellular systems relative to human liver tissue. Drug Metab Dispos. 2015 Apr;43(4):424-32.

Ballatori N, Christian WV, Lee JY, Dawson PA, Soroka CJ, Boyer JL, Madejczyk MS, Li N. OSTalpha-OSTbeta: a major basolateral bile acid and steroid transporter in human intestinal, renal, and biliary epithelia. Hepatology. 2005 Dec; 42(6):1270-9.

Ballatori N, Li N, Fang F, Boyer JL, Christian WV, Hammond CL. OST alpha-OST beta: a key membrane transporter of bile acids and conjugated steroids. Front Biosci. 2009 Jan 1; 14: 2829–2844.

Ban D, Kudo A, Sui S, Tanaka S, Nakamura N, Ito K, Suematsu M, Arii S. Decreased Mrp2-dependent bile flow in the post-warm ischemic rat liver. J Surg Res. 2009 May 15;153(2):310-6.

Banales JM, Masyuk TV, Bogert PS, Huang BQ, Gradilone SA, Lee SO, Stroope AJ, Masyuk AI, Medina JF, LaRusso NF. Hepatic cystogenesis is associated with abnormal expression and location of ion transporters and water channels in an animal model of autosomal recessive polycystic kidney disease. Am J Pathol. 2008 Dec;173(6):1637-46.

Bar-Meir S, Baron J, Seligson U, Gottesfeld F, Levy R, Gilat T. 99mTc-HIDA cholescintigraphy in Dubin-Johnson and Rotor syndromes. Radiology. 1982 Mar; 142(3):743-6.

Bellentani S, Scaglioni F, Marino M, Bedogni G. Epidemiology of non-alcoholic fatty liver disease. Dig Dis. 2010;28(1):155-61.

Benedetti A, Di Sario A, Marucci L, Svegliati-Baroni G, Schteingart CD, Ton-Nu HT, Hofmann AF. Carrier-mediated transport of conjugated bile acids across the basolateral membrane of biliary epithelial cells. Am J Physiol. 1997 Jun; 272(6 Pt 1):G1416-24.

Benedetti A, Di Sario A, Marucci L. et al. Carrier-mediated transport of conjugated bile acids across the basolateral membrane of biliary epithelial cells. Am J Physiol. 1997 Jun;272(6 Pt 1):G1416-24.

Bennink RJ, van Gulik TM. Liver function declines with increased age. HPB (Oxford). 2016 Aug;18(8):691-6.

Bergstrom M, Grahnen A, Langstrom B. Positron emission tomography microdosing: a new concept with application in tracer and early clinical drug development. Eur J Clin Pharmacol. 2003 Sep;59(5-6):357-66.

Bessems M, 't Hart NA, Tolba R, Doorschodt BM, Leuvenink HG, Ploeg RJ, Minor T, van Gulik TM. The isolated perfused rat liver: standardization of a time-honoured model. Lab Anim. 2006 Jul;40(3):236-46.

Campos JT, Sirlin CB, Choi JY. Focal hepatic lesions in Gd-EOB-DTPA enhanced MRI: the atlas. Insights Imaging. 2012 Oct; 3(5): 451–474.

Canet M, Cherrington N. Drug Disposition Alterations in Liver Disease: Extra-hepatic Effects in Cholestasis and Nonalcoholic Steatohepatitis. Expert Opin Drug Metab Toxicol. 2014a September; 10(9): 1209–1219.

Canet MJ, Hardwick RN, Lake AD, Dzierlenga AL, Clarke JD, Cherrington NJ. Modeling human nonalcoholic steatohepatitis-associated changes in drug transporter expression using experimental rodent models. Drug Metab Dispos. 2014b Apr;42(4):586-95.

Chai J, He Y, Cai SY, Jiang Z, Wang H, Li Q, Chen L, Peng Z, He X, Wu X, Xiao T, Wang R, Boyer JL, Chen W. Elevated hepatic multidrug resistance-associated protein 3/ATP-binding cassette subfamily C 3 expression in human obstructive cholestasis is mediated through tumor necrosis factor alpha and c-Jun NH2-terminal kinase/stress-activated protein kinase-signaling pathway. Hepatology. 2012 May;55(5):1485-94.

Chapman AB, Devuyst O, Eckardt KU, Gansevoort RT, Harris T, Horie S, Kasiske BL, Odland D, Pei Y, Perrone RD, Pirson Y, Schrier RW, Torra R, Torres VE, Watnick T, Wheeler DC; Conference Participants. Autosomal-dominant polycystic kidney disease (ADPKD): executive summary from a Kidney Disease: Improving Global Outcomes (KDIGO) Controversies Conference. Kidney Int. 2015 Jul;88(1):17-27.

Chauveau D, Fakhouri F, Grünfeld JP. Liver involvement in autosomal-dominant polycystic kidney disease: therapeutic dilemma. J Am Soc Nephrol. 2000 Sep;11(9):1767-75.

Chebib FT, Sussman CR, Wang X, Harris PC, Torres VE. Vasopressin and interactive calcium, cyclic AMP and purinergic signaling in Polycystic Kidney Disease. Nat Rev Nephrol. 2015 August; 11(8): 451–464.

Chen Y, Song X, Valanejad L, Vasilenko A, More V, Qiu X, Chen W, Lai Y, Slitt A, Stoner M, Yan B, Deng R. Bile salt export pump is dysregulated with altered farnesoid X receptor isoform expression in patients with hepatocellular carcinoma. Hepatology. 2013 Apr;57(4):1530-41.

Chiang J. Bile acids: regulation of synthesis. J Lipid Res. 2009 Oct; 50(10): 1955–1966.

Chu X, Korzekwa K, Elsby R, Fenner K, Galetin A, Lai Y, Matsson P, Moss A, Nagar S, Rosania GR, Bai JP, Polli JW, Sugiyama Y, Brouwer KL; International Transporter Consortium. Intracellular drug concentrations and transporters: measurement, modeling, and implications for the liver. Clin Pharmacol Ther. 2013 Jul;94(1):126-41.

Chu X, Korzekwa K, Elsby R, Fenner K, Galetin A, Lai Y, Matsson P, Moss A, Nagar S, Rosania GR, Bai JP, Polli JW, Sugiyama Y, Brouwer KL; International Transporter Consortium. Intracellular drug concentrations and transporters: measurement, modeling, and implications for the liver. Clin Pharmacol Ther. 2013 Jul;94(1):126-41.

Clarke JD, Hardwick RN, Lake AD, Canet MJ, Cherrington NJ. Experimental nonalcoholic steatohepatitis increases exposure to simvastatin hydroxy acid by decreasing hepatic organic anion transporting polypeptide expression. J Pharmacol Exp Ther. 2014 Mar;348(3):452-8.

Crocenzi FA, Mottino AD, Sánchez Pozzi EJ, Pellegrino JM, Rodríguez EA, Garay, Milkiewicz P, Vore M, Coleman R, and Roma MG. Impaired localisation and transport function of canalicular Bsep in taurolithocholate induced cholestasis in the rat. Gut. 2003 Aug; 52(8): 1170–1177.

Dahn MS, Lange MP, Benn S. The influence of hepatic venous oxygen saturation on the liver's synthetic response to metabolic stress. Proc Soc Exp Biol Med. 1999 May;221(1):39-45.

Davies NM, Wallace JL. Nonsteroidal anti-inflammatory drug-induced gastrointestinal toxicity: New insights into an old problem. J Gastroenterol. 1997 Feb;32(1):127-33.

Dawson S, Stahl S, Paul N, Barber J, Kenna JG. In vitro inhibition of the bile salt export pump correlates with risk of cholestatic drug-induced liver injury in humans. Drug Metab Dispos. 2012 Jan;40(1):130-8.

de Graaf W, Häusler S, Heger M, van Ginhoven TM, van Cappellen G, Bennink RJ, Kullak-Ublick GA, Hesselmann R, van Gulik TM, Stieger B. Transporters involved in the hepatic uptake of (99m)Tc-mebrofenin and indocyanine green. J Hepatol. 2011 Apr;54(4):738-45.

de Graaf W, Häusler S, Heger M, van Ginhoven TM, van Cappellen G, Bennink RJ, Kullak-Ublick GA, Hesselmann R, van Gulik TM, Stieger B. Transporters involved in the hepatic uptake of (99m)Tc-mebrofenin and indocyanine green. J Hepatol. 2011 Apr;54(4):738-45.

Denie C, Henrion J, Schapira M, Schmitz A, Heller FR. Spiramycin-induced cholestatic hepatitis. J Hepatol. 1992 Nov;16(3):386.

Di Mauro S, Ragusa M, Urbano F, Filippello A, Di Pino A, Scamporrino A, Pulvirenti A, Ferro A, Rabuazzo AM, Purrello M, Purrello F, Piro S. Intracellular and extracellular miRNome deregulation in cellular models of NAFLD or NASH: Clinical implications. Nutr Metab Cardiovasc Dis. 2016 Aug 20.

Dobrinska M. Enterohepatic circulation of drugs. J Clin Pharmacol 1989; 29: 577–80.

Donner MG, Keppler D. Up-regulation of basolateral multidrug resistance protein 3 (Mrp3) in cholestatic rat liver. Hepatology. 2001 Aug;34(2):351-9.

Erickson RP, Cherrington, NJ. Experimental non-alcoholic fatty liver disease results in decreased hepatic uptake transporter expression and function in rats. Eur J Pharmacol. 2009 613 119-127.

Feranchak AP, Sokol RJ. Cholangiocyte biology and cystic fibrosis liver disease. Semin Liver Dis. 2001 Nov;21(4):471-88.

Fisher CD, Lickteig, AJ, Augustine, LM, Oude Elferink, RP, Besselsen DG,

Fleming J, Conway J, Majoral C, Tossici-Bolt L, Katz I, Caillibotte G, Perchet D, Pichelin M, Muellinger B, Martonen T, Kroneberg P, Apiou-Sbirlea G. The use of combined single photon emission computed tomography and X-ray computed tomography to assess the fate of inhaled aerosol. J Aerosol Med Pulm Drug Deliv. 2011 Feb;24(1):49-60.

Fontana RJ. Pathogenesis of idiosyncratic drug-induced liver injury and clinical perspectives. Gastroenterology. 2014 Apr;146(4):914-28.

Gad MA, Krishnamurthy GT, Glowniak JV. Identification and differentiation of congenital gallbladder abnormality by quantitative technetium-99m IDA cholescintigraphy. J Nucl Med. 1992 Mar;33(3):431-4.

Garcia-Canaveras JC, Donato MT, Castell JV, Lahoz A. Targeted profiling of circulating and hepatic bile acids in human, mouse, and rat using a UPLC-MRM-MS-validated method. J Lipid Res. 2012 Oct;53:2231–41.

Geisel D, Lüdemann L, Fröling V, Malinowski M, Stockmann M, Baron A, Gebauer B, Seehofer D, Prasad V, Denecke T. Imaging-based evaluation of liver function: comparison of 99mTc-mebrofenin hepatobiliary scintigraphy and Gd-EOB-DTPA-enhanced MRI. Eur Radiol. 2015 May;25(5):1384-91.

Gencoglu E, Karakayali H, Moray G, Aktas A, Haberal M. Evaluation of pediatric liver transplant recipients using quantitative hepatobiliary scintigraphy. Transplant Proc. 2002 Sep;34(6):2160-2.

Gerk PM, Li W, Megaraj V, Vore M. Human multidrug resistance protein 2 transports the therapeutic bile salt tauroursodeoxycholate. J Pharmacol Exp Ther. 2007 Feb;320(2):893-9.

Gerk PM, Li W, Vore M. Estradiol 3-glucuronide is transported by the multidrug resistance-associated protein 2 but does not activate the allosteric site bound by estradiol 17-glucuronide. Drug Metab Dispos. 2004 Oct;32(10):1139-45.

Ghanem CI, Ruiz ML, Villanueva SS, Luquita M, Llesuy S, Catania VA, Bengochea LA, Mottino AD. Effect of repeated administration with subtoxic doses of acetaminophen to rats on enterohepatic recirculation of a subsequent toxic dose. Biochem Pharmacol. 2009 May 15;77(10):1621-8

Ghibellini G, Leslie EM, Pollack GM, Brouwer KL. Use of tc-99m mebrofenin as a clinical probe to assess altered hepatobiliary transport: integration of in vitro, pharmacokinetic modeling, and simulation studies. Pharm Res. 2008 Aug;25(8):1851-60.

Ghibellini G, Leslie EM, Pollack GM, Brouwer KL. Use of tc-99m mebrofenin as a clinical probe to assess altered hepatobiliary transport: integration of in vitro, pharmacokinetic modeling, and simulation studies. Pharm Res. 2008 Aug;25(8):1851-60.

Gradhand U, Lang T, Schaeffeler E, Glaeser H, Tegude H, Klein K, Fritz P, Jedlitschky G, Kroemer HK, Bachmakov I, Anwald B, Kerb R, Zanger UM, Eichelbaum M, Schwab M, Fromm MF. Variability in human hepatic MRP4 expression: influence of cholestasis and genotype. Pharmacogenomics J. 2008 Feb;8(1):42-52.

Greim H, Trülzsch D, Czygan P, Rudick J, Hutterer F, Schaffner F, Popper H. Mechanism of cholestasis. 6. Bile acids in human livers with or without biliary obstruction.Gastroenterology. 1972 Nov; 63(5):846-50.

Guidance for Industry (Draft): Drug Interaction Studies - Study Design, Data Analysis, Implications for Dosing, and Labeling Recommendations. <http://www.fda.gov/Drugs/GuidanceComplianceRegulatoryInformation/Guidances/ucm064982.htm>. Accessed 18 July 2016.).

Han TK, Proctor WR, Costales CL, Cai H, Everett RS, Thakker DR. Four cation-selective transporters contribute to apical uptake and accumulation of metformin in Caco-2 cell monolayers. J Pharmacol Exp Ther. 2015 Mar;352(3):519-28.

Hardwick RN, Fisher CD, Canet MJ, Scheffer GL, Cherrington NJ. Variations in ATP-binding cassette transporter regulation during the progression of human nonalcoholic fatty liver disease. Drug Metab Dispos. 2011 Dec;39(12):2395-402.

Hardwick RN, Fisher CD, Canet MJ, Scheffer GL, Cherrington NJ. Variations in ATP-binding cassette transporter regulation during the progression of human nonalcoholic fatty liver disease. Drug Metab Dispos. 2011 Dec;39(12):2395-402.

Haussinger D, Gerok W, Sies H. The effect of urea synthesis on extracellular pH in isolated perfused rat liver. Biochem J. 1986 May 15; 236(1): 261–265.

He J, Yu Y, Prasad B, Link J, Miyaoka RS, Chen X, Unadkat JD. PET imaging of Oatp-mediated hepatobiliary transport of [(11)C] rosuvastatin in the rat. Mol Pharm. 2014 Aug 4;11(8):2745-54.

Hirohashi T, Suzuki H, Takikawa H, Sugiyama Y. ATP-dependent transport of bile salts by rat multidrug resistance-associated protein 3 (Mrp3). J Biol Chem. 2000 Jan 28; 275(4):2905-10.

Ho RH, Kim RB. Transporters and drug therapy: implications for drug disposition and disease. Clin Pharmacol Ther. 2005 Sep;78(3):260-77.

Hofmann AF. Current concepts of biliary secretion. Dig Dis Sci. 1989;34:16S–20S.

Hogan MC, Abebe K, Torres VE, Chapman AB, Bae KT, Tao C, Sun H, Perrone RD, Steinman TI, Braun W, Winklhofer FT, Miskulin DC, Rahbari-Oskoui F, Brosnahan G, Masoumi A, Karpov IO, Spillane S, Flessner M, Moore CG, Schrier RW. Liver involvement in early autosomal-dominant polycystic kidney disease. Clin Gastroenterol Hepatol. 2015 Jan;13(1):155-64.

Holzinger F, Schteingart CD, Ton-Nu HT, Cerrè C, Steinbach JH, Yeh HZ, Hofmann AF. Transport of fluorescent bile acids by the isolated perfused rat liver: kinetics, sequestration, and mobilization. Hepatology. 1998 Aug;28(2):510-20.

Huang H, Wang H, Sinz M, Zoeckler M, Staudinger J, Redinbo MR, Teotico DG, Locker J, Kalpana GV, Mani S. Inhibition of drug metabolism by blocking the activation of nuclear receptors by ketoconazole. Oncogene. 2007 Jan 11;26(2):258-68.

Huang MJ, Liaw TF. Intravenous cholescintigraphy using Tc-99m-Labeled agents in the diagnosis of choledochalcyst. J Nuc Med. 1982; 23:113-116.

Huang SM, Strong JM, Zhang L, Reynolds KS, Nallani S, Temple R, Abraham S, Habet SA, Baweja RK, Burckart GJ, Chung S, Colangelo P, Frucht D, Green MD, Hepp P, Karnaukhova E, Ko HS, Lee JI, Marroum PJ, Norden JM, Qiu W, Rahman A, Sobel S, Stifano T, Thummel K, Wei XX, Yasuda S, Zheng JH, Zhao H, Lesko LJ. New era in drug interaction evaluation: US Food and Drug Administration update on CYP enzymes, transporters, and the guidance process. J Clin Pharmacol. 2008 Jun;48(6):662-70.

Ishikawa I, Chikamoto E, Nakamura M, Asaka M, Tomosugi N, Yuri T. High incidence of common bile duct dilatation in autosomal dominant polycystic kidney disease patients. Am J Kidney Dis. 1996 Mar;27(3):321-6.

Jaeschke H. Troglitazone hepatotoxicity: are we getting closer to understanding idiosyncratic liver injury? Toxicol Sci. 2007 May;97(1):1-3.

Kaplowitz N. Idiosyncratic Drug Hepatotoxicity. Nature Reviews Drug Discovery 2005 Jun;4(6): 489-499.

Khezrian M, Sheikholeslami B, Dadashzadeh S, Lavasani H, Rouini M.Effects of cyclosporine A on the hepatobiliary disposition and hepatic uptake of etoposide in an isolated perfused rat liver model. Cancer Chemother Pharmacol. 2015 May;75(5):961-8.

Kimura N, Masuda S, Tanihara Y, Ueo H, Okuda M, Katsura T, Inui K. Metformin is a superior substrate for renal organic cation transporter OCT2 rather than hepatic OCT1. Drug Metab Pharmacokinet. 2005 Oct;20(5):379-86.

Kitao A, Zen Y, Matsui O, et al. Hepatocellular carcinoma: signal intensity at gadoxetic acid-enhanced MR Imaging--correlation with molecular transporters and histopathologic features. Radiology. 2010;256(3):817–826.

Köck K, Ferslew BC, Netterberg I, Yang K, Urban TJ, Swaan PW, Stewart PW, Brouwer KL. Risk factors for development of cholestatic drug-induced liver injury: inhibition of hepatic basolateral bile acid transporters multidrug resistance-associated proteins 3 and 4. Drug Metab Dispos. 2014 Apr;42(4):665-74.

Kolodziejski TR, Safadi BY, Nakanuma Y, Milkes DE, Soetikno RM. Bile duct cysts in a patient with autosomal dominant polycystic kidney disease. Gastrointest Endosc. 2004 Jan;59(1):140-2.

König J, Müller F, Fromm MF. Transporters and drug-drug interactions: important determinants of drug disposition and effects. Pharmacol Rev. 2013 May 17;65(3):944-66.

Koruk M, Ozkilic S, Savas MC, Celen Z, Kadayifci A, Ozkilic C. Evaluation of hepatic functions and biliary dynamics in patients with liver cirrhosis by quantitative scintigraphy. Hepatogastroenterology. 2003 Nov-Dec;50(54):1803-5.

Lazaridis KN, Tietz P, Wu T, Kip S, Dawson PA, LaRusso NF. Alternative splicing of the rat sodium/bile acid transporter changes its cellular localization and transport properties. Proc Natl Acad Sci U S A. 2000 Sep 26; 97(20):11092-7.

Lee Z, Ljungberg M, Muzic RF Jr, Berridge MS. Usefulness and pitfalls of planar gamma-scintigraphy for measuring aerosol deposition in the lungs: a Monte Carlo investigation. J Nucl Med. 2001 Jul;42(7):1077-83.

Lerner ME, Roshkow JE, Smithline A, Ng C. Polycystic liver disease with obstructive jaundice: treatment with ultrasound-guided cyst aspiration. Gastrointest Radiol. 1992 Winter;17(1):46-8.

Leslie EM, Watkins PB, Kim RB, Brouwer KL. Differential inhibition of rat and human Na+-dependent taurocholate cotransporting polypeptide (NTCP/SLC10A1) by bosentan: a mechanism for species differences in hepatotoxicity. J Pharmacol Exp Ther. 2007 Jun;321:1170–8.

Lindell SL, Southard JH, Vreugdenhil P, Belzer FO. Kupffer cells depress hepatocyte protein synthesis on cold storage of the rat liver. Transplantation. 1994 Oct 27;58(8):869-74.

Loomba R, Sirlin CB, Schwimmer JB, Lavine JE. Advances in pediatric nonalcoholic fatty liver disease. Hepatology. 2009 Oct;50(4):1282-93.

Mairinger S, Erker T, Muller M, Langer O. PET and SPECT radiotracers to assess function and expression of ABC transporters in vivo. Curr Drug Metab. 2011 Oct;12(8):774-92.

Mariappan TT, Mandlekar S, Marathe P. Insight into tissue unbound concentration: utility in drug discovery and development. Curr Drug Metab. 2013 Mar;14(3):324-40.

Marion TL, Leslie EM, Brouwer KL Use of sandwich-cultured hepatocytes to evaluate impaired bile acid transport as a mechanism of drug-induced hepatotoxicity. Mol Pharm. 2007 Nov-Dec;4(6):911-8.

Mason SB, Liang Y, Sinders RM, Miller CA, Eggleston-Gulyas T, Crisler-Roberts R, Harris PC, Gattone VH 2nd. Disease stage characterization of hepatorenal fibrocystic pathology in the PCK rat model of ARPKD. Anat Rec (Hoboken). 2010 Aug;293(8):1279-88.

Masyuk TV, Huang BQ, Masyuk AI, Ritman EL, Torres VE, Wang X, Harris PC, Larusso NF. Biliary dysgenesis in the PCK rat, an orthologous model of autosomal recessive polycystic kidney disease. Am J Pathol. 2004 Nov;165(5):1719-30.

Matthews PM, Rabiner EA, Passchier J, and Roger N Gunn. Positron emission tomography molecular imaging for drug development. Br J Clin Pharmacol. 2012 Feb; 73(2): 175–186.

Mennone A, Soroka CJ, Cai SY, Harry K, Adachi M, Hagey L, Schuetz JD, Boyer JL. Mrp4-/- mice have an impaired cytoprotective response in obstructive cholestasis. Hepatology. 2006 May;43(5):1013-21.

Mennone A, Soroka CJ, Cai SY, Harry K, Adachi M, Hagey L, Schuetz JD, Boyer JL. Mrp4-/- mice have an impaired cytoprotective response in obstructive cholestasis. Hepatology. 2006 May;43(5):1013-21.

Milutinovic J, Fialkow PJ, Agodoa LY, Phillips LA, Rudd TG, Sutherland S. Clinical manifestations of autosomal dominant polycystic kidney disease in patients older than 50 years. Am J Kidney Dis. 1990 Mar;15(3):237-43.

Monte MJ, Marin JJ, Antelo A, and Jose Vazquez-Tato J. Bile acids: Chemistry, physiology, and pathophysiology. World J Gastroenterol. 2009 Feb 21; 15(7): 804–816.

Mooij MG, Schwarz UI, de Koning BA, Leeder JS, Gaedigk R, Samsom JN, Spaans E, van Goudoever JB, Tibboel D, Kim RB1, de Wildt SN. Ontogeny of human hepatic and intestinal transporter gene expression during childhood: age matters. Drug Metab Dispos. 2014 Aug;42(8):1268-74.

Morales A, Fernández-Checa JC, García-Ruiz C. Specific contribution of methionine and choline in nutritional nonalcoholic steatohepatitis: impact on mitochondrial S-adenosyl-L-methionine and glutathione. J Biol Chem. 2010 Jun 11;285(24):18528-36.

Morgan DJ, McLean AJ. Clinical pharmacokinetic and pharmacodynamic considerations in patients with liver disease. An update. Clin Pharmacokinet. 1995 Nov;29(5):370-91.

Morgan RE, Trauner M, van Staden CJ, Lee PH, Ramachandran B, Eschenberg M, Afshari CA, Qualls CW Jr, Lightfoot-Dunn R, Hamadeh HK. Interference with bile salt export pump function is a susceptibility factor for human liver injury in drug development. Toxicol Sci. 2010 Dec;118(2):485-500.

Morgan RE, van Staden CJ, Chen Y, Kalyanaraman N, Kalanzi J, Dunn RT 2nd, Afshari CA, Hamadeh HK. A multifactorial approach to hepatobiliary transporter assessment enables improved therapeutic compound development. Toxicol Sci. 2013 Nov;136(1):216-41.

Munoz-Garrido P, Marin JJ, Perugorria MJ, Urribarri AD, Erice O, Sáez E, Úriz M, Sarvide S, Portu A, Concepcion AR, Romero MR, Monte MJ, Santos-Laso Á, Hijona E, Jimenez-Agüero R, Marzioni M, Beuers U, Masyuk TV, LaRusso NF, Prieto J, Bujanda L, Drenth JP, Banales JM. Ursodeoxycholic acid inhibits hepatic cystogenesis in experimental models of polycystic liver disease. J Hepatol. 2015 Oct;63(4):952-61.

Nakahara T, Hyogo H, Kimura Y, Ishitobi T, Arihiro K, Aikata H, Takahashi S, Chayama K. Efficacy of rosuvastatin for the treatment of non-alcoholic steatohepatitis with dyslipidemia: An open-label, pilot study. Hepatol Res. 2012 Nov;42(11):1065-72.

Neuman MG, Voiculescu M, Nanau RM, Maor Y, Melzer E, Cohen LB, Opris M, Malnick S. Non-Alcoholic Steatohepatitis: Clinical and Translational Research. J Pharm Pharm Sci. 2016;19(1):8-24.

Neyt S, Huisman MT, Vanhove C, De Man H, Vliegen M, Moerman L, Dumolyn C, Mannens G, De Vos F. In vivo visualization and quantification of (Disturbed) Oatp-mediated hepatic uptake

and Mrp2-mediated biliary excretion of 99mTc-mebrofenin in mice. J Nucl Med. 2013 Apr;54(4):624-30.

Neyt S, Huisman MT, Vanhove C, De Man H, Vliegen M, Moerman L, Dumolyn C, Mannens G, De Vos F. In vivo visualization and quantification of (Disturbed) Oatp-mediated hepatic uptake and Mrp2-mediated biliary excretion of 99mTc-mebrofenin in mice. J Nucl Med. 2013 Apr;54(4):624-30.

Oi A, Morishita K, Awogi T, Ozaki A, Umezato M, Fujita S, Hosoki E, Morimoto H, Ishiharada N, Ishiyama H, Uesugi T, Miyatake M, Senba T, Shiragiku T, Nakagiri N, Ito N. Nonclinical safety profile of tolvaptan. Cardiovasc. Drugs Ther. 2011, S91–S99.

Ong MMK, Latchoumycandane C, Boelsterli UA. Troglitazone-induced hepatic necrosis in an animal model of silent genetic mitochondrial abnormalities. Toxicol. Sci. 2007 May;97(1), 205–213.

Palatini P, De Martin S. Pharmacokinetic drug interactions in liver disease: An update. World J Gastroenterol. 2016 Jan 21;22(3):1260-78.

Palmeira CM, Rolo AP. Mitochondrially-mediated toxicity of bile acids. Toxicology. 2004 Oct 15;203(1-3):1-15.

Patil DT, Yerian LM. Evolution of nonalcoholic fatty liver disease recurrence after liver transplantation. Liver Transpl. 2012 Oct;18(10):1147-53.

Perez MJ, Briz O. Bile-acid-induced cell injury and protection. World J Gastroenterol. 2009 Apr 14; 15(14): 1677–1689.

Perez MJ, Briz O. Bile-acid-induced cell injury and protection. World J Gastroenterol. 2009 Apr 14;15(14):1677-89.

Peters TS. Do preclinical strategies help predict human hepatotoxic potentials. Toxicol Pathol. 2005;33(1):146-54.

Pfeifer ND, Goss SL, Swift B, Ghibellini G, Ivanovic M, Heizer WD, Gangarosa LM, Brouwer KL. Effect of Ritonavir on (99m)Technetium-Mebrofenin Disposition in Humans: A Semi-PBPK Modeling and In Vitro Approach to Predict Transporter-Mediated DDIs. CPT Pharmacometrics Syst Pharmacol. 2013 Jan 2;2:e20.

Pitcairn, GR, Newman, SP. Tissue attenuation corrections in gamma scintigraphy. J Aerosol Med.1997;3,187-198.

Pou L, Brunet M, Cantarell C, Vidal E, Oppenheimer F, Monforte V, Vilardell J, Roman A, Martorell J, Capdevila L. Mycophenolic acid plasma concentrations: influence of comedication. Ther Drug Monit. 2001 Feb;23(1):35-8.

Radiation Protection Procedures, International atomic Energy Agency, Safety Series, No.38, pp 40-45, 1978.

Rahmim A, Zaidi H. PET versus SPECT: strengths, limitations and challenges. Nucl Med Commun. 2008 Mar;29(3):193-207.

Ringnér M. What is principal component analysis? Nature Biotechnology. 2008 26, 303–304.

Rodighiero V. Effects of liver disease on pharmacokinetics. An update. Clin Pharmacokinet. 1999 Nov;37(5):399-431.

Rodrigues AD, Lai Y, Cvijic ME, Elkin LL, Zvyaga T, Soars MG. Drug-induced perturbations of the bile acid pool, cholestasis, and hepatotoxicity: mechanistic considerations beyond the direct inhibition of the bile salt export pump. Drug Metab Dispos. 2014 Apr;42(4):566-74.

Rolo AP, Oliveira PJ, Moreno AJ, Palmeira CM. Bile acids affect liver mitochondrial bioenergetics: possible relevance for cholestasis therapy. Toxicol Sci. 2000 Sep;57(1):177-85.

Ryan JC, Dunn KW, Decker BS. Effects of chronic kidney disease on liver transport: quantitative intravital microscopy of fluorescein transport in the rat liver. Am J Physiol Regul Integr Comp Physiol. 2014 Dec 15;307(12):R1488-92.

Sager JE, Yu J, Ragueneau-Majlessi I, Isoherranen N. Physiologically Based Pharmacokinetic (PBPK) Modeling and Simulation Approaches: A Systematic Review of Published Models, Applications, and Model Verification. Drug Metab Dispos. 2015 Nov;43(11):1823-37.

Salam M, Keeffe EB. Liver cysts associated with polycystic kidney disease: role of Tc-99m hepatobiliary imaging. Clin Nucl Med. 1989 Nov;14(11):803-7.

Sanyal AJ, Chalasani N, Kowdley KV, McCullough A, Diehl AM, Bass NM, Neuschwander-Tetri BA, Lavine JE, Tonascia J, Unalp A, Van Natta M, Clark J, Brunt EM, Kleiner DE, Hoofnagle JH, Robuck PR; NASH CRN.. Pioglitazone, vitamin E, or placebo for nonalcoholic steatohepatitis. N Engl J Med. 2010 May 6;362(18):1675-85.

Schonhoff CM, Webster CR, Anwer MS. Cyclic AMP stimulates Mrp2 translocation by activating p38{alpha} MAPK in hepatic cells. Am J Physiol Gastrointest Liver Physiol. 2010 May;298(5):G667-74.

Schotland P, Bojunga N, Zien A, Trame MN, Lesko LJ. Improving drug safety with a systems pharmacology approach. Eur J Pharm Sci. 2016 Jun 7.

Sherstha R, McKinley C, Russ P, Scherzinger A, Bronner T, Showalter R, Everson GT. Postmenopausal estrogen therapy selectively stimulates hepatic enlargement in women with autosomal dominant polycystic kidney disease. Hepatology. 1997 Nov;26(5):1282-6.

Shingaki T, Takashima T, Ijuin R, Zhang X, Onoue T, Katayama Y, Okauchi T, Hayashinaka E, Cui Y, Wada Y, Suzuki M, Maeda K, Kusuhara H, Sugiyama Y, Watanabe Y. Evaluation of Oatp and Mrp2 activities in hepatobiliary excretion using newly developed positron emission tomography tracer [11C]dehydropravastatin in rats. J Pharmacol Exp Ther. 2013 Oct;347(1):193-202.

Shoaf SE, Bricmont P, Mallikaarjun S. Effects of CYP3A4 inhibition and induction on the pharmacokinetics and pharmacodynamics of tolvaptan, a non-peptide AVP antagonist in healthy subjects. Br J Clin Pharmacol. 2012 Apr;73(4):579-87.

Shoaf SE, Kim SR, Bricmont P, Mallikaarjun S. Pharmacokinetics and pharmacodynamics of single-dose oral tolvaptan in fasted and non-fasted states in healthy Caucasian and Japanese male subjects. Eur J Clin Pharmacol. 2012 Dec;68(12):1595-603.

Shoda LK, Woodhead JL, Siler SQ, Watkins PB, Howell BA. Linking physiology to toxicity using DILIsym®, a mechanistic mathematical model of drug-induced liver injury. Biopharm Drug Dispos. 2014 Jan;35(1):33-49.

Strelow J, Dewe W, Iversen PW, Brooks HB, Radding JA, McGee J, Weidner J. Mechanism of Action Assays for Enzymes. Advancing Translational Sciences; 2004-.
2012 May 1.

Swift B, Pfeifer ND, Brouwer KL. Sandwich-cultured hepatocytes: an in vitro model to evaluate hepatobiliary transporter-based drug interactions and hepatotoxicity. Drug Metab Rev. 2010 Aug;42(3):446-71.

Swift B, Tian X, Brouwer, KL. Integration of Preclinical and Clinical Data with Pharmacokinetic Modeling and Simulation to Evaluate Fexofenadine as a Probe for Hepatobiliary Transport Function. Pharm Res. 2009 Aug;26(8):1942-51

Swift B, Yue W, Brouwer KL. Evaluation of (99m)technetium-mebrofenin and (99m)technetium-sestamibi as specific probes for hepatic transport protein function in rat and human hepatocytes. Pharm Res. 2010 Sep;27(9):1987-98.

Tabibian JH, Masyuk AI, Masyuk TV, O'Hara SP, LaRusso NF. Physiology of Cholangiocytes. Compr Physiol. 2013 Jan; 3(1): 10.

Takahashi Y, Soejima Y, FukusatoT. Animal models of nonalcoholic fatty liver disease/nonalcoholic steatohepatitis. World J Gastroenterol. 2012 May 21; 18(19): 2300–2308.

Tammara BK, Sekar KS, Brumer SL. The disposition of a single dose of 14C OPC-41061 in healthy male volunteers. 1999 Ann. Meeting Am. Assoc. Pharm. Sci. Abstract 2025.

Testa A, Zanda M, Elmore CS, Sharma P. PET Tracers To Study Clinically Relevant Hepatic Transporters. Mol Pharm. 2015 Jul 6;12(7):2203-16.

Tian X, Li J, Zamek-Gliszczynski MJ, Bridges AS, Zhang P, Patel NJ, Raub TJ, Pollack GM, Brouwer KL. Roles of P-glycoprotein, Bcrp, and Mrp2 in biliary excretion of spiramycin in mice. Antimicrob Agents Chemother. 2007 Sep;51(9):3230-4.

Torres DM, Jones F, Shaw JC, Williams CD, Ward JA, Harrison SA. Rosiglitazone versus rosiglitazone and metformin versus rosiglitazone and losartan in the treatment of nonalcoholic steatohepatitis in humans: a 12-month randomized, prospective, open-label trial. Hepatology. 2011 Nov;54(5):1631-9.

Torres VE, Chapman AB, Devuyst O, Gansevoort RT, Grantham JJ, Higashihara E, Perrone RD, Krasa HB, Ouyang J, Czerwiec FS; TEMPO 3:4 Trial Investigators. Tolvaptan in patients with autosomal dominant polycystic kidney disease. N Engl J Med. 2012 Dec 20;367(25):2407-18.

Trauner M, Arrese M, Soroka CJ, Ananthanarayanan M, Koeppel TA, Schlosser SF, Suchy FJ, Keppler D, Boyer JL. The rat canalicular conjugate export pump (Mrp2) is down-regulated in intrahepatic and obstructive cholestasis. Gastroenterology. 1997 Jul;113(1):255-64.

Trottier J, Caron P, Straka RJ, Barbier O. Profile of serum bile acids in noncholestatic volunteers: gender-related differences in response to fenofibrate. Clin Pharmacol Ther. 2011;90:279–86.

Wang X, Gattone V 2nd, Harris PC, Torres VE. Effectiveness of vasopressin V2 receptor antagonists OPC-31260 and OPC-41061 on polycystic kidney disease development in the PCK rat. J Am Soc Nephrol. 2005 Apr;16(4):846-51.

Watkins PB, Lewis JH, Kaplowitz N, Alpers DH, Blais JD, Smotzer DM, Krasa H, Ouyang J, Torres VE, Czerwiec FS, Zimmer CA. Clinical Pattern of Tolvaptan-Associated Liver Injury in Subjects with Autosomal Dominant Polycystic Kidney Disease: Analysis of Clinical Trials Database. Drug Saf. 2015 Nov;38(11):1103-13.

Watkins PB. Idiosyncratic liver injury: challenges and approaches. Toxicologic pathology. 2005;33:1–5.

Woodhead JL, William J. Brock WJ, Roth SE, Shoaf SE, Brouwer KLR, Church R, Grammatopoulos TN, Stiles L, Siler SQ, Brett A. BA, Merrie M, Watkins PB, Shoda LKM. Application of a Mechanistic Model to Evaluate Putative Mechanisms of Tolvaptan Drug-Induced Liver Injury and Identify Patient Susceptibility Factors. Tox Sci. 2016 Sept 21.

Wu Y, Beland FA, Chen S, Liu F, Guo L, Fang JL. Mechanisms of tolvaptan-induced toxicity in HepG2 cells. Biochem Pharmacol. 2015 Jun 15;95(4):324-36.

Yang K, Pfeifer ND, Köck K, Brouwer KL. Species differences in hepatobiliary disposition of taurocholic acid in human and rat sandwich-cultured hepatocytes: implications for drug-induced liver injury. J Pharmacol Exp Ther. 2015 May;353(2):415-23.

Yang K, Woodhead JL, Watkins PB, Howell BA, Brouwer KL. Systems pharmacology modeling predicts delayed presentation and species differences in bile acid-mediated troglitazone hepatotoxicity. Clin Pharmacol Ther. 2014 Nov;96(5):589-98.

Younossi ZM, Koenig AB, Abdelatif D, Fazel Y, Henry L, Wymer M. Global epidemiology of nonalcoholic fatty liver disease-Meta-analytic assessment of prevalence, incidence, and outcomes. Hepatology. 2016 Jul;64(1):73-84.

Zamek-Gliszczynski MJ, Xiong H, Patel NJ, Turncliff RZ, Pollack GM, Brouwer KL. Pharmacokinetics of 5 (and 6)-carboxy-2',7'-dichlorofluorescein and its diacetate promoiety in the liver. J Pharmacol Exp Ther. 2003 Feb;304(2):801-9.

Zhao S, Iyengar R. Systems pharmacology: network analysis to identify multiscale mechanisms of drug action. Annu Rev Pharmacol Toxicol. 2012;52:505-21.

APPENDIX

Data Appendix

Appendix Table 2.1 Individual blood concentrations of MEB in healthy subjects (n=14) or patients with NASH (n=7)

	Subject ID (Healthy Subjects)													
	1	2	3	4	5	6	7	8	9	10	11	12	13	14
Time (min)	Concentration (nCi/mL)													
2.5	116	95.3	94.3	83.1	174	42	180	142	145	178	145	105	131	66.1
5.0	82.7	101	110	96.1	161	149	129	106	70.2	120	79.2	48.2	88.8	112
7.5	53.2	89.3	76.1	102	104	115	75.7	82.9	46.8	61.8	52.1	31.3	60.7	85.7
10	40.4	50.9	47.7	59.4	69.6	86.3	47.3	58.5	26.2	39.7	31.9	18.6	36.2	62.7
15	29.9	28.1	19.4	15.3	32.3	46.8	25.6	32.6	9.87	16.7	15.2	8.34	14.3	25.8

20	19.3	14.2	11.6	11.7	21.9	31.3	14.5	21.5	7.77	10.2	11.3	4.57	10.1	13.1
40	7.18	6.71	3.94	6.32	7.69	11.1	4.33	6.63	3.04	3.6	4.24	2.08	3.72	5.36
60	4.38	3.67	2.57	3.96	3.94	6.68	2.42	4.25	2.19	2.97	2.72	1.59	2.89	2.62
80	4.39	2.73	2.1	3.04	2.77	5.04	1.95	2.75	1.7	2.22	2	1.12	2.46	2.37
100	3.67	2.66	1.71	2.55	2.25	3.89	1.47	2.32	1.55	2.07	1.65	0.968	1.75	2.4
120	3.51	2.56	1.27	2.85	1.92	3.1	1.49	2.17	1.36	1.76	1.53	0.789	1.53	2.2
140	3.53	2.1	1.19	2.85	1.87	3.11	1.17	2.01	1.19	1.84	1.53	0.688	1.48	2.32
160	4.16	1.64	1.15	2.57	1.6	2.78	1.06	1.76	1.14	1.58	1.36	0.628	1.27	2.09
180	2.91	1.45	1.02	2.3	1.5	2.21	1.09	1.53	1.01	1.46	1.4	0.577	1.23	1.87
210	3.18	1.71	1.1	2.71	1.21	1.79	0.871	1.68	1.21	1.49	1.5	0.567	1.07	1.76
240	1.76	1.61	0.595	2.77	1.22	1.91	0.729	1.36	1	1.46	1.62	0.535	1.04	1.71
270	2.08	1.62	0.82	2.78	1.06	2.01	0.723	1.34	0.898	1.4	1.56	0.488	0.963	1.7
300	2.17	1.54	0.863	2.79	1.07	1.88	0.629	1.26	0.932	1.37	1.6	0.464	0.944	1.55

	Subject ID (NASH)						
	1	2	3	4	5	6	7
Time (min)	Concentration (nCi/mL)						
2.5	287	286	141	210	226	318	314
5.0	196	151	105	155	159	213	145
7.5	142	79.3	54.1	78.3	93.1	131	84.9
10	95.5	51.3	37.7	44.2	73.0	76.6	46.7
15	54.2	22.7	19.9	18.3	34.9	39.6	22.4
20	36.8	12.6	13.4	10.9	20.7	22.2	12.7
40	16.6	5.10	4.93	5.13	10.0	8.44	6.14
60	12.6	3.84	3.23	3.60	6.14	4.90	3.77
80	9.48	3.30	2.46	3.45	5.11	3.52	3.16
100	8.68	2.88	1.87	2.97	4.23	3.33	2.62

120	7.82	2.73	1.94	2.02	3.98	2.61	2.36
140	8.18	2.60	1.59	2.67	3.52	2.25	2.26
160	6.49	2.51	1.55	2.22	3.22	1.99	2.13
180	7.60	2.50	1.35	2.53	2.72	1.96	1.93
210	6.84	2.19	1.57	2.72	2.63	1.75	1.70
240	6.83	2.07	1.43	2.50	2.51	1.84	1.61
270	6.37	2.06	1.37	1.90	2.33	1.59	1.50
300	6.14	1.98	1.40	2.30	2.33	1.54	1.48

Appendix Table 2.2 Liver activity counts of MEB in healthy subjects (n=14) or patients with NASH (n=7)

	Subject ID (Healthy Subjects)													
	1	2	3	4	5	6	7	8	9	10	11	12	13	14
Time (min)	Liver Activity (counts/s)													
1	1420	2480	2360	543	555	482	370	540	666	1380	1380	1470	550	772
2	3180	5450	5800	3390	4510	2350	2900	2690	3320	4770	4840	5160	3690	3820
3	3890	6920	7890	5760	6680	3840	4470	4120	5080	6770	6910	7350	5600	5580
4	4500	7830	9360	7180	7980	4820	5490	5110	6300	8070	8160	8810	6860	6540
5	4980	8310	10500	8290	9100	5600	6450	5970	7360	9020	8980	9980	7820	7520
6	5350	8570	11300	9030	10100	6190	7120	6470	7970	9880	9840	10900	8370	8290
7	5640	8760	12000	9410	10900	6630	7520	7450	9180	10400	10100	11700	8820	8690
8	5940	8630	12500	9610	11600	7010	7540	7920	9760	10900	10700	12100	8990	8600
9	6100	8700	12300	9810	11900	7330	8240	8140	10000	11100	10500	12500	9320	8660

10	6300	8430	13300	10200	12300	7600	8440	8340	10300	11300	10600	12300	9430	8900
11	6440	8170	13300	10500	12800	7750	8690	8550	10500	11500	10400	12100	9360	8960
12	6610	7930	13400	10600	13100	7840	8690	8730	10800	11800	10900	12500	8890	8460
13	6650	7660	12100	10800	13300	7870	8650	8510	10500	11700	10600	12600	9080	8280
14	6730	7360	11600	10700	13500	7770	8830	8900	11000	11600	10600	12200	8550	8240
15	6790	6940	12200	10300	13500	7800	8900	9020	11100	11700	10600	12400	8610	8250
16	6800	6660	12100	9980	12800	7760	8670	8990	11100	11500	9860	12200	8320	8050
17	6760	6290	12100	9300	13500	7620	8000	8980	11100	11400	9720	11800	8010	7870
18	6750	6020	12200	8750	12800	7520	8510	8820	10900	11200	9330	12000	7840	7600
19	6720	5700	11100	8160	11700	7490	8400	8770	10800	10900	9010	10600	7440	7230
20	6710	5470	11400	7700	11500	7290	7810	8680	10700	10900	8700	10200	7300	6780
21	6710	5180	10800	7090	10500	7190	7700	8440	10400	10600	8310	10400	6990	6690
22	6700	4910	9830	6600	10800	7050	7170	8380	10300	10400	8020	9970	6610	6400

23	6580	4500	9020	5980	10400	6790	6600	7310	9000	10200	7690	9830	6440	6170
24	6470	4280	8880	6090	11000	6680	7170	7710	9500	10000	7380	9540	6150	5890
25	6380	4070	8170	6160	10900	6540	6920	7110	8760	9840	7080	7790	5850	5720
26	6340	3790	7320	5510	10800	6470	6800	6950	8570	9570	6950	7610	5650	5530
27	6470	3570	7030	5100	10300	6250	6460	6760	8340	8960	6640	7350	5450	5050
28	6200	3460	6560	4750	10900	6130	6320	6590	8120	7970	6520	7020	5230	4350
29	6040	3210	6180	5110	9430	5930	5990	7070	8720	8460	6170	6800	5080	4470
30	5870	3020	5830	4880	10200	5850	5390	6490	8000	8340	6090	6270	4870	4250
31	5740	2830	6000	4590	10000	5680	5360	5780	7120	7410	5940	5980	4720	3930
32	5640	2700	5390	4670	9390	5530	5410	5910	7280	7750	5580	5780	4590	3890
33	5500	2570	5450	4420	8960	5330	5180	5680	7000	7510	5320	5460	4470	3730
34	5490	2410	5140	4230	9090	5100	5120	5610	6910	7250	5220	4730	4310	3610
35	5380	2290	4820	3920	7990	4970	5050	5600	6900	7030	4890	4330	4150	3670

36	5230	2170	4530	3820	7700	4790	4680	5320	6560	6740	4590	3310	4080	3520
37	5140	2060	4320	3580	7490	4670	4510	4910	6050	6590	4310	3400	3960	3580
38	5050	1950	4230	3650	7120	4560	4430	4730	5830	6270	4250	3250	3850	3370
39	4860	1880	3800	3460	6780	4400	4160	4690	5780	6060	3990	3380	3690	3090
40	4570	1750	3740	3310	6390	4260	4150	4530	5580	5840	3530	3170	3610	3110
41	4570	1640	3500	3310	5970	4120	3960	4430	5460	5510	3470	3100	3500	3170
42	4460	1610	3460	3130	5900	3950	3990	4460	5500	5460	3200	3110	3370	3110
43	4260	1510	2980	3030	5540	3850	3830	4220	5200	5070	3270	2910	3330	2850
44	4020	1450	2850	3030	4860	3770	3440	3680	4530	4970	3040	2820	3200	2530
45	3840	1390	2530	2850	4960	3650	3380	3890	4800	4930	2790	2710	3180	2810
46	3710	1320	2290	2830	5060	3520	3220	3320	4090	4750	2590	2630	3040	2520
47	3530	1270	2480	2720	5190	3330	3230	3700	4560	4580	2540	2400	3020	2590
48	3310	1210	2330	2600	4690	2880	3060	3520	4340	4290	2590	2280	2940	2670

49	3130	1160	2220	2540	4420	3000	3020	3400	4190	4290	2480	2230	2760	2660
50	3040	1070	2150	2490	4150	2970	2920	3300	4070	4120	2380	2140	2810	2610
51	2890	1070	2090	2480	3880	2890	2960	3190	3930	3800	2260	2060	2640	2580
52	2760	999	2020	2370	3890	2820	2910	3050	3760	3730	2140	2030	2680	2350
53	2690	920	1880	2320	3680	2710	2740	3010	3700	3690	2030	1990	2570	2330
54	2590	940	1850	2250	3570	2630	2740	2940	3630	3260	1970	1960	2470	2210
55	2520	923	1810	2160	3320	2550	2500	2760	3400	3410	1870	1860	2420	2040
56	2410	857	1700	2050	3110	2470	2260	2640	3250	3430	1790	1840	2360	1960
57	2380	879	1670	2100	2750	2410	2160	2630	3250	3360	1680	1770	2300	1910
58	2300	867	1600	2000	2600	2330	2060	2580	3180	3190	1660	1720	2270	1870
59	2240	816	1570	1900	2590	2290	2030	2540	3140	3110	1570	1630	2200	1810
60	2210	800	1530	1820	2250	2200	1640	2410	2970	2910	1480	1540	2180	1930
61	2130	762	1520	1740	2280	2130	1570	2430	2990	2830	1510	1510	2110	1810

62	2080	742	1430	1720	2120	2030	1560	2410	2980	2670	1450	1500	2040	1760
63	2000	689	1330	1730	2210	1980	1390	2240	2770	2840	1380	1410	2020	1800
64	1990	679	1280	1810	1910	1900	1440	2180	2680	2540	1290	1350	1820	1650
65	1900	700	1260	1860	2020	1800	1370	1880	2320	2570	1180	1480	1860	1570
66	1890	701	1320	1940	1820	1740	1450	1800	2220	2480	1240	1490	1800	1560
67	1850	653	1220	1730	1870	1670	1440	1720	2120	2400	1180	1480	1790	1510
68	1810	664	1110	1770	1850	1620	1340	1690	2080	2290	1190	1040	1670	1510
69	1690	617	1080	1570	1470	1590	1320	1630	2010	2190	995	1220	1650	1380
70	1590	660	1070	1450	1840	1510	1320	1610	1980	2190	1000	1140	1680	1340
71	1650	626	1040	1440	1530	1450	1370	1630	2010	2150	955	1110	1660	1350
72	1630	590	1020	1470	1390	1430	1290	1590	1960	2070	877	1050	1580	1260
73	1580	576	995	1390	1430	1410	1330	1550	1910	2000	843	1040	1510	1250
74	1570	575	947	1330	1220	1360	1310	1480	1830	1970	854	1030	1520	1170

75	1550	578	928	1400	1390	1340	1320	1390	1720	1910	799	984	1450	1180
76	1510	567	918	1270	1220	1300	1350	1330	1640	1800	789	968	1460	1190
77	1460	567	825	1260	1210	1240	1300	1430	1760	1700	784	963	1410	1240
78	1410	598	840	1300	1300	1190	1280	1430	1770	1620	761	969	1380	1130
79	1420	569	785	1290	1250	1150	1230	1460	1800	1580	774	817	1370	1040
80	1340	577	825	1310	1360	1140	1030	1450	1790	1510	835	1050	1350	972
81	1320	625	784	1140	1240	1070	1070	1430	1760	1510	729	1120	1300	970
82	1250	711	779	614	1140	1070	1050	1430	1760	1490	674	1070	1270	980
83	1280	718	751	604	1110	1050	1170	1340	1650	1470	656	1010	1350	889
84	1260	736	747	640	1090	992	1030	1240	1530	1340	711	1030	1310	889
85	1250	710	671	587	1050	959	1000	1220	1510	1270	673	951	1200	846
86	1230	700	704	569	1270	938	1020	1260	1550	1340	636	858	1170	861
87	1160	766	671	536	1010	869	994	1300	1610	1360	661	789	1220	715

88	1130	758	590	513	1040	854	1040	1070	1320	1360	647	765	1180	694
89	1090	768	588	530	1100	845	1050	1230	1510	1270	660	725	1120	582
90	1070	753	576	529	1060	819	1020	1300	1610	1230	620	750	1140	698
91	1040	783	570	536	1090	810	897	1240	1530	1220	603	715	1080	678
92	994	748	526	532	920	795	946	1160	1430	1160	616	706	1160	721
93	1000	797	557	530	949	768	978	1100	1360	1140	589	801	1070	595
94	949	777	534	457	807	750	970	1150	1420	1120	593	777	1030	591
95	929	796	548	390	960	741	1000	1080	1330	1140	576	755	1020	641
96	892	791	514	525	788	704	963	1150	1420	1110	588	729	986	606
97	884	795	501	531	875	659	937	1130	1390	1140	583	726	1020	499
98	852	781	509	495	774	660	961	1060	1300	1100	550	689	1010	451
99	865	820	518	431	822	632	773	1080	1330	1070	570	662	982	412
100	821	828	533	415	886	617	805	1110	1360	1040	555	636	962	445

101	786	814	528	375	817	586	879	1060	1310	1000	631	654	955	432
102	756	884	557	391	762	581	925	986	1220	1010	594	591	911	312
103	723	850	558	392	776	542	802	848	1050	999	588	493	921	359
104	682	880	523	307	799	552	790	819	1010	992	582	502	883	376
105	678	872	535	337	791	534	800	815	1000	971	594	498	889	339
106	659	895	483	349	781	513	840	831	1020	952	518	496	882	389
107	655	950	497	377	767	492	843	779	960	918	530	483	874	382
108	616	963	452	373	773	492	808	780	961	907	569	455	876	354
109	611	980	451	330	782	485	840	781	963	870	557	453	876	442
110	578	974	453	345	684	464	850	745	918	874	545	451	887	373
111	579	1010	479	333	767	459	828	719	886	930	549	462	863	340
112	574	989	408	288	732	486	806	749	923	920	560	450	881	356
113	568	984	383	290	714	457	776	723	891	857	572	460	826	364

114	554	1020	420	298	657	433	825	768	946	839	551	487	866	381
115	523	1020	434	268	650	433	730	799	984	812	534	490	839	398
116	481	999	391	270	587	436	807	748	922	817	421	491	804	424
117	523	1010	443	294	638	416	814	704	868	783	376	447	807	78.9
118	517	1030	439	306	637	430	780	715	881	777	388	472	803	0.439
119	527	1010	416	296	578	398	794	709	873	783	374	453	792	0.314
120	491	1040	381	270	533	402	737	736	907	799	440	437	806	507
121	478	1040	384	258	463	385	692	773	953	755	388	419	782	1100
122	490	1010	386	248	503	379	863	834	1030	756	359	441	792	1130
123	464	1040	368	231	430	372	660	874	1080	693	319	443	779	1080
124	467	1040	369	217	469	362	836	780	961	713	315	426	792	1020
125	476	1030	339	237	497	367	792	885	1090	701	289	424	794	1020
126	474	982	352	219	491	342	836	770	949	717	328	412	773	1060

127	467	1030	341	220	489	335	846	781	962	729	345	411	810	1060
128	454	1010	305	267	461	352	820	902	1110	709	325	413	785	1060
129	457	1040	299	233	432	334	808	880	1080	671	288	382	811	1040
130	442	1000	272	218	396	320	752	956	1180	635	317	395	790	951
131	444	1010	344	218	486	312	792	904	1110	626	360	372	786	1030
132	447	987	331	185	450	330	815	670	826	640	386	367	772	989
133	455	984	314	182	388	320	694	582	717	625	393	393	742	955
134	436	924	301	183	449	324	833	572	704	677	326	377	799	1010
135	448	926	324	185	461	309	785	628	774	695	421	375	786	1010
136	450	950	311	188	318	312	728	609	750	688	381	365	762	1060
137	430	957	291	181	412	303	891	792	976	658	405	368	749	907
138	427	952	281	218	317	296	843	678	835	665	398	364	750	897
139	405	930	308	186	305	281	819	703	866	653	393	388	732	837

140	405	957	310	199	300	264	683	796	981	674	367	337	767	855
141	370	928	278	192	343	267	619	809	997	678	368	287	773	902
142	432	932	262	199	327	259	575	733	904	636	377	136	727	745
143	422	832	255	210	334	265	672	683	842	676	337	216	734	678
144	405	869	261	216	384	260	648	868	1070	670	303	285	724	702
145	388	868	244	210	443	271	613	814	1000	643	349	319	753	670
146	389	883	228	211	394	247	577	817	1010	680	324	264	733	651
147	379	896	210	203	382	270	609	719	886	576	312	215	713	711
148	384	891	184	183	405	260	686	748	922	631	288	407	755	758
149	351	917	185	190	406	253	682	758	934	636	297	409	740	780
150	379	906	192	184	424	258	585	644	793	673	267	418	724	784
151	378	946	184	165	480	258	575	606	747	679	274	385	710	811
152	388	908	201	155	459	263	593	602	742	707	277	355	704	750

153	381	885	200	150	472	245	545	677	834	630	271	358	711	760
154	363	853	169	172	368	240	521	783	965	658	265	370	679	726
155	359	874	179	144	364	251	508	677	835	672	262	378	705	725
156	357	920	177	137	418	225	447	704	867	639	244	370	669	620
157	377	911	168	140	424	239	493	799	985	695	252	373	561	475
158	352	882	182	144	415	245	510	882	1090	696	276	374	608	432
159	355	903	168	143	388	232	503	921	1130	693	267	377	629	487
160	341	865	171	153	374	221	498	1010	1240	659	263	324	591	466
161	334	897	167	145	360	226	520	846	1040	644	270	321	639	451
162	337	924	178	138	435	226	516	670	826	630	249	326	677	445
163	309	877	180	128	441	201	603	636	784	640	283	311	605	384
164	320	890	184	140	412	206	559	643	792	718	243	303	538	456
165	316	869	184	160	422	218	527	716	882	697	238	316	495	477

166	314	857	165	151	400	227	571	696	858	674	273	317	481	464
167	312	866	187	140	375	220	553	694	855	644	280	332	467	417
168	310	842	164	152	454	221	528	742	914	635	259	338	444	452
169	302	836	160	147	494	222	560	750	924	632	267	329	447	460
170	307	848	162	146	393	225	553	809	997	597	249	321	402	454
171	299	851	172	141	465	210	489	910	1120	624	254	319	384	378
172	300	858	138	153	456	203	551	885	1090	629	248	352	441	374
173	315	828	158	148	437	206	446	942	1160	645	236	332	492	365
174	303	852	154	142	454	214	567	897	1110	641	216	310	582	326
175	310	820	152	140	451	206	561	901	1110	599	241	201	582	518
176	306	807	146	145	483	200	546	785	967	708	227	265	554	641
177	275	798	144	122	440	213	542	904	1110	719	199	202	458	519
178	301	801	134	100	440	212	574	902	1110	680	182	264	429	361

179	288	782	138	101	457	215	546	809	997	684	177	236	472	343
180	294	773	132	110	445	206	509	874	1080	650	167	206	461	420

	Subject ID (NASH)						
	1	2	3	4	5	6	7
Time (min)	Liver Activity (counts/s)						
1	1430	2210	2830	815	1980	138	1180
2	4850	7850	9270	8680	4470	2320	6400
3	6680	11000	13000	13900	5830	4950	10400
4	7640	13300	16000	17100	6920	6410	12800
5	8600	15100	18200	19500	7610	7370	14600
6	9480	16400	19600	20800	8460	8110	15800
7	9900	17600	20600	22100	9000	8620	16600
8	10400	18400	20900	23400	9500	9020	17800

9	11100	18900	21500	23800	9150	9210	18700
10	11200	19400	21700	24300	8830	9610	19200
11	11600	19700	21400	24300	9460	9400	19200
12	12000	19700	20800	24300	9280	9320	19100
13	12200	19700	19600	24400	9410	9310	20100
14	12400	19800	18800	24400	8840	9360	20000
15	12500	19400	17600	24000	9800	9070	19600
16	12500	19300	17400	23700	9720	9130	19700
17	12600	18900	16900	23400	9040	8770	19600
18	12600	18900	16000	23200	8840	8630	19600
19	12700	18500	15300	22700	8660	8510	18900
20	12500	18200	14600	22300	8480	8320	18400
21	12800	17800	13900	22000	8780	8440	18000

22	12600	17300	13100	21500	7520	7900	17500
23	12600	17100	12500	20900	7280	7500	16900
24	12600	16600	12000	20400	7520	7290	16300
25	12400	16200	11300	19900	7940	6910	16200
26	12300	15900	10800	19300	7700	6840	15700
27	12200	15300	10300	18900	6660	6350	15000
28	12100	15000	9770	18400	6760	6140	14500
29	12000	14600	9340	18000	6470	6120	14500
30	11800	14100	8940	17400	4780	5930	13900
31	11700	13600	8720	16700	4530	5820	13400
32	11600	13200	8460	16300	4050	5580	13000
33	11300	12800	8040	15300	3840	5290	13500
34	11200	12400	7740	15000	3370	5160	12800

35	10900	12000	7620	15000	4060	4920	12900
36	10800	11700	7250	14500	3610	4800	12300
37	10800	11400	6990	14200	3590	4620	11800
38	10600	11000	6870	13600	3210	4500	11200
39	10600	10500	6540	12900	2820	4240	10800
40	10500	10300	6380	12800	2660	4000	10400
41	10300	10000	6170	12400	2950	3940	9990
42	10100	9820	6070	11700	3040	3800	9500
43	10100	9420	5900	11600	3380	3800	9300
44	9950	9020	5580	11100	3440	3700	8890
45	9700	8740	5330	10600	2810	3630	8600
46	9630	8520	5110	9930	3190	3600	8380
47	9580	8200	4920	9990	2960	3480	8030

48	9420	7920	4880	9760	2750	3400	7730
49	9380	7620	4670	9380	2810	3300	7860
50	9130	7350	4390	9030	2500	3200	7700
51	9130	7220	4290	8830	2730	3170	7260
52	8980	7100	4200	8550	2500	3070	6660
53	8810	7000	4200	8320	2850	3010	5950
54	8850	6630	3970	7720	2880	2900	5480
55	8620	6470	3690	7560	2920	2840	5290
56	8560	6220	3760	6950	2960	2780	5120
57	8360	5920	3700	6600	2950	2660	4950
58	8320	5910	3610	6360	2530	2640	4850
59	8280	5660	3520	6470	2370	2440	4780
60	8060	5500	3330	6020	1980	2390	4880

61	7980	5320	3280	6010	1840	2200	4880
62	7860	5180	3200	5690	2120	2250	4780
63	7750	4920	3260	5520	1700	2350	4120
64	7680	4840	3150	5220	1630	2070	4520
65	7660	4700	3010	5020	1900	2150	4320
66	7490	4640	2960	4960	2180	2170	4170
67	7380	4420	2750	4880	2160	2170	4010
68	7380	4340	2830	4700	2200	2110	3810
69	7110	4270	2570	4620	2140	2020	3780
70	7120	4190	2550	4360	2100	2050	3810
71	6880	3940	2520	4240	1860	1850	3860
72	6960	3990	2480	4160	2000	1700	3500
73	6790	4120	2530	3950	1940	1820	3330

74	6700	4010	2570	3830	2070	1780	3260
75	6710	3970	2370	3790	2350	1780	3280
76	6600	3880	2340	3750	2190	1780	3200
77	6390	3830	2150	3580	2250	1800	3240
78	6260	3710	2220	3490	2420	1800	3030
79	6320	3640	2090	3390	2210	1760	2890
80	6140	3490	2120	3350	2490	1710	2560
81	6130	3300	2000	3150	2320	1620	2560
82	6060	3390	1900	3070	2480	1350	2530
83	5980	3320	1860	3010	2180	1440	2490
84	5900	3200	1820	3030	2360	1410	2390
85	5820	3090	1780	2800	2290	1460	2310
86	5620	3070	1830	2720	2210	1470	2390

87	5670	3060	1730	2560	2220	1420	2150
88	5520	2980	1740	2610	2100	1400	2090
89	5530	2790	1740	2470	2110	1320	2180
90	5480	2790	1540	2480	1960	1360	2210
91	5310	2660	1520	2390	1800	1340	2250
92	5240	2620	1590	2380	1910	1310	2220
93	5080	2890	1500	2450	1890	1280	2250
94	5100	2930	1530	2270	1970	1490	2100
95	5140	2730	1470	2260	1890	1600	1770
96	4900	2720	1480	2110	1400	1580	1950
97	5020	2520	1490	1970	1700	1580	1930
98	4870	2380	1360	1960	1600	1630	1970
99	4770	2510	1380	1960	1630	1580	2030

100	4720	2490	1530	1840	1610	1620	1920
101	4700	2450	1380	1810	1560	1610	1960
102	4700	2380	1310	1820	1770	1630	1720
103	4550	2310	1340	1790	1690	1570	1750
104	4470	2260	1320	1710	1520	1600	1740
105	4400	2240	1240	1680	1540	1610	1680
106	4320	2110	1360	1610	1480	1570	1580
107	4150	2160	1420	1700	1440	1640	1550
108	4230	2220	1290	1610	1330	1620	1560
109	3980	2330	1300	1680	1520	1630	1510
110	4020	2030	1380	1580	1400	1590	1650
111	3990	2020	1270	1670	1550	1610	1580
112	3890	1920	1260	1510	1510	1620	1490

113	3880	2030	1220	1500	1540	1680	1390
114	3770	2020	1180	1500	1540	1630	1380
115	3600	1920	1230	1470	1560	1660	1500
116	3490	1810	1250	1490	1600	1600	1500
117	3510	1720	1220	1520	1710	1600	1600
118	3360	1670	1170	1500	1690	1590	1650
119	3370	1640	1170	1540	1590	1630	1700
120	3310	1580	1240	1340	1430	1620	1790
121	3140	1530	1180	1320	1380	1660	1890
122	3070	1500	1220	1230	1560	1730	1740
123	3090	1500	1250	1150	1700	1730	1740
124	3000	1470	1210	1200	1580	1660	1790
125	2920	1480	1150	1230	1220	1690	1800

126	2960	1600	1180	1110	1540	1680	1470
127	2920	1480	1280	1290	1520	1700	1600
128	2900	1320	1210	1260	1450	1660	1690
129	2730	1140	1280	1170	1580	1690	1480
130	2630	1010	1250	1160	1600	1700	1560
131	2610	1170	1300	1180	1220	1690	1420
132	2630	1220	1070	1140	1340	1660	1460
133	2510	1190	1250	1130	1510	1600	1460
134	2480	1140	1120	1130	1420	1650	1560
135	2390	1150	1000	1130	1450	1610	1560
136	2400	1240	1230	1210	1580	1620	1430
137	2300	1220	1270	1210	1420	1640	1450
138	2220	1190	1250	1250	1370	1660	1520

139	2290	1170	1210	1090	1370	1640	1390
140	2120	1230	1190	1080	1270	1650	1460
141	2090	1170	1220	1070	1320	1610	1470
142	2040	1150	1180	1010	1310	1590	1360
143	2050	1050	1210	1040	1340	1590	1320
144	2000	1120	1180	1050	1280	1650	1460
145	2030	1200	1290	1090	1300	1610	1500
146	1980	995	1190	1100	1260	1590	1570
147	1990	1020	1240	1120	1290	1570	1470
148	1890	1010	1080	1030	1950	1590	1350
149	1960	1080	1160	999	1930	1630	1210
150	1860	1070	1180	1020	1620	1640	1320
151	1830	1050	1180	932	1850	1630	1320

152	1830	997	1150	954	1830	1600	1220
153	1820	1020	1120	948	1750	1700	1320
154	1790	978	1200	1040	1810	1630	1340
155	1650	982	1190	973	1310	1670	1460
156	1780	931	1070	1010	1600	1700	1360
157	1660	923	1020	1000	1530	1720	1430
158	1610	915	1120	942	1480	1660	1150
159	1690	960	1030	921	1630	1690	1170
160	1680	942	1180	888	1780	1730	1210
161	1610	1030	1070	866	1610	1760	1270
162	1680	878	1040	916	1740	1640	1270
163	1630	1280	1110	896	1600	1710	1200
164	1630	1140	1230	852	1350	1650	1130

165	1590	710	1260	783	1650	1610	1170
166	1620	780	1230	858	1580	1650	1090
167	1580	749	1180	776	1380	1610	1230
168	1580	810	1120	789	1330	1550	1220
169	1530	737	1100	751	1160	1700	1220
170	1530	775	1060	805	1780	1750	1160
171	1550	937	1100	770	1700	1800	1090
172	1590	932	1160	723	1650	1720	1130
173	1550	869	1150	728	1880	1680	1170
174	1560	898	1080	687	1780	1640	1430
175	1490	993	1270	636	1750	1650	1050
176	1490	957	1020	679	1620	1510	1110
177	1470	917	1100	678	1560	1410	1120

178	1460	1030	1260	692	1480	1330	1040
179	1390	995	1190	675	1480	1290	1060
180	1280	832	1240	584	1360	1230	959

Data are not corrected for administered dose

Appendix Table 2.3 Blood Pharmacokinetics

Cohort	Subject	$Lamda_z$ (1/min)	T_{max} (min)	C_{max} (nCi/mL)	$AUC_{0\rightarrow last}$ (nCi*min/mL)	$AUC_{0\rightarrow\infty}$ (nCi*min/mL)	CL_{blood} (mL/min/kg)	f_u
Healthy	1	192	2.5	116	2070	2670	17.1	0.096
	2	276	5	101	1840	2460	16.7	0.0595
	3	195	5	110	1480	1720	15.5	0.117
	4	210	7.5	102	1940	2780	12.8	0.0722
	5	180	2.5	174	2340	2620	11.0	0.0384
	6	192	5	131	2300	2760	11.9	0.0988
	7	156	2.5	180	1790	1930	16.7	0.047
	8	226	2.5	142	2060	2470	14.0	0.0541
	9	302	2.5	145	1240	1650	19.1	0.0734
	10	380	2.5	178	1730	2480	17.6	0.0253
	11	278	2.5	145	1500	2140	16.8	0.0281
	12	215	2.5	118	937	1100	27.5	0.0715
	13	223	2.5	131	1440	1750	24.4	0.0347
	14	321	5	112	1770	2480	12.5	0.115

Cohort	Subject	$Lamda_z$ (1/min)	T_{max} (min)	C_{max} (nCi/mL)	$AUC_{0\rightarrow last}$ (nCi*min/mL)	$AUC_{0\rightarrow\infty}$ (nCi*min/mL)	CL_{blood} (mL/min/kg)	f_u
NASH	1	458	2.5	287	4870	8930	2.4	0.149
	2	357	2.5	286	2440	3460	5.59	0.113
	3	460	2.5	141	1660	2600	7.92	0.0425
	4	368	2.5	210	2240	3460	8.00	0.108
	5	219	2.5	226	2910	3640	6.54	0.0845
	6	212	2.5	318	3120	3590	8.42	0.0515
	7	232	2.5	314	2410	2910	10.3	0.0499

Appendix Table 2.4 Urine Pharmacokinetics

Cohort	Subject	Urinary excretion (μCi)	Urinary excretion (% of dose)	CL_{renal} (mL/min/kg)
Healthy	1	19.9	0.923	0.236
	2	20.8	0.831	0.206
	3	16.7	0.690	0.133
	4	19.4	0.806	0.177
	5	15.7	0.603	0.0787
	6	19.7	0.811	0.127
	7	12.0	0.514	0.0978
	8	13.4	0.549	0.101
	9	13.8	0.567	0.159
	10	6.91	0.274	0.0771
	11	7.60	0.299	0.0818
	12	7.10	0.292	0.102
	13	16.8	0.586	0.189
	14	5.10	0.200	0.0397
NASH	1	31.1	1.56	0.0823
	2	13.4	0.535	0.0474
	3	21.6	0.884	0.122
	4	15.3	0.564	0.0816
	5	26.3	1.06	0.0988
	6	17.5	0.663	0.0718
	7	18.5	0.681	0.0941

Appendix Table 2.5 Liver Pharmacokinetics

Cohort	Subject	Lamda$_z$¶ (1/min)	Half-life (min)	T_{max} (nCi/mL)	X_{max} (counts/s)	$AUC_{0\rightarrow last}$ (kcounts*min/s)	$AUC_{0\rightarrow\infty}$ (kcounts*min/s)
Healthy	1	0.0276	25.1	21	2830	174	182
	2	0.0282	24.6	9	2330	67.9	76.1
	3	0.0410	16.9	12	2180	71.1	71.8
	4	0.0267	26.0	13	2540	96.6	98.1
	5	0.0381	18.2	14	2320	106	110
	6	0.0307	22.5	15	2240	118	123
	7	0.0371	18.7	15	1990	76.7	78.6
	8	0.0304	22.8	15	2550	127	135
	9	0.0364	19.1	13	1840	59.7	60.2
	10	0.0312	22.2	12	2600	126	133
	11	0.0363	19.1	15	2630	120	123
	12	0.0323	21.5	12	2770	111	113
	13	0.0219	31.6	11	2080	112	123
	14	0.0239	29	11	2230	91.3	95.9

Cohort	Subject	$Lamda_z$¶ (1/min)	Half-life (min)	T_{max} (nCi/mL)	X_{max} (counts/s)	$AUC_{0\rightarrow last}$ (kcounts*min/s)	$AUC_{0\rightarrow \infty}$ (kcounts*min/s)
NASH	1	0.0103	67.6	21	2840	260	299
	2	0.0257	27.0	14	3690	208	218
	3	0.0259	26.7	10	4220	171	188
	4	0.0259	26.7	10	3970	161	176
	5	0.0116	59.6	15	2800	177	229
	6	0.0149	46.4	10	2270	153	187
	7	0.0290	23.9	13	3300	187	198

¶Calculated using the terminal slope from 30-80 min

Appendix Table 3.1 Effects of Tolvaptan on NTCP-mediated Uptake of ^{3}H-TCA

		Tolvaptan (μM)								TCDC (μM)
		0	0.01	0.1	1	5	10	25	50	100
Exp.	**Rep.**	**pmol/min/well (% of control)**								
1	1	3.02	NE	NE	3.83 (128)	NE	2.10 (70.0)	1.72 (57.3)	1.96 (65.4)	0.121 (4.02)
1	2	2.95	NE	NE	3.77 (126)	NE	2.03 (67.6)	1.92 (64.0)	1.28 (42.5)	0.0921 (3.07)
1	3	3.04	NE	NE	3.86 (129)	NE	1.22 (40.6)	1.72 (92.7)	1.83 (60.9)	0.197 (6.55)
Mean		3.00 (100)	-	-	3.82 (127)	-	2.78 (59.4)	2.14 (71.3)	1.69 (56.3)	0.136 (4.54)
SD		0.0487 (-)	-	-	0.468 (1.55)	-	0.491 (16.4)	0.565 (18.8)	0.364 (12.1)	0.0540 (1.80)
		pmol/min/well (% of control)								
2	1	1.50	1.56 (86.2)	1.47 (81.3)	2.32 (128)	1.65 (91.3)	1.55 (86.1)	1.43 (79.3)	1.39 (77.1)	BQL
2	2	2.00	1.47 (81.3)	1.28 (70.6)	2.42 (134)	1.16 (64.4)	1.25 (69.3)	1.12 (61.8)	0.849 (47.0)	BQL
2	3	1.92	1.43 (79.3)	1.22 (67.5)	1.36 (75.4)	1.47 (81.4)	1.40 (77.5)	1.19 (65.8)	1.04 (57.7)	BQL
Mean		1.81 (100)	1.49 (82.3)	1.32 (73.2)	2.03 (113)	1.43 (79.0)	1.40 (77.6)	1.25 (69.0)	1.09 (60.6)	BQL

SD		0.267 (-)	0.064 (3.57)	0.584 (7.23)	0.246 (32.3)	0.246 (13.6)	0.151 (8.39)	0.166 (9.17)	0.275 (15.3)	NC
					pmol/min/well (% of control)					
3	1	1.17	1.33 (112)	1.25 (105)	1.18 (99.6)	1.12 (94.5)	0.979 (82.4)	0.653 (55.0)	0.409 (34.5)	0.00439 (0.370)
3	2	0.874	1.29 (109)	1.22 (103)	1.22 (102)	1.01 (84.8)	0.853 (71.9)	0.479 (40.4)	0.411 (34.6)	0.00910 (0.767)
					Tolvaptan (µM)					**TCDC (µM)**
		0	0.01	0.1	1	5	10	25	50	100
Exp.	**Rep.**				**pmol/min/well (% of control)**					
3	3	1.18	1.36 (114)	1.23 (104)	1.24 (105)	1.19 (100)	0.904 (76.1)	0.548 (46.1)	0.422 (35.5)	0.0105 (0.888)
3	4	1.34	-	-	-	-	-	-	-	-
3	5	1.34	-	-	-	-	-	-	-	-
3	6	1.22	-	-	-	-	-	-	-	-
Mean		1.19 (100)	1.32 (112)	1.23 (104)	1.21 (102)	1.11 (93.2)	0.912 (76.8)	0.560 (47.2)	0.414 (34.8)	0.00801 (0.675)
SD		0.175 (-)	0.0329 (2.77)	0.0120 (1.01)	0.0306 (2.58)	0.0930 (7.84)	0.0630 (5.31)	0.0878 (7.39)	0.00677 (0.570)	0.00322 (0.271)

NE=not evaluated; 2 µM substrate (^{3}H-TCA) and < 1% organic solvent; BQL=below quantitation limit; NC=not calculable

Appendix Table 3.2 Effects of Tolvaptan on NTCP-mediated Uptake of ^{3}H-TCA (combined data)

	Tolvaptan (μM)								TCDC (μM)
	0	0.01	0.1	1	5	10	25	50	100
Exp.	**% of control**								
1	100	NE	NE	127	NE	59.4	71.3	56.3	4.54
2	100	82.3	73.2	113	79.0	77.6	70.0	60.6	BQL (0)
3	100	112	104	102	93.2	76.8	47.2	34.8	0.675
Mean	100	96.9	88.5	114	86.1	71.3	62.5	50.6	1.74
SD	-	*NC	*NC	12.6	*NC	10.3	13.3	13.8	*NC

NE=not evaluated; BQL=below quantitation limit; 2 μM substrate (^{3}H-TCA) and < 1% organic solvent; *n=2, standard deviation is not calculable (NC)

Appendix Table 3.3 Effects of DM-4103 on NTCP-mediated Uptake of ^{3}H-TCA

		DM-4103 (μM)								TCDC (μM)
		0	0.01	0.1	1	10	25	50	75	100
Exp.	**Rep.**	**pmol/min/well (% of control)**								
1	1	0.715	0.551 (65.1)	0.722 (85.2)	0.763 (90.1)	0.562 (66.4)	0.597 (70.5)	0.289 (34.1)	NE	BQL
1	2	0.946	0.606 (71.5)	0.524 (61.8)	0.632 (74.6)	0.434 (51.3)	0.463 (54.7)	0.281 (33.2)	NE	0.00384 (0.453)
1	3	0.880	0.630 (74.4)	0.794 (93.7)	0.649 (76.6)	0.471 (55.6)	0.588 (69.4)	0.197 (23.3)	NE	BQL
Mean		0.847 (100)	0.596 (70.3)	0.680 (80.3)	0.681 (80.4)	0.489 (57.8)	0.550 (64.9)	0.256 (30.2)	-	BQL
SD		0.119 (-)	0.0404 (4.77)	0.140 (17.0)	0.0713 (8.42)	0.0658 (7.77)	0.0746 (8.80)	0.0508 (6.00)	-	NC
		pmol/min/well (% of control)								
2	1	1.70	1.28 (70.4)	1.50 (82.7)	1.58 (87.0)	1.04 (57.2)	0.743 (41.0)	0.406 (22.3)	0.287 (15.8)	BQL
2	2	1.70	1.72 (94.9)	1.42 (78.2)	1.74 (95.8)	0.961 (52.9)	0.685 (37.7)	0.438 (24.1)	0.311 (17.1)	BQL
2	3	1.92	1.71 (94.5)	1.57 (86.2)	1.65 (90.8)	0.973 (53.6)	0.743 (40.9)	0.445 (24.5)	0.346 (19.1)	0.000705 (0.0389)

2	4	1.35	-	-	-	-	-	-	-	-
2	5	1.62	-	-	-	-	-	-	-	-
2	6	2.60	-	-	-	-	-	-	-	-
Mean		1.82 (100)	1.57 (86.6)	1.49 (82.4)	1.66 (91.2)	0.991 (54.6)	0.724 (39.9)	0.430 (23.7)	0.315 (17.3)	BQL
SD		0.426 (-)	0.254 (14.0)	0.0732 (4.03)	0.806 (4.44)	0.421 (2.32)	0.0333 (1.83)	0.0211 (1.16)	0.0296 (1.63)	NC
					DM-4103 (µM)					**TCDC (µM)**
		0	0.01	0.1	1	10	25	50	75	100
Exp.	**Rep.**				**pmol/min/well (% of control)**					
3	1	0.958	0.950 (91.0)	1.20 (115)	0.663 (63.6)	0.400 (38.2)	0.518 (49.6)	0.297 (28.5)	0.163 (15.6)	0.00401 (0.385)
3	2	1.36	1.17 (113)	1.27 (121)	1.16 (111)	0.576 (55.3)	0.466 (44.7)	0.218 (20.9)	0.150 (14.3)	0.00375 (0.359)
3	3	0.85	1.07 (102)	1.07 (103)	1.01 (97.2)	0.460 (44.1)	0.435 (41.7)	0.266 (25.5)	0.126 (12.1)	0.00199 (0.191)
3	4	0.949	-	-	-	-	-	-	-	-
3	5	1.10	-	-	-	-	-	-	-	-

3	6	MV	-	-	-	-	-	-	-	-
Mean		1.04 (100)	1.07 (102)	1.18 (113)	0.946 (90.7)	0.478 (45.9)	0.473 (45.4)	0.260 (25.0)	0.146 (14.0)	0.00325 (0.311)
SD		0.200 (-)	0.113 (10.8)	0.0986 (9.46)	0.256 (24.5)	0.0903 (8.66)	0.0417 (4.00)	0.0397 (3.81)	0.0185 (1.77)	0.00110 (0.105)

NE=not evaluated; 2 µM substrate (^{3}H-TCA) and < 1% organic solvent; BQL=below quantitation limit;
MV=missing value (pipette error)

Appendix Table 3.4 Effects of DM-4103 on NTCP-mediated Uptake of ^{3}H-TCA (combined data)

	DM-4103 (μM)								TCDC (μM)
	0	0.01	0.1	1	10	25	50	75	100
Exp.	**% of control**								
1	100	70.3	80.3	80.4	57.8	64.9	30.2	NE	BQL
2	100	86.6	82.4	91.2	54.6	39.9	23.7	17.3	BQL
3	100	102	113	90.7	45.9	45.4	25.0	14.0	0.311
Mean	100	86.3	92.0	87.4	52.7	50.0	26.3	15.7	BQL
SD	-	15.8	18.2	6.08	6.17	13.1	3.46	*NC	NC

NE=not evaluated; 2 μM substrate (^{3}H-TCA) and < 1% organic solvent; *n=2, standard deviation is not calculable (NC)

Appendix Table 3.5 Effects of DM-4107 on NTCP-mediated Uptake of ^{3}H-TCA

		DM-4107 (μM)									TCDC (μM)
		0	0.01	0.1	1	10	25	50	100	200	100
Exp.	**Rep.**	**pmol/min/well (% of control)**									
1	1	3.03	3.93 (124)	3.43 (108)	4.18 (131)	3.04 (95.5)	2.32 (72.8)	2.04 (64.20	1.77 (55.6)	1.26 (39.7)	0.0738 (2.34)
1	2	3.26	4.54 (143)	3.88 (122)	4.51 (142)	3.37 (106)	2.90 (91.0)	2.51 (79.0)	1.50 (47.2)	1.02 (32.1)	BQL (0)
1	3	3.26	4.48 (141)	4.42 (139)	4.63 (146)	3.67 (115)	2.27 (71.2)	2.79 (87.7)	1.50 (47.3)	1.11 (34.9)	0.0808 (2.55)
Mean		3.18 (100)	4.32 (136)	3.91 (123)	4.44 (140)	3.36 (106)	2.49 (78.4)	2.45 (77.0)	1.59 (50.0)	1.13 (35.6)	0.0515 (1.62)
SD		0.135 (-)	0.335 (10.5)	0.496 (15.6)	0.233 (7.32)	0.315 (9.91)	0.350 (11.0)	0.377 (12.0)	0.154 (4.86)	0.122 (3.82)	*NC
		pmol/min/well (% of control)									
2	1	1.88	1.66 (92.9)	1.45 (80.8)	1.17 (65.5)	1.30 (72.5)	NE	0.890 (49.8)	0.856 (47.8)	0.661 (36.9)	0.0111 (0.620)
2	2	1.71	1.65 (92.4)	1.53 (85.4)	1.33 (74.6)	1.52 (84.9)	NE	1.32 (74.0)	0.891 (49.8)	0.728 (40.7)	0.00861 (0.481)

`

	3	1.78	1.90 (106)	1.67 (93.0)	1.55 (86.5)	1.36 (75.7)	NE	1.22 (68.2)	0.931 (52.0)	0.416 (23.3)	0.00927 (0.518)
Mean		1.79 (100)	1.74 (97.1)	1.55 (86.4)	1.35 (75.5)	1.39 (77.7)	-	1.15 (64.0)	0.892 (49.9)	0.602 (33.6)	0.00966 (0.540)
SD		0.0841 (-)	0.139 (7.79)	0.111 (6.21)	0.189 (11.0)	0.115 (6.42)	-	0.227 (13.0)	0.0378 (2.11)	0.164 (9.17)	0.00130 (0.0724)
					pmol/min/well (% of control)						
3	1	1.11	1.27 (108)	1.33 (113)	0.935 (79.3)	0.500 (42.3)	NE	0.655 (55.6)	0.586 (49.7)	0.451 (38.2)	0.00604 (0.512)
3	2	1.18	*MV	1.38 (117)	*MV	0.836 (70.9)	NE	0.614 (52.0)	0.584 (49.5)	0.452 (38.3)	0.00697 (0.591)
					DM-4107 (µM)						**TCDC (µM)**
		0	0.01	0.1	1	10	25	50	100	200	100
Exp.	**Rep.**				**pmol/min/well (% of control)**						
3	3	1.25	1.12 (94.8)	1.18 (100)	*MV	0.860 (72.9)	NE	0.682 (57.8)	0.530 (45.0)	0.455 (38.5)	0.00407 (0.345)
Mean		1.18 (100)	1.20 (101)	1.30 (110)	0.935 (79.3)	0.731 (62.0)	-	0.650 (55.1)	0.567 (48.1)	0.453 (38.4)	0.00569 (0.483)
SD		0.0688 (-)	*NC	0.102 (8.66)	*NC	0.201 (17.1	-	0.0343 (2.90)	0.0314 (2.67)	0.00186 (0.157)	0.00148 (0.125)

NE=not evaluated; *n=1 or 2, standard deviation is not calculable (NC); 2 µM substrate (^{3}H-TCA) and < 1% organic solvent; BQL=below quantitation limit; *MV=missing value (cells not functional due to loss of cell media during shipment and low DPM counts)

Appendix Table 3.6 Effects of DM-4107 on NTCP-mediated Uptake of ^{3}H-TCA (combined data)

	DM-4107 (µM)									TCDC (µM)
	0	0.01	0.1	1	10	25	50	100	200	100
Exp.	**% of control**									
1	100	136	123	140	106	78.4	77.0	50.0	35.6	1.62
2	100	97.1	86.4	75.5	77.7	NE	64.0	49.9	33.6	0.540
3	100	101	110	79.3	62.0	NE	55.1	48.1	38.4	0.483
Mean	100	111	106	98.1	81.9	78.4	65.4	49.3	35.8	0.889
SD	-	21.2	18.5	35.9	22.3	*NC	11.0	1.10	2.39	0.635

NE=not evaluated; 2 µM substrate (^{3}H-TCA) and < 1% organic solvent; *n=1, standard deviation is not calculable (NC)

Appendix Table 3.7 Effects of Tolvaptan on BSEP-mediated ^{3}H-TCA Uptake

		Tolvaptan (µM)										RIF (µM)
		0	0.1	1	2	5	10	20	30	40	50	50
Exp.	**Rep.**	**BSEP-Mediated TCA Uptake (pmol/min/mg protein)**										
1	1	104	NE	NE	NE	107	59.2	46.5	43.7	23.3	15.2	38.0
1	2	106	NE	NE	NE	MV	46.8	37.5	26.9	25.2	16.7	37.0
1	3	93.8	NE	NE	NE	116	48.5	44.6	28.6	20.5	9.41	33.4
Mean		104	-	-	-	112	50.9	42.4	32.8	22.8	13.6	35.7
SD		6.35	-	-	-	NC	6.71	4.75	9.25	2.39	3.86	2.40
Exp.	**Rep.**	**BSEP-Mediated TCA Uptake (pmol/min/mg protein)**										
2	1	56.1	NE	NE	NE	70.9	100	63.2	34.5	18.5	10.1	NE
2	2	68.4	NE	NE	NE	89.1	88.1	68.8	32.4	19.7	9.16	NE
2	3	71.1	NE	NE	NE	72.6	86.2	50.1	26.8	18.5	9.83	NE
Mean		65.2	-	-	-	77.5	91.4	60.7	31.2	18.9	9.69	-
SD		8.01	-	-	-	10.1	7.55	9.59	4.00	0.692	0.480	-
Exp.	**Rep.**	**BSEP-Mediated TCA Uptake (pmol/min/mg protein)**										
3	1	68.8	89.6	84.8	94.7	99.2	73.1	66.6	43.9	19.0	12.3	24.5
3	2	69.0	80.5	79.1	89.3	78.8	76.4	54.9	31.3	12.3	19.6	19.7
3	3	68.7	84.9	68.6	91.3	91.8	82.4	59.4	30.5	6.63	10.9	10.6
Mean		68.8	85.0	77.5	91.7	81.5	77.3	60.3	36.1	12.6	14.2	18.3
SD		0.132	4.56	8.20	2.70	10.4	4.71	5.89	7.52	6.17	4.69	7.08
Exp.	**Rep.**	**TCA Uptake (% of control)**										
1	1	102	NE	NE	NE	106	58.5	46.0	43.3	23.1	15.0	37.6
1	2	105	NE	NE	NE	MV	46.2	37.1	26.6	24.9	16.5	36.6
1	3	92.8	NE	NE	NE	115	48.0	44.1	28.3	20.2	9.31	33.0
Mean		100	-	-	-	110	50.9	42.4	32.8	22.8	13.6	35.7

SD		6.28	-	-	-	6.38	8.68	6.33	11.8	1.30	1.06	0.73
Exp.	**Rep.**	**TCA Uptake (% of control)**										
2	1	86.0	NE	NE	NE	109	153	96.9	52.9	28.4	15.5	NE
2	2	105	NE	NE	NE	137	135	105	49.8	30.2	14.0	NE
2	3	109	NE	NE	NE	111	132	76.8	41.1	28.4	15.1	NE
Mean		100	-	-	-	119	140	93.1	47.9	29.0	14.9	-
SD		12.3	-	-	-	15.4	11.6	14.7	6.14	1.06	0.74	-
Exp.	**Rep.**	**TCA Uptake (% of control)**										
3	1	99.9	130	123	137	144	106	96.8	63.8	27.5	17.8	35.6
3	2	100	117	115	130	114	111	79.8	45.5	17.9	28.5	28.6
3	3	99.8	123	99.7	133	133	120	86.3	44.4	9.64	15.8	15.4
Mean		100	124	113	133	118	112	87.6	52.4	18.3	20.7	26.5
SD		0.192	6.63	11.9	3.93	15.0	6.85	8.55	10.9	8.96	6.81	10.3

2 µM substrate (^{3}H-TCA) and < 1% organic solvent; NC=not calculable; NE=not evaluated; MV=missing value (due to technical problem).

Appendix Table 3.8 K_i Determination of Tolvaptan on BSEP-mediated ^{3}H-TCA Uptake

Experiment 1

TCA (µM)		2	2	2	2	5	5	5	5	10	10	10	10
Tolvaptan(µM)		0	10	25	50	0	10	25	50	0	10	25	50
Exp.	**Rep.**	**BSEP-mediated TCA Uptake (pmol/min/mg protein)**											
1	**1**	87.0	63.6	44.5	15.2	186	150	63.4	44.5	269	250	175	62.1
1	**2**	75.0	79.2	35.9	6.77	165	135	62.4	51.3	179	274	128	26.9
1	**3**	83.2	51.2	39.2	8.32	149	114	79.7	36.1	210	216	155	42.9
Mean		81.7	64.7	39.9	10.1	167	133	68.5	44.0	219	247	153	44.0
SD		6.17	14.1	4.34	4.51	18.5	18.3	9.73	7.64	45.9	29.6	23.6	17.6
TCA (µM)		20	20	20	20	30	30	30	30				
Tolvaptan(µM)		0	10	25	50	0	10	25	50				
Exp.	**Rep.**	**BSEP-mediated TCA Uptake (pmol/min/mg protein)**											
1	**1**	479	372	211	47.7	316	288	239	153				
1	**2**	346	430	156	117	391	348	270	131				
1	**3**	347	335	153	129	358	206	218	48.0				
Mean		391	379	173	97.8	355	281	242	110				
SD		76.5	48.0	32.6	43.8	37.6	71.4	26.0	55.2				

Experiment 2

TCA (µM)		2	2	2	2	5	5	5	5	10	10	10	10
Tolvaptan (µM)		0	10	25	50	0	10	25	50	0	10	25	50
Exp.	**Rep.**	**BSEP-mediated TCA Uptake (pmol/min/mg protein)**											
2	**1**	104	95.5	60.0	20.1	188	185	139	44.9	279	356	238	94.1
2	**2**	101	94.2	55.7	23.8	161	195	163	44.5	299	274	216	111
2	**3**	99.7	81.8	44.4	17.0	139	285	131	42.0	212	299	207	100
Mean		101	90.5	53.4	20.3	163	215	144	43.8	257	310	220	102
SD		2.01	7.56	8.07	3.41	24.1	43.4	16.6	1.60	56.9	42.0	15.6	8.71

TCA (µM)		20	20	20	20	30	30	30	30
Tolvaptan (µM)		0	10	25	50	0	10	25	50
Exp.	**Rep.**	**BSEP-mediated TCA Uptake (pmol/min/mg protein)**							
2	**1**	386	377	228	140	589	533	305	271
2	**2**	450	306	293	36.9	454	381	363	264
2	**3**	353	353	331	36.7	508	446	302	132
Mean		396	345	284	71.2	517	453	323	222
SD		49.3	36.0	52.0	59.5	68.1	76.5	34.6	78.0

Experiment 3

TCA (µM)		2	2	2	2	5	5	5	5	10	10	10	10
Tolvaptan (µM)		0	10	25	50	0	10	25	50	0	10	25	50
Exp.	**Rep.**	**BSEP-mediated TCA Uptake (pmol/min/mg protein)**											
3	**1**	97.7	103	52.5	11.8	156	150	64.3	45.9	325	267	189	52.9
3	**2**	82.1	88.8	61.5	21.2	185	150	64.0	30.6	299	225	197	44.5
3	**3**	81.4	95.3	50.1	21.0	176	154	102	25.3	287	282	180	58.8
Mean		87.1	95.5	54.7	18.0	172	151	76.8	33.9	293	258	188	52.1
SD		9.24	6.87	6.03	5.37	14.6	2.00	21.9	10.7	19.5	29.8	8.46	7.14

TCA (µM)		20	20	20	20	30	30	30	30
Tolvaptan (µM)		0	10	25	50	0	10	25	50
Exp.	**Rep.**	**BSEP-mediated TCA Uptake (pmol/min/mg protein)**							
3	**1**	288	422	341	62.2	436	492	367	184
3	**2**	389	435	341	92.8	457	426	260	127
3	**3**	323	344	253	60.3	437	488	MV	131
Mean		333	400	312	71.7	444	469	313	147
SD		51.2	49.3	50.5	18.2	12.0	37.3	NC	31.7

MV=missing value (due to technical problem); NC=not calculable.

Appendix Table 3.9 Effects of DM-4103 on BSEP-mediated ^{3}H-TCA Uptake

		DM-4103 (μM)											
		0	0.1	0.3	1	2	5	10	20	30	40	50	75
Exp.	**Rep.**	**BSEP-mediated TCA Uptake (pmol/min/mg protein)**											
1	1	93.3	NE	NE	NE	NE	34.4	20.8	17.2	7.73	7.13	0.7	0
1	2	95.5	NE	NE	NE	NE	25.4	16.7	11.3	7.28	1.57	0	2.90
1	3	74.8	NE	NE	NE	NE	26.1	15.9	14.4	6.23	5.09	0	2.04
Mean		87.9	-	-	-	-	28.6	17.8	14.3	7.08	4.60	0	1.55
SD		11.4	-	-	-	-	5.02	2.65	2.97	0.77	2.81	NC	NC
		BSEP-mediated TCA Uptake (pmol/min/mg protein)											
2	1	68.7	83.7	64.8	64.5	48.1	37.4	26.6	14.3	NE	NE	NE	NE
2	2	70.8	74.3	62.0	61.2	50.6	35.2	12.0	9.49	NE	NE	NE	NE
2	3	67.0	68.7	53.7	55.6	50.4	31.0	20.5	11.7	NE	NE	NE	NE
Mean		68.9	75.6	60.1	60.4	49.7	34.5	19.7	11.8	-	-	-	-
SD		1.92	7.60	5.77	4.50	1.40	3.21	7.33	2.40	-	-	-	-
		BSEP-mediated TCA Uptake (pmol/min/mg protein)											
3	1	72.1	80.2	69.3	57.3	52.1	41.9	34.8	16.1	NE	NE	NE	NE
3	2	66.6	71.5	62.5	49.8	46.2	31.8	24.9	12.1	NE	NE	NE	NE
3	3	66.3	66.7	65.5	53.2	43.5	23.6	24.6	9.74	NE	NE	NE	NE
Mean		68.3	72.8	65.8	53.5	47.3	32.4	28.1	12.6	-	-	-	-
SD		3.31	6.87	3.39	3.73	4.39	9.16	5.77	3.20	-	-	-	-
		TCA Uptake (% of control)											
1	1	106	NE	NE	NE	NE	39.1	23.6	19.6	8.79	8.14	1.43	0
1	2	109	NE	NE	NE	NE	28.8	18.9	12.8	8.28	1.81	0	3.30
1	3	85.1	NE	NE	NE	NE	29.7	18.0	16.4	7.09	5.81	0	2.33
Mean		100	-	-	-	-	32.6	20.2	16.3	8.05	5.23	0	1.76
SD		12.9	-	-	-	-	5.70	3.02	3.38	0.87	3.20	NC	1.69

TCA Uptake (% of control)													
2	1	99.9	121	94.0	93.6	69.8	54.2	38.5	20.7	NE	NE	NE	NE
2	2	103	108	89.9	88.7	73.5	51.1	17.4	13.7	NE	NE	NE	NE
2	3	97.4	99.8	77.9	80.6	73.2	45.1	29.8	17.0	NE	NE	NE	NE
Mean		100	110	87.3	87.8	72.2	50.1	28.6	17.2	-	-	-	-
SD		2.79	11.0	8.38	6.53	2.04	4.66	10.6	3.48	-	-	-	-
TCA Uptake (% of control)													
3	1	106	117	101	83.8	76.3	61.3	50.9	23.5	NE	NE	NE	NE
3	2	97.4	105	91.5	73.0	67.6	46.5	36.5	17.7	NE	NE	NE	NE
3	3	97.0	97.6	95.9	77.9	63.7	34.5	36.1	14.3	NE	NE	NE	NE
Mean		100	107	96.3	78.2	69.2	47.4	41.1	18.5	-	-	-	-
SD		4.84	10.1	4.96	5.46	6.43	13.4	8.44	4.68	-	-	-	-

n=1 for initial concentration range (30-75 μM); n=2-3 for lower ranges (0.1-20 μM) used to determine IC50.
NC=not calculable; NE=not evaluated.

Appendix Table 3.10 Determination of Inhibition Constant (K_i) for DM-4103 on BSEP-mediated ^{3}H-TCA Uptake

Experiment 1

TCA (µM)		2	2	2	2	5	5	5	5	10	10	10	10
DM-4103(µM)		0	2	5	20	0	2	5	20	0	2	5	20
Exp.	**Rep.**	**BSEP-mediated TCA Uptake (pmol/min/mg protein)**											
1	**1**	73.0	63.2	40.6	12.4	190	130	84.5	43.9	365	258	100	89.0
1	**2**	79.2	53.0	41.3	12.2	203	127	77.1	34.2	274	241	152	82.1
1	**3**	80.7	56.5	33.5	9.70	228	141	77.0	28.7	298	297	106	71.7
Mean		77.6	57.5	38.5	11.4	207	132	79.5	35.6	312	265	119	80.9
SD		4.10	5.18	4.32	1.50	19.6	7.08	4.32	7.72	47.3	28.5	28.4	8.73
TCA (µM)		20	20	20	20	30	30	30	30				
DM-4103 (µM)		0	2	5	20	0	2	5	20				
Exp.	**Rep.**	**BSEP-mediated TCA Uptake (pmol/min/mg protein)**											
1	**1**	545	353	276	203	600	480	349	160				
1	**2**	511	380	311	155	530	579	334	217				
1	**3**	554	402	274	121	458	510	300	147				
Mean		537	378	287	159	529	523	328	175				
SD		22.7	24.5	20.5	41.3	71.3	50.9	25.3	37.0				

Experiment 2

TCA (µM)		2	2	2	2	5	5	5	5	10	10	10	10
DM-4103(µM)		0	2	5	20	0	2	5	20	0	2	5	20
Exp.	**Rep.**	**BSEP-mediated TCA Uptake (pmol/min/mg protein)**											
2	**1**	85.4	50.4	45.1	17.3	194	145	87.4	26.2	286	225	96.9	63.6
2	**2**	85.3	40.8	33.6	11.9	209	111	101	12.6	236	215	164	68.3
2	**3**	87.2	40.8	35.9	16.4	183	110	70.2	7.04	232	179	159	61.2

Mean		86.0	44.0	38.2	15.2	195	122	86.1	15.3	251	207	140	64.3
SD		1.07	5.51	6.10	2.87	12.7	20.0	15.4	9.88	30.0	24.0	37.4	3.61
TCA (µM)		20	20	20	20	30	30	30	30				
DM-4103 (µM)		0	2	5	20	0	2	5	20				
Exp.	**Rep.**	**BSEP-mediated TCA Uptake (pmol/min/mg protein)**											
2	**1**	299	347	216	48.7	437	394	350	182				
2	**2**	419	318	179	MV	516	505	440	188				
2	**3**	300	363	144	51.8	440	458	465	114				
Mean		340	343	180	50.3	464	452	418	162				
SD		69.1	22.8	35.9	NC	44.9	55.7	60.5	40.9				

MV=missing value (due to technical problem); NC=not calculable.

Experiment 3

TCA (µM)		2	2	2	2	5	5	5	5	10	10	10	10
DM-4103(µM)		0	2	5	20	0	2	5	20	0	2	5	20
Exp.	**Rep.**	**BSEP-mediated TCA Uptake (pmol/min/mg protein)**											
3	**1**	63.5	55.4	33.9	13.2	155	116	98.3	50.5	288	200	219	53.0
3	**2**	60.6	49.5	29.8	9.21	153	127	106	63.5	209	212	179	25.2
3	**3**	56.2	54.0	39.4	5.09	186	107	95.5	27.2	247	205	169	37.2
Mean		60.1	53.0	34.3	9.17	165	117	99.8	47.1	248	206	189	38.5
SD		3.68	3.09	4.81	4.06	18.5	9.87	5.20	18.4	39.5	6.10	26.5	13.9

TCA (µM)		20	20	20	20	30	30	30	30
DM-4103 (µM)		0	2	5	20	0	2	5	20
Exp.	**Rep.**	**BSEP-mediated TCA Uptake (pmol/min/mg protein)**							
3	**1**	382	314	202	0	418	394	277	221
3	**2**	580	225	293	0	548	296	417	192
3	**3**	315	236	242	0	377	434	321	131
Mean		426	258	246	0	448	375	339	182
SD		138	48.7	45.4	NC	89.1	70.9	71.6	46.0

NC=not calculable

Table 3.11 Effects of DM-4107 on BSEP-mediated ^{3}H-TCA Uptake

		DM-4107 (µM)							RIF (µM)
		0	10	20	50	100	150	200	50
Exp.	**Rep.**	**BSEP-mediated TCA Uptake (pmol/min/mg protein)**							
1	1	82.8	83.3	63.9	61.8	29.5	31.8	13.1	35.3
1	2	82.6	81.2	72.2	63.3	30.4	25.0	25.2	33.0
1	3	84.4	76.6	53.3	60.2	32.9	47.2	29.8	29.9
Mean		83.3	80.4	63.1	61.8	31.0	34.7	22.7	32.8
SD		1.01	3.46	9.43	1.54	1.76	11.4	8.62	2.70
BSEP-mediated TCA Uptake (pmol/min/mg protein)									
2	1	56.1	50.8	56.3	69.0	42.6	19.4	12.3	46.6
2	2	60.4	49.2	47.6	27.9	51.7	13.4	6.65	30.7
2	3	57.7	45.0	50.9	47.7	36.3	17.9	MV	23.5
Mean		58.1	48.3	51.6	48.2	43.5	16.9	9.49	33.6
SD		2.17	2.97	4.39	20.6	7.73	3.12	NC	11.8
BSEP-mediated TCA Uptake (pmol/min/mg protein)									
3	1	64.9	75.3	61.2	61.4	44.3	34.3	22.3	NE
3	2	60.9	69.7	50.7	61.2	37.8	36.2	17.9	NE
3	3	68.0	71.4	65.6	51.6	33.4	32.5	20.0	NE

Mean		64.6	72.1	59.1	58.1	38.5	34.4	20.1	-
SD		3.58	2.88	7.64	5.60	5.50	1.83	2.18	-
TCA Uptake (% of control)									
1	1	99.4	100	76.7	74.2	35.5	38.2	15.7	42.4
1	2	99.2	97.5	86.6	76.0	36.5	30.0	30.3	39.7
1	3	101	92.0	64.0	72.3	39.5	56.7	35.8	35.9
Mean		100	96.5	75.8	74.2	37.2	41.7	27.3	39.3
SD		1.22	4.16	11.3	1.85	2.12	13.7	10.4	3.24
TCA Uptake (% of control)									
2	1	96.6	87.4	97.0	119	73.3	33.4	21.3	76.6
2	2	104	84.7	82.0	48.0	88.9	23.1	11.5	49.2
2	3	99.4	77.5	87.7	82.2	62.4	30.8	MV	36.9
Mean		100	83.2	88.9	83.1	75.0	29.1	16.3	57.9
SD		3.73	5.12	7.57	35.4	13.3	5.36	NC	20.3
TCA Uptake (% of control)									
3	1	101	117	94.7	95.0	68.6	53.1	34.5	NE
3	2	94.2	108	78.5	94.8	58.5	56.1	27.8	NE
3	3	105	111	101	79.9	51.7	50.4	31.0	NE
Mean		100	112	91.6	89.9	59.6	53.2	31.1	-

SD	5.55	4.45	11.8	8.67	8.51	2.84	3.38	-

MV=missing value (due to technical problem); NC=not calculable; NE=not evaluated; 2 µM substrate (^{3}H-TCA) and < 1% organic solvent

Appendix Table 3.12 Effects of Tolvaptan on MRP2-mediated ^{3}H-$E_2$17G Uptake

		Tolvaptan (μM)							MK-571 (μM)
		0	0.1	1	3	10	20	50	50
Exp.	**Rep.**	**MRP2-Mediated $E_2$17G Uptake (pmol/min/mg protein)**							
1	1	2330	2560	2400	2400	3390	3130	2780	171
1	2	2350	2750	2330	2250	2940	3180	2340	175
1	3	2030	2290	2530	3290	2960	3030	2890	170
Mean		2240	2530	2420	2650	3090	3110	2670	172
SD		183	233	101	558	254	77.0	289	2.46
Exp.	**Rep.**	**MRP2-Mediated $E_2$17G Uptake (pmol/min/mg protein)**							
2	1	2100	2320	3120	3410	4130	3330	2630	45.1
2	2	2330	2480	3090	3780	3080	2920	2620	135
2	3	2360	2310	3020	3930	3000	3260	2720	87.1
Mean		2260	2370	3080	3710	3400	3170	2660	88.9
SD		146	95.3	51.1	268	628	220	55.9	44.8
Exp.	**Rep.**	**MRP2-Mediated $E_2$17G Uptake (pmol/min/mg protein)**							
3	1	2980	2490	3790	3400	3920	3400	3370	176
3	2	3170	2490	3220	3720	3630	2830	3220	195
3	3	2930	2120	3060	3050	3740	2830	3240	133
Mean		3030	2370	3360	3390	3760	3020	3270	168
SD		124	215	386	334	150	330	79.9	31.7
Exp.	**Rep.**	**MRP2-Mediated $E_2$17G Uptake (% of control)**							
1	1	104	114	107	108	151	140	124	7.64
1	2	105	123	104	101	131	142	105	7.82
1	3	90.6	102	113	147	132	135	129	7.61
Mean		100	113	108	118	138	139	119	7.69

SD		8.18	10.4	4.51	24.9	11.4	3.44	12.9	0.110
Exp.	**Rep.**	**MRP2-Mediated $E_2$17G Uptake (% of control)**							
2	1	93	102	138	151	182	147	116	1.99
2	2	103	109	137	167	136	129	116	5.95
2	3	104	102	134	173	133	144	120	3.85
Mean		100	105	136	164	150	140	117	3.93
SD		6.45	4.21	2.26	11.8	27.8	9.70	2.47	1.98
Exp.	**Rep.**	**MRP2-Mediated $E_2$17G Uptake (% of control)**							
3	1	98.6	82.1	125	112	130	112	111	5.80
3	2	105	82.4	106	123	120	93.6	106	6.44
3	3	96.8	70.0	101	101	123	93.6	107	4.39
Mean		100	78.2	111	112	124	100	108	5.54
SD		4.11	7.11	12.7	11.1	4.94	10.9	2.64	1.05

50 µM substrate (^{3}H- $E_2$17G) and < 1% organic solvent.

Appendix Table 3.13 Effects of Tolvaptan on MRP3-mediated ^{3}H- $E_2$17G Uptake

		Tolvaptan (μM)							MK-571 (μM)
		0	0.1	1	3	10	20	50	50
Exp.	**Rep.**	**MRP3-Mediated $E_2$17G Uptake (pmol/min/mg protein)**							
1	1	126	84.0	139	146	103	101	69.8	38.4
1	2	98.9	81.4	135	129	ND	95.0	71.5	48.2
1	3	114	97.9	127	122	123	91.2	65.1	53.5
Mean		113	87.8	134	132	113	95.8	68.8	46.7
SD		13.4	8.89	5.87	12.8	NC	5.11	3.30	7.66
Exp.	**Rep.**	**MRP3-Mediated $E_2$17G Uptake (pmol/min/mg protein)**							
2	1	123	136	137	151	102	151	94.2	45.1
2	2	139	144	143	148	101	128	64.8	135
2	3	152	149	120	134	133	108	71.5	87.1
Mean		138	143	133	144	112	129	76.8	88.9
SD		14.3	6.44	12.0	9.45	18.1	21.3	15.4	44.8
Exp.	**Rep.**	**MRP3-Mediated $E_2$17G Uptake (pmol/min/mg protein)**							
3	1	61.9	49.3	73.5	46.2	53.5	47.6	54.7	ND
3	2	52.3	50.5	57.3	73.6	48.0	61.3	50.3	6.7
3	3	43.0	ND	37.2	ND	38.8	39.1	46.4	23.8
Mean		52.4	49.9	56.0	59.9	46.8	49.4	50.5	15.3
SD		9.43	NC	18.2	19.3	7.44	11.2	4.14	NC
Exp.	**Rep.**	**MRP3-Mediated $E_2$17G Uptake (% of control)**							
1	1	111	74.5	123	130	91.1	89.9	62.0	34.1
1	2	87.7	72.3	120	114	ND	84.4	63.5	42.8
1	3	101	86.9	113	108	109	80.9	57.8	47.5
Mean		100	77.9	119	117	100	85.1	61.1	41.4

SD		11.9	7.89	5.21	11.3	NC	4.54	2.93	6.80
Exp.	**Rep.**	**MRP3-Mediated $E_2$17G Uptake (% of control)**							
2	1	89.3	98.3	99.4	109	73.5	109	68.1	32.4
2	2	101	104	103	107	73.1	92.3	46.8	27.1
2	3	110	108	86.6	96.6	96.1	78.4	51.7	22.0
Mean		100	103	96.3	104	80.9	93.3	55.5	27.2
SD		10.4	4.66	8.64	6.83	13.1	15.4	11.1	5.23
Exp.	**Rep.**	**MRP3-Mediated $E_2$17G Uptake (% of control)**							
3	1	118	94.0	140	88.2	102	90.9	104	ND
3	2	99.9	96.4	109	140	91.6	117	95.9	12.9
3	3	82.1	ND	71.0	ND	74.1	74.6	88.7	45.5
Mean		100	95.2	107	114	89.3	94.2	96.3	29.2
SD		18.0	1.63	34.7	NC	14.2	21.4	7.90	NC

10 µM substrate (^{3}H- $E_2$17G) and < 1% organic solvent; NC=not calculable; ND=not determined (sample processing error)

Appendix Table 3.14 Effects of Tolvaptan on MRP4-mediated ^{3}H-DHEAS Uptake

		Tolvaptan (µM)							MK-571 (µM)
		0	0.1	1	3	10	20	50	50
Exp.	**Rep.**	**MRP4-Mediated DHEAS Uptake (pmol/min/mg protein)**							
1	1	113	170	152	155	167	148	94.6	BQL (0)
1	2	128	166	141	154	140	139	120	BQL (0)
1	3	114	136	127	123	113	135	132	11.5
Mean		118	157	140	144	140	141	116	NC
SD		8.07	18.3	12.8	17.8	26.8	6.87	19.2	NC
Exp.	**Rep.**	**MRP4-Mediated DHEAS Uptake (pmol/min/mg protein)**							
2	1	196	224	189	166	224	259	153	BQL (0)
2	2	168	285	166	191	185	178	138	7.25
2	3	143	193	180	169	180	158	135	15.3
Mean		169	225	178	176	196	198	142	7.68
SD		26.4	32.5	11.3	13.7	24.1	53.2	9.55	7.53
Exp.	**Rep.**	**MRP4-Mediated DHEAS Uptake (pmol/min/mg protein)**							
3	1	212	196	221	174	176	190	178	BQL (0)
3	2	204	221	186	223	177	190	151	0.382
3	3	183	178	171	171	153	143	164	0.763
Mean		200	198	193	193	169	174	164	0.382
SD		14.9	21.5	25.2	35.1	13.6	27.0	13.6	0.382
Exp.	**Rep.**	**MRP4-Mediated DHEAS Uptake (% of control)**							
1	1	95.4	144	129	131	141	125	80.0	BQL (0)
1	2	108	140	120	130	119	118	101	BQL (0)
1	3	96.8	115	107	104	95.9	114	112	9.74
Mean		100	133	119	122	119	119	97.7	NC

SD		6.80	15.4	10.8	15.1	22.7	5.81	16.2	NC
Exp.	**Rep.**	**MRP4-Mediated DHEAS Uptake (% of control)**							
2	1	116	132	112	98.3	133	153	90.5	BQL (0)
2	2	99.4	153	98.4	113	109	106	81.6	4.29
2	3	84.7	114	106	100	107	93.4	80.0	9.07
Mean		100	133	106	104	116	117	84.0	4.54
SD		15.6	19.2	6.70	8.09	14.3	31.5	5.65	4.45
Exp.	**Rep.**	**MRP4-Mediated DHEAS Uptake (% of control)**							
3	1	106	98.2	110	86.9	88.1	95.2	89.1	BQL (0)
3	2	102	111	93.1	117	88.6	94.8	75.6	0.191
3	3	91.7	89.1	85.7	85.6	76.6	71.7	81.9	0.382
Mean		100	99.2	96.4	96.4	84.4	87.2	82.2	0.191
SD		7.46	10.8	12.6	17.5	6.80	13.5	6.78	0.191

2 µM substrate (^{3}H- DHEAS) and < 1% organic solvent; BQL=below quantitation limit; NC=not calculable

Appendix Table 3.15 Effects of DM-4103 on MRP2-mediated ^{3}H-$E_2$17G Uptake

		DM-4103 (μM)							MK-571 (μM)
		0	0.1	1	3	10	20	50	50
Exp.	**Rep.**	**MRP2-Mediated $E_2$17G Uptake (pmol/min/mg protein)**							
1	1	2760	3650	3860	3440	2760	2570	1050	62.7
1	2	2700	3190	3190	3330	2740	2730	961	92.4
1	3	3500	3980	3750	3270	2690	2500	1430	190
Mean		2980	3610	3600	3350	2730	2600	1150	115
SD		444	396	358	85.8	35.0	119	250	66.9
Exp.	**Rep.**	**MRP2-Mediated $E_2$17G Uptake (pmol/min/mg protein)**							
2	1	3160	3280	3870	2670	3170	2580	1230	103
2	2	2980	3290	3530	3340	2830	2310	1140	160
2	3	3140	3270	3910	2800	2660	2100	1210	181
Mean		3090	3280	3770	2940	2880	2330	1190	148
SD		100	12.7	209	356	258	244	47.1	40.4
Exp.	**Rep.**	**MRP2-Mediated $E_2$17G Uptake (pmol/min/mg protein)**							
3	1	2720	2770	2530	2700	2740	1670	894	36.1
3	2	2510	2670	2710	2860	2730	1840	1020	30.3
3	3	2870	2600	2310	2660	2520	2080	946	14.5
Mean		2700	2680	2520	2740	2660	1860	954	27.0
SD		180	88.1	196	107	126	202	63.7	11.2
Exp.	**Rep.**	**MRP2-Mediated $E_2$17G Uptake (% of control)**							
1	1	92.4	122	129	115	92.5	86.1	35.1	2.10
1	2	90.4	107	107	112	91.9	91.4	32.2	3.10
1	3	117	133	126	110	90.2	83.6	47.9	6.38
Mean		100	121	121	112	91.5	87.1	38.4	3.86

SD		14.9	13.3	12.0	2.88	1.17	3.99	8.36	2.24
Exp.	**Rep.**	**MRP2-Mediated $E_2$17G Uptake (% of control)**							
2	1	102	106	125	86.3	102	83.5	39.7	3.33
2	2	96.3	106	114	108	91.3	74.8	36.8	5.18
2	3	102	106	126	90.4	86.0	67.8	39.1	5.85
Mean		100	106	122	94.9	93.2	75.3	38.6	4.79
SD		3.23	0.411	6.77	11.5	8.33	7.88	1.52	1.31
Exp.	**Rep.**	**MRP2-Mediated $E_2$17G Uptake (% of control)**							
3	1	101	103	93.7	99.8	101	61.9	33.1	1.34
3	2	93.0	98.9	100	106	101	68.2	37.8	1.12
3	3	106	96.2	85.6	98.3	93.2	76.9	35.0	0.538
Mean		100	99.2	93.2	101	98.5	69.0	35.3	1.00
SD		6.65	3.26	7.26	3.96	4.67	7.49	2.36	0.413

50 µM substrate (^{3}H- $E_2$17G) and < 1% organic solvent; NC=not calculable

Appendix Table 3.16 Effects of DM-4103 on MRP3-mediated ^{3}H-$E_2$17G Uptake

		DM-4103 (μM)							MK-571 (μM)
		0	0.1	1	3	10	20	50	50
Exp.	**Rep.**	**MRP3-Mediated $E_2$17G Uptake (pmol/min/mg protein)**							
1	1	220	176	181	183	177	129	71.1	42.0
1	2	168	178	135	148	119	80.3	61.1	36.4
1	3	182	198	140	ND	115	109	62.3	46.8
Mean		190	184	152	166	137	106	64.8	41.7
SD		26.8	12.3	25.4	NC	34.9	24.3	5.47	5.20
Exp.	**Rep.**	**MRP3-Mediated $E_2$17G Uptake (pmol/min/mg protein)**							
2	1	163	170	129	106	156	137	56.8	51.7
2	2	143	131	167	109	121	147	82.6	57.3
2	3	126	130	194	174	146	98.4	68.0	40.2
Mean		144	144	163	130	141	127	69.1	49.7
SD		18.3	23.0	32.9	38.2	17.7	25.7	12.9	8.71
Exp.	**Rep.**	**MRP3-Mediated $E_2$17G Uptake (pmol/min/mg protein)**							
3	1	124	144	124	ND	113	105	43.8	35.9
3	2	135	144	140	184	136	120	63.9	28.1
3	3	158	ND	136	119	106	100	59.3	42.6
Mean		139	144	133	151	118	108	55.7	35.5
SD		17.4	NC	8.30	NC	15.7	10.3	10.5	7.25
Exp.	**Rep.**	**MRP3-Mediated $E_2$17G Uptake (% of control)**							
1	1	116	92.8	95.3	96.4	93.3	67.7	37.4	22.1
1	2	88.3	93.9	71.0	78.0	62.9	42.3	32.2	19.2
1	3	96.1	104	73.6	ND	60.3	57.3	32.8	24.6
Mean		100	97.1	80.0	87.2	72.2	55.8	34.1	22.0

SD		14.1	6.46	13.4	NC	18.4	12.8	2.88	2.74
Exp.	**Rep.**	**MRP3-Mediated $E_2$17G Uptake (% of control)**							
2	1	113	118	89.4	73.2	108	94.8	39.4	35.8
2	2	99.4	90.7	116	75.9	84.1	102	57.3	39.7
2	3	87.6	90.5	135	120	101	68.2	47.2	27.9
Mean		100	99.8	113	89.9	97.7	88.4	47.9	34.5
SD		12.7	16.0	22.8	26.5	12.3	17.8	8.96	6.04
Exp.	**Rep.**	**MRP3-Mediated $E_2$17G Uptake (% of control)**							
3	1	89.2	104	89.2	ND	81.2	75.4	31.5	25.8
3	2	97.1	104	101	132	97.6	86.1	46.0	20.2
3	3	114	ND	97.8	85.6	76.0	71.8	42.7	30.6
Mean		100	104	95.9	109	84.9	77.8	40.1	25.6
SD		12.5	NC	5.97	NC	11.3	7.44	7.58	5.22

10 µM substrate (^{3}H- $E_2$17G) and < 1% organic solvent; NC=not calculable; ND=not determined (sample processing error)

Appendix Table 3.17 Effects of DM-4103 on MRP4-mediated ^{3}H-DHEAS Uptake

		DM-4103 (µM)						MK-571 (µM)
		0	0.1	1	3	10	20	50
Exp.	**Rep.**	**MRP4-Mediated DHEAS Uptake (pmol/min/mg protein)**						
1	1	183	195	180	110	67.9	25.9	5.26
1	2	189	194	199	108	67.6	23.4	0.770
1	3	169	185	179	103	58.5	20.1	1.56
Mean		180	191	186	107	64.7	23.1	2.53
SD		10.1	5.53	11.3	3.22	5.32	2.90	2.40
Exp.	**Rep.**	**MRP4-Mediated DHEAS Uptake (pmol/min/mg protein)**						
2	1	228	237	196	135	63.9	35.0	2.72
2	2	229	217	181	121	43.2	30.1	3.27
2	3	217	197	162	124	43.0	20.2	1.30
Mean		225	217	180	127	50.0	28.4	2.43
SD		6.93	19.9	17.4	7.31	12.0	7.52	1.02
Exp.	**Rep.**	**MRP4-Mediated DHEAS Uptake (pmol/min/mg protein)**						
3	1	171	213	147	120	36.2	35.9	BQL (0)
3	2	155	117	135	107	30.4	33.7	BQL (0)
3	3	167	145	125	71.1	26.7	26.9	BQL (0)
Mean		164	158	136	99.6	31.1	32.1	NC
SD		7.97	49.0	11.1	25.5	4.76	4.69	NC
Exp.	**Rep.**	**MRP4-Mediated DHEAS Uptake (% of control)**						
1	1	101	108	99.8	60.9	37.7	14.4	2.92
1	2	105	107	110	59.7	37.5	13.0	0.427
1	3	93.8	103	99.4	57.4	32.5	11.2	0.863
Mean		100	106	103	59.3	35.9	12.9	1.40

SD		5.61	3.07	6.25	1.79	2.95	1.61	1.33
Exp.	**Rep.**	**MRP4-Mediated DHEAS Uptake (% of control)**						
2	1	102	106	87.5	60.1	28.5	15.6	1.21
2	2	102	96.9	80.5	54.0	19.2	13.4	1.46
2	3	96.4	87.9	72.0	55.3	19.2	9.00	0.578
Mean		100	96.9	80.0	56.5	22.3	12.7	1.08
SD		3.08	8.86	7.75	3.26	5.36	3.35	0.454
Exp.	**Rep.**	**MRP4-Mediated DHEAS Uptake (% of control)**						
3	1	104	129	89.6	73.2	22.0	21.8	BQL (0)
3	2	94.5	71.5	82.1	65.4	18.5	20.5	BQL (0)
3	3	102	88.2	76.1	43.2	16.3	16.4	BQL (0)
Mean		100	96.2	82.6	60.6	18.9	19.6	NC
SD		4.85	29.8	6.76	15.5	2.90	2.85	NC

2 µM substrate (^{3}H- DHEAS) and < 1% organic solvent; BQL=below quantitation limit; NC=not calculable

Appendix Table 3.18 Effects of DM-4107 on MRP2-mediated ^{3}H-$E_2$17G Uptake

		DM-4107 (µM)						MK-571 (µM)
		0	10	20	50	100	200	50
Exp.	**Rep.**	**MRP2-Mediated $E_2$17G Uptake (pmol/min/mg protein)**						
1	1	2600	2510	2590	3180	3170	1950	BQL (0)
1	2	ND	2470	2380	2930	2380	2630	149
1	3	ND	2330	2480	3120	2970	2070	BQL (0)
Mean		2600	2440	2480	3080	2840	2210	NC
SD		NC	97.7	106	129	416	362	NC
Exp.	**Rep.**	**MRP2-Mediated $E_2$17G Uptake (pmol/min/mg protein)**						
2	1	3290	2530	2850	3040	3050	1980	182
2	2	3130	2840	3070	2700	2940	1960	201
2	3	3170	2840	3020	2890	2770	1650	206
Mean		3200	2740	2980	2880	2920	1860	12.5
SD		84.2	180	112	173	138	185	196
Exp.	**Rep.**	**MRP2-Mediated $E_2$17G Uptake (pmol/min/mg protein)**						
3	1	2820	1940	2520	2620	2220	1570	187
3	2	2510	1580	2630	2550	2260	1560	131
3	3	2890	1520	2420	2350	2070	1610	106
Mean		2740	1680	2520	2510	2180	1580	141
SD		201	226	107	137	102	29.7	41.7
Exp.	**Rep.**	**MRP2-Mediated $E_2$17G Uptake (% of control)**						
1	1	100	96.6	100	122	122	74.9	BQL (0)
1	2	ND	95.0	91.4	113	91.3	101	5.75
1	3	ND	89.5	95.4	120	114	79.5	BQL (0)
Mean		100	93.7	95.5	118	109	85.1	NC

SD		NC	3.76	4.08	4.95	16.0	13.9	NC
Exp.	**Rep.**	**MRP2-Mediated $E_2$17G Uptake (% of control)**						
2	1	103	79.1	89.2	95.1	95.3	62.0	5.70
2	2	97.9	88.8	96.0	84.3	91.9	61.2	6.30
2	3	99.1	88.9	94.3	90.5	86.7	51.6	6.44
Mean		100	85.6	93.2	90.0	91.3	58.3	6.14
SD		2.63	5.64	3.50	5.40	4.31	5.77	0.392
Exp.	**Rep.**	**MRP2-Mediated $E_2$17G Uptake (% of control)**						
3	1	103	70.7	92.1	95.7	81.2	57.2	6.83
3	2	91.6	57.7	96.2	93.1	82.5	57.0	4.77
3	3	105	55.4	88.3	86.0	75.4	59.0	3.86
Mean		100	61.3	92.2	91.6	79.7	57.7	5.15
SD		7.35	8.27	3.93	5.00	3.74	1.09	1.53

50 µM substrate (^{3}H- $E_2$17G) and < 1% organic solvent; BQL=below quantitation limit; NC=not calculable; ND=not determined (sample processing error)

Appendix Table 3.19 Effects of DM-4107 on MRP3-mediated ^{3}H- $E_2$17G Uptake

		DM-4107 (μM)						MK-571 (μM)
		0	10	20	50	100	200	50
Exp.	**Rep.**	**MRP3-Mediated $E_2$17G Uptake (pmol/min/mg protein)**						
1	1	176	194	134	118	61.4	57.8	46.3
1	2	215	133	122	74.9	63.8	49.3	49.3
1	3	181	ND	136	ND	59.2	44.0	43.6
Mean		191	164	131	96.6	61.5	50.4	46.4
SD		21.0	NC	7.88	NC	2.28	6.94	2.89
Exp.	**Rep.**	**MRP3-Mediated $E_2$17G Uptake (pmol/min/mg protein)**						
2	1	130	123	97.1	86.2	67.4	57.3	57.3
2	2	155	144	113	70.2	55.0	50.5	55.0
2	3	168	125	94.3	93.6	47.1	48.6	37.8
Mean		151	131	101	83.4	56.5	52.1	50.0
SD		19.2	11.7	10.0	11.9	10.3	4.58	10.6
Exp.	**Rep.**	***MRP3-Mediated $E_2$17G Uptake (pmol/min/mg protein)**						
3	1	15.5	11.1	9.87	10.6	7.35	2.06	1.59
3	2	14.8	10.1	9.64	7.59	6.07	6.94	0.802
3	3	11.6	10.4	12.0	6.65	6.29	3.11	ND
Mean		14.0	10.5	10.5	8.26	6.57	4.04	1.20
SD		2.09	0.497	1.29	2.04	0.682	2.57	NC
Exp.	**Rep.**	**MRP3-Mediated $E_2$17G Uptake (% of control)**						
1	1	92.4	102	70.4	62.1	32.2	30.3	24.3
1	2	113	69.6	63.8	39.3	33.5	25.9	25.9
1	3	94.9	ND	71.5	ND	31.1	23.1	22.9
Mean		100	85.8	68.6	50.7	32.2	26.4	24.3

SD		11.0	NC	4.14	16.1	1.20	3.64	1.52
Exp.	**Rep.**	**MRP3-Mediated $E_2$17G Uptake (% of control)**						
2	1	86.1	81.3	64.3	57.1	44.6	37.9	37.9
2	2	103	95.3	74.7	46.5	36.4	33.4	36.4
2	3	111	82.9	62.4	62.0	31.2	32.2	25.0
Mean		100	86.5	67.1	55.2	37.4	34.5	33.1
SD		12.7	7.71	6.63	7.91	6.80	3.03	7.04
Exp.	**Rep.**	***MRP3-Mediated $E_2$17G Uptake (% of control)**						
3	1	111	79.2	70.6	75.5	52.6	14.8	11.4
3	2	106	72.2	69.0	54.3	43.4	49.6	5.74
3	3	83.0	74.6	85.7	47.6	45.0	22.2	ND
Mean		100	75.3	75.1	59.1	47.0	28.9	8.57
SD		14.9	3.56	9.22	14.6	4.88	18.4	NC

10 µM substrate (^{3}H- $E_2$17G) and < 1% organic solvent; NC=not calculable; ND=not determined (sample processing error);*MRP3 lot number 12-Feb-2015 was used for experiment 3

Appendix Table 3.20 Effects of DM-4107 on MRP4-mediated ^{3}H-DHEAS Uptake

		DM-4107 (µM)						MK-571 (µM)
		0	10	20	50	100	200	50
Exp.	**Rep.**	**MRP4-Mediated DHEAS Uptake (pmol/min/mg protein)**						
1	1	164	139	109	57.2	38.5	23.4	7.57
1	2	124	122	61.6	67.2	36.8	20.9	7.21
1	3	121	107	108	68.3	34.4	15.7	3.29
Mean		136	123	93.0	64.3	36.6	20.0	6.02
SD		23.8	15.9	27.2	6.12	2.03	3.90	2.37
Exp.	**Rep.**	**MRP4-Mediated DHEAS Uptake (pmol/min/mg protein)**						
2	1	259	184	136	89.0	38.9	27.0	8.1
2	2	226	187	139	82.2	63.0	20.6	BQL (0)
2	3	220	172	134	88.4	49.2	19.0	BQL (0)
Mean		235	181	136	86.5	50.4	22.2	NC
SD		20.8	7.75	2.42	3.78	12.1	4.22	NC
Exp.	**Rep.**	**MRP4-Mediated DHEAS Uptake (pmol/min/mg protein)**						
3	1	186	149	119	92.4	63.5	32.3	8.71
3	2	175	189	127	70.2	40.1	18.5	8.82
3	3	152	131	108	64.6	24.8	30.0	BQL (0)
Mean		171	157	118	75.7	42.8	26.9	5.85
SD		17.5	29.8	9.37	14.7	19.5	7.43	5.06
Exp.	**Rep.**	**MRP4-Mediated DHEAS Uptake (% of control)**						
1	1	120	101	80.0	41.9	28.2	17.1	5.55
1	2	91.0	89.7	45.1	49.3	27.0	15.3	5.28
1	3	88.9	78.2	79.4	50.1	25.2	11.5	2.41
Mean		100	89.8	68.2	47.1	26.8	14.6	4.41

SD		17.4	11.7	20.0	4.49	1.49	2.86	1.74
Exp.	**Rep.**	**MRP4-Mediated DHEAS Uptake (% of control)**						
2	1	110	78.2	57.7	37.8	16.5	11.5	3.44
2	2	96.2	79.3	58.9	34.9	26.8	8.75	BQL (0)
2	3	93.7	73.2	56.8	37.6	20.9	8.07	BQL (0)
Mean		100	76.9	57.8	36.8	21.4	9.44	NC
SD		8.86	3.29	1.03	1.61	5.14	1.79	NC
Exp.	**Rep.**	**MRP4-Mediated DHEAS Uptake (% of control)**						
3	1	109	87.1	69.4	54.1	37.2	18.9	5.10
3	2	102	111	74.4	41.1	23.5	10.8	5.16
3	3	88.8	76.9	63.4	37.8	14.5	17.6	BQL (0)
Mean		100	91.6	69.1	44.3	25.0	15.8	3.42
SD		10.2	17.4	5.48	8.60	11.4	4.35	2.96

2 µM substrate (^{3}H- DHEAS) and < 1% organic solvent; BQL=below quantitation limit; NC=not calculable

Appendix Table 3.21 Time- and temperature-dependent accumulation of tolvaptan in SCHH.

Time (min)	TVP (μM)	Total Accumulation (pmol/mg)	Cell Accumulation (pmol/mg)	BEI	$CL_{biliary}$ (mL/min/kg)	Intracellular concentration (μM)
5	15	3670 ± 260	3710 ± 250	<0	<0	483
10	15	3880 ± 79	3750 ± 480	4.4	2.7	488
20	15	3250 ± 520	3050 ± 60	6.1	2.2	396
10*	15	2970 ± 320	2740 ± 200	7.7	4.6	357

Data represent mean ±SD (n=3 replicates); *incubated at 4^{o}C

Appendix Table 3.22 Time-dependent accumulation of tolvaptan, DM-4103, and DM-4107 in SCHH.

Time (min)	TVP (μM)	Species	Total Accumulation (pmol/mg)	Cell Accumulation (pmol/mg)	BEI	$CL_{biliary}$ (mL/min/kg)	Intracellular concentration (μM)
10	15	Tolvaptan	4240 ± 350	4080 ± 550	3.82	16.7	530 ± 71
		DM-4103	11.6 ± 1.6	13.3 ± 2.2	0	NC	1.71 ± 0.28
		DM-4107	206 ± 34	183 ± 36	10.9	NC	35.6 ± 4.6

Data represent mean ±SD (n=3 replicates); NC=not calculable

Appendix Table 3.23 Accumulation of TCA, CDCA, TCDCA, and GCDCA in the presence and absence of tolvaptan in SCHH

Species	TVP (μM)	Total Accumulation (pmol/mg)	Cell Accumulation (pmol/mg)	BEI	$CL_{biliary}$ (mL/min/kg)	Intracellular concentration (μM)
TCA	0	215 ± 27	43.3 ± 4.5	79.8	20.3	5.64 ± 0.58
	15	145 ± 16	47.5 ± 2.1	67.3	11.6	6.18 ± 2.77
CDCA	0	580 ± 67	469 ± 60	19.1	13.1	61 ± 7.83
	15	658 ± 86	608 ± 31	7.52	5.86	79.1± 4.0
TCDCA	0	3.37 ± 0.37	0.545 ± 0.049	83.8	NC	NC
	15	3.32 ± 0.26	0.915 ± 0.224	71.0	NC	NC
GCDCA	0	8.28 ± 0.98	0.892 ± 0.065	89.2	NC	NC
	15	7.55 ± 1.28	1.93 ± 0.28	74.5	NC	NC

Data represent mean ±SD (n=3 replicates); BEI=biliary excretion index; NC=not calculable

Appendix Table 5.1 CDF (nM) in Outflow Perfusate of Wild-type or PCK rats

	Wild-type (animal number)					PCK (animal number)				
Time (min)	1	2	3	4	5	1	2	3	4	5
2	851	908	927	852	871	811	929	890	922	910
5	874	932	899	847	881	841	982	941	900	964
10	881	939	897	939	892	815	933	845	925	966
15	903	963	903	901	889	885	967	934	920	939
20	905	965	899	928	920	847	892	934	1000	964
25	848	904	903	908	895	845	1000	935	876	948
30	883	942	891	918	894	913	932	819	951	910
32	55.5	59.7	161	20.2	64.70	299	179	177	110	202
34	21.7	23.3	46.90	7.54	BQL	58.8	44.5	24	32.3	44.7
36	15.3	16.4	24.30	6.06	12.94	38.8	27.3	13.2	13.7	26.7
38	11	11.7	11.30	4.48	11.99	27.4	20.3	8.31	7.70	23.9
40	8.66	9.26	8.42	3.14	9.92	18.6	15.4	6.93	5.57	19.6
42	6.62	7.1	5.29	3.12	8.53	18.3	11.9	5.55	3.96	9.39

	Wild-type (animal number)						PCK (animal number)				
	1	2	3	1	2	3	1	2	3	1	2
44	5.26	5.66	4.51	2.49	6.93		12	11	3.5	3.00	5.74
46	4.04	4.380	3.93	2.13	5.28		9.27	8.65	3.17	2.12	4.52
48	2.39	2.66	2.71	BQL	5.59		9.16	8.74	2.7	2.21	3.62
50	BQL	BQL	1.85	BQL	5.29		6.32	6.36	2.27	2.00	2.52
52	BQL	BQL	2.22	BQL	4.44		6.48	5.74	2.28	BQL	2.43
54	BQL	BQL	2.63	BQL	3.64		5.70	6.42	BQL	BQL	2.19
56	BQL	BQL	BQL	BQL	2.98		4.26	4.77	BQL	BQL	BQL
58	BQL	BQL	BQL	BQL	2.25		3.50	4.09	BQL	BQL	BQL
60	BQL	BQL	BQL	BQL	BQL		2.36	3.66	BQL	BQL	BQL

Below quantitation limit (BQL); missing value (MV)

Appendix Table 5.2 CDF (nM) in Bile of Wild-type or PCK rats

Time (min)	Healthy (animal number)					PCK (animal number)				
	1	2	3	4	5	1	2	3	4	5
2.5	636	672	346	29.0	12.0	24.0	2.97	24.9	18.2	28.5
7.5	8820	9240	13700	9750	7650	BQL	2.43	26.1	267	6.88
12.5	15800	16500	27800	23600	11100	BQL	3.21	22.3	551	24.7
17.5	24200	25300	44100	35900	41200	18.7	6.09	21.8	657	27.3
22.5	28200	29500	59000	46800	62200	9.61	9.98	22.1	561	17.4
27.5	27800	29100	64500	56000	76200	10.5	14.7	24.6	602	23.0
32.5	57900	60600	74500	94400	99700	14.6	13.1	28.0	592	42.9
37.5	47700	50000	53600	73700	99100	14.4	13.0	23.8	335	73.6
42.5	26500	27600	35500	72300	81000	12.2	12.1	28.0	241	125
47.5	12100	12700	21800	28500	40500	11.4	10.2	22.8	213	130
52.5	7490	7850	13500	13900	28100	10.2	9.68	24.8	170	111
57.5	5970	6260	9190	8600	20500	7.66	8.44	19.1	151	91.0

Below quantitation limit (BQL)

Appendix Table 5.3 Bile Flow Rate

Time (min)	Wild-type (animal number)					PCK (animal number)				
	1	2	3	4	5	1	2	3	4	5
2.5	1.22	1.36	0.561	0.653	0.793	0.37	0.713	0.789	0.619	0.619
7.5	1.47	1.64	0.473	0.604	0.734	0.417	0.646	0.801	0.59	0.590
12.5	1.08	1.21	0.668	0.582	0.707	0.447	0.735	0.857	0.612	0.612
17.5	1.18	1.32	0.749	0.781	0.994	0.440	0.734	0.845	0.518	0.518
22.5	1.35	1.51	0.680	0.689	0.710	0.408	0.713	0.783	0.785	0.785
27.5	1.11	1.25	0.795	0.850	1.03	0.364	0.766	0.699	0.756	0.756
32.5	1.13	1.26	0.698	0.746	0.894	0.367	0.654	0.705	0.713	0.713
37.5	0.972	1.09	0.802	0.719	0.863	0.331	0.625	0.635	0.683	0.683
42.5	1.04	1.16	0.702	0.621	0.717	0.307	0.495	0.589	0.770	0.770
47.5	1.21	1.34	0.724	0.714	0.842	0.449	0.597	0.861	0.711	0.711
52.5	1.15	1.28	0.688	0.552	0.670	0.368	0.543	0.706	0.676	0.676
57.5	1.09	1.21	0.741	0.625	0.760	0.369	0.589	0.709	0.639	0.639

Data expressed as μL/min/g liver

Appendix Table 5.4 Rat Physiological Parameters

	Wild-type (animal number)					PCK (animal number)				
	1	2	3	4	5	1	2	3	4	5
Body weight (g)	525	534	564	542	532	494	506	572	558	548
Liver weight (g)	18.4	17.3	16.4	23.0	15.4	55.0	48.5	28.7	27.9	37.5
Total Kidney weight (g)	3.01	2.88	2.98	4.06	3.02	5.70	7.45	5.26	5.19	6.07

Appendix Table 5.5 Simulated Bile Rate (nmol/min)

Time (min)	Control	Scenario 1	Scenario 2	Scenario 3	Scenario 4	Scenario 5	Scenario 6	Scenario 7
0.27252	0.0000000	0.0000000	0.0000000	0.0000000	0.0000000	0.0000000	0.0000000	0.0000000
1.02252	0.0000000	0.0000000	0.0000000	0.0000000	0.0000000	0.0000000	0.0000000	0.0000000
1.77252	2.58E-09	2.46E-09	2.58E-09	2.58E-09	3.03E-09	1.61E-09	1.29E-09	3.28E-11
2.52252	2.58E-05	2.46E-05	2.58E-05	2.58E-05	3.03E-05	1.61E-05	1.29E-05	3.28E-07
2.58258	0.002754	0.002236	0.001786	0.000786	5.63E-05	0.001115	0.000393	9.99E-06
2.64264	0.00512	0.004157	0.00332	0.001461	8.23E-05	0.002072	0.000731	1.86E-05
2.7027	0.007486	0.006078	0.004853	0.002136	0.000108	0.003029	0.001069	2.72E-05
2.76276	0.009853	0.008	0.006388	0.002811	0.000134	0.003987	0.001407	3.57E-05
2.82282	0.012219	0.009921	0.007922	0.003487	0.00016	0.004944	0.001745	4.43E-05
2.88288	0.014585	0.011842	0.009456	0.004162	0.000186	0.005901	0.002083	5.29E-05
2.94294	0.016952	0.013764	0.010991	0.004837	0.000212	0.006859	0.002421	6.15E-05
3.003	0.019318	0.015685	0.012525	0.005512	0.000238	0.007817	0.002759	7.01E-05
3.06306	0.021685	0.017607	0.014059	0.006188	0.000264	0.008774	0.003097	7.87E-05
3.12312	0.024051	0.019528	0.015593	0.006863	0.00029	0.009732	0.003435	8.72E-05
3.18318	0.026417	0.021449	0.017127	0.007538	0.000316	0.010689	0.003773	9.58E-05
3.24324	0.028784	0.02337	0.018662	0.008213	0.000342	0.011647	0.004111	0.000104
3.3033	0.03115	0.025291	0.020196	0.008888	0.000368	0.012604	0.004448	0.000113
3.36336	0.033516	0.027212	0.02173	0.009564	0.000394	0.013562	0.004787	0.000122
3.42342	0.035883	0.029134	0.023264	0.010239	0.00042	0.014519	0.005125	0.00013
3.48348	0.038249	0.031055	0.024798	0.010914	0.000446	0.015476	0.005462	0.000139
3.54354	0.040615	0.032976	0.026332	0.011589	0.000472	0.016434	0.0058	0.000147
3.6036	0.042982	0.034898	0.027867	0.012265	0.000498	0.017392	0.006139	0.000156
3.66366	0.045348	0.036819	0.029401	0.01294	0.000524	0.018349	0.006476	0.000165
3.72372	0.047715	0.038741	0.030936	0.013615	0.00055	0.019307	0.006814	0.000173
3.78378	0.050081	0.040662	0.03247	0.01429	0.000576	0.020265	0.007152	0.000182
3.84384	0.052447	0.042583	0.034004	0.014965	0.000602	0.021222	0.00749	0.00019
3.9039	0.054814	0.044505	0.035538	0.015641	0.000628	0.022179	0.007828	0.000199
3.96396	0.05718	0.046426	0.037072	0.016316	0.000654	0.023137	0.008166	0.000207
4.02402	0.059546	0.048347	0.038606	0.016991	0.00068	0.024094	0.008504	0.000216
4.08408	0.061913	0.050268	0.040141	0.017666	0.000706	0.025052	0.008842	0.000225
4.14414	0.064279	0.052189	0.041675	0.018342	0.000732	0.026009	0.00918	0.000233
4.2042	0.066645	0.05411	0.043209	0.019017	0.000758	0.026967	0.009518	0.000242
4.26426	0.069012	0.056032	0.044743	0.019692	0.000784	0.027924	0.009856	0.00025
4.32432	0.071378	0.057953	0.046277	0.020367	0.00081	0.028881	0.010194	0.000259
4.38438	0.073745	0.059875	0.047812	0.021043	0.000836	0.029839	0.010532	0.000268
4.44444	0.076111	0.061796	0.049346	0.021718	0.000862	0.030797	0.01087	0.000276
4.5045	0.078477	0.063717	0.05088	0.022393	0.000888	0.031754	0.011208	0.000285
4.56456	0.080844	0.065639	0.052415	0.023068	0.000914	0.032712	0.011546	0.000293
4.62462	0.08321	0.06756	0.053949	0.023743	0.00094	0.03367	0.011883	0.000302
4.68468	0.085576	0.069481	0.055483	0.024418	0.000966	0.034627	0.012221	0.00031
4.74474	0.087943	0.071403	0.057017	0.025094	0.000992	0.035584	0.01256	0.000319
4.8048	0.090309	0.073324	0.058551	0.025769	0.001018	0.036542	0.012897	0.000328
4.86486	0.092675	0.075245	0.060085	0.026444	0.001044	0.037499	0.013235	0.000336
4.92492	0.095042	0.077167	0.06162	0.02712	0.00107	0.038457	0.013574	0.000345
4.98498	0.097408	0.079088	0.063154	0.027795	0.001096	0.039414	0.013911	0.000353
5.04505	0.099775	0.081009	0.064688	0.02847	0.001122	0.040372	0.014249	0.000362
5.10511	0.102141	0.08293	0.066222	0.029145	0.001148	0.041329	0.014587	0.000371
5.16517	0.104508	0.084852	0.067757	0.029821	0.001174	0.042287	0.014925	0.000379
5.22523	0.106874	0.086773	0.069291	0.030496	0.0012	0.043245	0.015263	0.000388
5.28529	0.10924	0.088694	0.070825	0.031171	0.001226	0.044202	0.015601	0.000396
5.34535	0.111607	0.090616	0.07236	0.031846	0.001252	0.04516	0.015939	0.000405
5.40541	0.113973	0.092537	0.073894	0.032521	0.001278	0.046117	0.016277	0.000413
5.46547	0.11634	0.094459	0.075428	0.033197	0.001304	0.047075	0.016615	0.000422
5.52553	0.118706	0.09638	0.076962	0.033872	0.00133	0.048032	0.016953	0.000431
5.58559	0.121072	0.098301	0.078496	0.034547	0.001356	0.048989	0.017291	0.000439
5.64565	0.123439	0.100223	0.080031	0.035222	0.001382	0.049947	0.017629	0.000448

5.70571	0.125805	0.102144	0.081565	0.035897	0.001408	0.050905	0.017966	0.000456
5.76577	0.128171	0.104065	0.083099	0.036573	0.001434	0.051862	0.018305	0.000465
5.82583	0.130538	0.105987	0.084633	0.037248	0.00146	0.052819	0.018643	0.000474
5.88589	0.132904	0.107908	0.086167	0.037923	0.001486	0.053777	0.01898	0.000482
5.94595	0.13527	0.109829	0.087701	0.038598	0.001512	0.054734	0.019318	0.000491
6.00601	0.137637	0.11175	0.089236	0.039274	0.001538	0.055692	0.019657	0.000499
6.06607	0.140003	0.113671	0.09077	0.039949	0.001565	0.05665	0.019994	0.000508
6.12613	0.14237	0.115593	0.092304	0.040624	0.001591	0.057607	0.020332	0.000516
6.18619	0.144736	0.117514	0.093838	0.041299	0.001617	0.058564	0.02067	0.000525
6.24625	0.147102	0.119435	0.095372	0.041974	0.001643	0.059522	0.021008	0.000534
6.30631	0.149469	0.121357	0.096907	0.04265	0.001669	0.06048	0.021346	0.000542
6.36637	0.151835	0.123278	0.098441	0.043325	0.001695	0.061437	0.021684	0.000551
6.42643	0.154201	0.125199	0.099975	0.044	0.001721	0.062394	0.022022	0.000559
6.48649	0.156568	0.127121	0.10151	0.044675	0.001747	0.063352	0.02236	0.000568
6.54655	0.158934	0.129042	0.103044	0.045351	0.001773	0.06431	0.022698	0.000577
6.60661	0.1613	0.130963	0.104578	0.046026	0.001799	0.065267	0.023036	0.000585
6.66667	0.163667	0.132885	0.106112	0.046701	0.001825	0.066225	0.023374	0.000594
6.72673	0.166033	0.134806	0.107646	0.047376	0.001851	0.067182	0.023712	0.000602
6.78679	0.1684	0.136728	0.109181	0.048052	0.001877	0.06814	0.02405	0.000611
6.84685	0.170766	0.138649	0.110715	0.048727	0.001903	0.069097	0.024388	0.000619
6.90691	0.173132	0.14057	0.112249	0.049402	0.001929	0.070055	0.024726	0.000628
6.96697	0.175499	0.142491	0.113783	0.050077	0.001955	0.071012	0.025064	0.000637
7.02703	0.177865	0.144412	0.115317	0.050752	0.001981	0.071969	0.025401	0.000645
7.08709	0.180231	0.146333	0.116851	0.051428	0.002007	0.072927	0.02574	0.000654
7.14715	0.182598	0.148255	0.118386	0.052103	0.002033	0.073885	0.026078	0.000662
7.20721	0.184964	0.150176	0.11992	0.052778	0.002059	0.074842	0.026415	0.000671
7.26727	0.18733	0.152097	0.121454	0.053453	0.002085	0.075799	0.026753	0.00068
7.32733	0.189697	0.154019	0.122989	0.054129	0.002111	0.076757	0.027092	0.000688
7.38739	0.192063	0.15594	0.124523	0.054804	0.002137	0.077715	0.027429	0.000697
7.44745	0.19443	0.157862	0.126057	0.055479	0.002159	0.078672	0.027767	0.000705
7.50751	0.196491	0.159535	0.127393	0.056067	0.002185	0.079506	0.028062	0.000713
7.56757	0.198822	0.161428	0.128905	0.056732	0.00221	0.08045	0.028394	0.000721
7.62763	0.201152	0.16332	0.130415	0.057397	0.002236	0.081392	0.028727	0.00073
7.68769	0.203482	0.165211	0.131926	0.058062	0.002262	0.082335	0.02906	0.000738
7.74775	0.205813	0.167104	0.133437	0.058727	0.002287	0.083278	0.029393	0.000747
7.80781	0.208143	0.168996	0.134948	0.059392	0.002313	0.084221	0.029726	0.000755
7.86787	0.210473	0.170888	0.136459	0.060057	0.002339	0.085164	0.030059	0.000763
7.92793	0.212804	0.17278	0.13797	0.060722	0.002364	0.086107	0.030391	0.000772
7.98799	0.215134	0.174672	0.13948	0.061387	0.00239	0.087049	0.030724	0.00078
8.04805	0.217464	0.176564	0.140991	0.062052	0.002415	0.087992	0.031057	0.000789
8.10811	0.219795	0.178456	0.142502	0.062717	0.002441	0.088935	0.03139	0.000797
8.16817	0.222125	0.180348	0.144013	0.063382	0.002467	0.089879	0.031723	0.000806
8.22823	0.224455	0.18224	0.145524	0.064047	0.002492	0.090822	0.032056	0.000814
8.28829	0.226786	0.184132	0.147035	0.064712	0.002518	0.091765	0.032388	0.000823
8.34835	0.229116	0.186024	0.148546	0.065376	0.002543	0.092708	0.032721	0.000831
8.40841	0.231446	0.187916	0.150056	0.066041	0.002569	0.09365	0.033054	0.00084
8.46847	0.233777	0.189809	0.151568	0.066706	0.002595	0.094594	0.033386	0.000848
8.52853	0.236107	0.1917	0.153078	0.067371	0.00262	0.095536	0.033719	0.000856
8.58859	0.238437	0.193592	0.154589	0.068036	0.002646	0.096479	0.034052	0.000865
8.64865	0.240768	0.195485	0.1561	0.068701	0.002671	0.097422	0.034385	0.000873
8.70871	0.243098	0.197376	0.157611	0.069366	0.002697	0.098365	0.034718	0.000882
8.76877	0.245428	0.199268	0.159121	0.070031	0.002723	0.099307	0.035051	0.00089
8.82883	0.247759	0.201161	0.160633	0.070696	0.002748	0.100251	0.035383	0.000899
8.88889	0.250089	0.203053	0.162143	0.071361	0.002774	0.101193	0.035716	0.000907
8.94895	0.252419	0.204944	0.163654	0.072026	0.002799	0.102137	0.036049	0.000916
9.00901	0.25475	0.206837	0.165165	0.072691	0.002825	0.10308	0.036382	0.000924
9.06907	0.25708	0.208729	0.166676	0.073356	0.002851	0.104023	0.036715	0.000933
9.12913	0.25941	0.21062	0.168186	0.074021	0.002876	0.104965	0.037048	0.000941
9.18919	0.261741	0.212513	0.169698	0.074686	0.002902	0.105909	0.03738	0.000949

9.24925	0.264071	0.214405	0.171208	0.075351	0.002927	0.106851	0.037713	0.000958
9.30931	0.266401	0.216297	0.172719	0.076015	0.002953	0.107794	0.038046	0.000966
9.36937	0.268732	0.218189	0.17423	0.076681	0.002979	0.108737	0.038379	0.000975
9.42943	0.271062	0.220081	0.175741	0.077345	0.003004	0.10968	0.038711	0.000983
9.48949	0.273392	0.221973	0.177252	0.07801	0.00303	0.110623	0.039044	0.000992
9.54955	0.275723	0.223865	0.178763	0.078675	0.003056	0.111566	0.039377	0.001
9.60961	0.278053	0.225757	0.180274	0.07934	0.003081	0.112509	0.03971	0.001009
9.66967	0.280383	0.227649	0.181784	0.080005	0.003107	0.113451	0.040043	0.001017
9.72973	0.282714	0.229542	0.183295	0.08067	0.003132	0.114394	0.040375	0.001026
9.78979	0.285044	0.231433	0.184806	0.081335	0.003158	0.115337	0.040708	0.001034
9.84985	0.287374	0.233325	0.186317	0.082	0.003184	0.11628	0.041041	0.001042
9.90991	0.289705	0.235218	0.187828	0.082665	0.003209	0.117224	0.041374	0.001051
9.96997	0.292035	0.237109	0.189339	0.08333	0.003235	0.118167	0.041707	0.001059
10.03	0.294364	0.239	0.190849	0.083995	0.00326	0.119109	0.04204	0.001068
10.0901	0.296696	0.240894	0.192361	0.08466	0.003286	0.120053	0.042372	0.001076
10.1502	0.299028	0.242787	0.193873	0.085325	0.003312	0.120996	0.042705	0.001085
10.2102	0.301356	0.244677	0.195382	0.08599	0.003337	0.121938	0.043038	0.001093
10.2703	0.303688	0.246571	0.196894	0.086655	0.003363	0.122882	0.043371	0.001102
10.3303	0.306016	0.248461	0.198403	0.087319	0.003388	0.123823	0.043703	0.00111
10.3904	0.308348	0.250354	0.199915	0.087985	0.003414	0.124767	0.044036	0.001119
10.4505	0.310679	0.252247	0.201426	0.08865	0.00344	0.12571	0.044369	0.001127
10.5105	0.313007	0.254137	0.202936	0.089314	0.003465	0.126652	0.044702	0.001135
10.5706	0.315339	0.25603	0.204448	0.08998	0.003491	0.127596	0.045035	0.001144
10.6306	0.317667	0.25792	0.205957	0.090644	0.003516	0.128538	0.045367	0.001152
10.6907	0.319999	0.259814	0.207469	0.091309	0.003542	0.129481	0.0457	0.001161
10.7508	0.322331	0.261707	0.208981	0.091975	0.003568	0.130425	0.046033	0.001169
10.8108	0.324659	0.263597	0.21049	0.092639	0.003593	0.131367	0.046366	0.001178
10.8709	0.326991	0.265491	0.212002	0.093304	0.003619	0.132311	0.046699	0.001186
10.9309	0.329319	0.267381	0.213511	0.093969	0.003645	0.133252	0.047031	0.001195
10.991	0.331651	0.269274	0.215023	0.094634	0.00367	0.134196	0.047364	0.001203
11.0511	0.333983	0.271168	0.216535	0.095299	0.003696	0.13514	0.047697	0.001212
11.1111	0.336311	0.273058	0.218045	0.095964	0.003721	0.136082	0.04803	0.00122
11.1712	0.338643	0.274951	0.219557	0.096629	0.003747	0.137026	0.048363	0.001228
11.2312	0.340971	0.276842	0.221066	0.097293	0.003773	0.137967	0.048695	0.001237
11.2913	0.343302	0.278734	0.222577	0.097959	0.003798	0.13891	0.049028	0.001245
11.3514	0.345634	0.280628	0.224089	0.098624	0.003824	0.139854	0.049361	0.001254
11.4114	0.347962	0.282518	0.225598	0.099288	0.003849	0.140796	0.049694	0.001262
11.4715	0.350294	0.284411	0.22711	0.099954	0.003875	0.141739	0.050027	0.001271
11.5315	0.352622	0.286301	0.22862	0.100618	0.003901	0.142682	0.050359	0.001279
11.5916	0.354954	0.288195	0.230132	0.101283	0.003926	0.143625	0.050692	0.001288
11.6517	0.357286	0.290088	0.231644	0.101949	0.003952	0.144569	0.051025	0.001296
11.7117	0.359614	0.291978	0.233153	0.102613	0.003977	0.145511	0.051358	0.001304
11.7718	0.361946	0.293872	0.234665	0.103279	0.004003	0.146454	0.051691	0.001313
11.8318	0.364274	0.295762	0.236174	0.103943	0.004029	0.147396	0.052023	0.001321
11.8919	0.366606	0.297655	0.237686	0.104608	0.004054	0.14834	0.052356	0.00133
11.952	0.368938	0.299548	0.239198	0.105274	0.00408	0.149284	0.05269	0.001338
12.012	0.371266	0.301439	0.240707	0.105938	0.004105	0.150225	0.053022	0.001347
12.0721	0.373597	0.303331	0.242219	0.106603	0.004131	0.151169	0.053355	0.001355
12.1321	0.375925	0.305221	0.243728	0.107267	0.004157	0.152111	0.053687	0.001364
12.1922	0.378257	0.307115	0.24524	0.107933	0.004182	0.153054	0.05402	0.001372
12.2523	0.380589	0.309008	0.246752	0.108598	0.004208	0.153998	0.054353	0.001381
12.3123	0.382917	0.310898	0.248261	0.109262	0.004234	0.15494	0.054686	0.001389
12.3724	0.385249	0.312792	0.249773	0.109928	0.004259	0.155883	0.055019	0.001397
12.4324	0.387577	0.314682	0.251283	0.110592	0.004285	0.156826	0.055351	0.001406
12.4925	0.389909	0.316575	0.252794	0.111258	0.00431	0.157769	0.055685	0.001414
12.5526	0.392241	0.318469	0.254306	0.111923	0.004336	0.158712	0.056017	0.001423
12.6126	0.394569	0.320359	0.255816	0.112587	0.004362	0.159655	0.05635	0.001431
12.6727	0.396901	0.322252	0.257328	0.113253	0.004387	0.160598	0.056683	0.00144
12.7327	0.399229	0.324142	0.258837	0.113917	0.004413	0.16154	0.057015	0.001448

12.7928	0.401561	0.326036	0.260349	0.114582	0.004438	0.162484	0.057348	0.001457
12.8529	0.403893	0.327929	0.261861	0.115248	0.004464	0.163428	0.057682	0.001465
12.9129	0.406221	0.329819	0.26337	0.115912	0.00449	0.164369	0.058014	0.001474
12.973	0.408552	0.331712	0.264882	0.116577	0.004515	0.165313	0.058347	0.001482
13.033	0.41088	0.333602	0.266391	0.117241	0.004541	0.166255	0.058679	0.00149
13.0931	0.413212	0.335496	0.267903	0.117907	0.004566	0.167198	0.059012	0.001499
13.1532	0.415544	0.337389	0.269415	0.118572	0.004592	0.168142	0.059345	0.001507
13.2132	0.417872	0.339279	0.270924	0.119237	0.004618	0.169084	0.059678	0.001516
13.2733	0.420204	0.341172	0.272436	0.119902	0.004643	0.170027	0.060011	0.001524
13.3333	0.422532	0.343063	0.273945	0.120566	0.004669	0.170969	0.060343	0.001533
13.3934	0.424864	0.344956	0.275457	0.121232	0.004694	0.171913	0.060677	0.001541
13.4535	0.427196	0.346849	0.276969	0.121897	0.00472	0.172856	0.061009	0.00155
13.5135	0.429524	0.34874	0.278479	0.122561	0.004746	0.173799	0.061342	0.001558
13.5736	0.431856	0.350633	0.279991	0.123227	0.004771	0.174742	0.061675	0.001567
13.6336	0.434184	0.352523	0.2815	0.123891	0.004797	0.175684	0.062007	0.001575
13.6937	0.436516	0.354417	0.283012	0.124556	0.004822	0.176628	0.06234	0.001583
13.7538	0.438847	0.356309	0.284523	0.125222	0.004848	0.177571	0.062674	0.001592
13.8138	0.441175	0.358199	0.286032	0.125886	0.004874	0.178513	0.063006	0.0016
13.8739	0.443507	0.360093	0.287544	0.126551	0.004899	0.179456	0.063339	0.001609
13.9339	0.445835	0.361983	0.289054	0.127216	0.004925	0.180399	0.063672	0.001617
13.994	0.448167	0.363876	0.290566	0.127881	0.004951	0.181342	0.064004	0.001626
14.0541	0.450499	0.36577	0.292078	0.128546	0.004976	0.182286	0.064337	0.001634
14.1141	0.452827	0.36766	0.293587	0.129211	0.005002	0.183228	0.06467	0.001643
14.1742	0.455159	0.369553	0.295099	0.129876	0.005027	0.184171	0.065003	0.001651
14.2342	0.457487	0.371443	0.296608	0.13054	0.005053	0.185113	0.065335	0.00166
14.2943	0.459819	0.373337	0.29812	0.131206	0.005079	0.186057	0.065669	0.001668
14.3544	0.462151	0.37523	0.299632	0.131871	0.005104	0.187	0.066001	0.001676
14.4144	0.464479	0.37712	0.301141	0.132536	0.00513	0.187942	0.066334	0.001685
14.4745	0.466811	0.379014	0.302653	0.133201	0.005155	0.188886	0.066667	0.001693
14.5345	0.469139	0.380904	0.304163	0.133865	0.005181	0.189828	0.066999	0.001702
14.5946	0.47147	0.382796	0.305674	0.13453	0.005207	0.190771	0.067332	0.00171
14.6547	0.473802	0.38469	0.307186	0.135196	0.005232	0.191715	0.067666	0.001719
14.7147	0.47613	0.38658	0.308695	0.13586	0.005258	0.192657	0.067998	0.001727
14.7748	0.478462	0.388473	0.310207	0.136525	0.005283	0.1936	0.068331	0.001736
14.8348	0.48079	0.390363	0.311716	0.13719	0.005309	0.194542	0.068664	0.001744
14.8949	0.483122	0.392257	0.313228	0.137855	0.005335	0.195486	0.068996	0.001753
14.955	0.485454	0.39415	0.31474	0.138521	0.00536	0.196429	0.06933	0.001761
15.015	0.487782	0.39604	0.31625	0.139185	0.005386	0.197372	0.069662	0.001769
15.0751	0.490114	0.397934	0.317762	0.13985	0.005411	0.198315	0.069995	0.001778
15.1351	0.492442	0.399824	0.319271	0.140515	0.005437	0.199257	0.070328	0.001786
15.1952	0.494774	0.401717	0.320783	0.14118	0.005463	0.200201	0.070661	0.001795
15.2553	0.497106	0.403611	0.322295	0.141845	0.005488	0.201144	0.070993	0.001803
15.3153	0.499434	0.405501	0.323804	0.14251	0.005514	0.202086	0.071326	0.001812
15.3754	0.501766	0.407394	0.325316	0.143175	0.005539	0.20303	0.071659	0.00182
15.4354	0.504094	0.409284	0.326825	0.143839	0.005565	0.203972	0.071991	0.001829
15.4955	0.506425	0.411177	0.328337	0.144504	0.005591	0.204915	0.072324	0.001837
15.5556	0.508757	0.413071	0.329849	0.14517	0.005616	0.205859	0.072658	0.001846
15.6156	0.511085	0.414961	0.331358	0.145834	0.005642	0.206801	0.07299	0.001854
15.6757	0.513417	0.416854	0.33287	0.1465	0.005668	0.207744	0.073323	0.001862
15.7357	0.515745	0.418744	0.334379	0.147164	0.005693	0.208686	0.073656	0.001871
15.7958	0.518077	0.420638	0.335891	0.147829	0.005719	0.20963	0.073988	0.001879
15.8559	0.520409	0.422531	0.337403	0.148495	0.005744	0.210573	0.074322	0.001888
15.9159	0.522737	0.424421	0.338913	0.149159	0.00577	0.211516	0.074654	0.001896
15.976	0.525069	0.426315	0.340424	0.149824	0.005796	0.212459	0.074987	0.001905
16.036	0.527397	0.428205	0.341934	0.150489	0.005821	0.213401	0.07532	0.001913
16.0961	0.529729	0.430098	0.343446	0.151154	0.005847	0.214345	0.075653	0.001922
16.1562	0.532061	0.431992	0.344958	0.15182	0.005872	0.215288	0.075986	0.00193
16.2162	0.534389	0.433882	0.346467	0.152484	0.005898	0.21623	0.076318	0.001938
16.2763	0.53672	0.435774	0.347978	0.153149	0.005924	0.217173	0.076651	0.001947

16.3363	0.539048	0.437664	0.349488	0.153813	0.005949	0.218116	0.076983	0.001955
16.3964	0.54138	0.439558	0.351	0.154479	0.005975	0.219059	0.077317	0.001964
16.4565	0.543712	0.441451	0.352511	0.155144	0.006	0.220002	0.07765	0.001972
16.5165	0.54604	0.443341	0.354021	0.155808	0.006026	0.220945	0.077982	0.001981
16.5766	0.548372	0.445235	0.355533	0.156474	0.006052	0.221888	0.078315	0.001989
16.6366	0.5507	0.447125	0.357042	0.157138	0.006077	0.22283	0.078648	0.001998
16.6967	0.553032	0.449018	0.358554	0.157803	0.006103	0.223774	0.07898	0.002006
16.7568	0.555364	0.450912	0.360066	0.158469	0.006128	0.224717	0.079314	0.002015
16.8168	0.557692	0.452802	0.361575	0.159133	0.006154	0.225659	0.079646	0.002023
16.8769	0.560024	0.454695	0.363087	0.159799	0.00618	0.226603	0.079979	0.002031
16.9369	0.562352	0.456585	0.364597	0.160463	0.006205	0.227545	0.080312	0.00204
16.997	0.564684	0.458479	0.366109	0.161128	0.006231	0.228489	0.080645	0.002048
17.0571	0.567015	0.460371	0.36762	0.161793	0.006257	0.229432	0.080977	0.002057
17.1171	0.569343	0.462262	0.369129	0.162458	0.006282	0.230373	0.08131	0.002065
17.1772	0.571675	0.464155	0.370641	0.163123	0.006308	0.231317	0.081643	0.002074
17.2372	0.574003	0.466045	0.37215	0.163787	0.006333	0.232259	0.081975	0.002082
17.2973	0.576335	0.467938	0.373662	0.164453	0.006359	0.233203	0.082309	0.002091
17.3574	0.578667	0.469832	0.375174	0.165118	0.006385	0.234146	0.082642	0.002099
17.4174	0.580995	0.471722	0.376684	0.165782	0.00641	0.235089	0.082974	0.002108
17.4775	0.583327	0.473615	0.378196	0.166448	0.006436	0.236032	0.083307	0.002116
17.5375	0.585655	0.475506	0.379705	0.167112	0.006461	0.236974	0.08364	0.002124
17.5976	0.587987	0.477399	0.381217	0.167778	0.006487	0.237918	0.083973	0.002133
17.6577	0.590319	0.479292	0.382729	0.168443	0.006513	0.238861	0.084306	0.002141
17.7177	0.592647	0.481183	0.384238	0.169107	0.006538	0.239803	0.084638	0.00215
17.7778	0.594979	0.483076	0.38575	0.169773	0.006564	0.240747	0.084971	0.002158
17.8378	0.597307	0.484966	0.387259	0.170437	0.006589	0.241688	0.085304	0.002167
17.8979	0.599639	0.486859	0.388771	0.171102	0.006615	0.242632	0.085637	0.002175
17.958	0.60197	0.488752	0.390283	0.171768	0.006641	0.243576	0.08597	0.002184
18.018	0.604298	0.490642	0.391792	0.172432	0.006666	0.244517	0.086302	0.002192
18.0781	0.60663	0.492536	0.393304	0.173097	0.006692	0.245461	0.086635	0.002201
18.1381	0.608958	0.494426	0.394813	0.173762	0.006717	0.246403	0.086968	0.002209
18.1982	0.61129	0.496319	0.396325	0.174427	0.006743	0.247346	0.087301	0.002217
18.2583	0.613622	0.498213	0.397837	0.175092	0.006769	0.24829	0.087634	0.002226
18.3183	0.61595	0.500103	0.399346	0.175757	0.006794	0.249232	0.087966	0.002234
18.3784	0.618282	0.501996	0.400858	0.176422	0.00682	0.250176	0.088299	0.002243
18.4384	0.62061	0.503886	0.402368	0.177086	0.006846	0.251118	0.088632	0.002251
18.4985	0.622942	0.50578	0.40388	0.177752	0.006871	0.252062	0.088965	0.00226
18.5586	0.625274	0.507673	0.405392	0.178417	0.006897	0.253005	0.089298	0.002268
18.6186	0.627602	0.509563	0.406901	0.179081	0.006922	0.253947	0.08963	0.002277
18.6787	0.629934	0.511457	0.408413	0.179747	0.006948	0.254891	0.089963	0.002285
18.7387	0.632262	0.513347	0.409922	0.180411	0.006974	0.255832	0.090296	0.002294
18.7988	0.634593	0.515239	0.411433	0.181076	0.006999	0.256775	0.090629	0.002302
18.8589	0.636925	0.517133	0.412945	0.181742	0.007025	0.257719	0.090962	0.00231
18.9189	0.639253	0.519023	0.414455	0.182406	0.00705	0.258661	0.091294	0.002319
18.979	0.641585	0.520916	0.415967	0.183071	0.007076	0.259605	0.091627	0.002327
19.039	0.643913	0.522807	0.417476	0.183736	0.007102	0.260547	0.09196	0.002336
19.0991	0.646245	0.5247	0.418988	0.184401	0.007127	0.26149	0.092293	0.002344
19.1592	0.648577	0.526593	0.4205	0.185066	0.007153	0.262434	0.092626	0.002353
19.2192	0.650905	0.528484	0.422009	0.185731	0.007178	0.263376	0.092958	0.002361
19.2793	0.653237	0.530377	0.423521	0.186396	0.007204	0.264319	0.093291	0.00237
19.3393	0.655565	0.532267	0.425031	0.18706	0.00723	0.265262	0.093624	0.002378
19.3994	0.657897	0.53416	0.426542	0.187726	0.007255	0.266205	0.093957	0.002387
19.4595	0.660229	0.536054	0.428054	0.188391	0.007281	0.267149	0.09429	0.002395
19.5195	0.662557	0.537944	0.429564	0.189056	0.007306	0.268091	0.094623	0.002403
19.5796	0.664888	0.539837	0.431075	0.189721	0.007332	0.269034	0.094955	0.002412
19.6396	0.667216	0.541727	0.432584	0.190385	0.007358	0.269976	0.095288	0.00242
19.6997	0.669548	0.54362	0.434096	0.19105	0.007383	0.270919	0.095621	0.002429
19.7598	0.67188	0.545514	0.435608	0.191716	0.007409	0.271863	0.095954	0.002437
19.8198	0.674208	0.547404	0.437118	0.19238	0.007435	0.272805	0.096286	0.002446

19.8799	0.67654	0.549297	0.438629	0.193046	0.00746	0.273748	0.09662	0.002454
19.9399	0.678868	0.551187	0.440139	0.19371	0.007486	0.274691	0.096952	0.002463
20	0.6812	0.553081	0.441651	0.194375	0.007511	0.275634	0.097285	0.002471
20.0601	0.683532	0.554974	0.443163	0.195041	0.007537	0.276578	0.097618	0.002479
20.1201	0.68586	0.556864	0.444672	0.195705	0.007563	0.27752	0.09795	0.002488
20.1802	0.688192	0.558758	0.446184	0.19637	0.007588	0.278463	0.098283	0.002496
20.2402	0.69052	0.560648	0.447693	0.197035	0.007614	0.279405	0.098616	0.002505
20.3003	0.692852	0.562541	0.449205	0.1977	0.007639	0.280349	0.098949	0.002513
20.3604	0.695184	0.564435	0.450717	0.198365	0.007665	0.281293	0.099282	0.002522
20.4204	0.697512	0.566325	0.452227	0.19903	0.007691	0.282235	0.099615	0.00253
20.4805	0.699843	0.568217	0.453738	0.199695	0.007716	0.283178	0.099947	0.002539
20.5405	0.702171	0.570107	0.455247	0.200359	0.007742	0.28412	0.10028	0.002547
20.6006	0.704503	0.572001	0.456759	0.201025	0.007767	0.285063	0.100613	0.002556
20.6607	0.706835	0.573894	0.458271	0.20169	0.007793	0.286007	0.100946	0.002564
20.7207	0.709163	0.575784	0.45978	0.202354	0.007819	0.286949	0.101278	0.002572
20.7808	0.711495	0.577678	0.461292	0.20302	0.007844	0.287892	0.101612	0.002581
20.8408	0.713823	0.579568	0.462802	0.203684	0.00787	0.288835	0.101944	0.002589
20.9009	0.716155	0.581461	0.464314	0.204349	0.007895	0.289778	0.102277	0.002598
20.961	0.718487	0.583355	0.465826	0.205015	0.007921	0.290722	0.10261	0.002606
21.021	0.720815	0.585245	0.467335	0.205679	0.007947	0.291664	0.102942	0.002615
21.0811	0.723147	0.587138	0.468847	0.206344	0.007972	0.292607	0.103275	0.002623
21.1411	0.725475	0.589028	0.470356	0.207009	0.007998	0.293549	0.103608	0.002632
21.2012	0.727807	0.590922	0.471868	0.207674	0.008023	0.294493	0.103941	0.00264
21.2613	0.730138	0.592814	0.473379	0.208339	0.008049	0.295436	0.104274	0.002649
21.3213	0.732466	0.594704	0.474889	0.209004	0.008075	0.296378	0.104607	0.002657
21.3814	0.734798	0.596598	0.476401	0.209669	0.0081	0.297322	0.104939	0.002665
21.4414	0.737126	0.598488	0.47791	0.210333	0.008126	0.298264	0.105272	0.002674
21.5015	0.739458	0.600381	0.479422	0.210999	0.008152	0.299207	0.105605	0.002682
21.5616	0.74179	0.602275	0.480934	0.211664	0.008177	0.300151	0.105938	0.002691
21.6216	0.744118	0.604165	0.482443	0.212328	0.008203	0.301093	0.10627	0.002699
21.6817	0.74645	0.606058	0.483955	0.212994	0.008228	0.302036	0.106604	0.002708
21.7417	0.748778	0.607949	0.485464	0.213658	0.008254	0.302978	0.106936	0.002716
21.8018	0.75111	0.609842	0.486976	0.214323	0.00828	0.303922	0.107269	0.002725
21.8619	0.753442	0.611735	0.488488	0.214989	0.008305	0.304865	0.107602	0.002733
21.9219	0.75577	0.613625	0.489998	0.215653	0.008331	0.305808	0.107934	0.002742
21.982	0.758102	0.615519	0.49151	0.216319	0.008356	0.306751	0.108268	0.00275
22.042	0.76043	0.617409	0.493019	0.216983	0.008382	0.307693	0.1086	0.002758
22.1021	0.762761	0.619302	0.49453	0.217648	0.008408	0.308636	0.108933	0.002767
22.1622	0.765093	0.621195	0.496042	0.218313	0.008433	0.30958	0.109266	0.002775
22.2222	0.767421	0.623085	0.497551	0.218978	0.008459	0.310522	0.109599	0.002784
22.2823	0.769753	0.624979	0.499063	0.219643	0.008484	0.311465	0.109931	0.002792
22.3423	0.772081	0.626869	0.500573	0.220307	0.00851	0.312408	0.110264	0.002801
22.4024	0.774413	0.628762	0.502085	0.220973	0.008536	0.313351	0.110597	0.002809
22.4625	0.776745	0.630656	0.503597	0.221638	0.008561	0.314295	0.11093	0.002818
22.5225	0.779073	0.632546	0.505106	0.222303	0.008587	0.315237	0.111263	0.002826
22.5826	0.781405	0.634439	0.506618	0.222968	0.008612	0.31618	0.111596	0.002835
22.6426	0.783733	0.636329	0.508127	0.223632	0.008638	0.317122	0.111928	0.002843
22.7027	0.786065	0.638223	0.509639	0.224298	0.008664	0.318066	0.112261	0.002851
22.7628	0.788397	0.640116	0.511151	0.224963	0.008689	0.319009	0.112594	0.00286
22.8228	0.790725	0.642006	0.51266	0.225627	0.008715	0.319951	0.112926	0.002868
22.8829	0.793057	0.6439	0.514172	0.226293	0.00874	0.320895	0.11326	0.002877
22.9429	0.795385	0.64579	0.515682	0.226957	0.008766	0.321837	0.113592	0.002885
23.003	0.797716	0.647682	0.517193	0.227622	0.008792	0.32278	0.113925	0.002894
23.0631	0.800048	0.649576	0.518705	0.228288	0.008817	0.323724	0.114258	0.002902
23.1231	0.802376	0.651466	0.520214	0.228952	0.008843	0.324666	0.114591	0.002911
23.1832	0.804708	0.653359	0.521726	0.229617	0.008869	0.325609	0.114923	0.002919
23.2432	0.807036	0.655249	0.523236	0.230282	0.008894	0.326552	0.115256	0.002928
23.3033	0.809368	0.657143	0.524748	0.230947	0.00892	0.327495	0.115589	0.002936
23.3634	0.8117	0.659036	0.526259	0.231612	0.008945	0.328438	0.115922	0.002944

23.4234	0.814028	0.660926	0.527769	0.232277	0.008971	0.329381	0.116255	0.002953
23.4835	0.81636	0.66282	0.529281	0.232942	0.008997	0.330324	0.116588	0.002961
23.5435	0.818688	0.66471	0.53079	0.233606	0.009022	0.331266	0.11692	0.00297
23.6036	0.82102	0.666603	0.532302	0.234272	0.009048	0.33221	0.117253	0.002978
23.6637	0.823352	0.668497	0.533814	0.234937	0.009073	0.333153	0.117586	0.002987
23.7237	0.82568	0.670387	0.535323	0.235601	0.009099	0.334095	0.117918	0.002995
23.7838	0.828011	0.67228	0.536835	0.236267	0.009125	0.335039	0.118252	0.003004
23.8438	0.830339	0.67417	0.538344	0.236931	0.00915	0.335981	0.118584	0.003012
23.9039	0.832671	0.676063	0.539856	0.237596	0.009176	0.336924	0.118917	0.00302
23.964	0.835003	0.677956	0.541368	0.238262	0.009201	0.337868	0.11925	0.003029
24.024	0.837331	0.679847	0.542877	0.238926	0.009227	0.33881	0.119583	0.003037
24.0841	0.839663	0.68174	0.544389	0.239591	0.009253	0.339753	0.119915	0.003046
24.1441	0.841991	0.68363	0.545898	0.240256	0.009278	0.340695	0.120248	0.003054
24.2042	0.844323	0.685524	0.54741	0.240921	0.009304	0.341639	0.120581	0.003063
24.2643	0.846655	0.687417	0.548922	0.241587	0.009329	0.342582	0.120914	0.003071
24.3243	0.848983	0.689307	0.550432	0.242251	0.009355	0.343525	0.121247	0.00308
24.3844	0.851315	0.6912	0.551944	0.242916	0.009381	0.344468	0.12158	0.003088
24.4444	0.853643	0.693091	0.553453	0.24358	0.009406	0.34541	0.121912	0.003097
24.5045	0.855975	0.694984	0.554965	0.244246	0.009432	0.346354	0.122245	0.003105
24.5646	0.858306	0.696877	0.556476	0.244911	0.009458	0.347297	0.122578	0.003113
24.6246	0.860634	0.698767	0.557985	0.245575	0.009483	0.348238	0.12291	0.003122
24.6847	0.862966	0.70066	0.559497	0.246241	0.009509	0.349182	0.123244	0.00313
24.7447	0.865294	0.70255	0.561007	0.246905	0.009534	0.350125	0.123576	0.003139
24.8048	0.867626	0.704444	0.562519	0.24757	0.00956	0.351068	0.123909	0.003147
24.8649	0.869958	0.706337	0.564031	0.248236	0.009586	0.352012	0.124242	0.003156
24.9249	0.872286	0.708227	0.56554	0.2489	0.009611	0.352954	0.124575	0.003164
24.985	0.874618	0.710121	0.567052	0.249566	0.009637	0.353897	0.124908	0.003173
25.045	0.876946	0.712011	0.568561	0.25023	0.009662	0.354839	0.12524	0.003181
25.1051	0.879278	0.713904	0.570073	0.250895	0.009688	0.355783	0.125573	0.00319
25.1652	0.88161	0.715798	0.571585	0.251561	0.009714	0.356726	0.125906	0.003198
25.2252	0.883938	0.717688	0.573094	0.252225	0.009739	0.357668	0.126239	0.003206
25.2853	0.88627	0.719581	0.574606	0.25289	0.009765	0.358612	0.126571	0.003215
25.3453	0.888598	0.721471	0.576116	0.253555	0.00979	0.359554	0.126904	0.003223
25.4054	0.89093	0.723365	0.577628	0.25422	0.009816	0.360498	0.127237	0.003232
25.4655	0.893261	0.725257	0.579139	0.254885	0.009842	0.361441	0.12757	0.00324
25.5255	0.895589	0.727148	0.580648	0.255549	0.009867	0.362382	0.127902	0.003249
25.5856	0.897921	0.729041	0.58216	0.256215	0.009893	0.363326	0.128236	0.003257
25.6456	0.900249	0.730931	0.58367	0.256879	0.009918	0.364269	0.128568	0.003266
25.7057	0.902581	0.732824	0.585181	0.257545	0.009944	0.365212	0.128901	0.003274
25.7658	0.904913	0.734718	0.586693	0.25821	0.00997	0.366155	0.129234	0.003283
25.8258	0.907241	0.736608	0.588203	0.258874	0.009995	0.367098	0.129566	0.003291
25.8859	0.909573	0.738501	0.589715	0.25954	0.010021	0.368041	0.1299	0.003299
25.9459	0.911901	0.740392	0.591224	0.260204	0.010047	0.368983	0.130232	0.003308
26.006	0.914233	0.742285	0.592736	0.260869	0.010072	0.369927	0.130565	0.003316
26.0661	0.916565	0.744178	0.594248	0.261535	0.010098	0.37087	0.130898	0.003325
26.1261	0.918893	0.746068	0.595757	0.262199	0.010123	0.371812	0.131231	0.003333
26.1862	0.921225	0.747962	0.597269	0.262864	0.010149	0.372756	0.131563	0.003342
26.2462	0.923553	0.749852	0.598778	0.263529	0.010175	0.373697	0.131896	0.00335
26.3063	0.925884	0.751745	0.60029	0.264194	0.0102	0.374641	0.132229	0.003359
26.3664	0.928216	0.753638	0.601802	0.264859	0.010226	0.375585	0.132562	0.003367
26.4264	0.930544	0.755528	0.603311	0.265524	0.010251	0.376526	0.132895	0.003376
26.4865	0.932876	0.757422	0.604823	0.266189	0.010277	0.37747	0.133228	0.003384
26.5465	0.935204	0.759312	0.606332	0.266853	0.010303	0.378412	0.13356	0.003392
26.6066	0.937536	0.761205	0.607844	0.267519	0.010328	0.379355	0.133893	0.003401
26.6667	0.939868	0.763099	0.609356	0.268184	0.010354	0.380299	0.134226	0.003409
26.7267	0.942196	0.764989	0.610866	0.268848	0.010379	0.381242	0.134558	0.003418
26.7868	0.944528	0.766882	0.612377	0.269514	0.010405	0.382185	0.134892	0.003426
26.8468	0.946856	0.768772	0.613887	0.270178	0.010431	0.383127	0.135224	0.003435
26.9069	0.949188	0.770666	0.615399	0.270844	0.010456	0.384071	0.135557	0.003443

26.967	0.95152	0.772559	0.616911	0.271509	0.010482	0.385014	0.13589	0.003452
27.027	0.953848	0.774449	0.61842	0.272173	0.010507	0.385956	0.136223	0.00346
27.0871	0.956179	0.776342	0.619931	0.272838	0.010533	0.386899	0.136555	0.003469
27.1471	0.958507	0.778232	0.621441	0.273503	0.010559	0.387841	0.136888	0.003477
27.2072	0.960839	0.780125	0.622953	0.274168	0.010584	0.388785	0.137221	0.003485
27.2673	0.963171	0.782019	0.624465	0.274833	0.01061	0.389729	0.137554	0.003494
27.3273	0.965499	0.783909	0.625974	0.275498	0.010636	0.39067	0.137887	0.003502
27.3874	0.967831	0.785802	0.627486	0.276163	0.010661	0.391614	0.13822	0.003511
27.4474	0.970159	0.787692	0.628995	0.276827	0.010687	0.392556	0.138552	0.003519
27.5075	0.972491	0.789586	0.630507	0.277493	0.010683	0.393499	0.138885	0.003528
27.5676	0.972151	0.78931	0.630287	0.277396	0.010694	0.393362	0.138837	0.003526
27.6276	0.973151	0.790122	0.630935	0.277681	0.010694	0.393767	0.138979	0.00353
27.6877	0.973151	0.790122	0.630935	0.277681	0.010705	0.393767	0.138979	0.00353
27.7477	0.974151	0.790934	0.631583	0.277967	0.010705	0.394171	0.139123	0.003534
27.8078	0.974151	0.790934	0.631583	0.277967	0.010716	0.394171	0.139123	0.003534
27.8679	0.975151	0.791745	0.632232	0.278252	0.010716	0.394576	0.139265	0.003537
27.9279	0.975151	0.791745	0.632232	0.278252	0.010727	0.394576	0.139265	0.003537
27.988	0.976151	0.792557	0.63288	0.278537	0.010727	0.39498	0.139408	0.003541
28.048	0.976151	0.792557	0.63288	0.278537	0.010738	0.39498	0.139408	0.003541
28.1081	0.977151	0.793369	0.633528	0.278823	0.010738	0.395385	0.139551	0.003545
28.1682	0.977151	0.793369	0.633528	0.278823	0.010749	0.395385	0.139551	0.003545
28.2282	0.978151	0.794181	0.634177	0.279108	0.010749	0.39579	0.139694	0.003548
28.2883	0.978151	0.794181	0.634177	0.279108	0.01076	0.39579	0.139694	0.003548
28.3483	0.979151	0.794993	0.634825	0.279393	0.01076	0.396194	0.139836	0.003552
28.4084	0.979151	0.794993	0.634825	0.279393	0.010771	0.396194	0.139836	0.003552
28.4685	0.980151	0.795805	0.635473	0.279679	0.010771	0.396599	0.139979	0.003555
28.5285	0.980151	0.795805	0.635473	0.279679	0.010782	0.396599	0.139979	0.003555
28.5886	0.981151	0.796617	0.636122	0.279964	0.010782	0.397004	0.140122	0.003559
28.6486	0.981151	0.796617	0.636122	0.279964	0.010793	0.397004	0.140122	0.003559
28.7087	0.982151	0.797429	0.63677	0.280249	0.010793	0.397408	0.140265	0.003563
28.7688	0.982151	0.797429	0.63677	0.280249	0.010804	0.397408	0.140265	0.003563
28.8288	0.983151	0.798241	0.637418	0.280535	0.010804	0.397813	0.140408	0.003566
28.8889	0.983151	0.798241	0.637418	0.280535	0.010815	0.397813	0.140408	0.003566
28.9489	0.984151	0.799053	0.638067	0.28082	0.010815	0.398218	0.14055	0.00357
29.009	0.984151	0.799053	0.638067	0.28082	0.010826	0.398218	0.14055	0.00357
29.0691	0.985151	0.799865	0.638715	0.281105	0.010826	0.398622	0.140693	0.003574
29.1291	0.985151	0.799865	0.638715	0.281105	0.010837	0.398622	0.140693	0.003574
29.1892	0.986151	0.800677	0.639363	0.281391	0.010837	0.399027	0.140836	0.003577
29.2492	0.986151	0.800677	0.639363	0.281391	0.010848	0.399027	0.140836	0.003577
29.3093	0.987151	0.801489	0.640012	0.281676	0.010848	0.399432	0.140979	0.003581
29.3694	0.987151	0.801489	0.640012	0.281676	0.010859	0.399432	0.140979	0.003581
29.4294	0.988151	0.802301	0.64066	0.281961	0.010859	0.399836	0.141122	0.003584
29.4895	0.988151	0.802301	0.64066	0.281961	0.01087	0.399836	0.141122	0.003584
29.5495	0.989151	0.803112	0.641308	0.282247	0.01087	0.40024	0.141265	0.003588
29.6096	0.989151	0.803112	0.641308	0.282247	0.010881	0.40024	0.141265	0.003588
29.6697	0.990151	0.803924	0.641957	0.282532	0.010881	0.400645	0.141407	0.003592
29.7297	0.990151	0.803924	0.641957	0.282532	0.010892	0.400645	0.141407	0.003592
29.7898	0.991151	0.804736	0.642605	0.282817	0.010892	0.40105	0.14155	0.003595
29.8498	0.991151	0.804736	0.642605	0.282817	0.010903	0.40105	0.14155	0.003595
29.9099	0.992151	0.805548	0.643253	0.283103	0.010903	0.401454	0.141693	0.003599
29.97	0.992151	0.805548	0.643253	0.283103	0.010914	0.401454	0.141693	0.003599
30.03	0.993151	0.80636	0.643902	0.283388	0.01025	0.401859	0.141836	0.003603
27.5676	0.972151	0.78931	0.630287	0.277396	0.010694	0.393362	0.138837	0.003526
27.6276	0.973151	0.790122	0.630935	0.277681	0.010694	0.393767	0.138979	0.00353
27.6877	0.973151	0.790122	0.630935	0.277681	0.010705	0.393767	0.138979	0.00353
27.7477	0.974151	0.790934	0.631583	0.277967	0.010705	0.394171	0.139123	0.003534
27.8078	0.974151	0.790934	0.631583	0.277967	0.010716	0.394171	0.139123	0.003534
27.8679	0.975151	0.791745	0.632232	0.278252	0.010716	0.394576	0.139265	0.003537
27.9279	0.975151	0.791745	0.632232	0.278252	0.010727	0.394576	0.139265	0.003537

27.988	0.976151	0.792557	0.63288	0.278537	0.010727	0.39498	0.139408	0.003541
28.048	0.976151	0.792557	0.63288	0.278537	0.010738	0.39498	0.139408	0.003541
28.1081	0.977151	0.793369	0.633528	0.278823	0.010738	0.395385	0.139551	0.003545
28.1682	0.977151	0.793369	0.633528	0.278823	0.010749	0.395385	0.139551	0.003545
28.2282	0.978151	0.794181	0.634177	0.279108	0.010749	0.39579	0.139694	0.003548
28.2883	0.978151	0.794181	0.634177	0.279108	0.01076	0.39579	0.139694	0.003548
28.3483	0.979151	0.794993	0.634825	0.279393	0.01076	0.396194	0.139836	0.003552
28.4084	0.979151	0.794993	0.634825	0.279393	0.010771	0.396194	0.139836	0.003552
28.4685	0.980151	0.795805	0.635473	0.279679	0.010771	0.396599	0.139979	0.003555
28.5285	0.980151	0.795805	0.635473	0.279679	0.010782	0.396599	0.139979	0.003555
28.5886	0.981151	0.796617	0.636122	0.279964	0.010782	0.397004	0.140122	0.003559
28.6486	0.981151	0.796617	0.636122	0.279964	0.010793	0.397004	0.140122	0.003559
28.7087	0.982151	0.797429	0.63677	0.280249	0.010793	0.397408	0.140265	0.003563
28.7688	0.982151	0.797429	0.63677	0.280249	0.010804	0.397408	0.140265	0.003563
28.8288	0.983151	0.798241	0.637418	0.280535	0.010804	0.397813	0.140408	0.003566
28.8889	0.983151	0.798241	0.637418	0.280535	0.010815	0.397813	0.140408	0.003566
28.9489	0.984151	0.799053	0.638067	0.28082	0.010815	0.398218	0.14055	0.00357
29.009	0.984151	0.799053	0.638067	0.28082	0.010826	0.398218	0.14055	0.00357
29.0691	0.985151	0.799865	0.638715	0.281105	0.010826	0.398622	0.140693	0.003574
29.1291	0.985151	0.799865	0.638715	0.281105	0.010837	0.398622	0.140693	0.003574
29.1892	0.986151	0.800677	0.639363	0.281391	0.010837	0.399027	0.140836	0.003577
29.2492	0.986151	0.800677	0.639363	0.281391	0.010848	0.399027	0.140836	0.003577
29.3093	0.987151	0.801489	0.640012	0.281676	0.010848	0.399432	0.140979	0.003581
29.3694	0.987151	0.801489	0.640012	0.281676	0.010859	0.399432	0.140979	0.003581
29.4294	0.988151	0.802301	0.64066	0.281961	0.010859	0.399836	0.141122	0.003584
29.4895	0.988151	0.802301	0.64066	0.281961	0.01087	0.399836	0.141122	0.003584
29.5495	0.989151	0.803112	0.641308	0.282247	0.01087	0.40024	0.141265	0.003588
29.6096	0.989151	0.803112	0.641308	0.282247	0.010881	0.40024	0.141265	0.003588
29.6697	0.990151	0.803924	0.641957	0.282532	0.010881	0.400645	0.141407	0.003592
29.7297	0.990151	0.803924	0.641957	0.282532	0.010892	0.400645	0.141407	0.003592
29.7898	0.991151	0.804736	0.642605	0.282817	0.010892	0.40105	0.14155	0.003595
29.8498	0.991151	0.804736	0.642605	0.282817	0.010903	0.40105	0.14155	0.003595
29.9099	0.992151	0.805548	0.643253	0.283103	0.010903	0.401454	0.141693	0.003599
29.97	0.992151	0.805548	0.643253	0.283103	0.010914	0.401454	0.141693	0.003599
30	0.993151	0.80636	0.643902	0.283388	0.01025	0.401859	0.141836	0.003603
29.7297	0.990151	0.803924	0.641957	0.282532	0.010892	0.400645	0.141407	0.003592
29.7898	0.991151	0.804736	0.642605	0.282817	0.010892	0.40105	0.14155	0.003595
29.8498	0.991151	0.804736	0.642605	0.282817	0.010903	0.40105	0.14155	0.003595
29.9099	0.992151	0.805548	0.643253	0.283103	0.010903	0.401454	0.141693	0.003599
29.97	0.992151	0.805548	0.643253	0.283103	0.010914	0.401454	0.141693	0.003599
30	0.993151	0.80636	0.643902	0.283388	0.01025	0.401859	0.141836	0.003603

The parameters for the control simulation were based on the mean values from wild-type rats (Chapter 5; Table 5.1); where scenario 1 is a 3-fold increase in $k_{perfusate}$; scenario 2 is a 5-fold increase in $k_{perfusate}$; scenario 3 is a 10-fold increase in $k_{perfusate}$; scenario 4 is a 100-fold increase in $k_{perfusate}$; scenario 5 is a 3-fold increase in $k_{perfusate}$ and 0.5-fold decrease in CL_{up}; scenario 6 is a 10-fold increase in $k_{perfusate}$ and 0.5-fold decrease in CL_{up}; scenario 7 is a 200-fold increase in $k_{perfusate}$.